Investigation of some traditional Chinese medicines used to treat cancer

Fang, Rui

INVESTIGATION OF SOME TRADITIONAL CHINESE MEDICINES USED TO TREAT CANCER

A THESIS
Submitted to University of London
For the degree of

DOCTOR OF PHILOSOPHY

RUI FANG

Drug Discovery Group
Pharmaceutical Sciences Research Division
School of Biomedical & Health Sciences
King's College London
University of London

2006

ABSTRACT

The aim of the present project is to study five Traditional Chinese Medicines (TCM) used traditionally in China for the treatment of cancer. They are *Dolichos lablab* L., *Gekko swinhonis* Gunther, *Illicium verum* Hook. *f*, *Lonicera japonica* Thunb. and *Iris tectorum* Maxim.

Solvent extractions of the TCMs were subjected to bioassay-guided fractionation and isolation, yielding series of fractions with increasing purity and cytotoxicity. The cytotoxicity assay used comprised four human cancer cell lines (COR-L23, C32, MCF-7 and HepG2) and two human normal cell lines (MRC-5 and 16HBE14o-).

The separation of organic components was carried out mainly by means of TLC, VLC and HPLC. Isolation and purification of bioactive compounds from the active extract of *I. tectorum*, the most potent source tested, led to the identification of two known flavonoids (tectorigenin and 7-*O*-methyl-aromadendrin), two known triterpenes (isoiridogermanal and iridobelamal A) and two novel triterpenes. The structures of the latter were determined by mass spectrometry and infrared and 2D nuclear magnetic resonance spectroscopic techniques.

Induction of apoptosis by the isolated compounds was investigated using flow cytometry with quadrant analysis, and confirmed by fluorescence microscopy. Furthermore, cell cycle specific cytotoxicity was determined by DNA analysis. The selectivity of cytotoxicity activity, modes of action and structure-activity relationships of the compounds are discussed.

Also, a cell culture-based prodrug assay was established for high-throughput screening of potential glucosides, which are inactive *in vitro* but may be metabolized to active aglycones *in vivo*.

In summary, the results obtained showed that selection based on ethnopharmacology, together with a robust and reliable method to detect biological activity, can be a useful approach for exploring traditional medicines for novel cytotoxic substances.

ACKNOWLEDGEMENTS

My appreciation and gratitude goes to my first supervisor, Professor Peter J Hylands for his excellent supervision and constructive support during the course of practical work and the preparation of the thesis. His enthusiasm, patience and dedication to his students and research are unparalleled and deserve the utmost respect and appreciation.

I would like to express my thanks to my second supervisor, Professor Peter J Houghton for his kindness, understanding and invaluable guidance in the initiation of the present project. His continuous encouragement, kind support and mentoring supervision throughout my PhD course are highly appreciated.

My thanks also go to Christine Leon and the staff of the Royal Botanic Gardens, Kew, for their kind helps in the authentication of plant materials of the present project.

I would also like to acknowledge: Dr Alex F Drake and Dr Tam Bui of the Pharmaceutical Optical and Chiroptical Spectroscopy Centre, Department of Pharmacy, King's College London for optical rotation and circular dichroism measurements; Dr Jane Hawkes and Mr Jonathan Cobb, NMR Unit, Chemistry Department, King's College London, for constructive discussions and NMR spectroscopic measurements; Dr Roger Tye and Dr Andy Cakebread of mass spectrometry Unit, King's College London for mass spectrometry measurements; Professor Robert Hider and Dr Ding Yong Liu, Pharmacy Department, and Dr Helen Collins and Dr John Murphy, Life Sciences Research Division for their instrumental support in experiments of HPLC and flow cytometry, respectively; Mr Mike Faux and Dr Cynthia Bosquillon for technical assistance during the course of the research work; and members of pharmacognosy research group for their friendship and encouragement.

The financial support of the Henry Lester Trust Limited, Great Britain-China Educational Trust and Sino-British Fellowship Trust are gratefully acknowledged.

Most importantly, my love and gratitude goes to my parents, my wife, Chunliu Deng, and her parents, for their love, kindness, patience and understanding through which have enabled me to complete the project.

TABLE OF CONTENTS

LIST OF TABLES

LIST OF FIGURES

ABBREVIATIONS

A	=	absorbance
Ac	=	acetyl
Ann	=	annexin V-FITC (phospholipid-binding protein conjugated with FITC)
β-glu	=	*β*-glucosidase
c	=	concentration
CD	=	circular dichroism
$CDCl_3$	=	deuterated chloroform
CD_3OD	=	deuterated methanol
$CHCl_3$	=	chloroform
CIMS	=	chemical ionization mass spectrometry
cm	=	centimetre
conc.	=	concentration
comp.	=	compound
COR-L23	=	human non-small cell lung cancer
COSY	=	correlated spectroscopy
C32	=	human amelanotic melanoma
^{13}C NMR	=	carbon 13 nuclear magnetic resonance
°C	=	degree celsius
d	=	doublet (for description of NMR spectra)
DCM	=	dichloromethane
DEPT	=	distortionless enhancement by polarisation transfer
DL	=	*Dolichos lablab* L.
DMEM	=	Dulbecco's modified eagle medium
DMSO	=	dimethyl sulphoxide
DMSO-d_6	=	deuterated dimethyl sulphoxide
EDTA	=	ethylenediamine tetraacetic acid
EIMS	=	electron ionization mass spectrometry
ESIMS	=	electrospray ionization mass spectrometry
EtOAc	=	ethyl acetate
EtOH	=	ethanol
λ	=	wavelength
FBS	=	foetal bovine serum

FDA	=	fluorescein diacetate
FITC	=	fluorescein isothiocyanate
g	=	gram
Glc	=	glucose
GK	=	*Gekko swinhonis* Gunther
h	=	hour
HepG2	=	hepatocellular carcinoma
HMBC	=	heteronuclear multiple bond connectivity
HMQC	=	heteronuclear multiple quantum coherence
^{1}H NMR	=	proton nuclear magnetic resonance
IG_{50}	=	concentration required to inhibit cell growth by 50%
Iris	=	*Iris tectorum* Maxim.
IR	=	infrared spectrascopy
IV	=	*Illicium verum* Hook. *f*
J	=	nuclear spin-spin coupling constant (Hz)
kg	=	kilogram
LJ	=	*Lonicera japonica* Thunb.
ml	=	millilitre
m	=	multiplet (for description of NMR spectra)
M^+	=	molecular ion
MCF-7	=	human Caucasian breast adenocarcinoma
Me	=	methyl
MeO	=	methoxyl
MeOH	=	methanol
mg	=	milligram
MHz	=	mega Hertz
min	=	minute
ml	=	millilitre
mm	=	millimetre
mM	=	millimolar
MRC-5	=	human foetal lung fibroblast
MS	=	mass spectrometry
MTT	=	3-(4,5-dimethylthiazol-2-yl)-2,5-diphenyltetrazolium bromide
m/z	=	mass to charge ratio
µg	=	microgram

µl	=	microlitre
µM	=	micromolar
nM	=	nanomolar
NMR	=	nuclear magnetic resonance
NOESY	=	nuclear overhauser effect spectroscopy
OD	=	optical density
PBS	=	phosphate buffer saline
PE	=	phycoerythrin (a red protein)
PI	=	propidium iodide
ppm	=	parts per million
q	=	quartet (for description of NMR spectra)
R_f	=	retardation factor
Rha	=	rhamnose
rpm	=	revolutions per minute
R_T	=	retention time
s	=	singlet (for description of NMR spectra)
SEM	=	standard error of the mean
SRB	=	sulphorhodamine B
t	=	triplet (for description of NMR spectra)
TCA	=	trichloroacetic acid
TLC	=	thin-layer chromatography
TMS	=	tetramethylsilane
UV	=	ultraviolet
VLC	=	vacuum liquid chromatography
v/v	=	volume by volume
w/v	=	weight by volume
δ	=	chemical shift (ppm, for description of NMR spectra)
[α]	=	specific rotation
16HBE14o-	=	human bronchial epithelial cell line

CHAPTER 1
INTRODUCTION

1.1 Classification of cancer

Generally, a cell population that evolves to be able to disregard the normal controls of proliferation and territory becomes a cancer (Ponder, 2001). Neoplasms are classified as being benign or malignant; malignant neoplasms are equivalent to cancer. Different cancers are described according to their cell of origin and the tissue in which they arise (Roger *et al.*, 2006) (see Table 1-1).

Epithelium (carcinoma)	• Glandular, e.g., prostate: adenocarcinoma • Squamous, e.g., cervix: carcinoma
Mesenchyma (sarcoma)	• Smooth muscle: leiomyosarcoma; benign hyperproliferation is called a leiomyoma (fibroid) • Bone: osteosarcoma • Fat cells: liposarcoma; benign hyperproliferation is called a lipoma
Nervous system	• Eye: retinoblastoma • Astrocytes: astrocytoma
White bood cells (leukaemia)	• Myeloid cells: myelocytic leukaemia • Lymphocytes: lymphocytic leukaemia • Lymphoma: solid tumour derived from B- or T-lymphocytes

Table 1-1: Terminology of cancer (from Roger *et al.*, 2006)

Indeed, cancer is many diseases. There are several initiating causes, several cofactors and promoters, and several kinds of cellular damage inflicted on the body's own cells. Cancer arises from cells in the body that were once normal cells. The factors that determine the incidence are largely exogenous. Exogenous causative agents or factors

that have been identified in human include: cigarette smoking, occupational and environmental chemicals, radiation. dietary factors, lifestyle and socioeconomic factors, and specific viruses (Anonymous, 2006).

1.2 Epidemiology of cancer

Cancer is a major cause of morbidity in the United Kingdom (Anonymous, 2006a). Each year more than a quarter of a million people are newly diagnosed with cancer. Overall it is estimated that more than one in three people will develop some form of cancer during their lifetime (Anonymous, 2006a). As shown in Figure 1-1, there are more than 200 different types of cancer, but four of them (breast, lung, large bowel [colorectal] and prostate cancer) account for over half of all new cases in 2002. Breast cancer is the most common cancer in the UK despite the fact that it is rare in men. Prostate cancer has overtaken lung cancer to become the most commonly diagnosed cancer in UK males, with more than 31,000 cases diagnosed in 2002. Lung cancer is the second most common cancer for males, with around 23,000 cases annually (Anonymous, 2006a). In 2004, 153,397 people died of cancer in the UK, deaths from cancers of the lung (22%), bowel (11%), breast (8%) and prostate (6%) together account for around 47% of all cancer deaths (Anonymous, 2006b).

In the United States, cancer is the second most common cause of death, exceeded only by heart disease. In the US, cancer accounts for 1 of every 4 deaths. About 564,380 Americans are expected to die of cancer in 2006, more than 1,500 people a day (Anonymous, 2006).

The global burden of cancer continues to increase. In the year 2000, 5.3 million men and 4.7 million women developed a malignant tumour and 6.2 million died of the disease. Given the present trends in smoking prevalence and the adoption of unhealthy lifestyles, the number of new cases is expected to reach 15 million by 2020. Worldwide, 12% of people die of cancer and in industrialized countries more than one in four will die of the disease (Stewart and Kleihues, 2003).

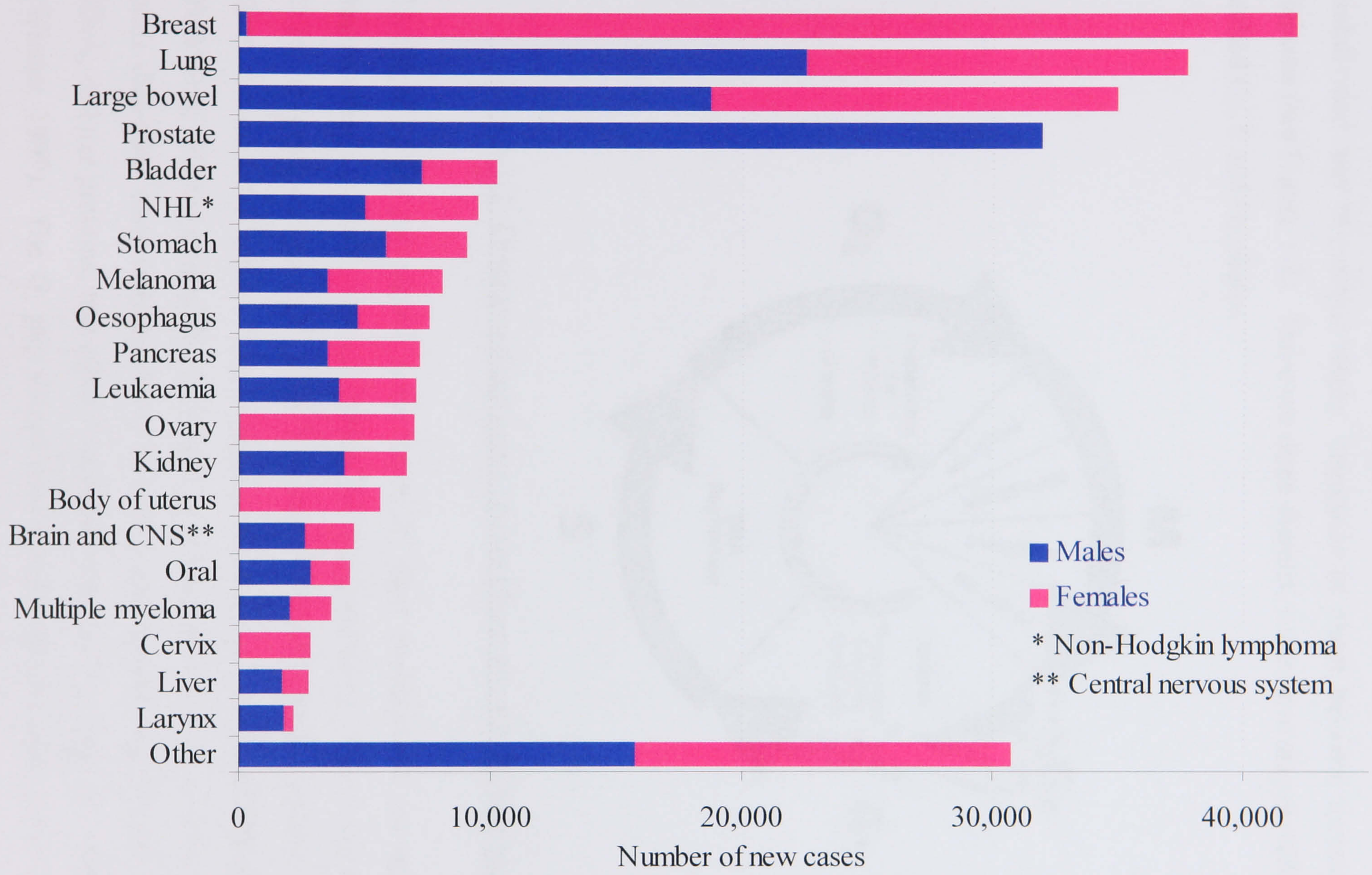

Figure 1-1: The 20 most commonly diagnosed cancers in UK, 2002 (Anonymous, 2006a)

1.3 Cell biology

The eukaryotic cell cycle consists of a series of events that are involved in the growth, replication, and division of cells (Lodish and Darnell, 1995). The cell cycle can be subdivided into two major stages, interphase (a phase between mitotic events) and mitosis (see Figure 1-2). There are three distinct, successive stages within interphase, called G_1, S and G_2 phases.

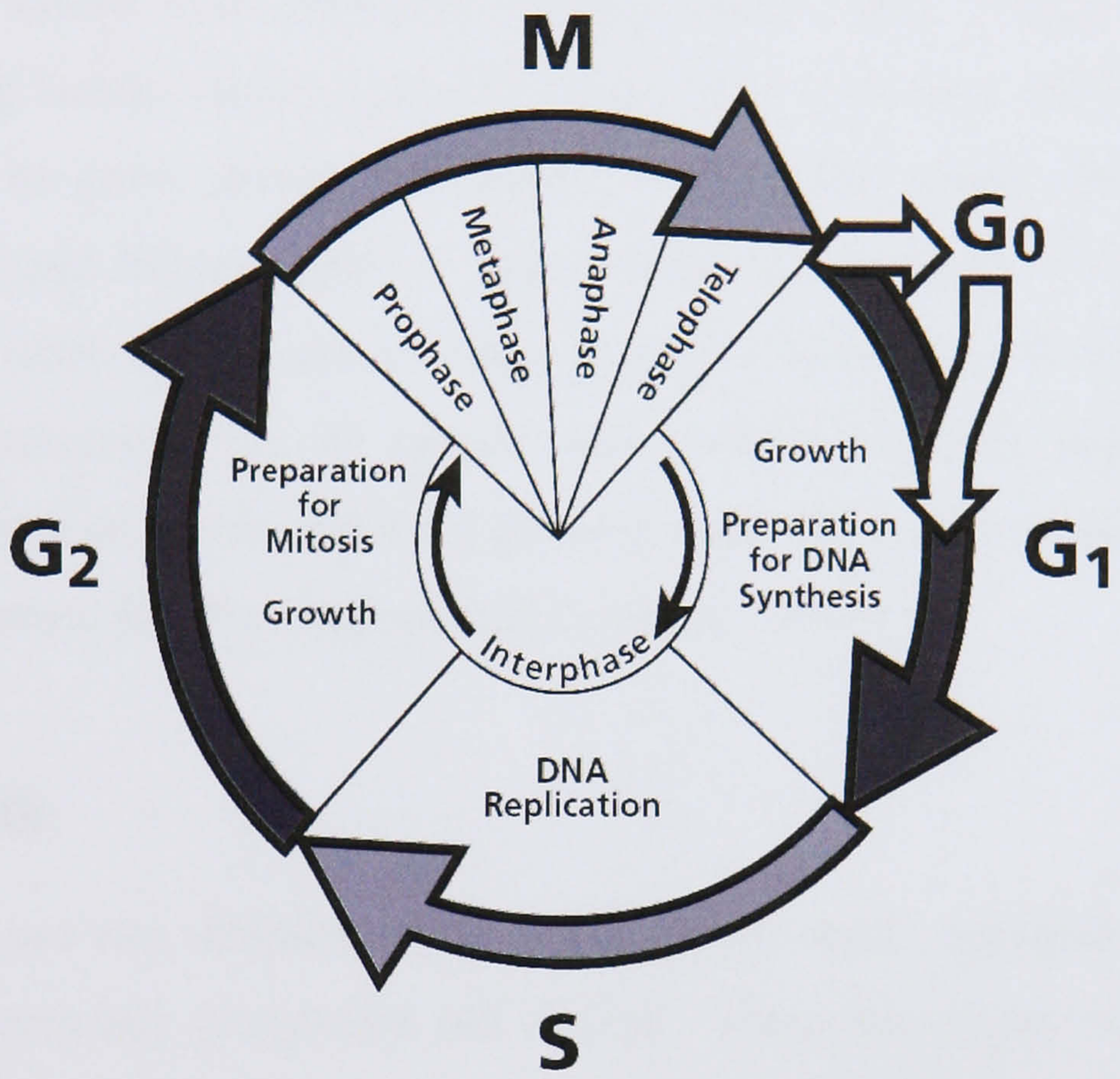

Figure 1-2: Diagram of cell cycle phases (from www.bdbiosciences.com)

During G_1 (first gap phase), cells "monitor" their environment and upon receipt of requisite signals, they grow (synthesize RNA and proteins). The ploidy of a cell in G_1 is $2n$. If conditions are right, cells "commit" to DNA synthesis (S phase) and replicate their chromosomal DNA. The ploidy of cells during S phase is between $2n$ and $4n$. Following DNA duplication, cells enter a second growth phase called G_2, in which cells duplicate their infrastructure, including the quantity of ribosomes, ribosomal RNA, cellular proteins, and other functional elements in preparation for cell division (Wieder, 1999). The G_2 gap allows time for the cell to ensure DNA replication is complete before initiating mitosis. In mitosis, there are four successive phases called prophase, metaphase, anaphase and telophase that are accompanied by cytokinesis giving rise to two daughter cells (Murray and Hunt, 1993). For the most part, upon

completion of the process, each daughter cell contains the same genetic material as the original parent cell. In addition to these specific stages, the G_0 phase has been described for cells that exit the cell cycle and enter a quiescent, non-dividing state. In response to external stimuli, some quiescent cells may undergo reactivation and express early response genes, so that they can leave G_0 and enter the G_1 phase of the cell cycle. For instance, KI-67 protein is a marker for distinguishing proliferating G_1 from G_0 cells (Stein and Pardee, 2004).

In many ways, cancer cells resemble undifferentiated cells, which exhibit similar properties during normal embryogenesis. They differ from their normal counterparts by their ability to grow, divide and invade, without the normal restraining forces operating (Price and Sikora, 2002). Thus, unlike normal cells, which can enter a quiescent stage when their numbers reach a certain level (stop dividing by contact inhibition), transformed cells or cancer cells, which lose this aspect of growth regulation, continue to divide and keep growing until the supply of nutrients or some other factor becomes limiting (Pollard and Earnshaw, 2002).

1.4 Cell death

Generally, there are two different mechanisms of cell death, apoptosis (programmed cell death) and necrosis (accidental cell death). These two types of cell death are demonstrated in Figure 1-3. Remarkably, necrosis is the consequence of a passive, degenerative process, which is identified primarily by loss of membrane integrity.

1.4.1 Apoptosis

It is generally accepted that all cells have the ability to under go an internally controlled cell suicide process known as apoptosis, or programmed cell death, in response to a given stimulus or environmental agent (Schwartzman and Cidlowski, 1993). The term "apoptosis" itself derives from a Greek word that describes phenomena such as the falling of leaves from trees. Apoptosis is a mode of cell death that facilitates such fundamental processes as development (for example, removal of unwanted tissue during embryogenesis) and the immune response (for example, elimination of self-reactive T cells) (Allen *et al.*, 1993).

Apoptosis is characterized by a distinct set of morphological and biochemical features

including cell shrinkage, nuclear condensation, proteolysis, internucleosomal DNA cleavage, and apoptotic body formation (Martin *et al.*, 1994). In the process of apoptosis, DNA fragmentation involves endonuclease, which characteristically breaks the DNA between the clumps of chromatin that are referred to as nucleosomes, the consequence of this is that the DNA breaks into fragments of rather precise sizes that are multiples of about 200 DNA base pairs in length. Whilst these processes of DNA cleavage are going on, the nucleus begins to break into fragments and the cell likewise splits into pieces; thus the original dying cell generates a number of cellular apoptotic bodies or apoptotic fragments. This used to be referred to as karyorrhexis. Finally, these fragments are engulfed by the specialised migrating macrophages or healthy neighbouring epithelial cells by a process called phagocytosis. This phagocytic process results in apoptotic bodies enclosed in a membrane-bound vesicle in a cell called a phagosome (see Figure 1-3). The host cell then gradually digests the apoptotic body (Potten and Wilson, 2004).

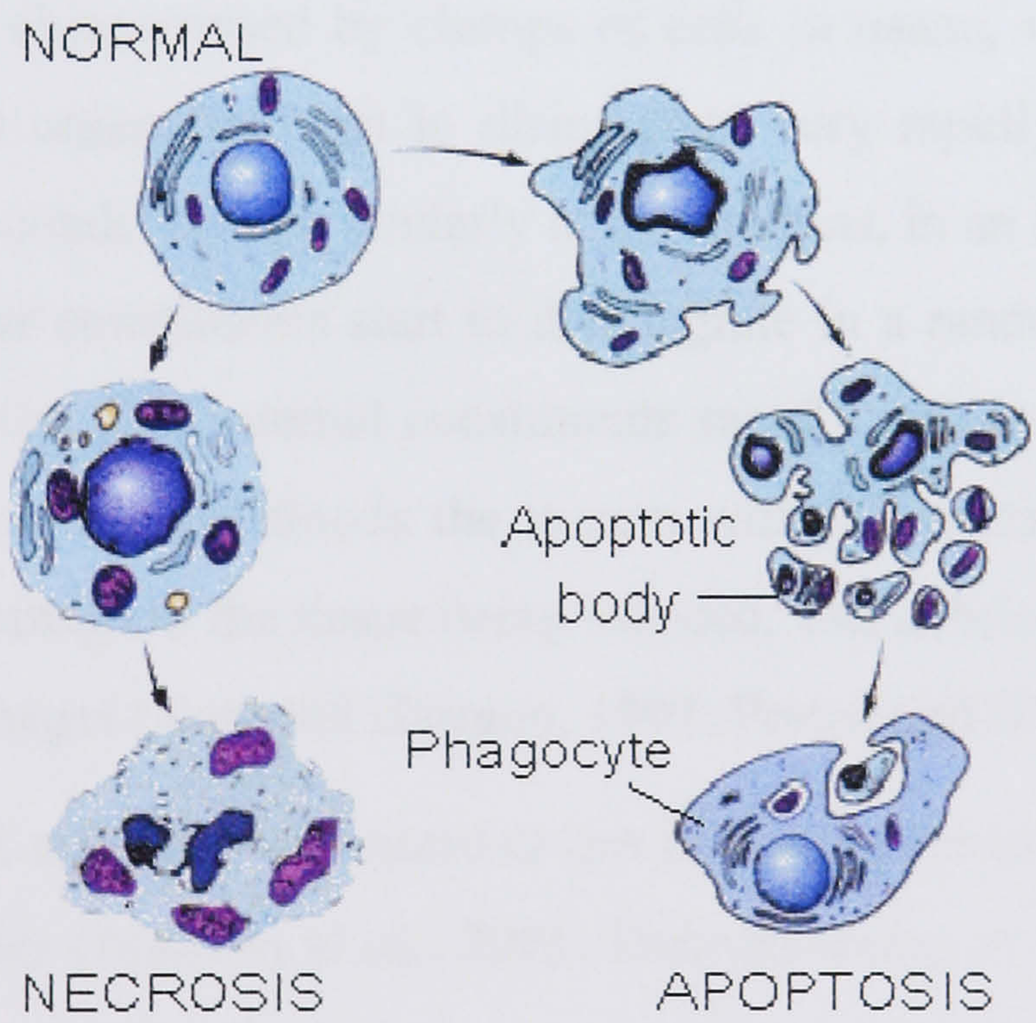

Figure 1-3: Morphological illustration of apoptosis and necrosis (from http://www.cecs.cl/web/cecs)

In oncology, the interest in apoptosis originates from the observations that ionizing radiation or interactions of antitumour drugs with their respective intracellular targets often result in this mode of cell death, and that the efficacy of several antitumour drugs correlates with their ability to induce apoptosis (Kaufmann, 1989; Krishan and

Frei, 1975; Szende *et al.*, 1989). The possibility, therefore, of modulating this process can open new strategies for improving chemotherapy. In addition, the ability to monitor early signs of apoptosis in samples from patient tumours may be predictive for the outcome of treatment protocols (Darzynkiewicz *et al.*, 1992).

1.4.2 Necrosis

In contrast to apoptosis, or programmed cell death, necrosis is a non-specific mode of cell death. It can be caused by excessively high concentrations of toxic agents (Lennon *et al.*, 1991). When cells die by an accidental cell death process known as necrosis, the cells swell. This cellular swelling is caused by the early loss of energy and cell membrane integrity from the cell permitting the movement of both ions, mostly sodium, and water into the cell. Necrotic cells eventually lyse, in turn triggering an inflammatory response, which is not observed during apoptosis (Studzinski, 1999).

Practically, necrosis can be induced by either physical disruption or severe metabolic poisons. It is often characterised by clumps of cells in tissue, where the cells swell and the cytoplasmic organelles start to disintegrate very rapidly. Furthermore, the DNA in the nucleus condenses, particularly at the margins, in an irregular fashion and the DNA and cellular constituents start to disintegrate in a random and uncontrolled fashion. Subsequently, vital internal constituents rapidly leak out of the cell and the host tissue recognises this and floods the system with inflammatory lymphocytes to stop infection and damage to the tissue being induced. The debris is then engulfed and removed by macrophages (Kerr and Harmon, 1991; Potten and Wilson, 2004).

As seen in Table 1-2, apoptosis and necrosis can be distinguished from one another by a set of characteristics (Mattson *et al.*, 2001; Darzynkiewicz *et al.*, 1994; Shi *et al.*, 1997):

Apoptosis	**Necrosis**
Cell morphology	
Cell shrinks dramatically due to blebbing and produces apoptotic bodies	Cell swells and loses integrity of cell membrane due to influx of H_2O
Membranes and organelles remain intact	Outer membrane and organelle membranes rupture leading to non-specific release of damaging enzymes like DNAases and proteases
Nucleus condenses	Nucleus swells
Pyknosis and karyorrhexis (dense condensation of chromatin)	Karyolysis preceded by irregular chromatin clumping
DNA degradation	
Apoptosis exhibits internucleosomal DNA degradation	Necrosis exhibits random DNA degradation
Caused by activation of specific nucleases	Caused by intracellular enzymes released upon organelle membrane rupture or caused by random interaction with random enzymes
Inflammatory response	
No inflammatory response because membranes remain intact	Extensive inflammatory response due to release of intracellular material from the necrotic cell
Synthesis of anti-inflammatory agents occurs that results from actual upregulation of certain apoptotic gene products	Inflammation can further damage normal tissue
Activation of proteases	
Activation of caspases (cysteine proteases) that specifically cleave substrates with aspartic acid residue	Lysosomal rupture leads to release of many non-specific proteases which cause non-specific destruction of cell proteins
Genetic regulation	
Under strict genetic control	Induced by harsh cellular environment

Table 1-2: Comparison of apoptosis with necrosis (summarised from Mattson *et al.*, 2001; Darzynkiewicz *et al.*, 1994; Shi *et al.*, 1997)

1.5 Cancer treatment

1.5.1 Surgery

Surgery is the oldest and most frequently used cancer therapy. It is most efficacious in the treatment of local disease in the region of the primary tumour and in regional lymphatics. Although surgery is still preferred in a high percentage of cases, it is no longer considered as the sole therapy for many neoplasms. Once a neoplasm has spread from the primary site to a distant organ, especially multiple metastasis, surgery should have little role in management of the disease (Holland *et al.*, 1993). Therefore, the use of chemotherapy and radiation therapy in combination with surgery has considerably reduced the extent of operation needed to manage many types of cancer.

1.5.2 Radiation

In modern decades, radiotherapy has become a standard treatment option for a wide range of malignancies. Data from the US Surveillance, Epidemiology, and End Results (SEER) program show that radiation treatment is commonly included in primary oncological treatment. If subsequent palliative interventions are included, more than half of cancer patients receive radiotherapy at least once in their care (DeVita *et al.*, 2005).

1.5.3 Chemotherapy

Chemotherapy began in 1946 when nitrogen mustard was used to treat patients with lymphoma and leukaemia (Goodman *et al.*, 1946). Over the past 20 years new therapies have emerged and innovation in this area is constantly evolving. Nowadays, it has become one of the most significant treatment modalities in cancer care. Currently there are over 500 molecules in clinical development by 43 pharmaceutical companies. It is likely that fewer than 30 will actually make it to the marketplace, and fewer than five will make a big impact on cancer care. The high-cost drugs can achieve extension of life for patients, however, people have to assess how much they are willing to pay for a month of reasonable-quality life (Price and Sikora, 2002). As a result, the demand for a cheap source of chemotherapeutic drug with high efficacy is still quite high.

Based on cancer cell kinetic data, it is reasonable to assume that even small tumours, when clinically detectable, already have resistant clone(s) of cells (Garrett and Workman, 1999). The use of cytotoxic agents of different groups in combination, which attack different biochemical targets should give a broader range of cover of resistant cell lines in a heterogeneous tumour population (Shah and Schwartz, 2000). The development of new resistant cell lines is thus slowed or prevented, thereby giving maximum cell kill, which is impossible with a single-agent regimen. Therefore, the more novel chemotherapeutic molecules are developed, the higher are the chances to eliminate drug-resistant cancer cells.

1.5.4 Chemoprevention

New drugs are developed and tested to prevent cancer, in contrast to classical chemotherapy for treatment of existing disease. This new pharmacological approach to arrest or reverse the process of carcinogenesis, and thus to prevent cancer, is called chemoprevention (Sporn and Liby, 2005). It has been shown convincingly that the use of chemopreventive agents in men and women with premalignant lesions can substantially reduce the subsequent development of truly invasive cancer. Chemoprevention is now recognized as both a clinical and basic science (Alberts *et al.*, 1999).

Carcinogenesis often proceeds through multiple stages, such as initiation, promotion, progression, *etc*. As a result, the transitions between successive stages of carcinogenesis can be enhanced or inhibited by various agents. Several types of evidence indicate that at least half of human cancer is potentially preventable (Alberts *et al.*, 1999).

Plant foods contain a wide variety of anticancer phytochemicals with many potential bioactivities that may reduce cancer susceptibility. Using a panel of *in-vitro* bioassays to monitor chromatographic fractionation, a diverse group of plant secondary metabolites has been identified as potential cancer chemopreventive agents from mainly edible plants. Flavonoids and isoflavonoids are especially promising candidates for cancer prevention (Kinghorn *et al.*, 2004; Birt *et al.*, 2001). They are biosynthesized by plants and have strong antioxidant activity in scavenging free radicals which are involved in cell damage and tumour promotion (Mitchell *et al.*, 1998). At the same time, flavonoids are known to suppress tumour cell growth, which

is mediated by different types of cell cycle arrest and induction of apoptosis in several tumour cell lines. For instance, genistein, the principal isoflavonoid contained in soybeans, is thought to be particularly effective in the prevention of prostate. breast and colon cancers (Adlercreutz *et al.*, 1995).

1.6 Natural products in anticancer treatments

Generally, the accelerated pace of (aberrant) gene identification, and the new technologies of combinatorial chemistry and high-throughput screening, should provide access to a wide range of new, totally synthetic drugs. On the other hand, natural products are likely to provide many of the lead structures, and these will be used as templates for the construction of novel compounds with enhanced biological properties (Mann, 2002).

Plants have been used as medicine for millennia. Out of estimated 250,000 to 350,000 plant species identified so far, about 35,000 are used worldwide for medicinal purposes (Kong *et al.*, 2003). Its has been confirmed by WHO that herbal medicines serve the health needs of about 80 percent of the world's population; especially for millions of people in the vast rural areas of developing countries (Anonymous, 2002). The search for anticancer agents from plant sources started in earnest in the 1950s with the discovery of vinblastine in the Madagascar periwinkle, and the isolation of the cytotoxic podophyllotoxins (Cragg and Newman, 2005). It has been estimated that in the mid-1990s over 200 companies and research organizations worldwide are screening plant and animal compounds for medicinal properties. Especially, the National Cancer Institute (NCI) (of the US) initiated an extensive plant collection program in 1960, focused mainly in temperate regions, and began to screen plant extracts for anticancer activity. This led to the discovery of many novel chemotypes showing a range of cytotoxic activities, including the taxoids and camptothecins. Natural compounds isolated from medicinal plants, as rich sources of novel anticancer drugs, have been of increasing interest since then (Cai *et al.*, 2004). As a result, over 60% of currently used anticancer agents are derived in one way or another from natural sources, including plants. marine organisms and micro-organisms (Newman *et al.*, 2003).

The most efficient method of discovering drugs such as novel anticancer agents is

bioactivity-guided fractionation of natural products (Pezzuto. 1997). It is certain that more natural product drugs, some of which should be useful for the treatment of humans, remain to be discovered. Moreover, for the commercial procurement of structurally complex natural product drugs, isolation from plant material may be most practical. There are many well known anticancer drugs which were developed from natural products (see Table 1-3). For instance, paclitaxel is now the first drug of choice in several cancers including breast cancer. Vinblastine is the first drug of choice in many forms of leukemia and since the 1950s it has increased the survival rate of childhood leukemias by 80% (Kong *et al.*, 2003).

Besides those compounds with unusual structure and very high cytotoxicity recognized as anticancer agents, a variety of polyphenolic compounds of plant origin are known to inhibit cancer (Yang *et al.*, 2001). These compounds are relatively less cytotoxic and may affect cancer progression as a result of their effects on cell cycle progression, growth, differentiation as well as their antioxidant, apoptotic and antiangiogenic effects.

The antioxidant activities of polyphenols are well recognized and may be responsible for various health benefits. Free radicals are produced by pollutants in our food, water and air; oxidation-reduction reactions of lipids and metal ions; and continuous mitochondrial electron transport reactions in the body (Liu *et al.*, 2002). Catechins in green and black tea and red wine can deactivate these aggressive superoxide, alkyl and hydroxyl free radicals by providing an electron, thereby preventing attack on DNA and other cell components (Brownson *et al.*, 2002). The radicals produce free radical chain reactions, which leads potentially to heart disease, stroke, memory loss and cancer. In one step, catechins help subvert these health problems by converting damaging free radicals to inactive compounds while themselves becoming low-energy harmless catechin free radicals. In addition to being powerful antioxidants, catechins such as epigallocatechin gallate (EGCG) in green tea absorb ultraviolet light in the 280–320nm range, preventing the promotion of photoinduced skin cancer. EGCG also has substantial inhibitory effects against a wide variety of tumours *in vivo* and against cancer cell lines *in vitro* (Kavanagh *et al.*, 2001; Yang *et al.*, 2001a).

Compounds	Drug name	Source	Cancer use	Mode of Action	Arrested cell cycle
Doxorubicin	Adriamycin® Rubex®	*Streptomyces peucetius* var. *caesius* (Microbe)	Lymphoma, breast, ovary, lung and sarcomas	Topoisomerase II inhibition and DNA-binding	G_2/M phase
Etoposide	Etopophos® VePesid®	*Podophyllum peltatum* (Plant)	Testicular and small cell lung cancer	Topoisomerase II inhibition	S and G_2/M phases
Mitomycin C	Mutamycin®	*Streptomyces lavendulae* (Microbe)	Gastric, colorectal, anal and lung cancer	DNA alkylation and cross-linking	Non-specific
Paclitaxel	Taxol®	*Taxus brevifolia* (Plant)	Overy, breast, lung, bladder, and head and neck cancer	Microtubule stabilisation	G_2/M phase
Topotecan	Hycamtin®	*Camptotheca acuminata* (Plant)	Ovarian, lung and paediatric cancer	Topoisomerase I inhibition	S and G_2/M phases
Vinblastine	Velban® Velbe®	*Catharanthus roseus* (Plant)	Bladder, kidney, lung, leukemia prostate and germ-cell ovarian cancer	Microtubule assembly inhibition	M phase
Vincristine	Oncovin® Vincrex®	*Catharanthus roseus* (Plant)	Leukemia, lymphoma, neuroblastoma and rhabdomyosarcoma	Microtubule assembly inhibition	M phase

Table 1-3: Summary of anticancer agents derived from natural products (Mao *et al.*, 1999; Yun *et al.*, 2005; Tolis *et al.*, 1999; da Rocha *et al.*, 2001; Anonymous, 2006c; Potter *et al.*, 2002; Zhu *et al.*, 2005; Endresen *et al.*, 1995; Wang *et al.*, 2000 and Manca *et al.*, 1990)

Some isoflavones have been shown to exert antiproliferative effects on cancer cells by steroid receptor signalling (Thelen *et al.*, 2005). Some of these compounds have oestrogenic (or antioestrogenic) activity and are commonly referred to as phyto-oestrogens. Progression from latent stages into clinically significant cancer is a process that generally requires several years. During this period of time dietary phytochemical, such as genistein from soy may have chemopreventive effects. which could slow or obviate hormone-dependent cancer development (Denis *et al.*, 1999).

1.7 Traditional Chinese Medicine in anticancer treatment

Ancient China is a source of information about the early medicinal uses of plants. "***Ben Cao Gang Mu***" (Compendium of Materia Medica), a pharmacopoeia of TCM that was actually written in 1578, contained thousands of herbal cures (Kong *et al.*, 2003). The long tradition of herbal medicine continues to the present day in China. As a result, almost 5,000 plants have been used in traditional Chinese medicine (Wakdikar, 2004).

In recently published monographs on anticancer Chinese medicines, more than 400 Traditional Chinese Medicinal (TCM) species were summarized and documented as being associated with anticancer treatment, based on long-term practical experience of the use of TCM for anticancer purposes (Cai *et al.*, 2006). The TCMs selected for the present study have been recorded to be used for anticancer treatment in China (Ji, 1999), but have not been investigated very well for their active components with bioactivity for anticancer purposes.

1.7.1 TCMs Investigated

1.7.1.1 *Dolichos lablab* L.

Dolichos lablab L. is a perennial vine belonging to the Fabaceae. It is widely cultivated in China. In TCM, the white seeds of *Dolichos lablab* L. (see Figure 1-4), so called "***Bai Bian Dou***" (Chinese pin yin name), have been prescribed for stomachic, antidote and antialcoholism purposes (Yoshikawa *et al.*, 1998). It was frequently involved in some complex prescriptions of TCM for treatment of gastric cancer, hepatoma and cervical carcinoma (Ji, 1999).

It was reported that the glycoside mixture obtained from the white seeds of *Dolichos lablab* L. showed potent adjuvant activity (induction of the antibody response against chicken ovalbumin in mice) (Oda *et al.*, 2000). In continuing studies, several saponin constituents, such as lablabosides A ~ C (**1** ~ **3**) have been isolated from the glycosidic fraction with the adjuvant activity (Yoshikawa *et al.*, 1998). Chikusetsusaponin IVa (**4**) and lablabsaponin I (**5**) were also isolated from the seeds. Moreover, lablabsaponin I (**5**) exhibited strong superoxide dismutase-like activity on the hypoxanthine-XOD system (Yoshiki *et al.*, 1995).

Figure 1-4: Seed of *Dolichos lablab* L.

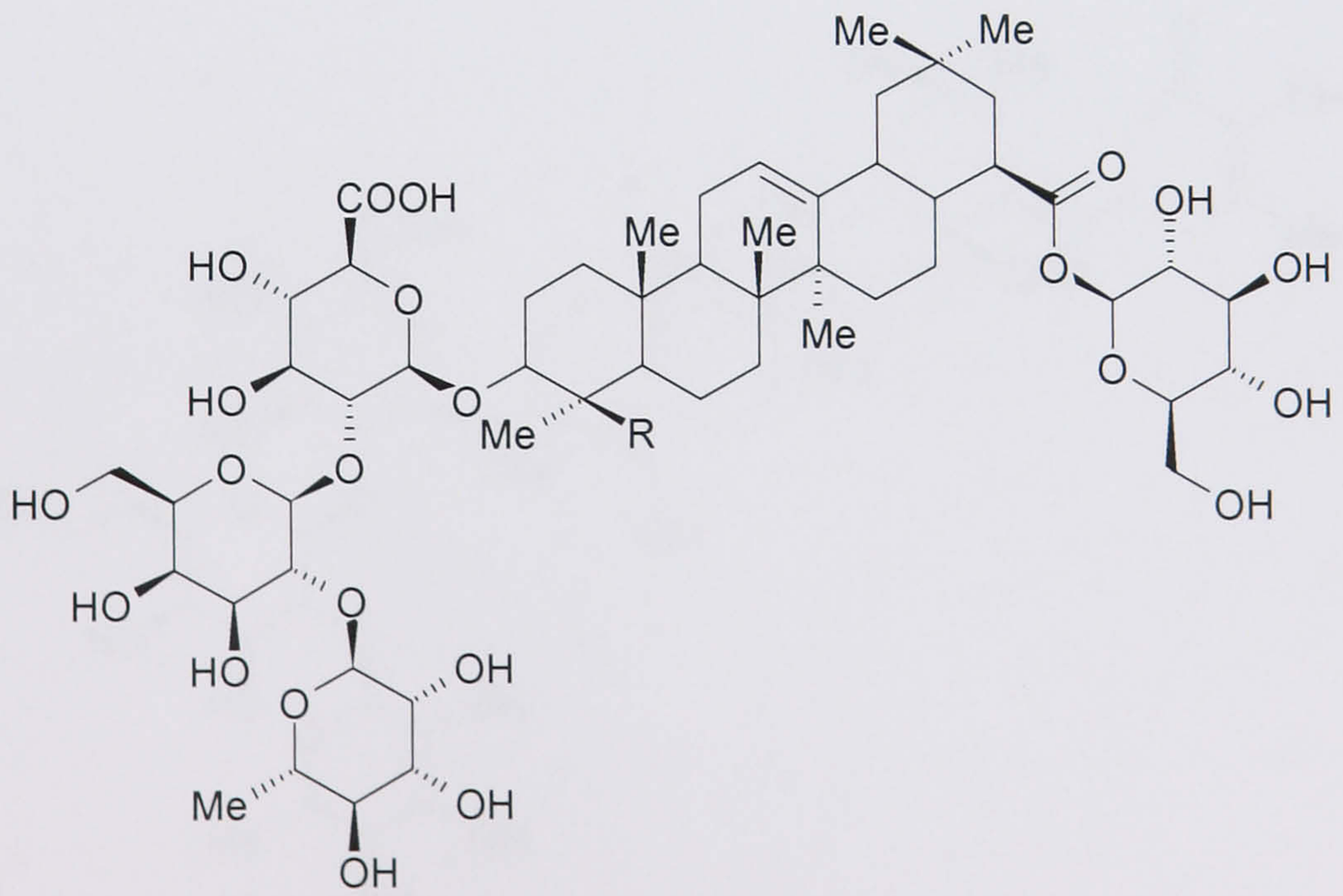

1: R = Me
2: R = CH_2OH

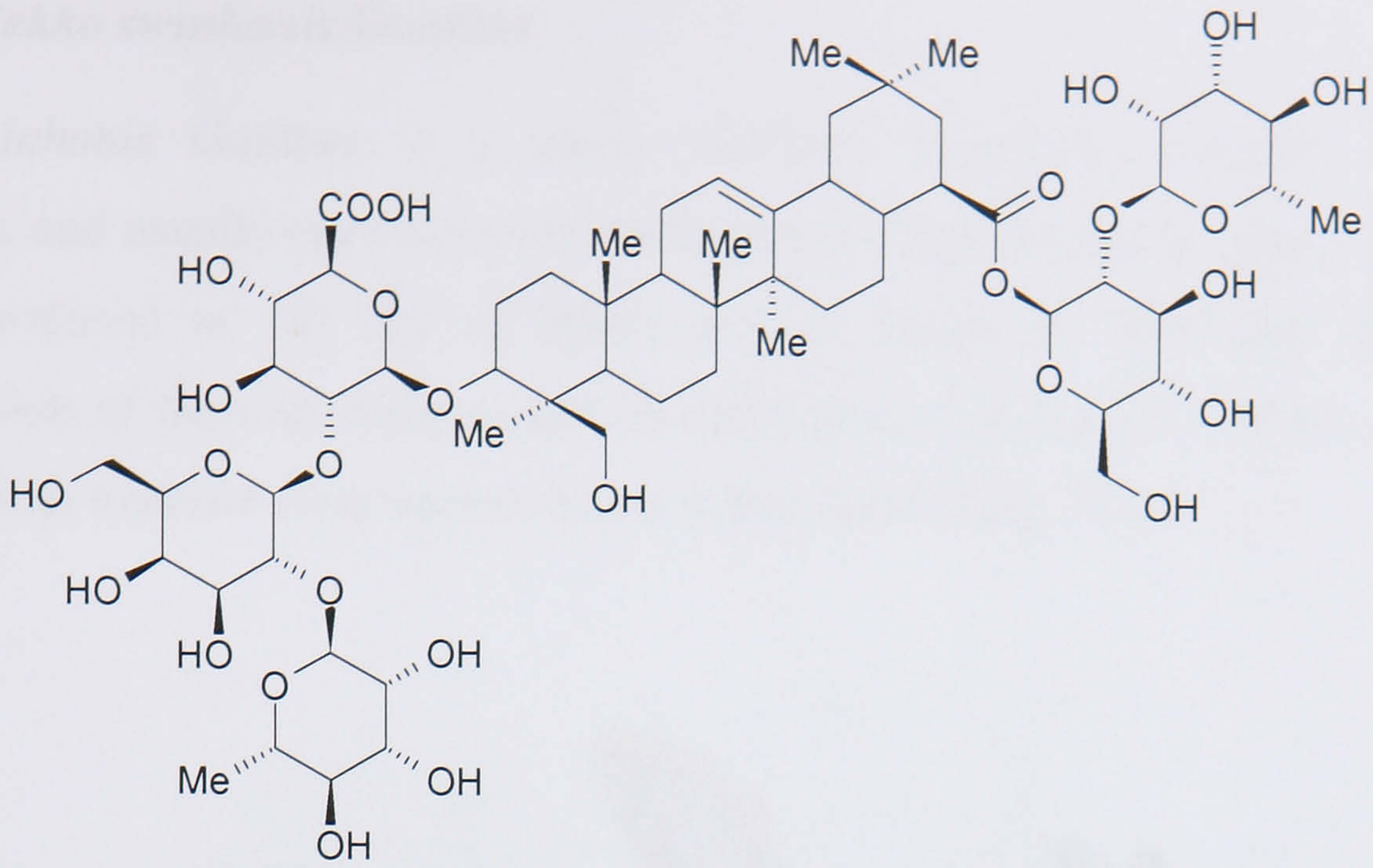
Me
Me
OH
HO
OH
O
O
Me
COOH
HO
O
Me
Me
Me
O
HO
O
Me
OH
O
O
OH
O
OH
OH
HO
O
HO
O
HO
O
OH
Me
OH
OH

3

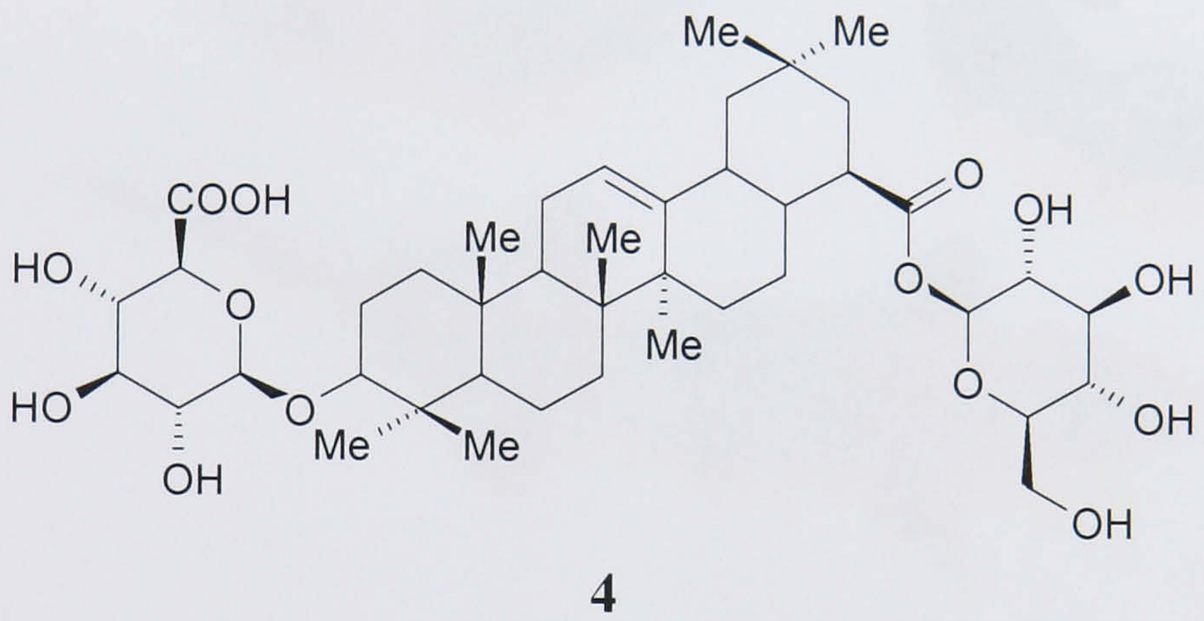
Me
Me
COOH
HO
O
Me
Me
O
OH
OH
HO
O
Me
Me
Me
O
OH
OH
HO
O
OH
OH

4

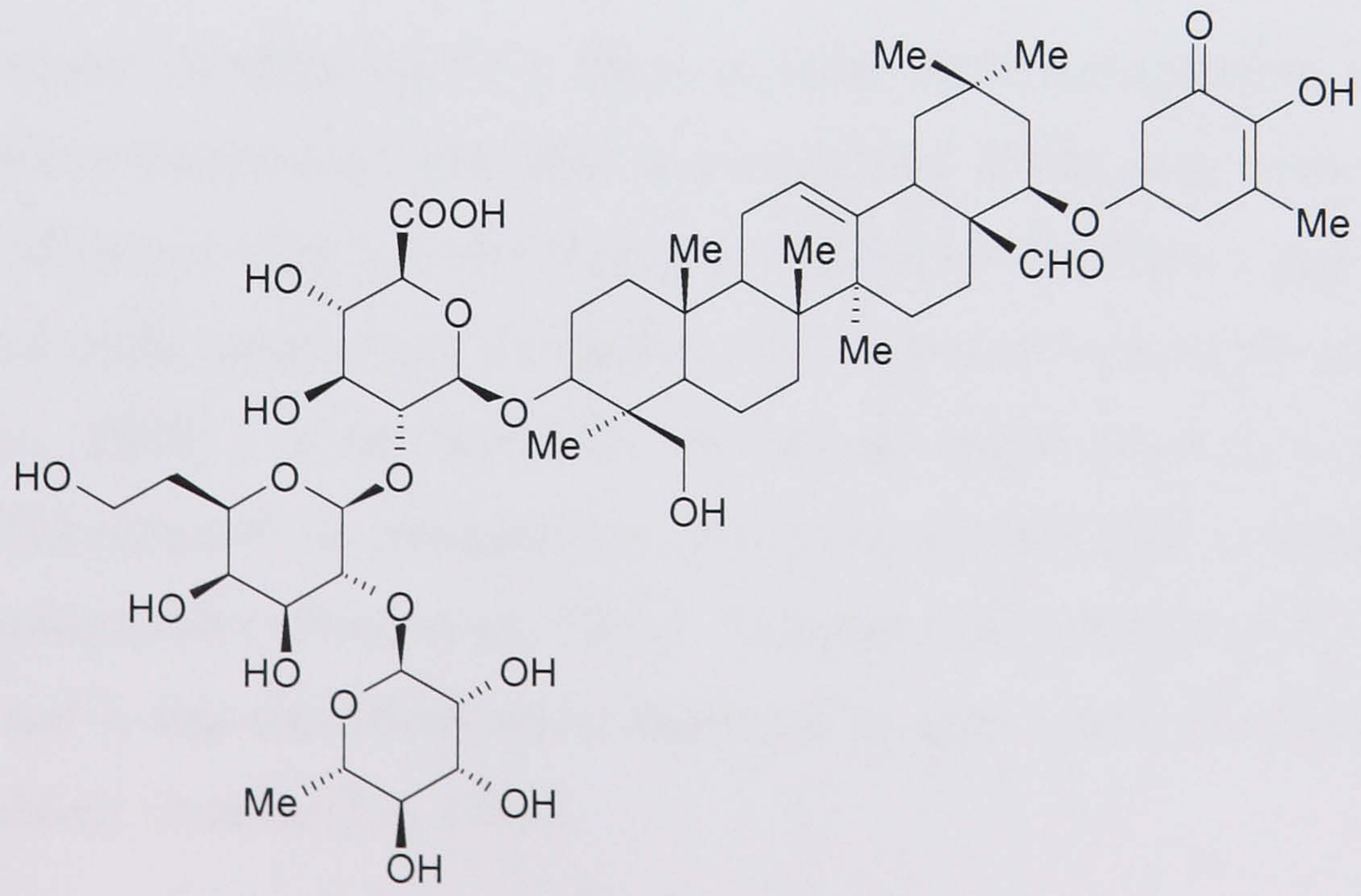
Me
Me
O
OH
Me
COOH
HO
O
Me
Me
Me
CHO
O
HO
O
Me
HO
O
O
OH
O
OH
HO
O
HO
O
OH
Me
OH
OH

5

1.7.1.2 *Gekko swinhonis* Gunther

Gekko swinhonis Gunther is a small vertebrate frequently adapted to human habitations, and usually crawls around walls and ceilings at night in search of insects. It was introduced as "***Bi Hu***" (Chinese pin yin name) in "***Ben Cao Gang Mu***" (Compendium of Materia Medica) and its dried body (see Figure 1-5) has been used as a medicinal material from ancient times (Chen and Huang, 2001).

Figure 1-5: Dry body of *Gekko swinhonis* Gunther as used as raw medicine

Gekko swinhonis Gunther has been listed in some TCM prescriptions used to treat arthritis, carious osteitis and carbuncle. In recent years, it was commonly used to treat many kind of cancer, such as nasopharyngeal carcinoma, lymphoma and lung cancer. Most clinical trials reported are treatments against gastric carcinoma and hepatoma (Chen *et al.*, 1988). More than 28% of patients were cured in a clinical trial (involving 118 patients) for two complex prescriptions with *Gekko swinhonis* Gunther as the major ingredient (Song *et al.*, 1996). To some extent, the lives of patients were prolonged and living conditions were improved in most cases of cancer treated by *Gekko swinhonis* Gunther (Lu, 1985).

1.7.1.3 *Illicium verum* Hook. *f*

Star anise (see Figure 1-6) is the fruit of *Illicium verum* Hook. *f*, which is an evergreen tree belonging to the Illiciaceae. It is an important spice and a well known TCM used in the treatment of stomach ache (Nakamura *et al.*, 1996). However, it is easily confused with the extremely poisonous *Illicium anisatum*, containing anisatin (**6**).

Figure 1-6: Fruit of *Illicium verum* Hook. *f*

Star anise (the fruit of *Illicium verum*), known as "***Ba Jiao***" in TCM, has been shown to possess potent antimicrobial properties effectively against bacteria, yeast and fungal strains (De *et al.*, 2002). Further investigation suggested that a major portion of this antimicrobial property is due to anethole (**7**) present in the dried fruit. It is one of the major components of the fruit and accounting for 76% of the extracted volatile oil (Yan *et al.*, 2002). The butanol extract of star anise showed inhibitory activity (IG_{50}=44μg/ml) on the tube-like formation induced by human umbilical venous endothelial cells in the *in-vitro* angiogenesis assay (Nam *et al.*, 2003). That might contribute to its anticancer action. Other compounds isolated from *Illicium verum* include 1-(4'-methoxyphenyl)-1,2-propanediol (**8**), veranisatin A ~ C (**9, 10** and **11**), verimol C (**12**), verimol D (**13**), verimol F (**14**) and verimol K (**15**) (Sy and Brown, 1998). It was reported that veranisatins caused convulsions and showed lethal toxicity in mice at a dose of 3mg/kg. They caused hypothermia at lower doses (Nakamura *et al.*, 1996).

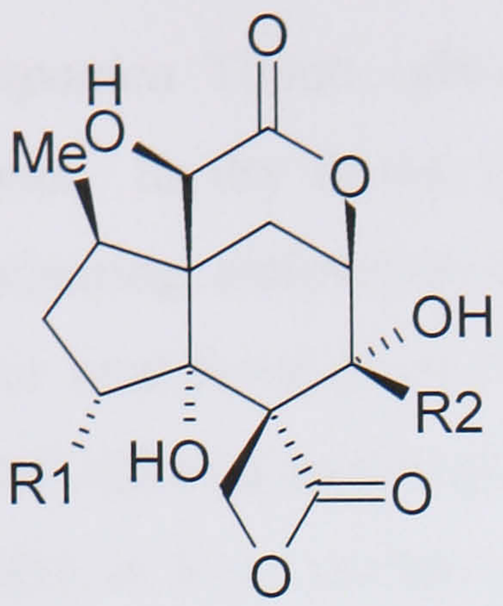

	R1	R2
6:	OH	Me
9:	H	CH_2OMe
10:	H	COOMe
11:	OH	COOMe

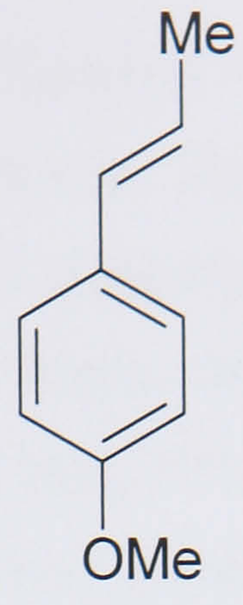

7

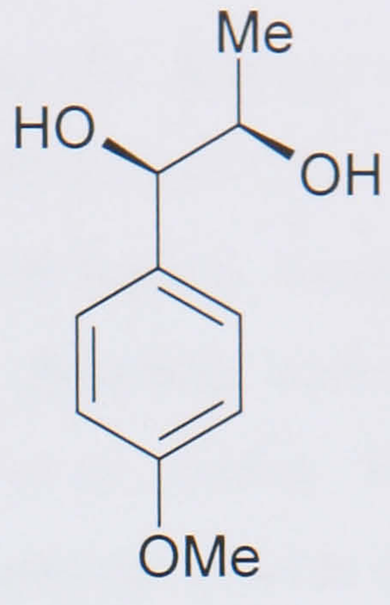

8

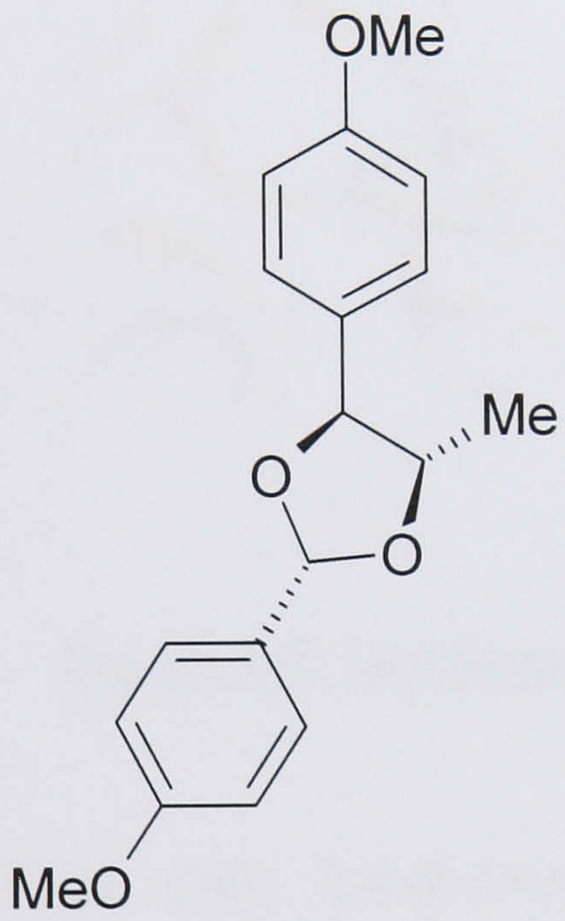

12

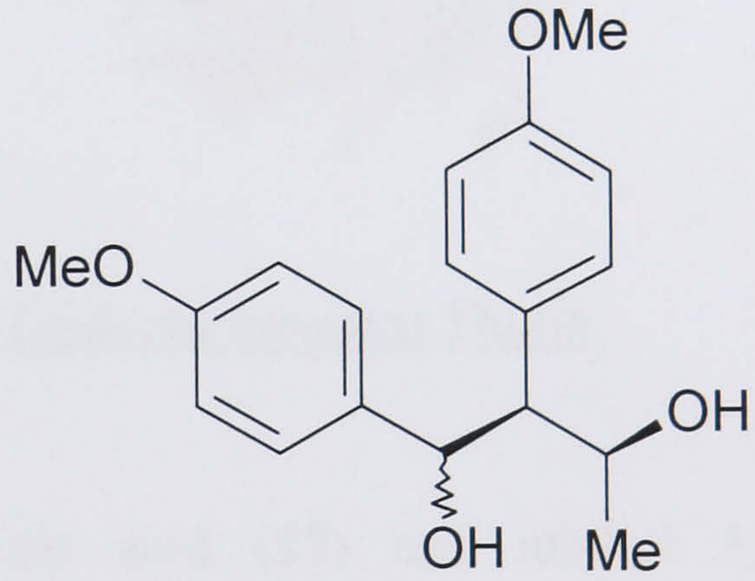

13

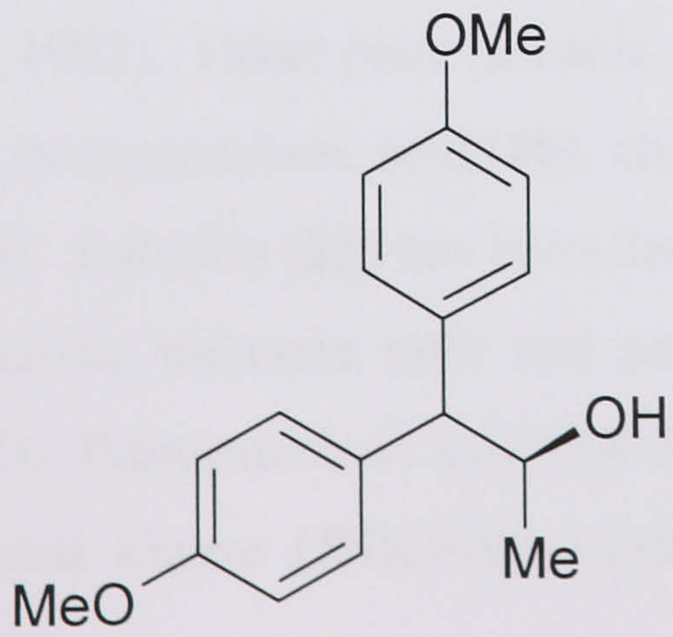

14

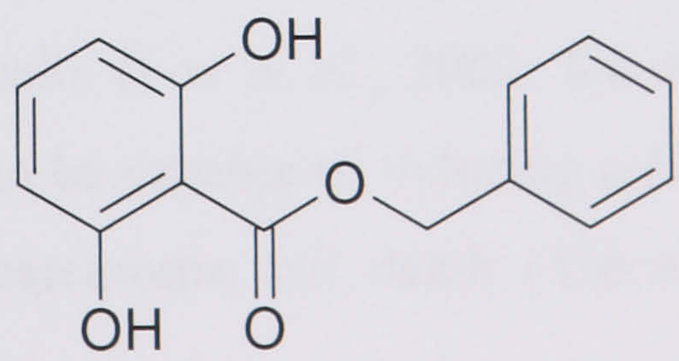

15

1.7.1.4 *Lonicera japonica* Thunb.

Lonicera japonica Thunb., also known as Japanese honeysuckle, belongs to the Caprifoliaceae. Its dry flower buds are known as "***Jin Yin Hua***" in TCM. It has latent-heat-clearing, antipyretic, detoxicant and anti-inflammatory actions, therefore is prescribed to treat fever caused by common febrile diseases, dysentery, carbuncles, furuncles and infected swellings (Chang and Hsu, 1992; Lee *et al.*, 1998). It is an important herb in many complex prescriptions of TCM for treatment of skin cancer, nasopharyngeal carcinoma and rectal cancer (Ji, 1999).

Figure 1-7: Dry flower buds of *Lonicera japonica* Thunb.

Methyl caffeate (**16**), 3,4-di-*O*-caffeoylquinic acid (**17**) and methyl 3,4-di-*O*-caffeoylquinate (**18**) are polyphenolic compounds isolated from *Lonicera japonica*. They had exhibited strong inhibitory effect on human platelet aggregation (Chang and Hsu, 1992). Other plant phenols found in *Lonicera japonica* include chlorogenic acid (**19**), protocatechuic acid (**20**), chrysin (**21**), luteolin (**22**) and rutin (**23**) (Kumar *et al.*, 2005). Luteolin (**22**) has been demonstrated to have an effect on various cancers such as human leukemia cells and pancreatic tumour cells (Lee *et al.*, 2002; Ko *et al.*, 2002). Protocatechuic acid (**20**) has been showed to be capable of inducing c-Jun *N*-terminal kinase (JNK)-dependent hepatocellular carcinoma cell death (Yip *et al.*, 2006).

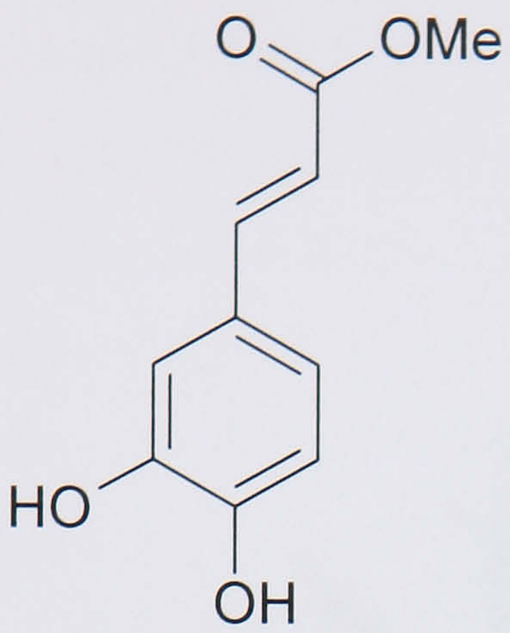

16

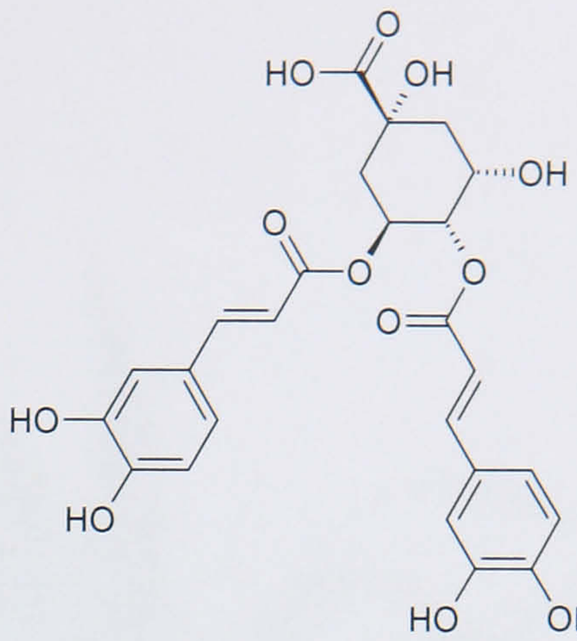

17

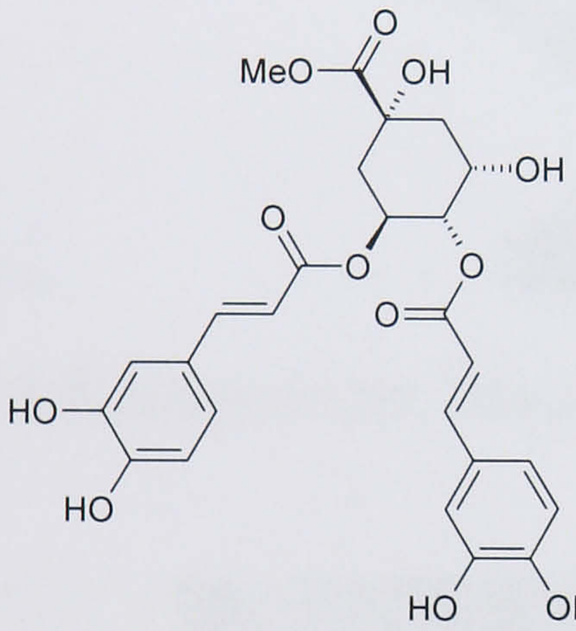

18

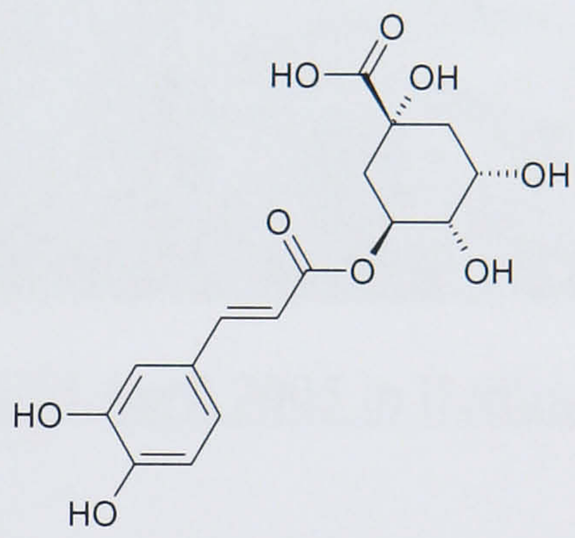

19

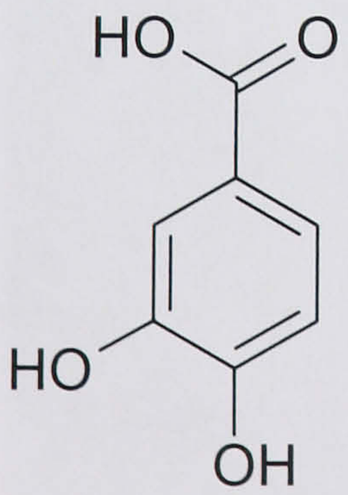

20

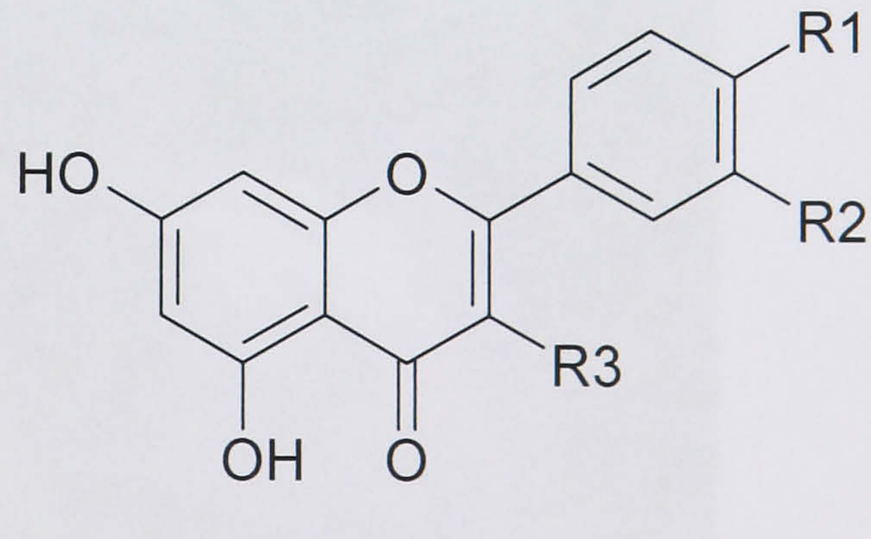

	R1	R2	R3
21	H	H	H
22	OH	OH	H
23	OH	OH	-*O*-Glc-Rha

1.7.1.5 *Iris tectorum* Maxim.

Figure 1-8: *Iris tectorum* Maxim. (blooming on 25 April 2005 in Beijing, China)

Figure 1-9: Flower of *Iris tectorum* Maxim. (blooming on 25 April 2005 in Beijing, China)

Iris tectorum Maxim. belongs to the Iridaceae. It is a perennial herb which is native to China. Its Chinese common name is "蓝蝴蝶", means blue butterfly. It also known as Japanese Roof Iris in some papers, because that is where it was first observed by the Russian botanist, Carl Maximowicz (1827-1891). At that time, Japanese people planted it on straw-thatched roof of houses (Klingaman, 2005). The distinctive characteristic of its flower is the cockscomb-like frill at the outer petal (as shown in Figure 1-9). *Iris tectorum* has yellowish green leaves emerging directly from the ground in basal fans, broadly sword-shaped, curved and have no midrib (see Figure 1-8). Its rhizome is creeping and thick. Generally, it grows 12- to 18-inches tall producing blue flowers in April and May. The favourable environments are forest margins, sunny banks, meadows, damp places and beside water; its distribution altitude is 500–3,500 meters. It is wide spread in China and easily seen in Anhui, Fujian, Gansu, Guangdong, Guangxi, Guizhou, Hainan, Hubei, Hunan, Jiangsu, Jiangxi, Qinghai, Shanxi, Sichuan, Xizang, Yunnan and Zhejiang provinces (Zhao *et al.*, 2000).

The rhizome of *Iris tectorum* (Figure 1-10) was introduced as a medicine in the first Chinese monograph of herbal medicines "***Shen Nong Ben Cao Jing***", which was written about two thousand years ago. Where it was introduced as a bitter medicine to treat some disorders described as "癥瘕积聚" (in ancient Chinese). These syndromes are very similar to the descriptions of tumours in modern medical knowledge. It was also commonly used as an anti-helminthic TCM in China. In recent years, however, this plant is seldom seen in TCM prescription because it is not available in modern TCM shops any longer. Actually, *Iris tectorum* has become a decorative plant in gardens and used to beautify the environment of cities in China.

The idea of exploring the *Iris tectorum*-derived compounds as anticancer drug is rather new. The rhizome of *Iris tectorum* Maxim. has been used as herbal medicine in China for thousands of years, however, it was usually used as a substitution of *Belamcanda chinensis* in some area of China (Xiao *et al.*, 2002). According to the latest edition of Chinese Pharmacopoeia (Anonymous, 2005), it is referred as "***Chuan She Gan***", used to treat sore throat, disperse phlegm, heat-clearing and detoxicating. It was also recorded to treat abdominal distension and hepatic cirrhosis (Song *et al.*, 2001) in China. In Japan it is used as an emetic and a laxative (Seki *et al.*, 1994). A field study and investigation in the present study revealed that the rhizome of *Iris*

tectorum has been used as traditional folk medicine for the treatment of cancer in Tongren, a small town in Guizhou province, South China.

Figure 1-10: Dry rhizome of *Iris tectorum* (cut into pieces) as raw TCM

The major compounds in the root of *Iris tectorum* are tectorigenin (**24**), tectoridin (**25**) and irigenin (**26**) (Wu and Xu, 1992). Other compounds isolated from *Iris tectorum* include the flavonoids, iristectorigenin A (**27**), iristectorigenin B (**28**), iristectorin A (**29**) and iristectorin B (**30**) (Morita *et al.*, 1972), and the terpenoids: iridotectoral A (**31**) and iridotectoral B (**32**), (6*R*, 10*S*, 11*R*)-26-ξ-hydroxy-(13*R*)-oxaspiroirid-16-enal (**33**) and 28-deacetyl-belamcandal (**34**) (Takahashi *et al.*, 2000). Further investigation lead to the isolation of seven triterpene esters, named iristectorenes A ~ G (**35** ~ **41**) (Seki *et al.*, 1994) and eight tetracyclic esters, named iristectorones A ~ H (**42** ~ **49**) (Seki *et al.*, 1994a) from the seed oil of *Iris tectorum*.

28-Deacetybelamcandal (**34**) was isolated from a methanolic extract of the rhizomes of *Iris tectorum* and demonstrated as a tumour-promoting triterpenoid with activation of protein kinase C and induction of TNF-α release from HL-60 cells (human promyelocytic leukemia) (Takahashi *et al.*, 1999).

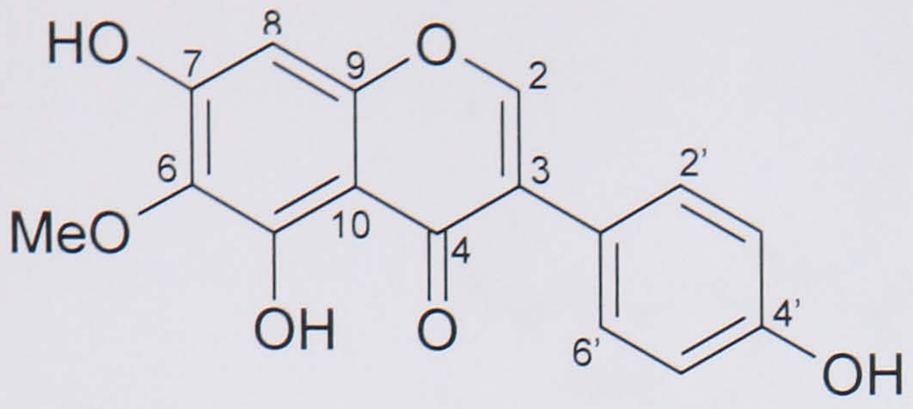

24

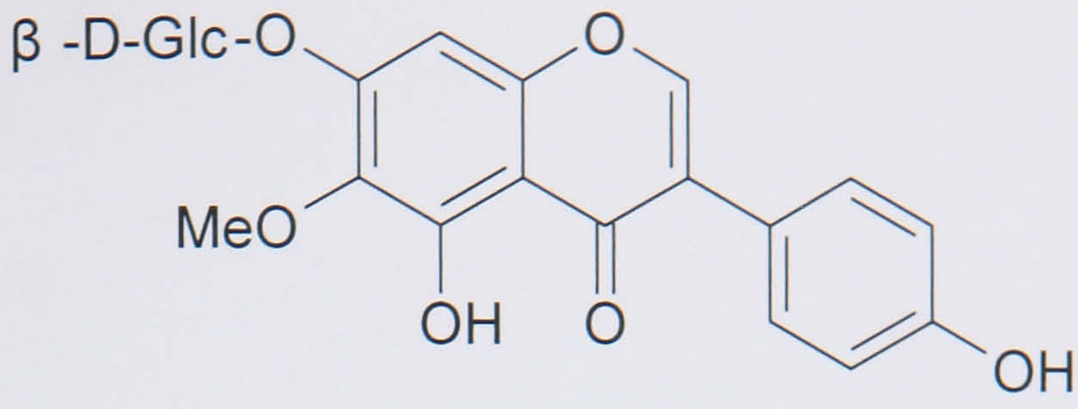

25

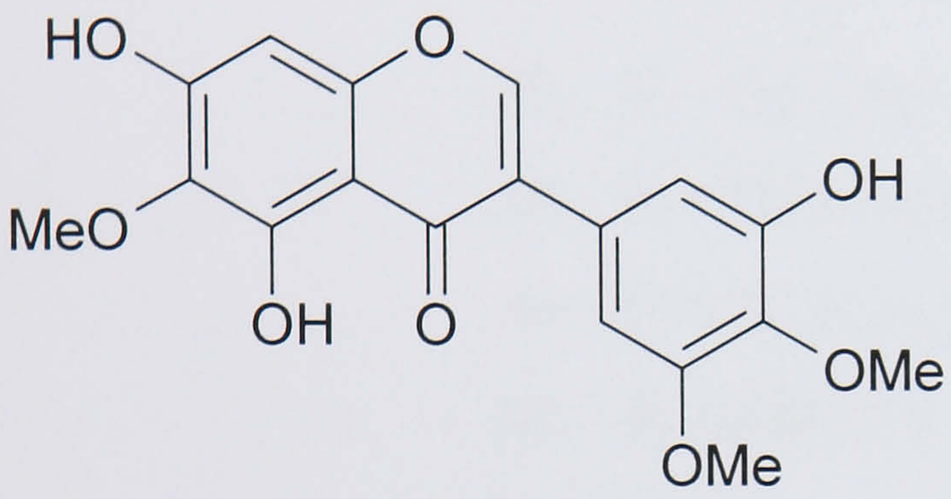

26

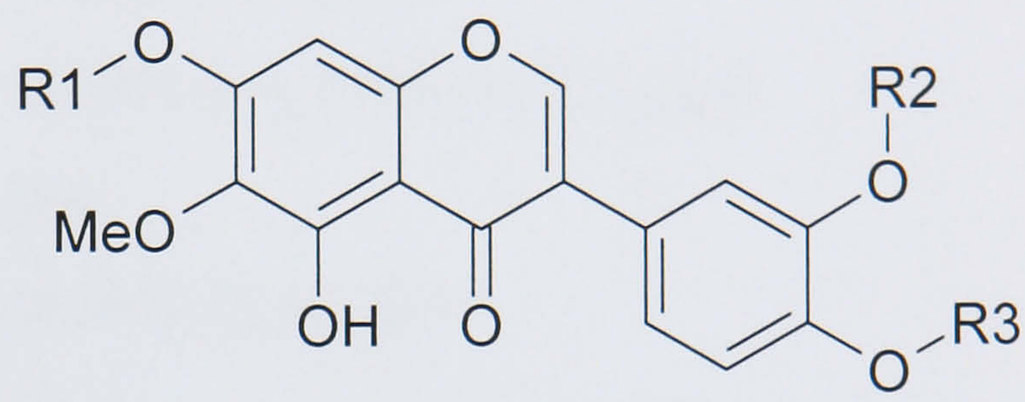

	R1	R2	R3
27:	H	H	Me
28:	H	Me	H
29:	Gl	H	Me
30:	Glc or H	Me	H or Glc

*Glc=glucose

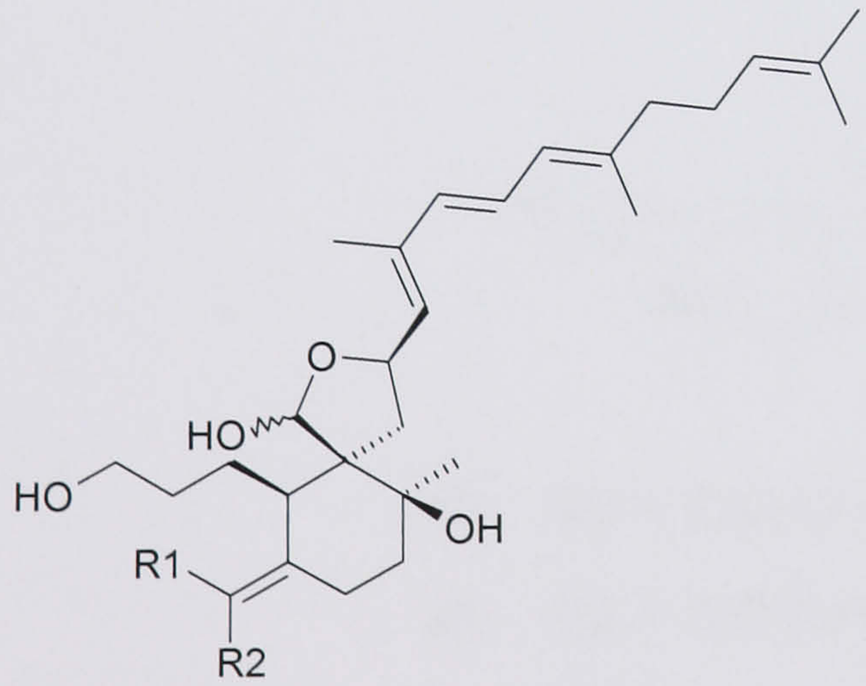

	R1	R2
31:	Me	CHO
33:	CHO	Me

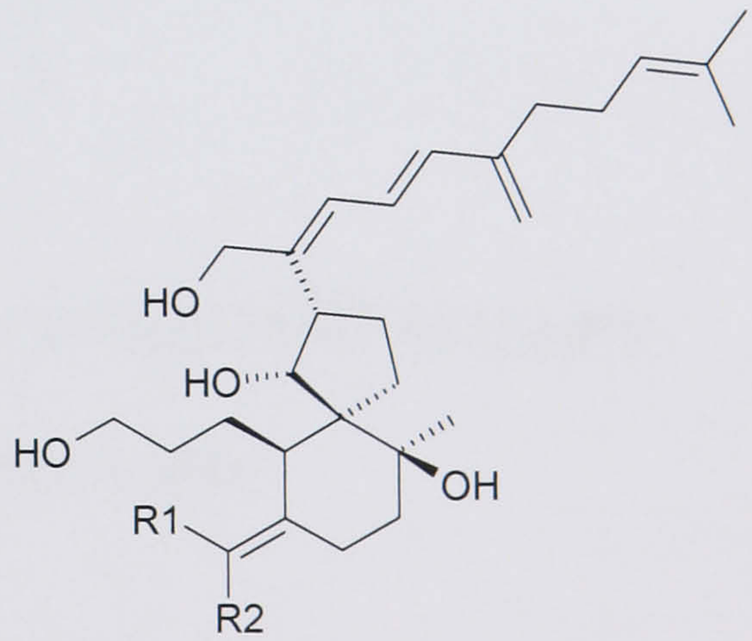

	R1	R2
32:	Me	CHO
34:	CHO	Me

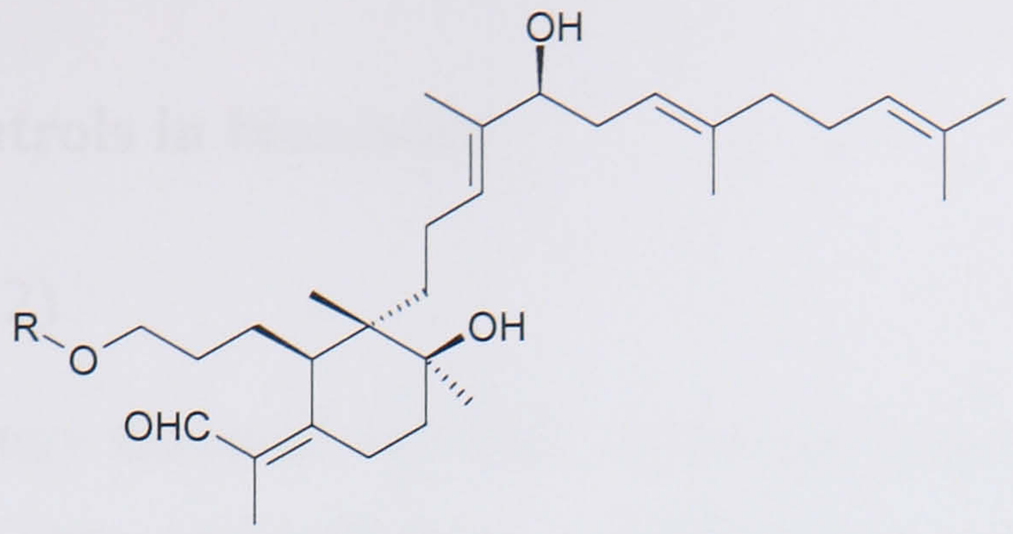

35: R = $CO(CH_2)_7CH^{cis}{=}CH(CH_2)_3Me$

36: R = $CO(CH_2)_{12}Me$

37: R = $CO(CH_2)_9CH^{cis}{=}CH(CH_2)_3Me$

38: R = $CO(CH_2)_7CH^{cis}{=}CHCH_2CH^{cis}{=}CH(CH_2)_4Me$

39: R = $CO(CH_2)_{14}Me$

40: R = $CO(CH_2)_9CH^{cis}{=}CH(CH_2)_5Me$

41: R = $CO(CH_2)_{16}Me$

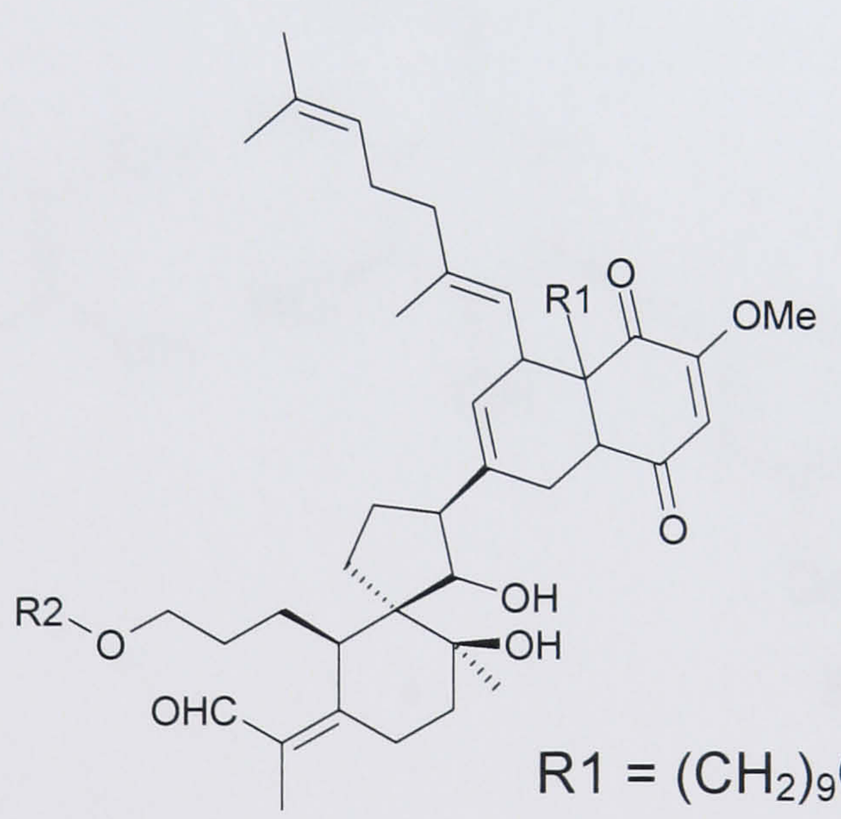

R1 = $(CH_2)_9CH^{cis}{=}CH(CH_2)_3Me$

42: R2 = $CO(CH_2)_7CH^{cis}{=}CH(CH_2)_3Me$

43: R2 = $CO(CH_2)_{12}Me$

44: R2 = $CO(CH_2)_9CH^{cis}{=}CH(CH_2)_3Me$

45: R2 = $CO(CH_2)_7CH^{cis}{=}CHCH_2CH^{cis}{=}CH(CH_2)_4Me$

46: R2 = $CO(CH_2)_{14}Me$

47: R2 = $CO(CH_2)_9CH^{cis}{=}CH(CH_2)_5Me$

48: R2 = $CO(CH_2)_{11}CH^{cis}{=}CH(CH_2)_3Me$

49: R2 = $CO(CH_2)_{16}Me$

1.8 Positive controls in bioassays

1.8.1 Luteolin (22)

Luteolin (**22**), a dietary flavonoid with high antioxidant activity (Lee *et al.*, 1995), commonly found in some medicinal plants, usually occurs as glycosylated forms in celery, green pepper, perilla leaf and camomile tea, *etc*., and as an aglycone in perilla seeds (Ko *et al.*, 2002; Shi *et al.*, 2005). It has been reported to exhibit anti-inflammatory activity (Harris *et al.*, 2006) as well.

Previous research work had demonstrated that luteolin (**22**) inhibited tumour growth and angiogenesis in a murine xenograft model (Bagli *et al.*, 2004). Also, it inhibited vascular endothelial growth factor (VEGF)-induced *in-vivo* angiogenesis in the rabbit corneal assay. Those results might explain the protective action of plant-based diets on the incidence of cancer.

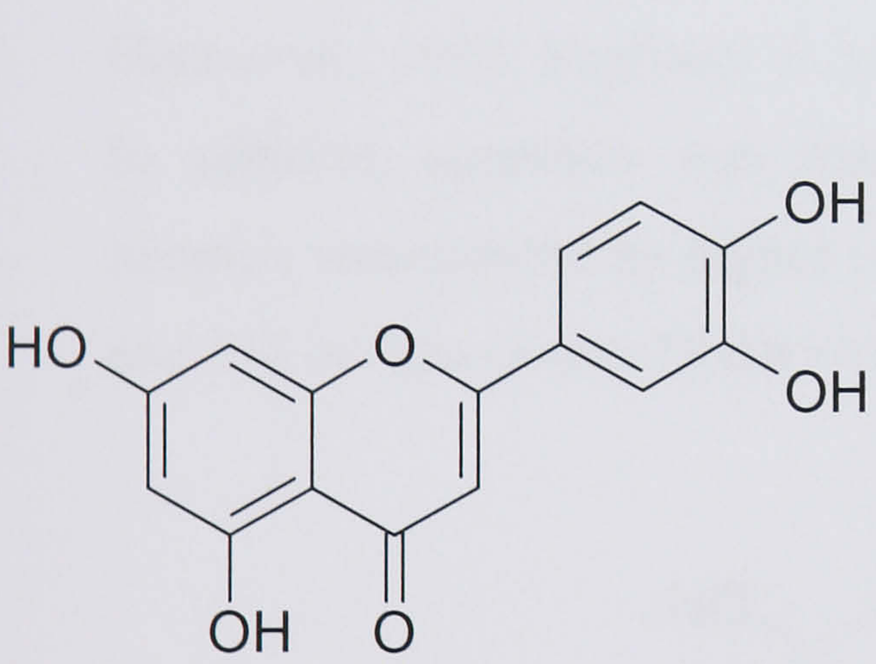

22

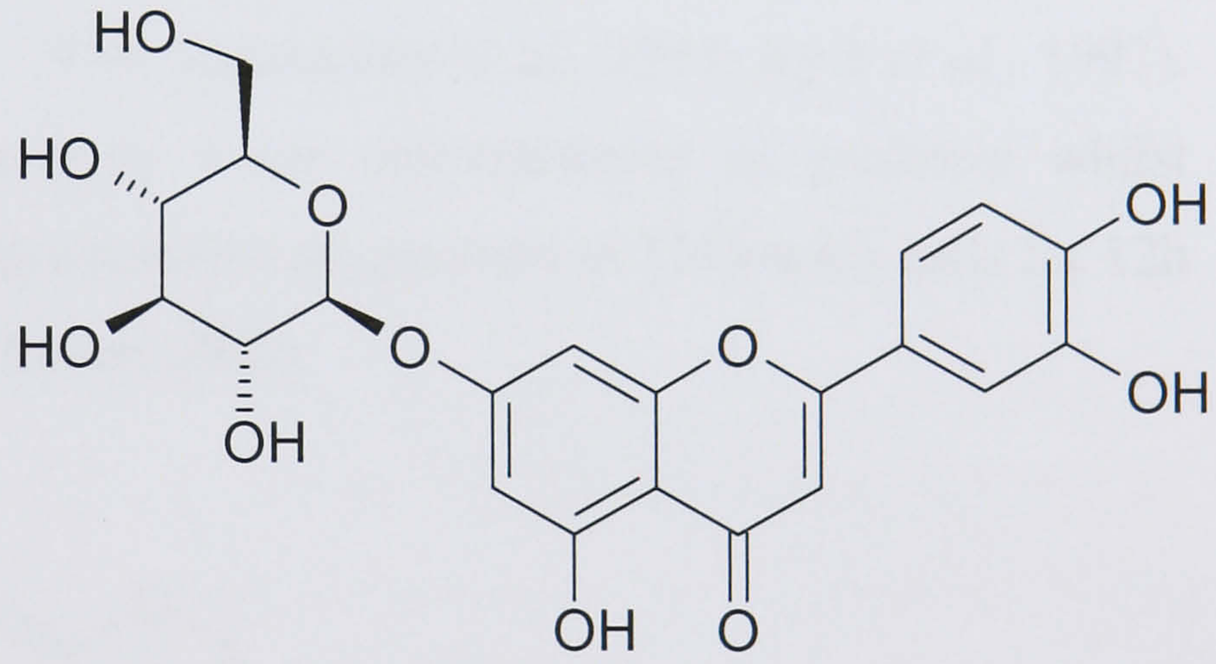

50

Moreover, it has shown inhibition of proliferation as well as apoptotic effect on various cancers such as a human leukaemia cell line and pancreatic tumour cells (Ko *et al.*, 2002; Lee *et al.*, 2002). Several reports suggested that luteolin (**22**) is an inhibitor of topoisomerase I and II (Chowdhury *et al.*, 2002; Webb and Ebeler, 2003). Furthermore, a recent study revealed that the apoptosis induced by luteolin (**22**) is mediated through death receptor 5 (DR5) up-regulation (Horinaka *et al.*, 2005). These results further support its therapeutic potential as a lead anticancer compound. Thereby, luteolin (**22**) was employed as a cytotoxic flavonoid aglycone of luteolin-7-*O*-glucoside (**50**) for the establishment of prodrug assay in the present study.

1.8.2 Genistein (51)

Genistein (4′,5,7-trihydroxyisoflavone) (**51**) was selected as a positive control for apoptosis assays in present study. Genistein (**51**), as a natural product, has been identified as having anti-proliferative and apoptotic effects on various malignant cell types derived from solid tumours (Park *et al.*, 2005; Yu *et al.*, 2004). Epidemiological studies have shown a lower incidence of breast, prostate, and colon cancers in Asian countries, particularly China and Japan, than in the United States. Therefore, it is believed that a diet rich in isoflavonoids may play an important role in cancer prevention (Messina *et al.*, 1994; Markovits *et al.*, 1989). As a isoflavone, genistein (**51**) is believed to be a metabolite of soy produced by the gut floral bacteria (Adlercreutz *et al.*, 1995). Studies of the effects of genistein (**51**) against different types of malignant cells have been carried out in both *in vitro* and *in vivo* experiments (Polkowski and Mazurek, 2000). A number of studies have shown that genistein (**51**) induced cell cycle progression arrest at the G_2/M phase and induced apoptosis in leukaemia, breast, gastric, colon and prostate cancer cell lines (Traganos *et al.*, 1992; Hotz *et al.*, 1992; Pagliacci *et al.*, 1994; Matsukawa *et al.*, 1993; Kyle *et al.*, 1997). In addition, apoptosis was induced by lower concentrations of genistein whilst necrosis was induced by higher concentrations of genistein in TM4 testis cells for 12h and 24h *in vitro* (Kumi-Diaka and Butler, 2000).

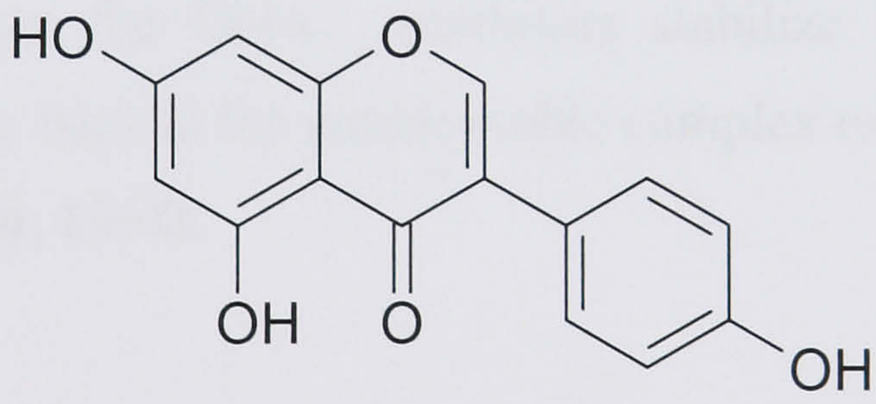

51

1.8.2.1 Tyrosine kinase inhibition effect

The mechanisms of anticancer effects of genistein were also investigated in previous studies. It was suggested to be a potent inhibitor of epidermal growth factor receptor, a tyrosine-specific protein kinase (Akiyama *et al.*, 1987; Linassier *et al.*, 1990; Spinozzi *et al.*, 1994). Epidermal growth factor (EGF) is a key driver for cell growth.

Moreover, tyrosine kinase receptors for EGF has been widely implicated in promoting proliferation and progression of malignant cells including those of the lung, breast, prostate, colon, ovary, head and neck. Consequently, these receptors and their signalling pathways are targets for the development of novel anticancer therapies (Wells, 2000).

1.8.2.2 Topoisomerase II inhibition effect

A multitude of studies revealed that genistein inhibits DNA topoisomerases II *in vitro* (Markovits *et al.*, 1989; Ding *et al.*, 2001; Salti *et al.*, 2000; McCabe and Orrenius, 1993). A possible mechanism of induction of apoptosis is through either stabilization of DNA topoisomerase II complexes consequently blocking DNA religation or blocking the enzyme's catalytic activity (Beck *et al.*, 2001). Topoisomerase II first interacts with DNA by reversibly forming a noncovalent complex. At this stage no DNA strand breaks have been made and, because abrupt removal of the enzyme would leave no residual damage, this initial complex is termed "noncleavable". The enzyme then cuts both DNA strands, forming a covalent bond between each protein subunit and one of the newly formed 5'-phosphate ends of the DNA. This complex is considered "cleavable", since removal or disruption of the protein would result in a permanent double-strand break. In the absence of inhibitors the cleavable complex is either rapidly converted back to the noncleavable complex or, after accomplishing a topological change by strand passage or rotation, the breaks are resealed and the enzyme dissociates from the DNA. Inhibitors stabilize the cleavable complex, preventing it from going back to the noncleavable complex or from completing strand passage or rotation (Pratt, 1994).

1.8.3 Vinblastine (52)

Vinblastine (**52**) is an alkaloid which was isolated from the periwinkle plant *Catharanthus roseus* (previously known as *Vinca rosea*). Initially, extracts of *Catharanthus roseus* were investigated because it was reputed to be useful in the treatment of diabetes, however, it led to the discovery and isolation of two complex indole alkaloids, vinblastine and vincristine, which have been used in the clinical treatment of a variety of cancers (Noble, 1990). The so called "vinca alkaloids", including vinblastine (**52**), vincristine (**53**), vindesine (**54**) and vinorelbine (**55**) (semisynthetic derivatives of vinblastine) have become clinically useful since the discovery of their antitumour properties in 1958 (Fox, 1991; Zhou and Rahmani, 1992; Curran and Plosker, 2002).

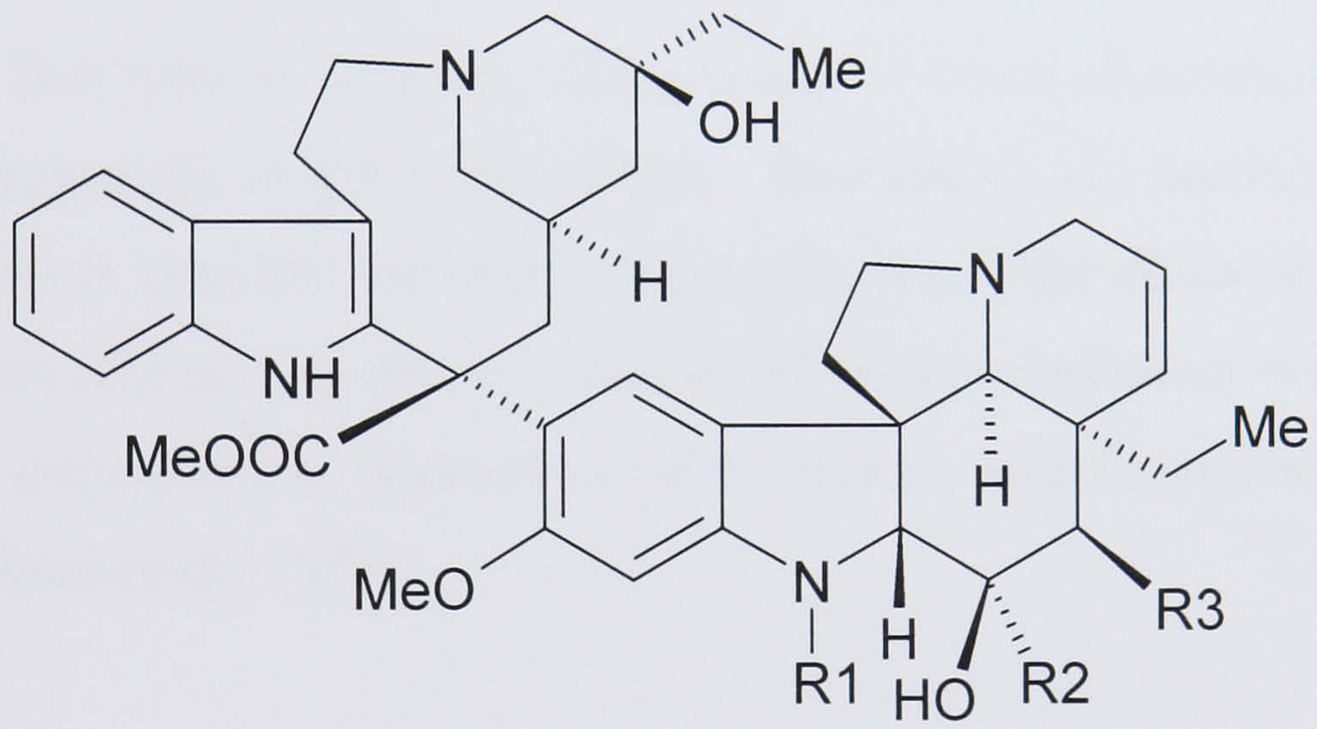

	R1	R2	R3
52:	Me	COOMe	OCOMe
53:	CHO	COOMe	OCOMe
54:	Me	$CONH_2$	OH

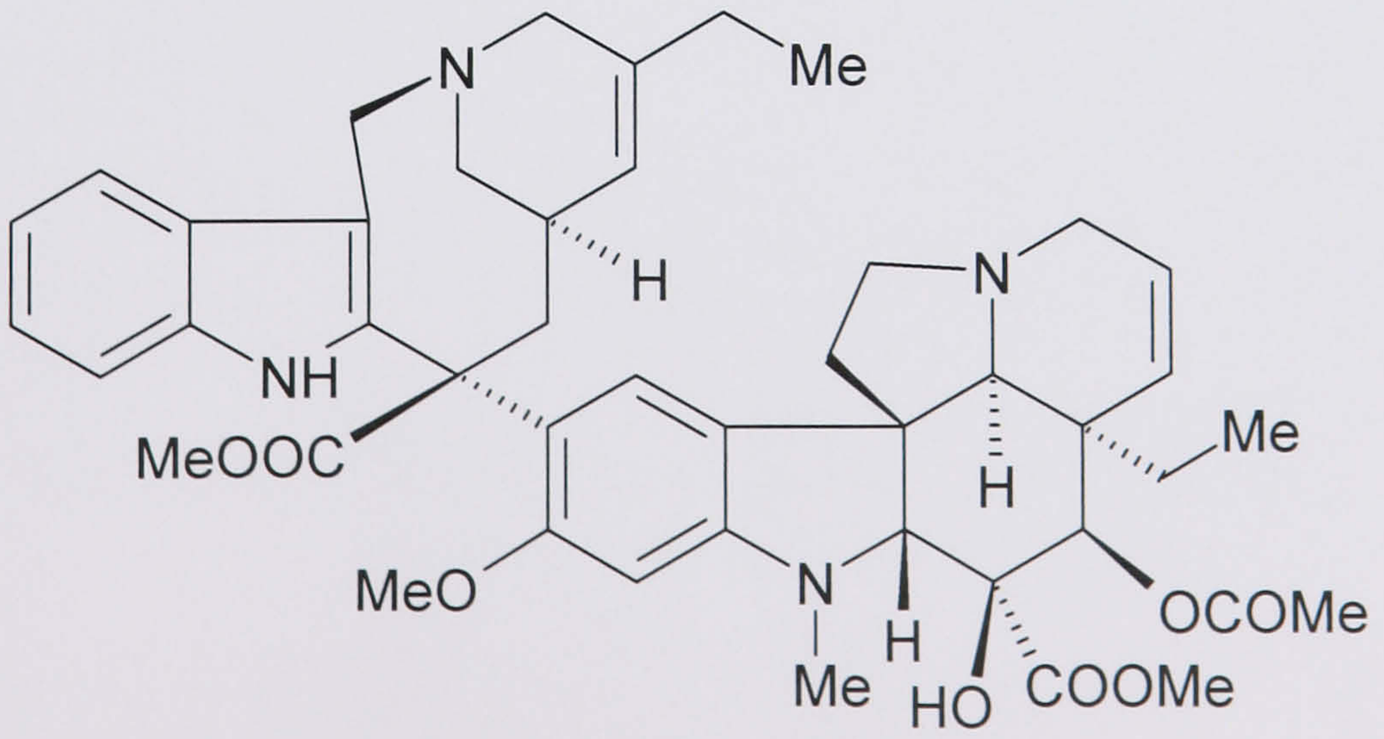

55

Further study revealed that vinblastine (**52**) is a cell cycle-specific agent, which arrests many mammalian cells in metaphase of mitosis by an action on microtubules (Toso *et al.*, 1993). Thus, vinblastine sulphate (**69**) was used as a positive control for *in-vitro* bioassays in present study.

1.8.3.1 Microtubule inhibition effect

The central function of mitosis is to segregate the two sets of chromosomes that are present in the cell after S phase. Chromosome segregation is carried out by the mitotic spindle, which pulls the sister chromatids apart and moves a complete set of chromosomes to each pole of the cell, where they are packaged into daughter nuclei. The mitotic spindle is based on a bipolar array of microtubules, which are highly dynamic polymers that continuously grow and shrink, the major component of microtubules is tubulin (Jordan, 2002; Scholey *et al.*, 2003). Vinca alkaloids bind specifically to free tubulin dimmers. Once bound to Vinca alkaloids, tubulin dimers are unable to aggregate to form microtubles. This effectively decreases the pool of free tubulin dimers available for microtubule assembly. The effect of disrupting the balance between microtubule polymerization and depolymerization results in the net dissolution of microtubules, destruction of the mitotic spindle and arrest of cell in metaphase (Wilson *et al.*, 1975).

CHAPTER 2
PHYTOCHEMICAL INVESTIGATION

2.1 General techniques and materials

The TCM samples: *Dolichos lablab* L., *Gekko swinhonis* Gunther and *Lonicera japonica* Thunb. were obtained from Tong Ren Tang herbal shop in Beijing. *Illicium verum* Hook. *f* was kindly donated by Natural Product Research group in Royal Botanic Gardens, Kew. *Iris tectorum* Maxim. was obtained from a local herbal shop in Tongren (a town in Guizhou province, China). All TCM samples were authenticated by staff in Royal Botanic Gardens, Kew. Reference samples are deposited in the collection of the Pharmacy Department, King's College London. The record of vouchers is summarized in Table 2-1.

A limited amount of the TCMs were firstly extracted with four solvents (hexane, $CHCl_3$, MeOH and water) in a Soxhlet apparatus, each extract was obtained by ten-cycle extraction (see Figure 2-1). Afterwards, the crude extracts were subject to primary screening for inhibition against cancer cells. All solvents were from BDH Supplies, UK, and chemicals and medium were from Sigma-Aldrich, UK, unless otherwise indicated.

Plant name	Date	Part used	Voucher No.
Dolichos lablab L.	Jan. 2003	Seed	DO21-K1
Gekko swinhonis Gunther	Jan. 2003	Dry body	GE101-E1
Iris tectorum Maxim.	July 2004	Rhizome	TCMK 598*
Illicium verum Hook. *f*	Dec. 2002	Fruit	IL22-L9
Lonicera japonica Thunb.	Jan. 2003	Flower bud	LO41-J1

Table 2-1: Voucher record of TCM materials used in the present study (* Voucher No. of *Iris tectorum* Maxim. reserved in the Kew Herbarium.)

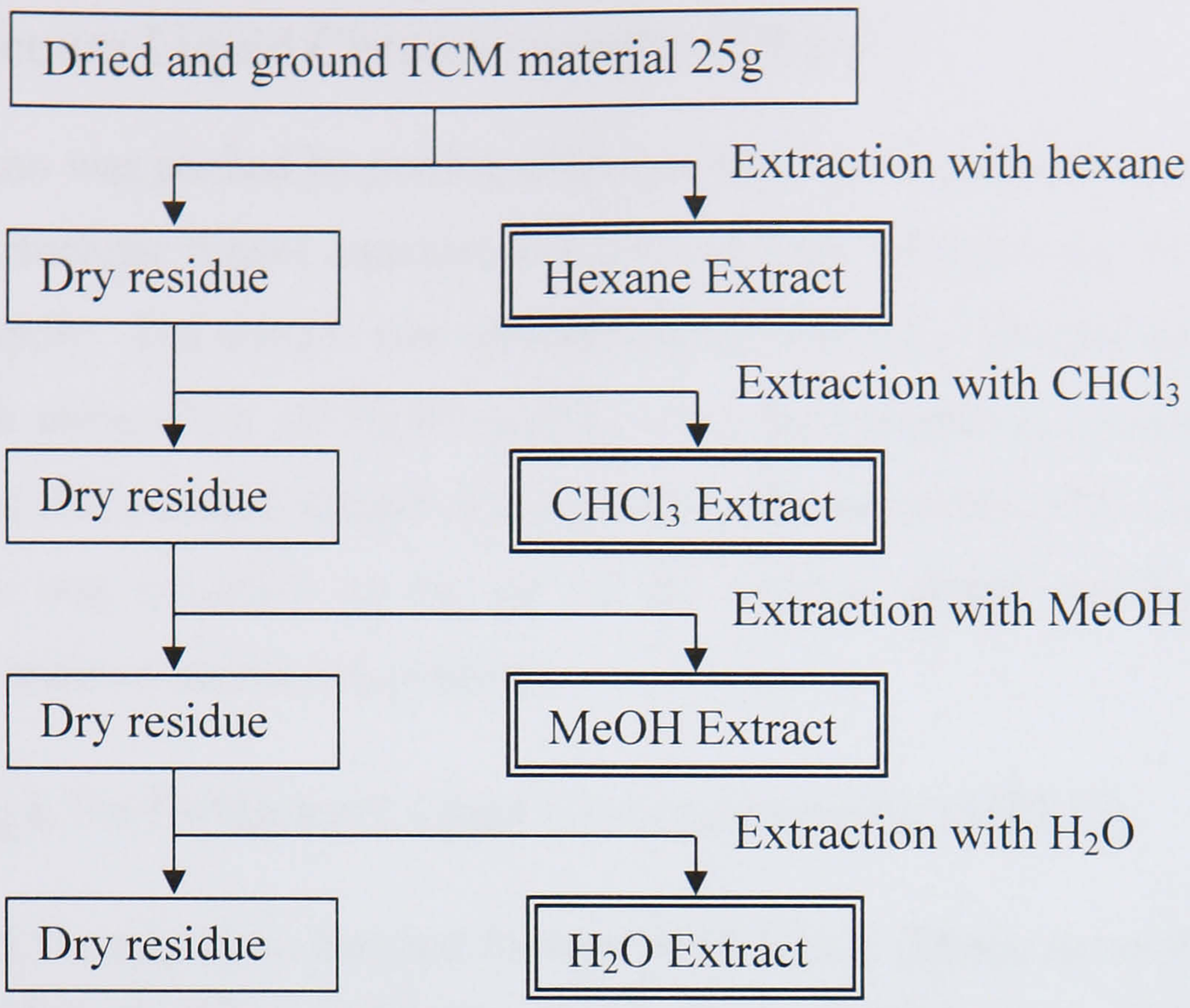

Figure 2-1: Extraction procedure for preliminary screening. (A Soxhlet apparatus was used for all extractions)

2.1.1 Thin-layer Chromatography (TLC)

Analytical TLC:

Pre-coated aluminium backed plates of Silica Gel 60 F_{254} (0.25mm thickness) were obtained from Merck Ltd., Magna Park, UK.

Preparative TLC:

Silica gel 60 PF_{254} (Merck Ltd, Magna Park, UK), 1mm thick, made on glasses (20×20cm), dried at 105°C for 6 hours before use. Zones on the developed TLC plates were observed and marked with a pencil under UV, then scraped off, eluted with solvent, filtered and fractions evaporated to dryness under reduced pressure.

Mobile phases of TLC:

- DS1= $CHCl_3$:EtOAc:MeOH (6:3:1)
- DS2= CH_2Cl_2:EtOH (22:3)

Detection: The zones were detected under UV (at 254nm and 366nm) or by spraying with acidic anisaldehyde reagent (Gibbons and Gray, 1998).

2.1.2 Vacuum Liquid Chromatography (VLC)

VLC column was packed by putting silica gel 60 PF_{254} saturated with the initial eluant, in a glass Buchner funnel attached to a conical flask with the side arm connected to vacuum supply. The sample was reconstituted in a small amount of desirable solvent, mixed with some silica gel 60 PF_{254} (1:1, w/w), then ground in a mortar and allowed to dry. The silica-coated sample was applied to the top of the VLC column, and after the sample was adsorbed on the top of the column, eluant was added in a fixed volume in order of increasing polarity.

2.1.3 High Performance Liquid Chromatography (HPLC)

- HPLC equipment: Hewlett Packard 1090 HPLC (Diode Array detector).
- Analytical HPLC column: ACE® C-18 (particle size 5μm, length×I.D.: 150mm×4mm)
- Semi-Preparative HPLC column: Discovery® HS C18 (particle size 5μm, length×I.D.: 250mm×10mm) obtained from Sigma-Aldrich (Cat. 568533-U).
- HPLC grade solvents (acetonitrile and water) were obtained from Fisher Scientific UK.

2.1.4 Infrared Spectroscopy (IR)

The infrared spectra of isolated compounds were measured with a Perkin Elmer Spectrum One® FT-IR spectrometer with diamond attenuated total reflectance (DATR) technique. It allows collection of good-quality infrared spectra from virtually any solid or liquid sample with almost no sample preparation. In addition, due to the small size of the detection interface on the diamond crystal, the amount of sample required is quite small compared to other infrared spectrometers.

2.1.5 Ultraviolet and circular dichroism spectroscopy

UV/CD spectra of isolated compounds were obtained on a Jasco J720 spectrpolarimeter. Samples were prepared as MeCN solutions, and scanned in a rectangular cell of pathlength 1mm over the region 420 ~ 180nm.

2.1.6 Optical rotation

Perkin-Elmer 141 polarimeter. Sodium D line (589nm) was used for the measurement of optical rotation. Samples were prepared as CH_2Cl_2 solution and detected in a

cylindrical cell of pathlenth 10cm.

2.1.7 Mass spectrometry

Low resolution EIMS was measured on a JEOL JMS-AX505W double Focusing mass spectrometer; low resolution ESIMS was measured on a Waters QToF mass spectrometer and high resolution ESIMS (HRESIMS) were measured on a Bruker Apex III FT, ion cyclotron resonance mass spectrometer in the department of chemistry, King's College London.

2.1.8 NMR spectroscopy

^{1}H and ^{13}C NMR spectra were measured on a Bruker DRX500 (500MHz) NMR spectrometer in $CDCl_3$ or DMSO-d_6 using TMS as internal standard. (500MHz for ^{1}H and 125 MHz for ^{13}C) in the department of chemistry, King's College London.

2.2 Cell culture and cytotoxicity test

Cytotoxicity testing in microplates has been widely used for *in-vitro* anticancer screening. The endpoint can be determined by a variety of colorimetric staining procedures including trypan blue, crystal violet, neutral red and MTT assay. Using these assays, a large number of tests can be carried out in a rapid and automated fashion. Most cell viability tests rely on a breakdown in membrane integrity that is determined by the uptake of a dye to which the cell is normally impermeable (*e.g.*, trypan blue) or the release of a dye normally taken up and retained by viable cells (*e.g.*, neutral red). However, this effect does not always predict ultimate survival (Freshney, 2000). Many of these techniques are labour intensive with long processing time, some are subject to artifacts and sensitive to incubation time, which result in poor reproducibility (Fricker, 1994).

The development of the sulphorhodamine B (SRB) (**56**) protein staining assay for the *in-vitro* measurement of cellular protein content of adherent and suspension cultures was established by Skehan *et al.* in 1990; subsequently it has been adopted for routine use of *in-vitro* antitumour screening in the National Cancer Institute since 1990 (Skehan *et al.*, 1990). Sulphorhodamine B (**56**) is a bright pink aminoxanthene dye with two sulphonic groups. In mildly acidic conditions, it binds to basic amino acids of residues of TCA-fixed proteins. Thus, colorimetric measurement of the bound dye

provides a sensitive index of cell protein that is linear with cell number over a cell density range of more than 100-fold (Monks *et al.*, 1991). Comparing with other protein and biomass stains, it provides the best combination of staining intensity and signal-to-noise ratio in microtitre assays (Skehan *et al.*, 1990). The SRB assay has a number of advantages including better linearity, higher sensitivity, a stable end-point that dose not require time-sensitive measurement and lower cost (Rubinstein *et al.*, 1990). These features make it applicable to large-scale screenings of anticancer drug candidates from natural extracts or synthetic chemicals.

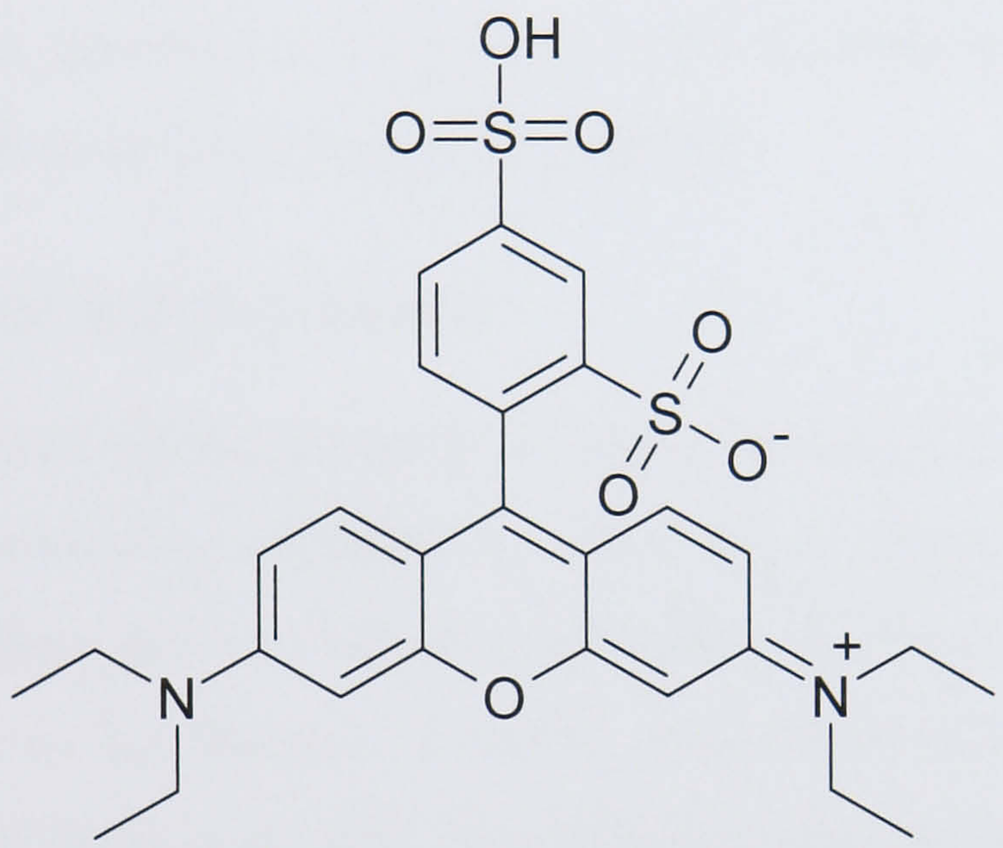

2.2.1 Harvesting cells

1. Cells were incubated in appropriate culture medium at 37°C in 5% CO_2 until 75% confluent.
2. Cells were rinsed with 5ml Ca^{2+}-, Mg^{2+}-free phosphate-buffered saline (PBS) and aspirated.
3. Cells were subjected to incubation with 2ml 0.05% trypsin/0.5mM EDTA for 3 minutes at 37°C.
4. Cell culture flask was tapped on the edge with horizontal force until the cells detached. If necessary, the flask was incubated for an additional 1 min, so allowing the cells to be detached completely.
5. The detached cells were triturated with a 1ml pipette several times to disrupt

cell clumps and produce a single cell suspension.

6. 5ml medium containing 10% foetal bovine serum was added to inactivate the trypsin.
7. The cell suspension was transfered to a 15ml conical tube and centrifuged at 1,500 rpm for 5min, then the cells were resuspended in culture medium or PBS as appropriate.

2.2.2 Seeding density

Seeding density was chosen according to the cell cycle time determined individually for each cell line. For assays over 3 ~ 5 days, 5×10^3 cells per well in 96-well plate is appropriate for all cell lines (as described on page 57).

2.2.3 Preincubation and dissociation

Chemical and enzymatic dissociation are traumatic processes that certainly kill some cells, meanwhile, sensitizing survivors to other toxic insults. As a result, this sensitization can produce false-positive artifacts when cells are subsequently exposed to growth inhibitors or cytotoxins. Thereby, dissociated cells require a recovery period before an experiment is started. Normally, one day preincubation was found to be sufficient (Monks *et al.*, 1991).

2.2.4 Drug solubilization

Stock solutions of polar compounds were made in dimethyl sulphoxide (DMSO), then diluted in total growth medium to appropriate concentration. All stock solutions were sterilized by filtration (0.22μm pore size).

Preliminary experiments determined that the toxicity-threshold concentrations of DMSO for tested cell lines were in the range of 0.5 ~ 1%. 1% DMSO in culture medium can result in up to 10% inhibition of cell proliferation. Thus, the final concentration of DMSO in cell culture experiments was no more than 0.5%.

2.2.5 Cell fixation

Trichloroacetic acid (TCA) was the fixative for SRB assay. It fixes cells instantly, permeabilizes their membranes so allowing rapid penetration of dye, and great strengthening of cell adhesion, and hardening of cells to withstand rough handling

(Skehan, 1999).

2.2.6 Human cell lines

Four cell lines (COR-L23, C32, MCF-7 and MRC-5) used in this project were purchased from the European Collection of Cell Cultures (ECACC). Hepatocellular carcinoma (HepG2) was obtained from American Type Culture Collection (ATCC). 16HBE14o- was kindly donated by Dr Ben Forbes (Department of Pharmacy, King's College London) (see Table 2-2).

All cells cultured with appropriate medium and supplemented with 10% foetal bovine serum (FBS), 1% penicillin (104U/ml)/streptomycin (10mg/ml) and 1% *L*-glutamine (200mM). Biochemical agents were purchased from Sigma-Aldrich unless specified. At about 70-80% confluence, cells were trypsinised to form a cell suspension and counted using a haemocytometer before inoculation. Cells were plated in 96-well plate (Costar, 3359) or 6-well plate (Costar, 3516) at appropriate density which ensured that the cells were in exponential growth (as described in Figure 2-2 and Figure 2-3) and left to attach for 24 hours prior to addition of extract or compound.

Cell lines	Description	ECACC No.	Medium
COR-L23	Human non-small cell lung cancer	92031919	RPMI-1640
C32	Human amelanotic melanoma	87090201	DMEM
HepG2	Hepatocellular carcinoma	HB-8065	EMEM
MCF-7	Human Caucasian breast adenocarcinoma	86012803	EMEM
MRC-5	Human foetal lung fibroblast*	84101801	DMEM
16HBE14o-	Human bronchial epithelial cell line*	—	DMEM

Table 2-2: Six cell lines employed in bioassays (* Normal cell lines)

2.2.7 Doubling time determination

In order to investigate the doubling time (total cell cycle time) for each cell line used in the present project, cells were seeded into 96-well plates over a range from 1×10^3 cells/well to 7×10^3 cells/well and incubated for 5 days (120h). The growth curve of

cells in exponential proliferation is S-shaped when plotted on linear co-ordinates (see Figure 2-2) and linear when plotted on semi-log coordinates (the log of cell number *vs* time on a linear scale as shown in Figure 2-3).

General formula that describes the growth of cells is:

$$A = A_0 2^{T/Tc}$$

Where A is the number of cells at any time, A_0 is the number of cells at an initial point. T is the time elapsed and T_c is the doubling time of the cell. Thus the proliferation formula can be written as (Wieder, 1999):

$$T_c = 0.3T / \log(A/A_0)$$

As shown in Table 2-3, the total cell cycle time is determined between two time points (day 0 and day 5) where the shape of the growth curve on the semi-log plot is a straight line (see Figure 2-3). This exponential part of the growth curve represents the time when, in principle, nearly all of the cells are dividing.

Obviously, the higher seeding density results in a shorter doubling time, which means cells proliferate more quickly to an appropriate density. For example, COR-L23 and HepG2 exhibit doubling time of 150h and 108h, respectively, at the seeding density of 1×10^3 cells/well. However, when they were incubated at 7×10^3 cells/well, their corresponding doubling time dropped down to 41h and 30h respectively (see Table 2-3). As shown in Figure 2-2 and Figure 2-3, cell seeding at 5×10^3 and 7×10^3 cells/well exhibited exponential proliferation, and led to a reasonable cell cycle time (≤48h) for use in the bioassays in the present study. In addition to contact inhibition, cells growing at a high density, exhaust nutrients much more quickly than in moderate density. In addition, the capability of the cell culture plate and the cost of the growing medium and supplements also limit the applicable cell seeding density.

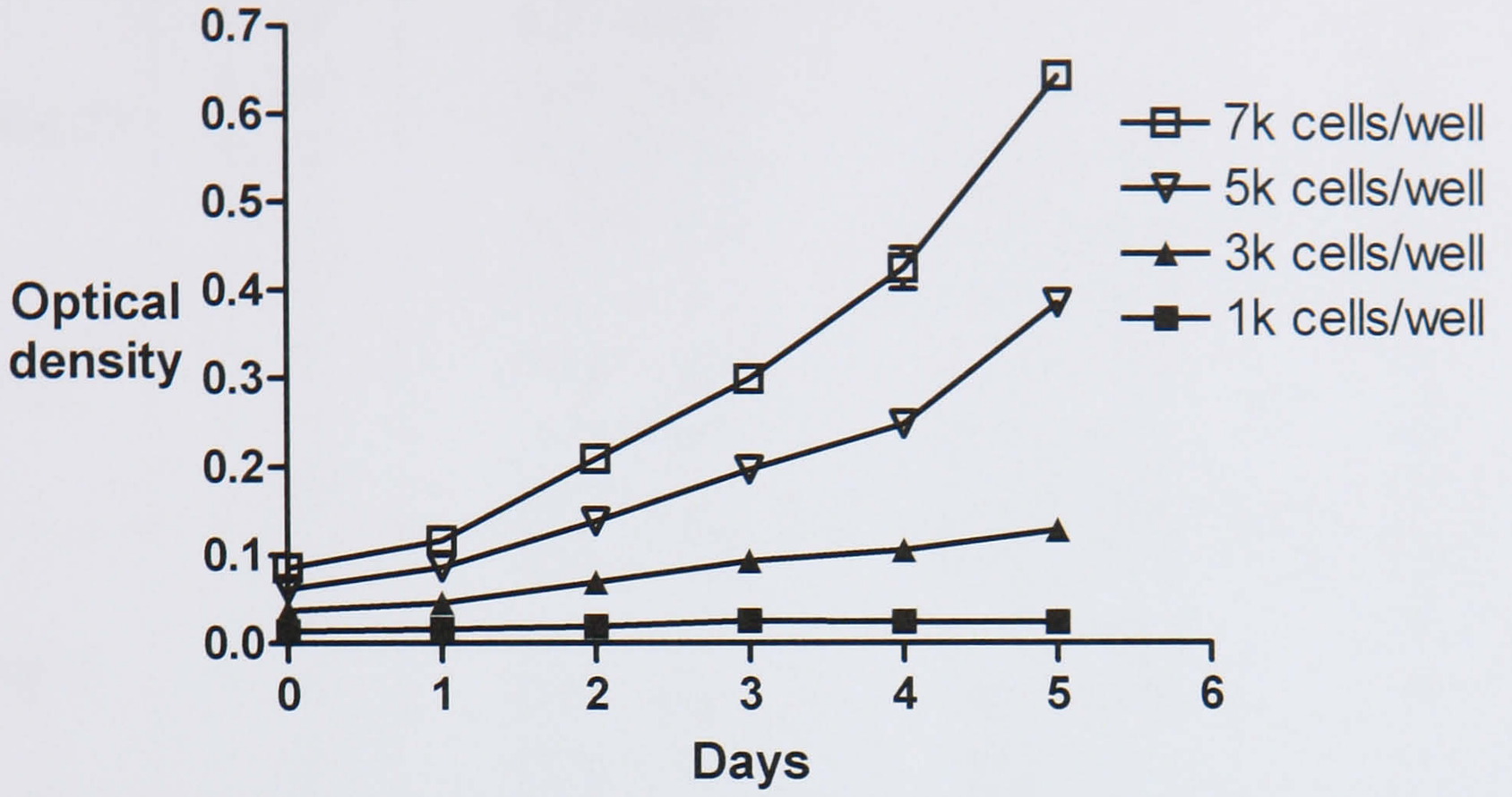

Figure 2-2: Growth curve of COR-L23 cells plotted on linear coordinates (k=×10^3, n=2, mean±SEM)

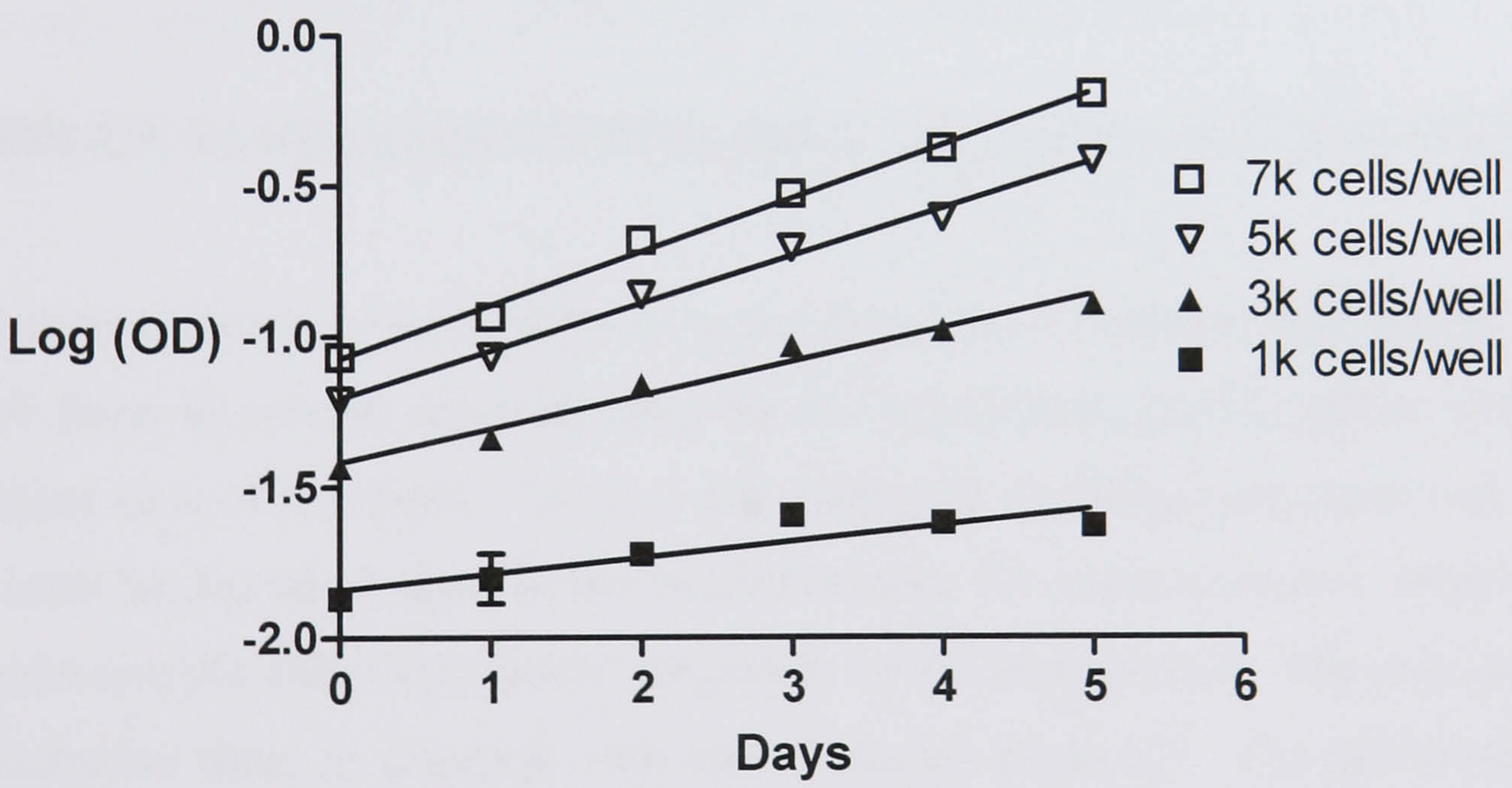

Figure 2-3: Growth curve of COR-L23 cells plotted on semi-log coordinates (k=×10^3, n=2, mean±SEM)

Cell lines	Seeding density	Optical density		Doubling time (hours)
		Day 0	Day 5	
COR-L23	1×10^3	0.01±0.001	0.02±0.002	150
	3×10^3	0.04±0.002	0.13±0.004	66
	5×10^3	0.06±0.001	0.38±0.001	45
	7×10^3	0.09±0.002	0.64±0.000	41
C32	1×10^3	0.02±0.001	0.05±0.001	67
	3×10^3	0.04±0.000	0.21±0.004	51
	5×10^3	0.08±0.005	0.42±0.002	48
	7×10^3	0.08±0.006	0.59±0.020	42
HepG2	1×10^3	0.01±0.001	0.02±0.001	108
	3×10^3	0.03±0.000	0.13±0.012	52
	5×10^3	0.04±0.001	0.49±0.029	34
	7×10^3	0.06±0.003	1.00±0.024	30
MCF-7	1×10^3	0.01±0.002	0.05±0.002	59
	3×10^3	0.03±0.002	0.23±0.008	43
	5×10^3	0.06±0.007	0.54±0.008	38
	7×10^3	0.08±0.003	0.77±0.005	36
MRC-5	1×10^3	0.01±0.001	0.02±0.002	82
	3×10^3	0.02±0.001	0.12±0.003	41
	5×10^3	0.03±0.003	0.26±0.003	36
	7×10^3	0.04±0.001	0.38±0.001	36

Table 2-3: Determination of doubling time of five cell lines (n=2, mean±SEM)

There are two criteria to be considered for the selection of preferred cell density. First, all cell lines in control must be keep in the exponential growth phase over the incubation time of bioassays. On the other hand, the doubling time (total cell cycle time) must be shorter or equal to the incubation time for some bioassays, otherwise a cell cycle-specific effect may not be observed. In the present study, 48h was used for the incubation time, in common with most bioassay protocols. The optimized cell seeding density for all cell lines was thus 5×10^3 cells/well.

2.2.8 Sample preparation

40mg extract sample was dissolved in 1ml of dimethyl sulphoxide (DMSO) and sterilized through a 0.22μm pore size filter, and kept at –20°C as stock solutions of 40mg/ml. On the day of inoculation, the testing solutions were made by dilution of the stocks. Each extract was prepared in 6 concentrations: 200μg/ml, 100μg/ml,

50μg/ml, 10μg/ml, 2μg/ml and 0.4μg/ml. After adding the sample solutions to test plates and mixing with 100μl growth medium per well, the testing concentrations in the wells were thus: 100μg/ml, 50μg/ml, 25μg/ml, 5μg/ml, 1μg/ml and 0.2μg/ml. The final testing concentrations of pure compounds were prepared at molar concentrations (μM or nM).

2.2.9 Sulphorhodamine B assay (protocol)

1. Cells were incubated with the samples for 48h, after which the cells were fixed with ice-cold 40% (w/v) trichloroacetic acid (TCA) for 1 hour at 4°C. Then the plates were washed 5 times in distilled water and allowed to dry in the air.
2. 0.4% (w/v) of SRB (Sigma-Aldrich, S1402) solution was prepared in 1% acetic acid. This pink solution was added to the dry 96-well plates at 50μl/well and allowed to stain at room temperature for 30 minutes.
3. After removal of the SRB solution, the plates were quickly washed with 1% acetic acid, 5 times, to remove unbound dye.
4. The washed plates were dried in the air. Total protein produced by the cells was stained pink.
5. Bound SRB was solubilized by adding 100μl of 10mM unbuffered Tris Base (pH 10.5) to each well and shaking for 5min on a shaker platform.

The plates were read in a 96-well plate reader (SpectraMax-190, Molecular Devices, Sunnydale, USA), the working wavelength was 492nm (Keawpradub *et al.*, 1999). As a result, the optical density (OD) of SRB was directly proportional to the cell number.

The results of primary screening are shown as percentage of the remaining cells and the cytotoxic activity of potent compounds are indicated by IG_{50} (growth inhibition of 50%). There are three required measurements: the OD of the treated cells (T), OD of control cells (C) and OD of cells at time zero (T_0), which is from a reference plate of inoculated cells fixed with TCA prior to drug addition to the test plates. Data are expressed in terms of percentage of remaining cells $[(T/C)\times100]$, as a measure of cell viability and survival in the presence of the extracts. For pure compounds and standard positive controls, their activity is shown as IG_{50}, which is the drug concentration causing a 50% reduction in the net protein increase in control cells

[$100\times(T-T_0)/(C-T_0)$] during the drug incubation (Monks *et al.*, 1991).

Data was analysed by using "Analysing Dose-Response Data" in GraphPad Prism version 4.00 for Windows to obtain values of IG_{50}. Firstly, the values of optical density (OD) were normalized as the percentage of proliferation of tested cells comparing with control. Then, the values of concentrations were transformed to their respective logarithms using X=Log(X). These manipulations were required to produce a conventional dose-response graph with response values plotted against the logarithm of drug concentration. At the same time, IG_{50} was determined by means of "Nonlinear Regression (Curve Fit)". As an example, typical results are shown in Figure 2-4. The cytotoxicity against MCF-7 cells of a active compound "A" isolated later was 4 times higher than that of another less toxic compound "B" and their dose-response regression curves were also remarkably different.

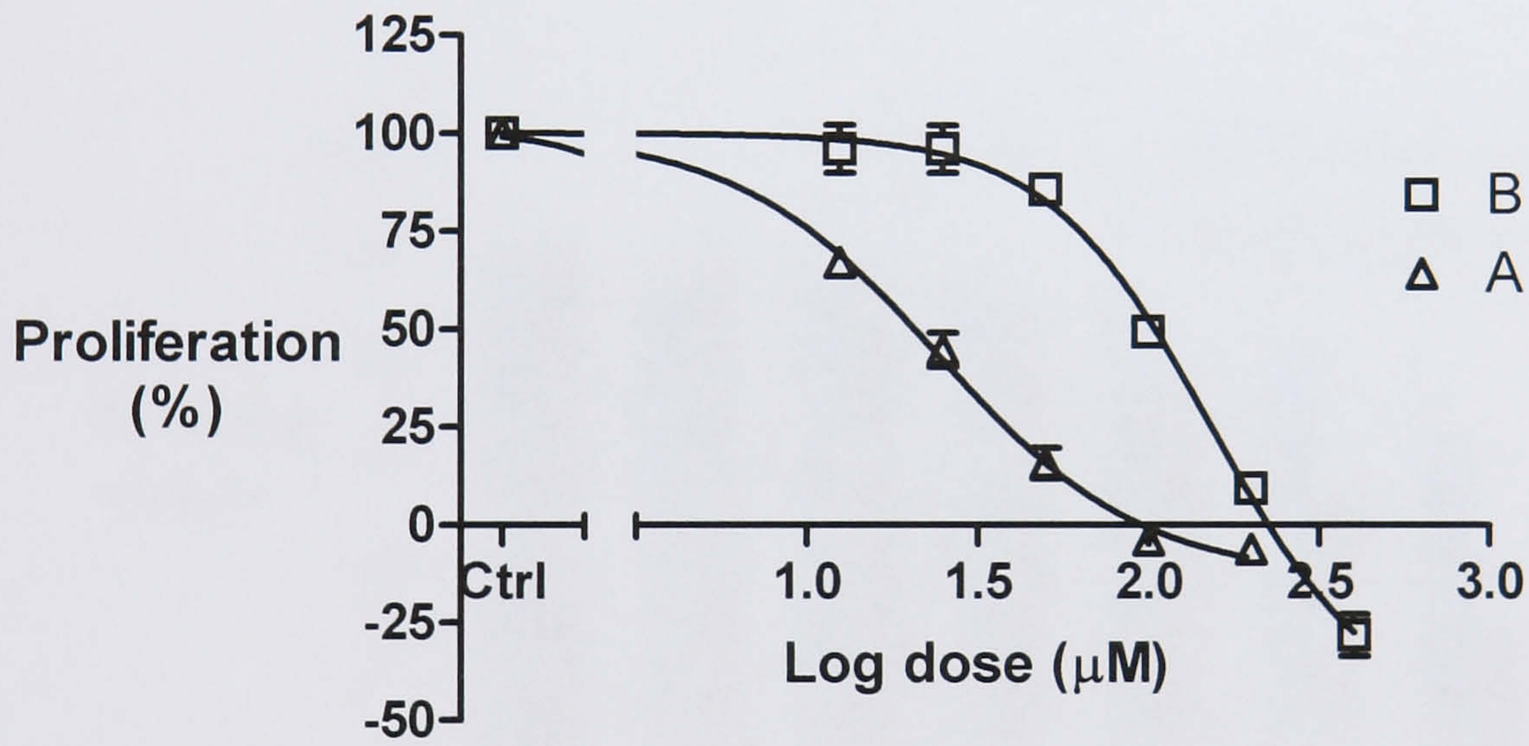

Figure 2-4: Dose-response curves of illustrative examples of isolated compounds against MCF-7 cells

2.2.10 Optimization of cytotoxicity assay

Genistein (**51**) was prepared in solutions over a range of 12.5μM to 400μM and incubated with COR-L23 cells (5×10^3 cells/well) for 24h and 48h. As shown in Figure 2-5, higher doses and longer treatment times resulted in stronger inhibition effect on cell proliferation. 61% cells survived in the first 24h treatment with 400μM genistein (**51**), however, the proportion decreased to 25% when the exposure time has extended to 48h. Because COR-L23 cell line has a doubling time of 45h and genistein (**51**) is a cell cycle-specific (G_2/M phase) agent, insufficient exposure time may result in some cells (in a different cell cycle phase) avoiding attack of the cell cycle-specific cytotoxic agent. The remarkably different results between the 24h and 48h treatments clearly suggested that the shorter exposure time (less than that for one cell cycle) may lead to an inaccurate cytotoxicity evaluation. So, in the present work, the incubation time used was 48h.

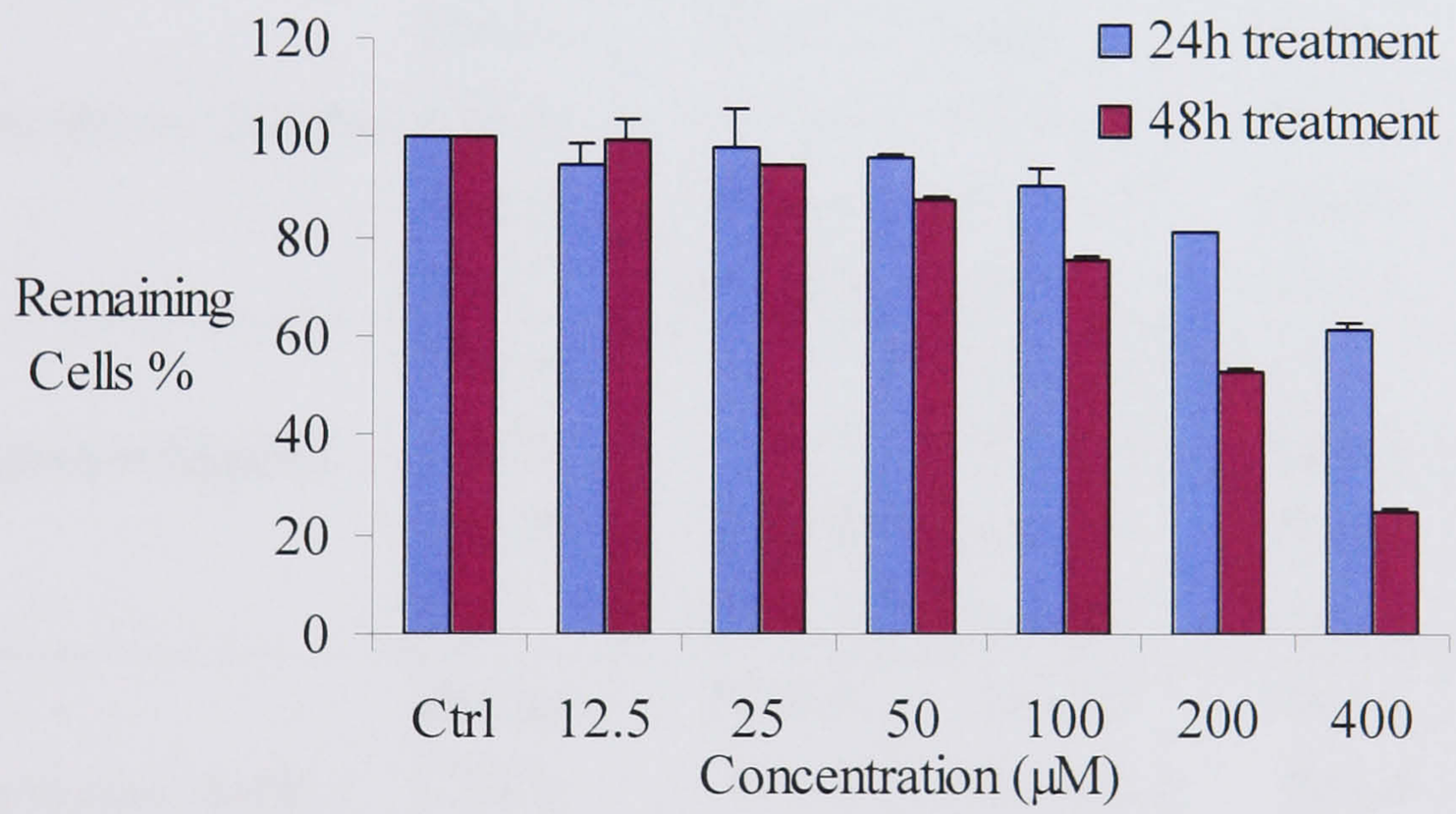

Figure 2-5: Time-dependent and dose-dependent cytotoxicity of genistein (**51**) against COR-L23 cells (n=2)

2.3 Results of the preliminary screening

The aim of preliminary screening was to select the most active extracts from the initial 18 extracts of the organisms tested. The extracts were firstly dissolved in DMSO to produce 40mg/ml stock solutions, and then diluted with medium to obtain the desired concentrations. All extracts were tested at 100μg/ml and tested against COR-L23, C32, MCF-7, and HepG2 cell lines. Cells were exposed to crude extracts for 48h. As shown on Table 2-4, active extracts inhibit proliferation of cells.

Plants and extracts		**Remaining cells(%) ±SEM**			
		COR-L23	**C32**	**MCF-7**	**HepG2**
Dolichos lablab L.	Hexane	105±1.8	118±5.0	102±2.4	155±5.1
	$CHCl_3$	116±1.9	106±3.4	110±1.9	185±8.3
	MeOH	103±0.8	113±0.2	101±5.2	160±1.0
	H_2O	118±1.5	118±4.5	107±1.8	205±4.1
Gekko swinhonis Gunther	Hexane	90±2.2	118±3.4	92±6.4	146±4.3
	$CHCl_3$	101±1.6	103±0.6	99±3.5	195±10.3
	MeOH	86±4.4	107±0.8	93±4.4	211±32.5
	H_2O	101±0.5	111±1.1	103±2.1	148±1.9
Iris tectorum Maxim.	Hexane	—	—	—	—
	$CHCl_3$	7±0.7	27±1.5	16±0.5	12±0.9
	MeOH	86±0.8	103±1.1	92±0.6	163±15.2
	H_2O	101±1.3	109±0.1	97±1.1	141±5.0
Illicium verum Hook. *f*	Hexane	11±0.5	86±2.6	14±1.3	130±5.8
	$CHCl_3$	8±0.3	63±15.2	9±5.4	79±2.0
	MeOH	85±0.9	101±2.3	83±9.4	142±2.3
	H_2O	91±0.1	103±1.2	90±3.3	103±0.7
Lonicera japonica Thunb.	Hexane	—	—	—	—
	$CHCl_3$	10±1.4	68±2.3	13±7.6	88±7.0
	MeOH	36±1.2	92±1.0	41±2.1	209±35.1
	H_2O	93±2.3	112±0.1	91±4.1	128±4.1

Table 2-4: Percentage of remaining cells of four cancer cell lines after exposure to plant extracts at 100μg/ml for 48h (n=3, mean±SEM)

Those extracts which caused the proportion of remaining cells lower than 50% were considered to be active and worth following by further bioassay-guided isolation and purification. As shown in Table 2-4, $CHCl_3$ extracts of *Iris tectorum* Maxim., *Illicium verum* Hook. *f* and *Lonicera japonica* Thunb. showed considerable cytotoxicity against cancer cells. In particular, the $CHCl_3$ extract of *Iris tectorum* Maxim. was the most active one against all types of cancer cell lines. The other two TCMs were only active against C32 and MCF-7 cell lines. Because of the limited time and financial support for present study, only the most active extract was selected for further work. Therefore, only *Iris tectorum* Maxim. was subjected to further phytochimcal investigation and bioassays.

2.4 Phytochemical investigation of *Iris tectorum* Maxim.

2.4.1 Bioactivity-directed fractionation

Results from the preliminary assay for cytotoxic activity indicated promising active constituents included in $CHCl_3$ extract of *Iris tectorum* Maxim. A large scale fractionation and isolation for the active compounds from *Iris tectorum* Maxim. was carried out and described in Figure 2-6.

Firstly, 2kg of powdered rhizome was extracted by supercritical fluid extraction (with liquid CO_2) in Shenzhen Neptunus Bioengineering Co. Ltd., China. In this step most volatile components that could be extracted into hexane were removed. This was confirmed by analytical TLC shown as Figure 2-7. The dry residue was exhaustively extracted with $CHCl_3$ by Soxhlet extraction for 3 times. The $CHCl_3$ extract was taken to dryness under reduced pressure, yielding 152g of dried extract.

In further cytotoxicity assay the chloroform extract of *Iris tectorum* Maxim. showed cytotoxicity against lung cancer (CORL-23) and breast cancer (MCF-7) cell lines, with IG_{50} values of 36.9μg/ml and 35.6μg/ml respectively. However, human melanotic melanoma (C32) was less sensitive to this extract and showed an IG_{50} of 75.1μg/ml (see Figure 2-8).

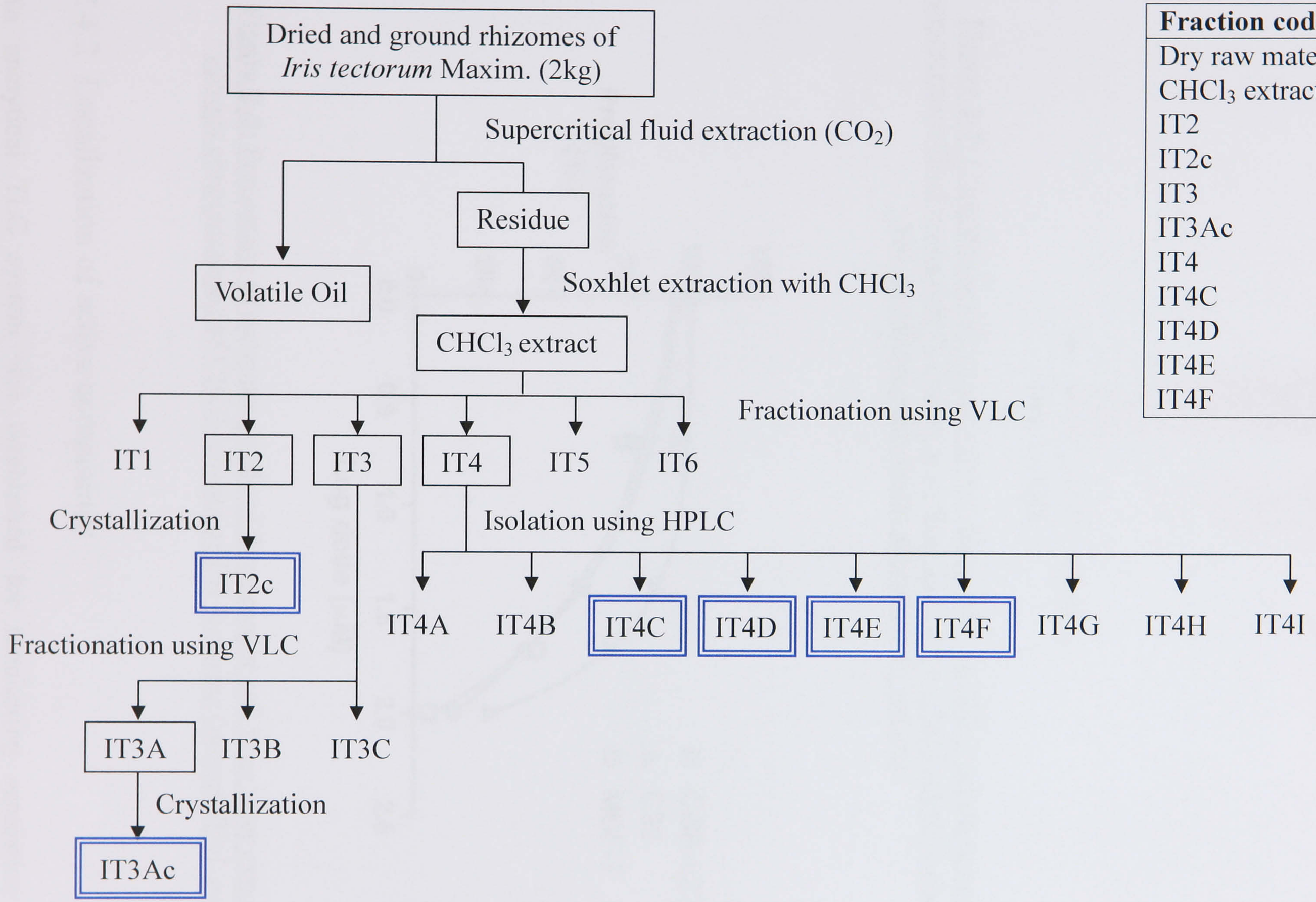

Fraction code	Weight
Dry raw material	2kg
$CHCl_3$ extract	152g
IT2	3.6g
IT2c	12.2mg
IT3	52g
IT3Ac	1.4g
IT4	17g
IT4C	11.2mg
IT4D	13.1mg
IT4E	5.6mg
IT4F	26.8mg

Figure 2-6: Flow chart of fractionation and isolation of compounds from *Iris tectorum* Maxim.

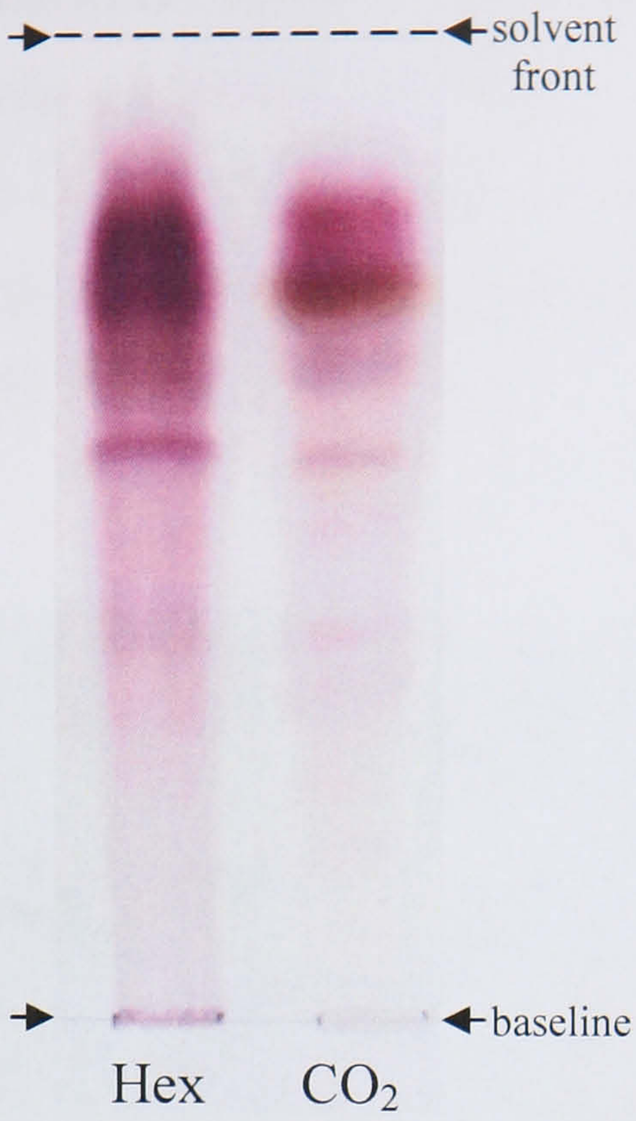

Figure 2-7: Comparison of hexane extract (Hex) with volatile fraction removed by supercritical fluid extraction (CO_2) on analytical TLC developed in mobile phase DS1 and visualized with acidic anisaldehyde reagent

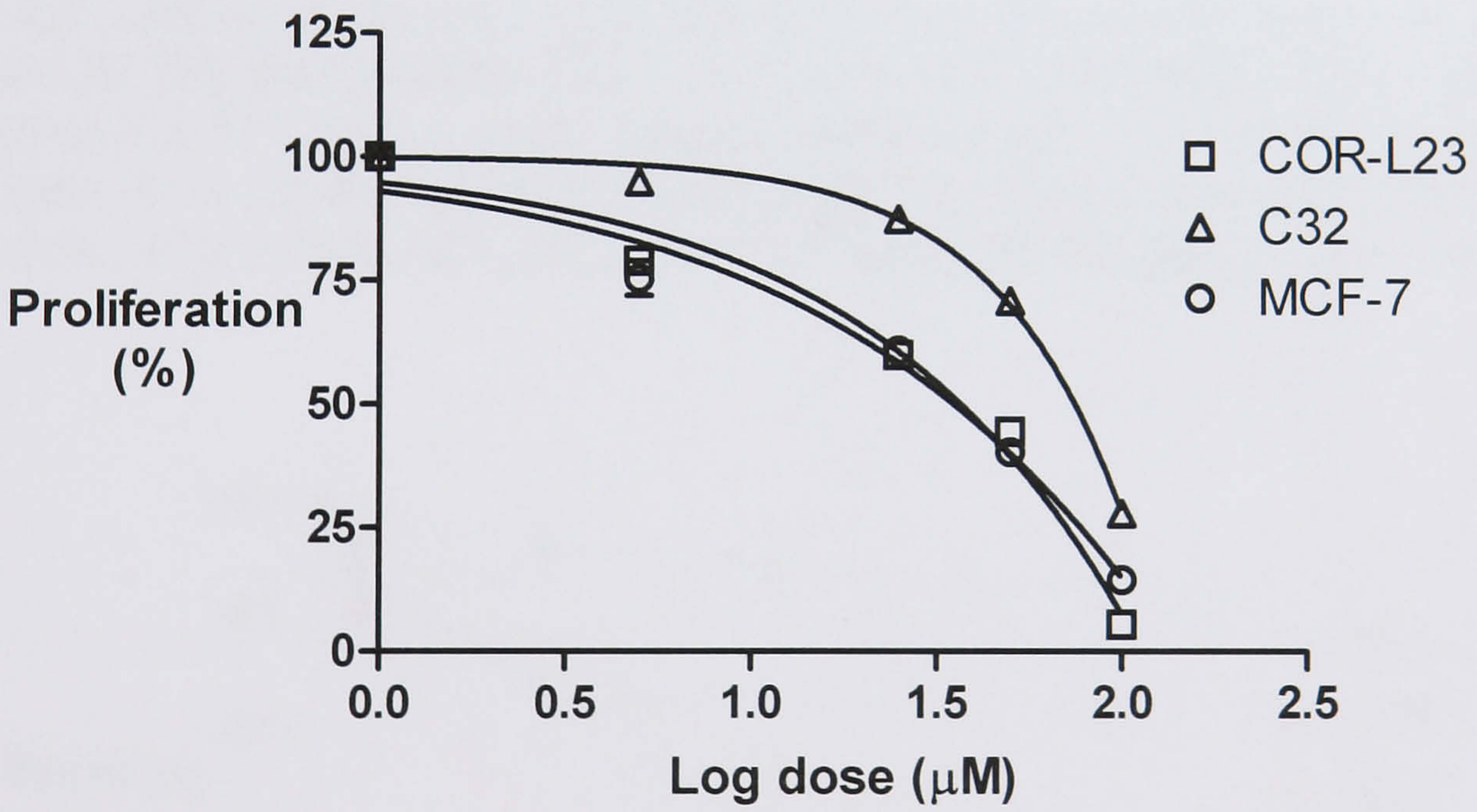

Figure 2-8: Percentage of remaining cells of three cancer cell lines after exposure to various concentrations of $CHCl_3$ extract of *Iris tectorum* (mean±SEM, n=2)

2.4.2 Localization of active compounds

An analytical TLC system was established for monitoring separation of the compounds in $CHCl_3$ extract as displayed in Figure 2-9. The four distinguishable

zones (PT1 ~ PT4) were collected from 12 preparative TLC plates, which were developed in the same mobile phase system (DS1). Then these four sub-fractions were tested for cytotoxicity against cancer cell lines. Figure 2-10 indicates the fraction PT2 contains a group of cytotoxic components (R_f = 0.3 ~ 0.4 on the TLC plate in Figure 2-9) in the $CHCl_3$ extract.

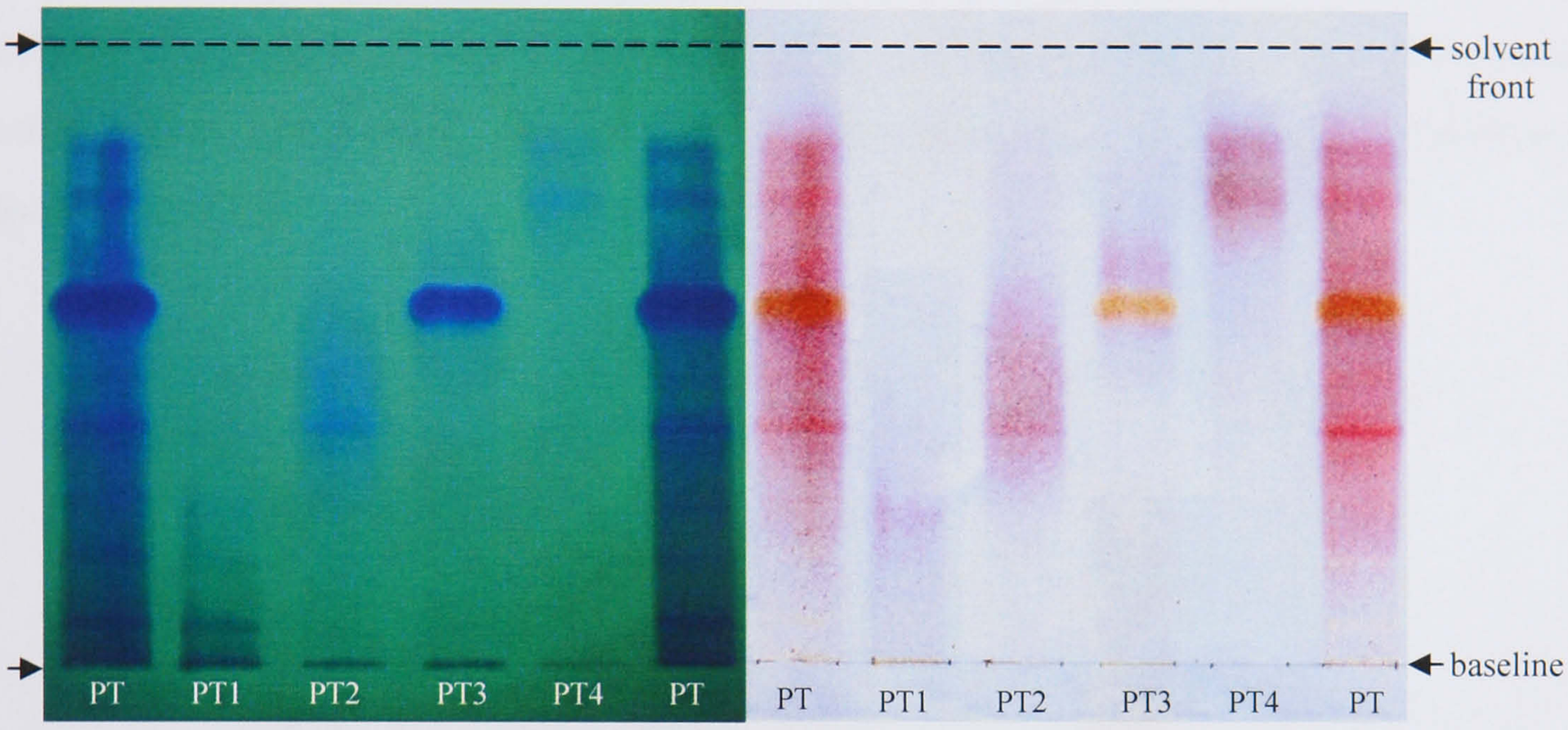

Figure 2-9: Thin-layer chromatogram of total $CHCl_3$ extract of *Iris tectorum* Maxim. (PT) and its four sub-fractions (PT1 ~ PT4) produced by preparative TLC. (It was developed in DS1 mobile system. The left-hand side picture shows the developed TLC plate observed under 254nm UV; the right-hand side picture shows the same TLC plate under normal light after visualisation with acidic anisaldehyde reagent)

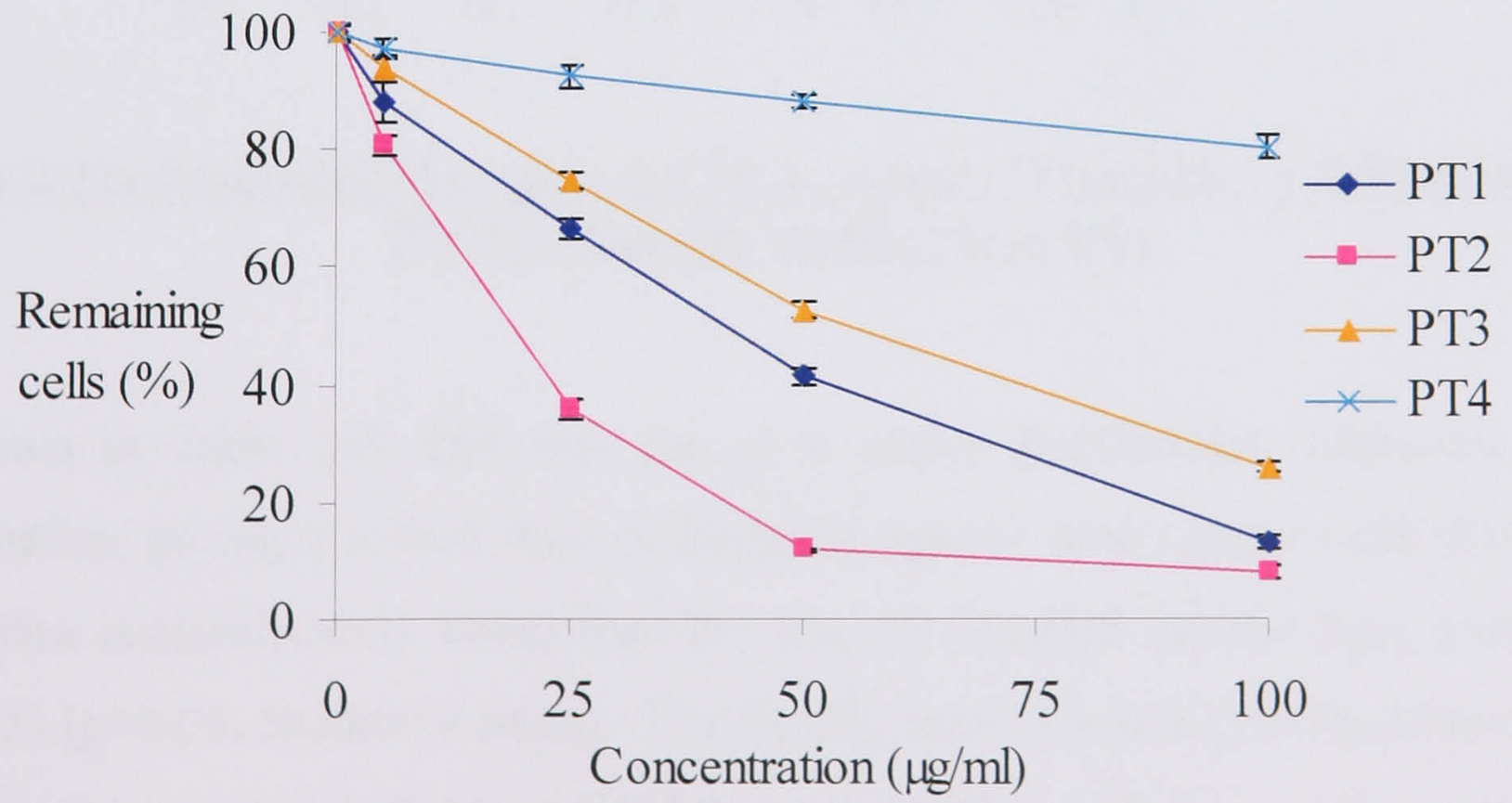

Figure 2-10: Percentage of remaining cells of COR-L23 after exposure to various concentrations of sub-fractions (PT1 ~ PT4) for 48h (mean±SEM, n=2)

2.4.3 Isolation and purification of compounds

After the cytotoxicity test for the sub-fractions (PT1 ~ PT4), the component within PT2 band (R_f =0.3 ~ 0.4 on TLC plate developed by mobile phase DS1) was recognized as the location for the active compounds on TLC plates. Meanwhile, a sub-fraction IT4 eluted by VLC in a large scale isolation (Figure 2-6 on page 63) had almost identical mobility (R_f =0.38) in the same TLC system (Figure 2-11). Further cytotoxicity analysis of the VLC fractions IT1 ~ IT6 also confirmed that IT4 was the most active sub-fraction (Figure 2-12). Therefore, the isolation and purification focused on IT4.

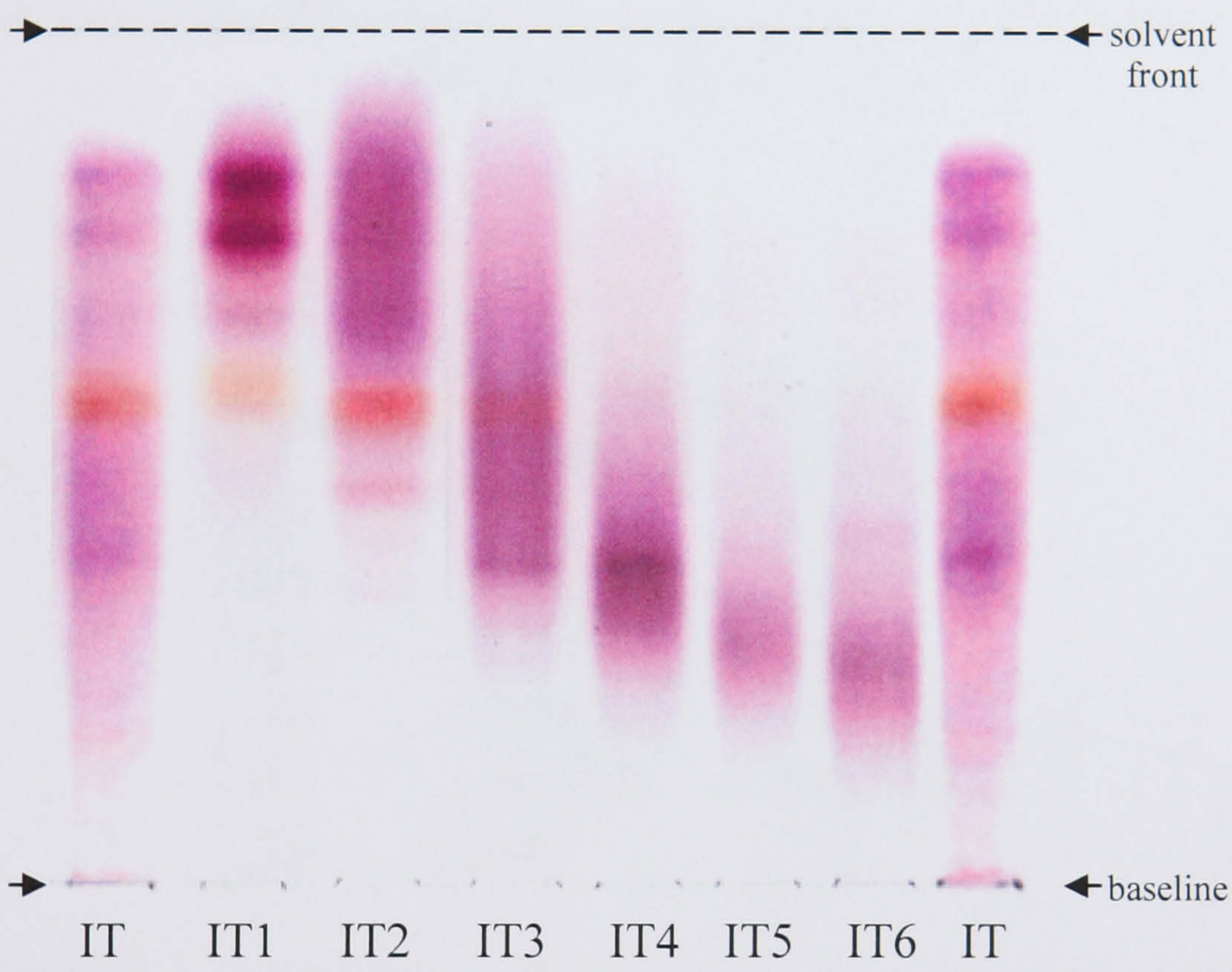

Figure 2-11: Analytical TLC plate of $CHCl_3$ extract (IT) and its VLC-fractions IT1 ~ IT6 developed in mobile phase DS1

As shown in Table 2-5, IT4 was the most active fraction for inhibition of cells proliferation, giving a lowest IG_{50} of 25μg/ml against lung cancer cells (COR-L23). This value is significantly lower than the IG_{50} of 35μg/ml against lung normal cells (MRC-5) (p<0.05, Student's t-test). Practically, both IT3 and IT4 fractions exhibited selective cytotoxicity between COR-L23 and MRC-5 cell lines. That means at a certain concentration of IT3 or IT4 the proliferation of COR-L23 cells is inhibited more than that of MRC-5 cells.

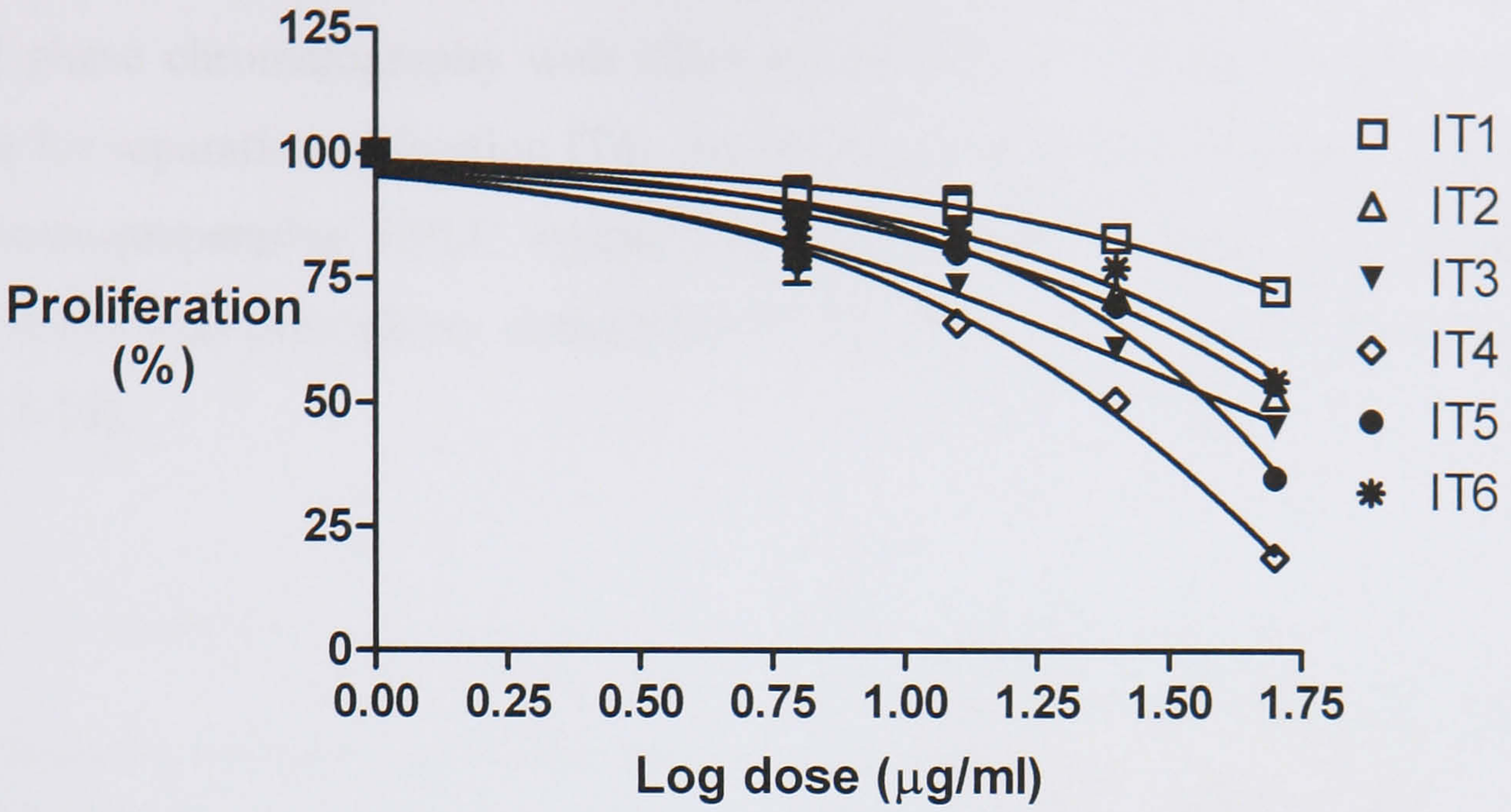

Figure 2-12: Inhibition effect of sub-fractions IT1 ~ IT6 on proliferation of COR-L23 cells (mean±SEM, n=2)

Fractions	IG_{50} (μg/ml)	
	COR-L23	**MRC-5**
IT1	>50	>50
IT2	>50	>50
IT3	39±1.00	>50
IT4	25±0.62*	35±1.55
IT5	40±0.28	42±2.40
IT6	>50	>50

Table 2-5: The IG_{50} values (μg/ml) of sub-fractions IT1 ~ IT6 against COR-L23 (lung cancer) and MRC-5 (normal lung fibroblast) cells (IG_{50}±SEM, n=2); * IG_{50} Value of IT4 against COR-L23 was significantly lower than that against MRC-5 (p<0.05).

Crystallization of VLC fractions IT2 and IT3A from MeOH yielded compounds IT2c and IT3Ac (Figure 2-6 on page 63). They showed almost identical R_f values (0.56) on TLC as shown in Figure 2-13. However, IT2c did not quench UV(254nm), while the spot of IT3Ac was observed as a dark spot. This observation indicated that IT2c is a relatively saturated compound.

After development in DS2 mobile phase system, IT3B and IT3C (sub-fractions of IT3) showed significant bands at R_f=0.37 which are in common with IT4. Thereby, they

were recombined with IT4 for further isolation. An extra experiment revealed that normal phase chromatography with silica gel 60 PF_{254} in an open column was not feasible for separation of fraction IT4. As previously described (section 2.1.3 on page 50) a semi-preparative HPLC system was applied for separation and purification. That yielded four pure glassy compounds IT4C, IT4D, IT4E and IT4F (as shown in Figure 2-14).

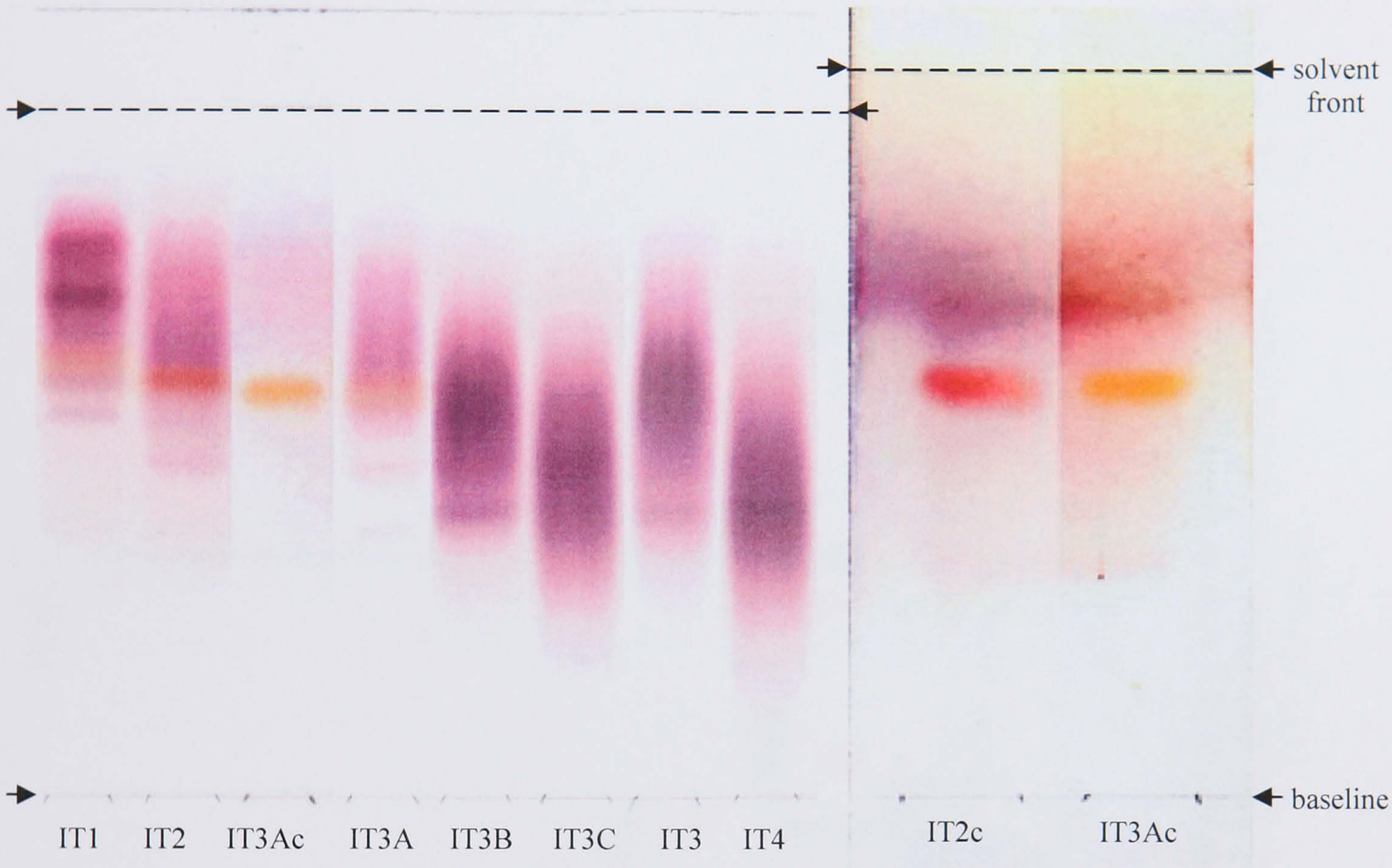

Figure 2-13: Analytical TLC plate of fractions: IT1 ~ IT4, sub-fractions: IT3A ~ IT3C and compounds IT2c and IT3Ac. Left: IT3B IT3C and IT4 have dark bands around R_f=0.37 on the same TLC plate developed in DS2 mobile phase; Right: TLC plate of IT2c and IT3Ac developed in mobile phase DS1.

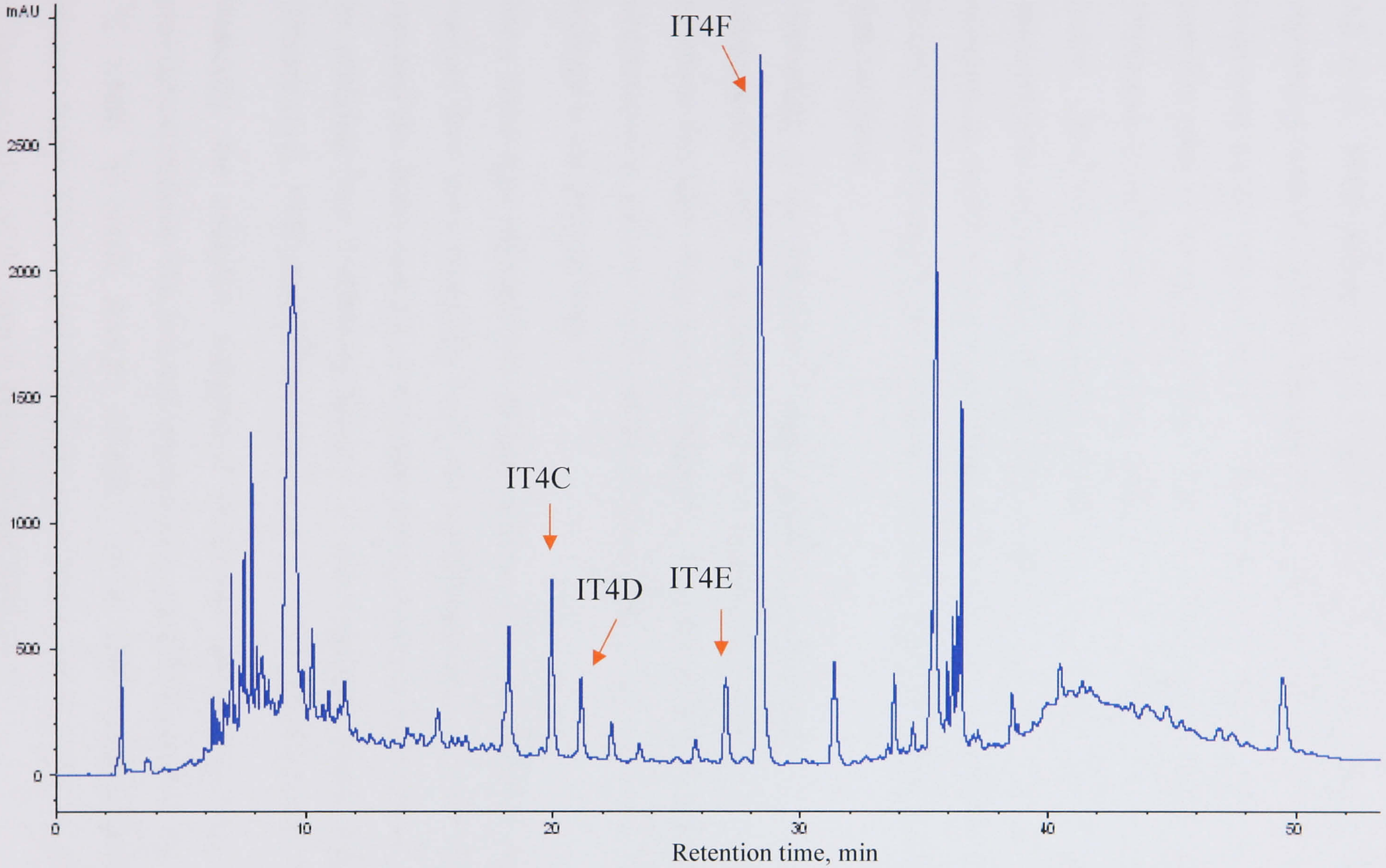

Figure 2-14: HPLC chromatogram of IT4 sub-fraction analysed by semi-preparative column: Discovery® HS C18. Gradient conditions: Acetonitrile/water=30/70→70/30, 0-30min; 70/30→100/0, 30-55min. Retention times: IT4C=20min; IT4D=21.3min; IT4E=27min; IT4F=28.5min.

2.5 Structural elucidation

In the past two decades, many phytochemicals such as isoflavonoids, quinones and iridals have been discovered in the rhizomes of Iridaceous plants (Seki *et al.*, 1994a; Ali *et al.*, 1983; Minami *et al.*, 1996). Iridal-type triterpenoids are biogenetically interesting natural products because they were exclusively found in the rhizomes of Iridaceous plants (Marner *et al.*, 1982; Seki *et al.*, 1994; Abe *et al.*, 1991). Some possible roles in living plant cells, such as antioxidant function (Marner and Kerp, 1992) and drought-resistant activity (Bonfils *et al.*, 1994) have been suggested for the iridals. This type of monocyclic and bicyclic triterpenoids have been recognized as characteristic metabolites of Iridaceous plants. In the present work, four pure compounds, which were isolated from the most active fraction IT4 by RP C-18 HPLC system were eventually elucidated as iridal-type triterpenoids by several spectroscopic technologies.

According to the literature a major group of compounds from *Iris tectorum* are triterpenoids with a saturated six-membered ring bonded to an α,β-unsaturated aldehyde function. Moreover, an aliphatic unsaturated hydrocarbon is present. These characteristics can be easily observed from the NMR results of those compounds isolated in the present work.

Most iridal-type triterpenoids do not produce crystals, therefore, it is impossible to analyse their stereochemistry by X-ray crystallography. Nevertheless, some workers reported the determination of absolute configuration of some iridal-type triterpenoids by studying their 2-methoxy-2phenyl-2-(trifluoromethyl)acetic acid (MTPA) esters (Ohtani *et al.*, 1991) and CD spectra (Ito *et al.*, 1999; Miyake *et al.*, 1997).

Basically, the complete assignment of proton and carbon, and hence structure elucidation of these four isolated triterpenoids were facilitated by the measurements of ^{13}C NMR, ^{1}H NMR, HMQC, HMBC, ^{1}H-^{1}H COSY and NOESY spectra in the present study. The isolated triterpenes were numbered as in **57**, **60**, **61** and **65** for ease of interpretation of the data in Table 2-6 and Table 2-7.

2.5.1 Structural elucidation of compounds IT4E and IT4F

IT4F was obtained as a yellowish glassy solid, and showed a major peak at 28.5 min on the HPLC chromatogram of active sub fraction IT4. This suggests that IT4F could be a major compound in *I. tectorum*. Mass spectral investigation by ESIMS and CIMS gave peaks at *m/z* 497 $[M+Na]^+$ and *m/z* 492 $[M+NH_4]^+$ (consistent with formula of $C_{30}H_{50}O_4Na$ and $C_{30}H_{50}O_4NH_4$, indicating a molecular formula of $C_{30}H_{50}O_4$ for IT4F). Such a formula is in keeping with the known occurrence of triterpenes such as isoiridogermanal (formula: $C_{30}H_{50}O_4$) previously found in *Iris pallida* (Krick *et al.*, 1983). The ^1H and ^{13}C NMR data of IT4F are superimposable with those of isoiridogermanal (**57**) in the literature (Krick *et al.*, 1983; Seki *et al.*, 1994b; Takahashi *et al.*, 2000).

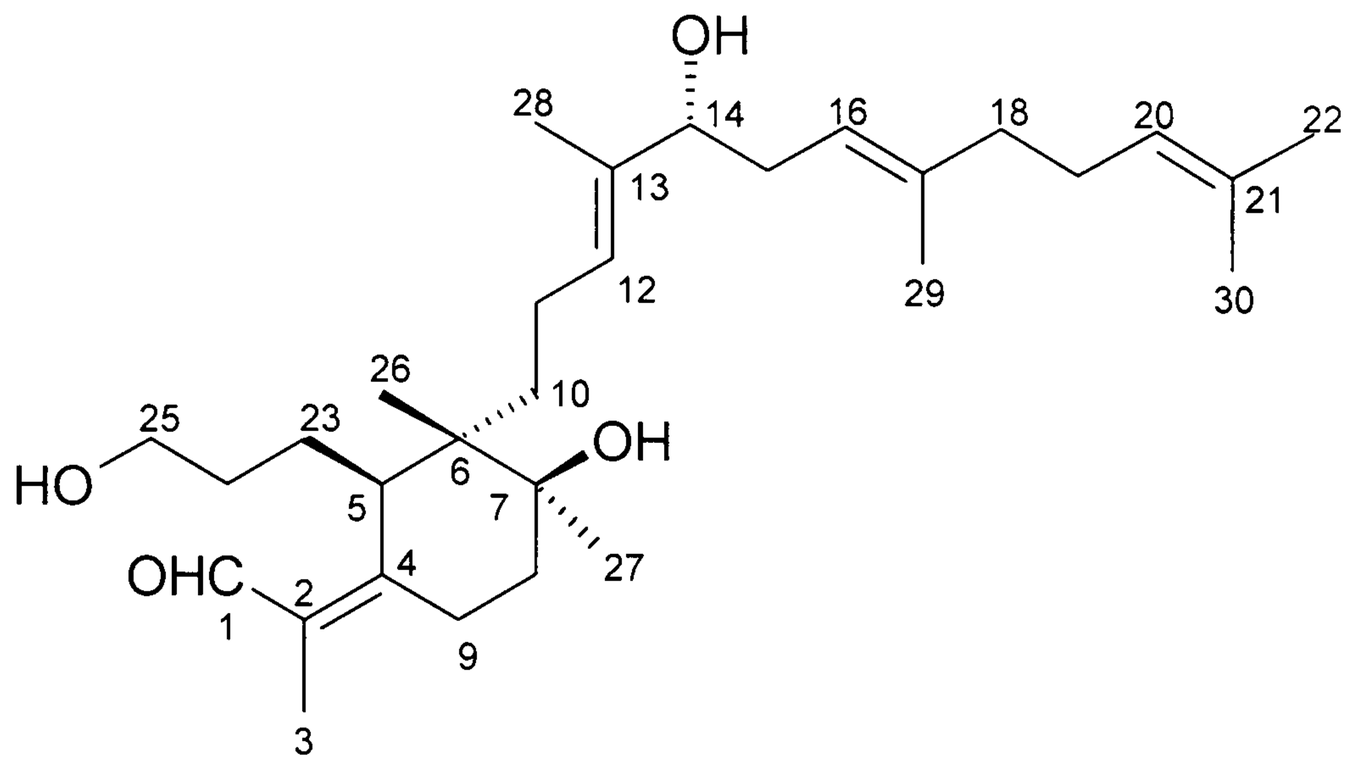

57

Isoiridogermanal (**57**) was first isolated from *Iris pallida* and *Iris florentina* in 1983 (Krick *et al.*, 1983) and subsequently from rhizomes of *Belamcanda chinensis*, *Iris cristata* Solander, *Iris germanica*, *Iris japonica* and bulbs and leaves of *Tigridia pavonia* (Bonfils and Sauvaire, 1996; Taillet *et al.*, 1999; Takahashi *et al.*, 2000; Effers *et al.*, 1999), all Iridaceae. The absolute configuration has been well established as that shown in **57** by means of chemical and physical analysis (Ito *et al.*, 1999). Furthermore, the absolute stereochemistry of the related compounds γ-irigermanal (**58**) and iriflorental (**59**) had previously been unequivocally established by X-ray crystallography (Marner *et al.*, 1982; Miyake *et al.*, 1997). On the basis of the above data, IT4F is identified as isoiridogermanal, **57**. The possible biosynthetic

route of IT4F (**57**) from terpenes is shown in Figure 2-15 (modified from Seki, 1994).

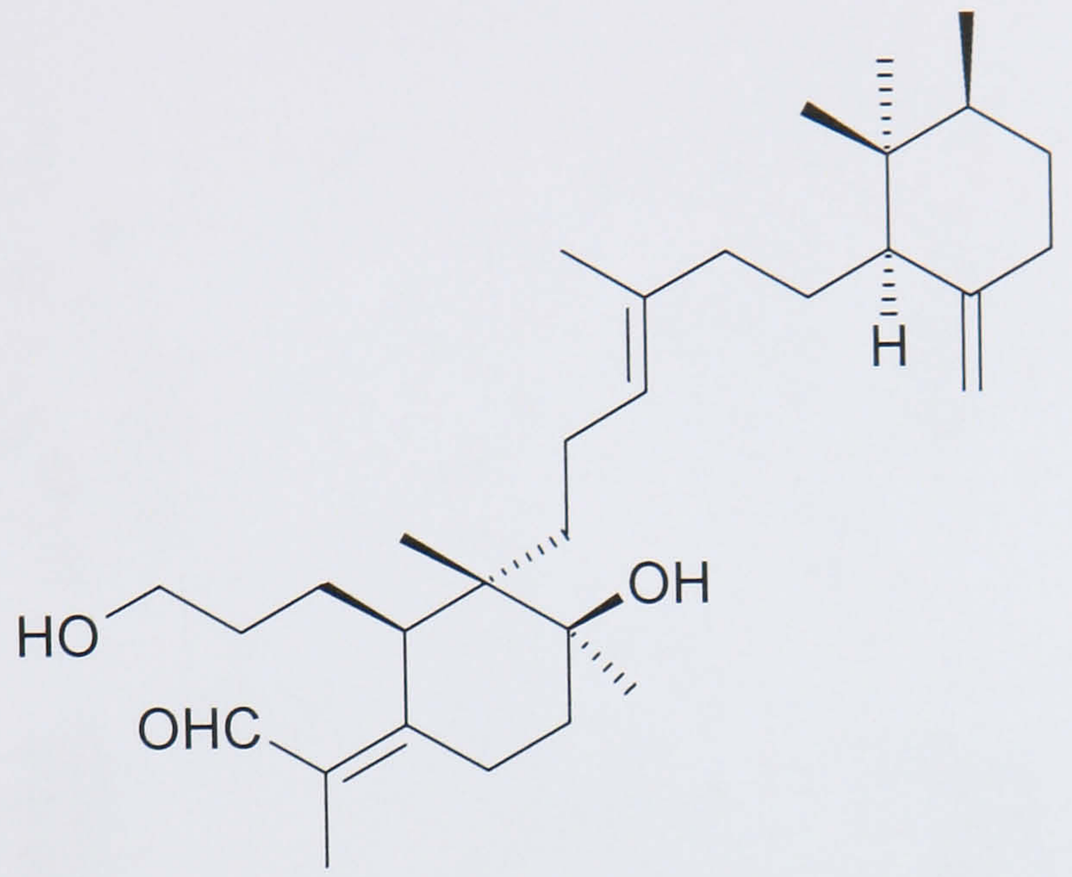

58

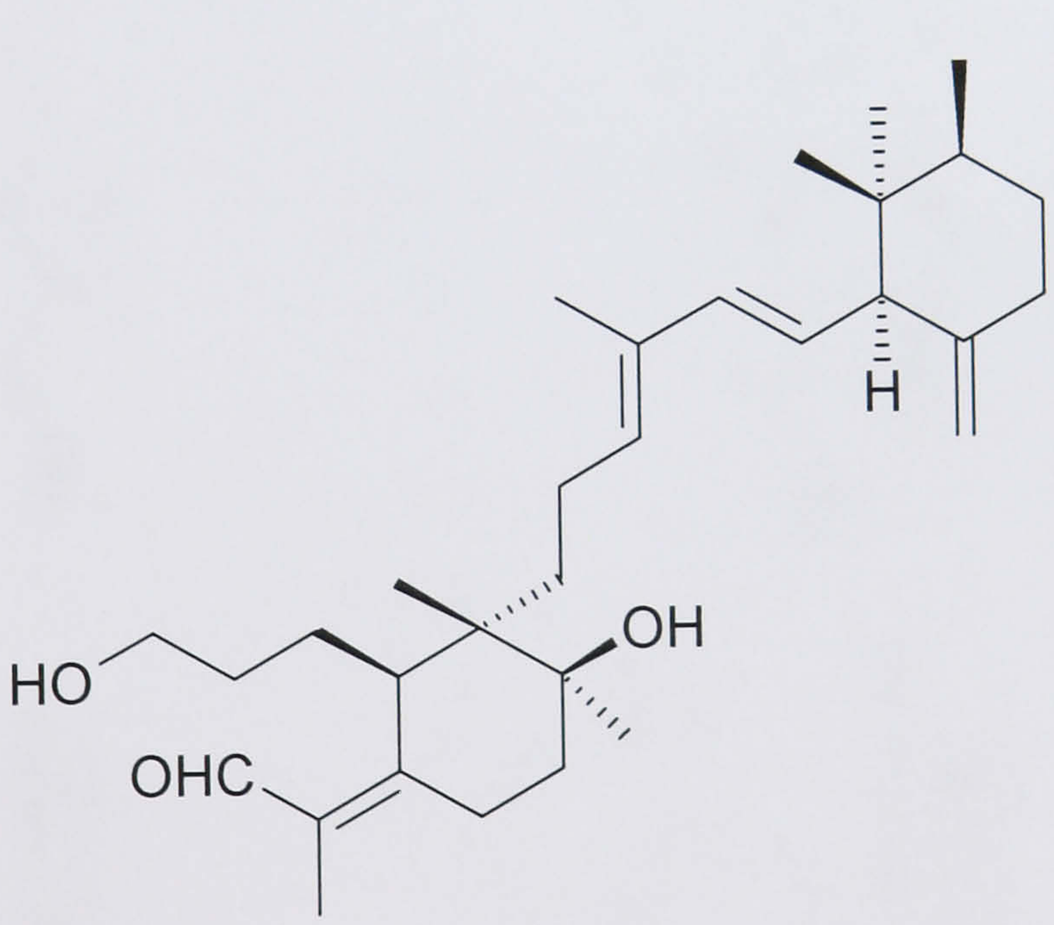

59

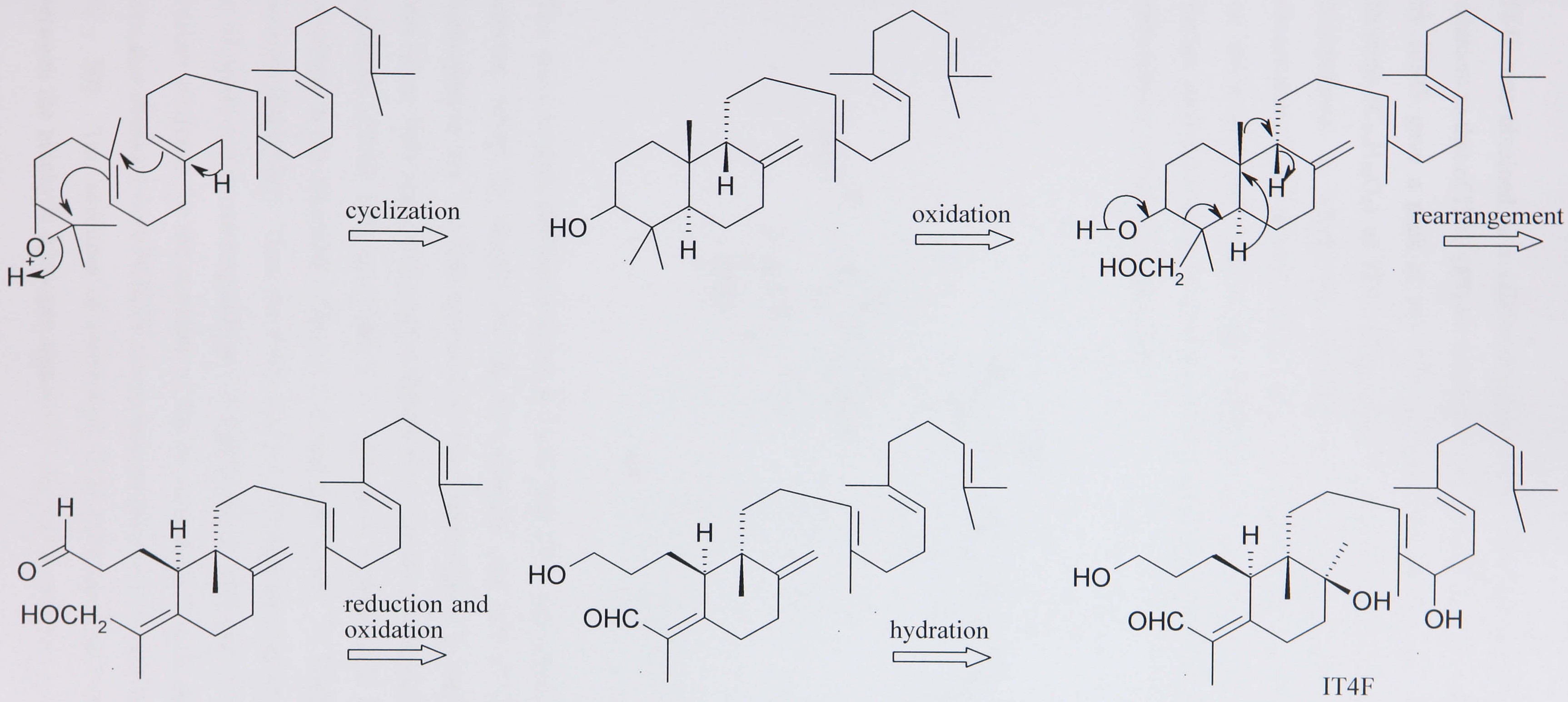

Figure 2-15: Possible biosynthetic route of IT4F (**57**) from terpenes (modified from Seki, 1994)

IT4E was obtained as a yellowish glassy solid. It showed a small peak at 27 min. adjacent to that of IT4F (**57**) on the HPLC chromatogram. Mass spectral investigation by EIMS gave a peak at *m/z* 474, suggesting it might have the same molecular formula ($C_{30}H_{50}O_4$) as IT4F (**57**). Such a formula is also identical with that of iridobelamal A, which was reported as a colourless viscous oil (according to observations in the present study, it is solid after being dried under N_2 gas), an isomer of isoiridogermanal, with similar NMR signal values (Takahashi *et al.*, 2000). In further investigation, the NMR data of IT4E were identical to those of iridobelamal A (**60**) (shown in Table 2-6 and Table 2-7).

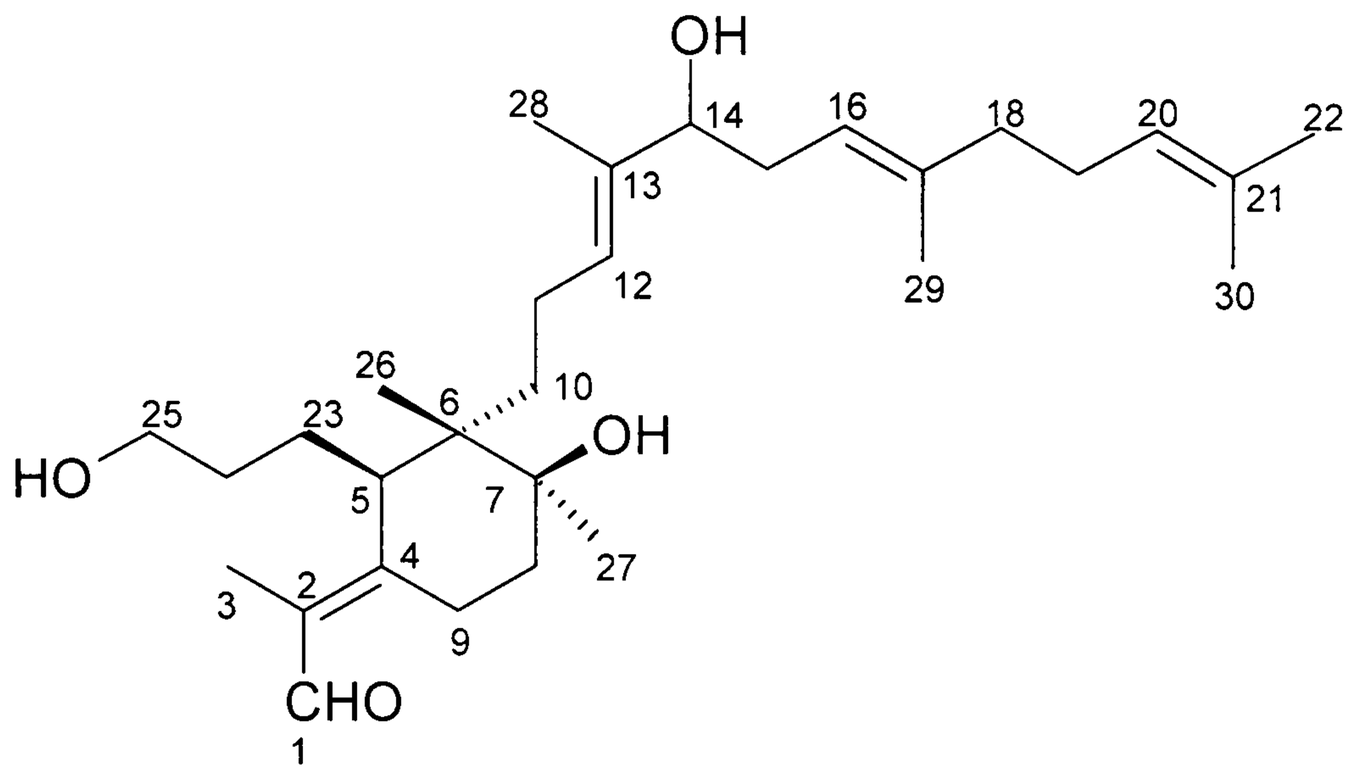

60

The most evident difference between IT4E and IT4F was observed in their NMR spectra, where the signals for the H-5 methine and one of the H-9 methylene hydrogens in the ^1H NMR spectrum of IT4E were shifted to higher ($\Delta\delta_H$ 0.52ppm) and lower field ($\Delta\delta_H$ 0.67ppm), respectively, than the corresponding signals in the spectrum of IT4F (**57**) (see Table 2-7). Moreover, a remarkable difference was also observed in the chemical shifts of C-5 and C-9 in the ^{13}C NMR spectra of these isomers (Table 2-6). Thus, for IT4E, $\delta_C(5)$ = 47.3ppm whereas for IT4F $\delta_C(5)$ occurs at 43.4ppm and the corresponding C-9 signals are at 20.0 and 23.8ppm, respectively. Further evidence for the structure of the six-membered ring in these two molecules was also obtained from NOESY measurements (Figure 2-16 and Figure 2-17 on page 79 ~ 80). The spectrum of compound IT4F (**57**) exhibited NOESY correlations between the aldehyde hydrogen signal H-1 (δ_H 10.18) and that of H-5 (δ_H 3.31), and

between the signals of the C-3 vinyl methyl hydrogen (δ_H 1.83) and one of the C-9 methylene hydrogens (δ_H 2.55). Meanwhile, in the spectrum of compound IT4E, the aldehyde hydrogen signal H-1 (δ_H 10.24) and the signal for the vinyl methyl (carbon 3) (δ_H 1.80) showed NOE correlations with one of the C-9 methylene hydrogen signals (δ_H 3.22) and the H-5 (δ_H 2.79), respectively. Those observations clearly indicated that IT4E is likely to be the geometrical isomer of IT4F (**57**) at the α,β-unsaturated aldehyde moiety ($\Delta^{2(4)}$). IT4E is thus identified as iridobelamal A, **60**.

As seen in Table 2-6, both sets of observed data of IT4F and IT4E superimposed well with those of isoiridogermanal (**57**) and iridobelamal A (**60**), respectively. Moreover, the only difference between **57** and **60** is the stereochemistry of the vinyl CH_3 and CHO: **57** is the *Z* isomer while **60** is the *E*. This evident difference was clearly observed between IT4F and IT4E, as shown in Figure 2-16 and Figure 2-17. Therefore, IT4F (**57**) and IT4E (**60**) were identified as isoiridogermanal (**57**) and iridobelamal A (**60**), respectively.

Carbon No.		IT4E	Iridobelamal A	Carbon	IT4F	isoiridogermanal
1	CHO	190.7	190.4	CHO	190.0	189.7
2	C	133.1	132.7	C	133.2	132.7
3	CH_3	11.9	11.6	CH_3	11.0	10.9
4	C	163.5	163.1	C	162.8	162.8
5	CH	47.3	47.0	CH	43.4	43.4
6	C	45.2	44.9	C	44.7	44.7
7	C	75.2	74.8	C	75.0	75.0
8	CH_2	38.0	37.7	CH_2	37.0	37.0
9	CH_2	20.0	19.7	CH_2	23.8	23.8
10	CH_2	36.9	36.6	CH_2	36.9	36.9
11	CH_2	23.0	22.6	CH_2	21.8	21.8
12	CH	125.7	125.4	CH	125.3	125.0
13	C	136.9	136.6	C	137.0	136.7
14	CH	76.8	76.4	CH	76.7	76.7
15	CH_2	34.3	33.9	CH_2	34.2	34.2
16	CH	119.9	119.6	CH	119.9	119.6
17	C	138.9	138.5	C	138.8	138.4
18	CH_2	39.8	39.5	CH_2	39.8	39.8
19	CH_2	26.5	26.2	CH_2	26.5	26.5
20	CH	124.1	123.8	CH	124.1	123.8
21	C	131.7	131.3	C	131.7	131.3
22	CH_3	25.7	25.4	CH_3	25.7	25.7
23	CH_2	27.1	26.8	CH_2	26.6	26.6
24	CH_2	32.0	31.7	CH_2	32.7	32.7
25	CH_2	63.2	62.9	CH_2	63.1	63.0
26	CH_3	17.8	17.5	CH_3	18.0	17.9
27	CH_3	26.4	26.0	CH_3	26.3	26.3
28	CH_3	11.9	11.6	CH_3	11.9	11.9
29	CH_3	16.3	16.0	CH_3	16.3	16.4
30	CH_3	17.7	17.4	CH_3	17.7	17.7

Table 2-6: Comparison of the ^{13}C NMR data (δ, at 125MHz, in $CDCl_3$) of IT4E (**60**) and IT4F (**57**) with those of iridobelamal A and isoiridogermanal, from Takahashi, 2000.

Carbon No.		IT4E	Iridobelamal A	Carbon	IT4F	isoiridogermanal
1	CHO	10.24 *s*	10.23 *s*	CHO	10.18 *s*	10.18 *s*
3	CH_3	1.80 *s*	1.81 *br s*	CH_3	1.83 *s*	1.83 *br s*
5	CH	2.79 *br d* (*J*=9.9Hz)	2.79 *br d* (*J*=9Hz)	CH	3.31 *br d* (*J*=11.1Hz)	3.31 *br d* (*J*=9Hz)
8	CH_2	1.62-1.71 *m* 1.79-1.87 *m*	1.83 *m*	CH_2	1.65 *m* 1.87 *m*	1.67 *m* 1.85 *m*
9	CH_2	3.22 apparent *br d* (*J*=13.9Hz) 2.59 apparent *td* (*J*=13.9, 2.3Hz)	3.22 *br d* (*J*=14Hz) 2.59 br *td* (*J*=14, 4Hz)	CH_2	2.55 apparent *br t* (*J*=13.5Hz) 2.60 apparent *td* (*J*=14.0, 4.7Hz)	2.54 *br d* (*J*=14Hz) 2.60 *td* (*J*=14, 4Hz)
10	CH_2	1.13 -1.32 *m*	1.95 *m*	CH_2	1.18 *m* 1.32 *m*	1.17 *m* 1.35 *m*
11	CH_2	1.90-1.96 *m* 1.99-2.10 *m*	?	CH_2	1.86 *m* 1.96 *m*	1.92 *m* 2.00 *m*
12	CH	5.26 *t* (*J*=6.8Hz)	5.26 *br t* (*J*=7Hz)	CH	5.25 *t* (*J*=7Hz)	5.24 *br t* (*J*=7Hz)
14	CH	3.93 *dd* (*J*=7.5, 5.1Hz)	3.94 *br t* (*J*=7Hz)	CH	3.92 *dd* (*J*=7.8, 5.1Hz)	3.92 *dd* (*J*=7, 5Hz)

Continued on next page

Table 2-7: Comparison of the ^{1}H NMR spectral data (δ, at 500MHz, in $CDCl_3$) of IT4E (**60**) and IT4F (**57**) with published data of iridobelamal A and isoiridogermanal (Takahashi *et al.*, 2000); *Data missing from the literature are replaced by question marks.

Continued from previous page

Carbon No.		IT4E	Iridobelamal A	Carbon	IT4F	isoiridogermanal
15	CH_2	2.13-2.33 *m*	2.24 *td* (*J*=13, 7Hz) 2.27 *td* (*J*=13, 7Hz)	CH_2	2.22 *m*	2.21 *td* (*J*=13, 7Hz) 2.33 *td* (*J*=13,7Hz)
16	CH	5.07 *m*	5.08 *m*	CH	5.07 *m*	5.07 *m*
18	CH_2	2.02 *br d* (*J*=6.5Hz)	2.03 *m*	CH_2	2.02 *m*	2.03 *m*
19	CH_2	2.07 *br s*	?	CH_2	2.07 *m*	2.07 *m*
20	CH	5.06 *m*	5.06 *m*	CH	5.06 *m*	5.06 *m*
22	CH_3	1.68 *s*	1.68 *br s*	CH_3	1.68 *s*	1.68 *br s*
23	CH_2	1.80 *m* 2.10 *m*	?-2.10 *m*	CH_2	1.79 *m* 2.03 *m*	1.83 *m* 2.02 *m*
24	CH_2	1.33-1.41 *m*	1.2 *m* 1.37 *m*	CH_2	1.26 *m* 1.40 *m*	1.27 *m* 1.37 *m*
25	CH_2	3.61 apparent *td* (*J*=6.3, 2.3Hz)	3.61 *t* (*J*=6Hz)	CH_2	3.61 apparent *t* (*J*=6.4Hz)	3.61 *t* (*J*=6Hz)
26	CH_3	1.09 *s*	1.08 *s*	CH_3	1.10 *s*	1.09 *s*
27	CH_3	1.16 *s*	1.16 *s*	CH_3	1.16 *s*	1.15 *s*
28	CH_3	1.60 *s*	1.60 br *s*	CH_3	1.55 *s*	1.55 br *s*
29	CH_3	1.63 *s*	1.62 br *s*	CH_3	1.62 *s*	1.62 br *s*
30	CH_3	1.60 *s*	1.59 br *s*	CH_3	1.60 *s*	1.59 br *s*

Table 2-7: Comparison of the ^{1}H NMR spectral data (δ, at 500MHz, in $CDCl_3$) of IT4E (**60**) and IT4F (**57**) with those of iridobelamal A and isoiridogermanal (Takahashi *et al.*, 2000) *Data missing from the literature are replaced by question marks.

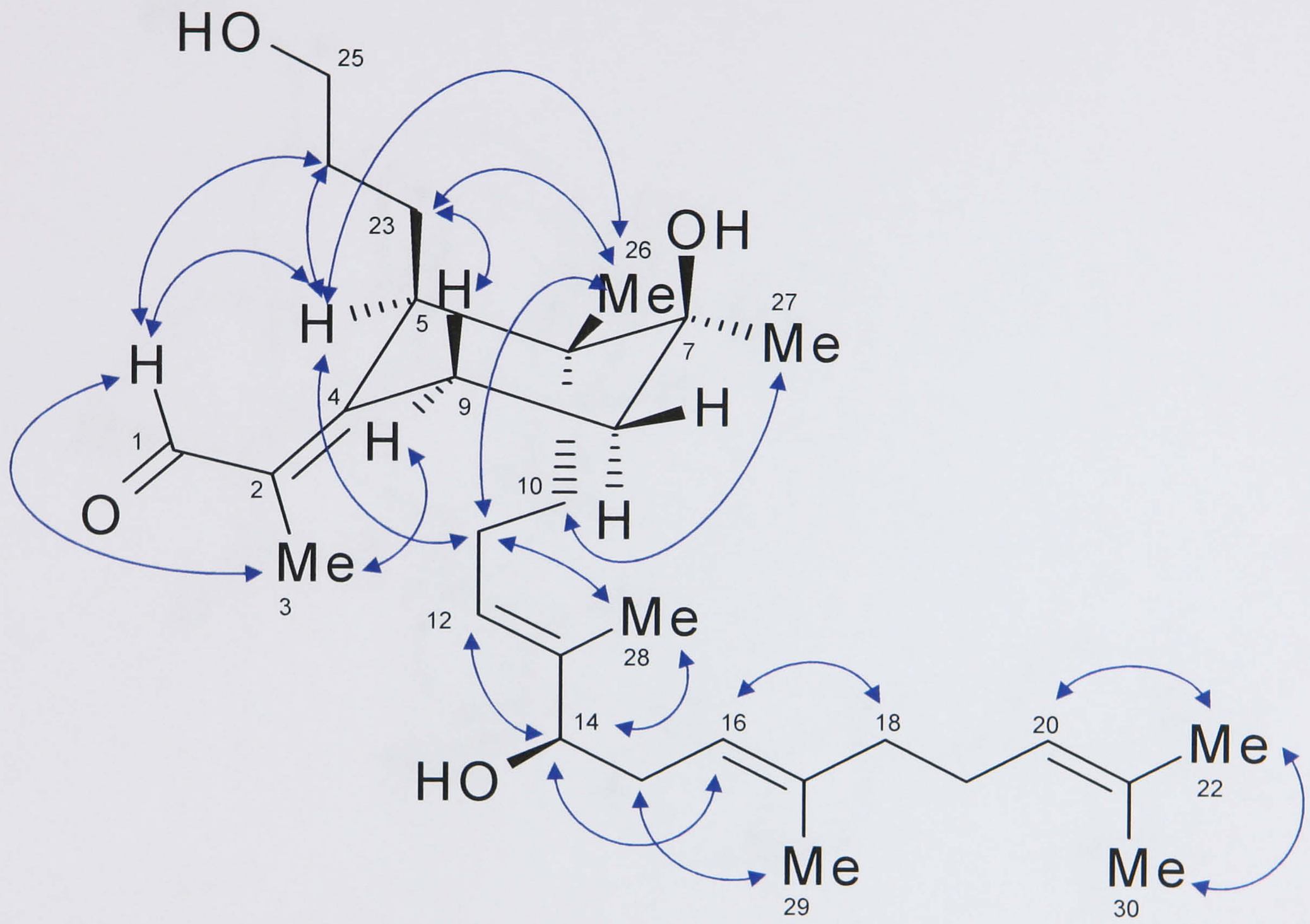

Figure 2-16: Observed NOESY ^{1}H-^{1}H correlation signals and proposed stereostructure of IT4F (**57**) (Some hydrogen atoms omitted for clarity).

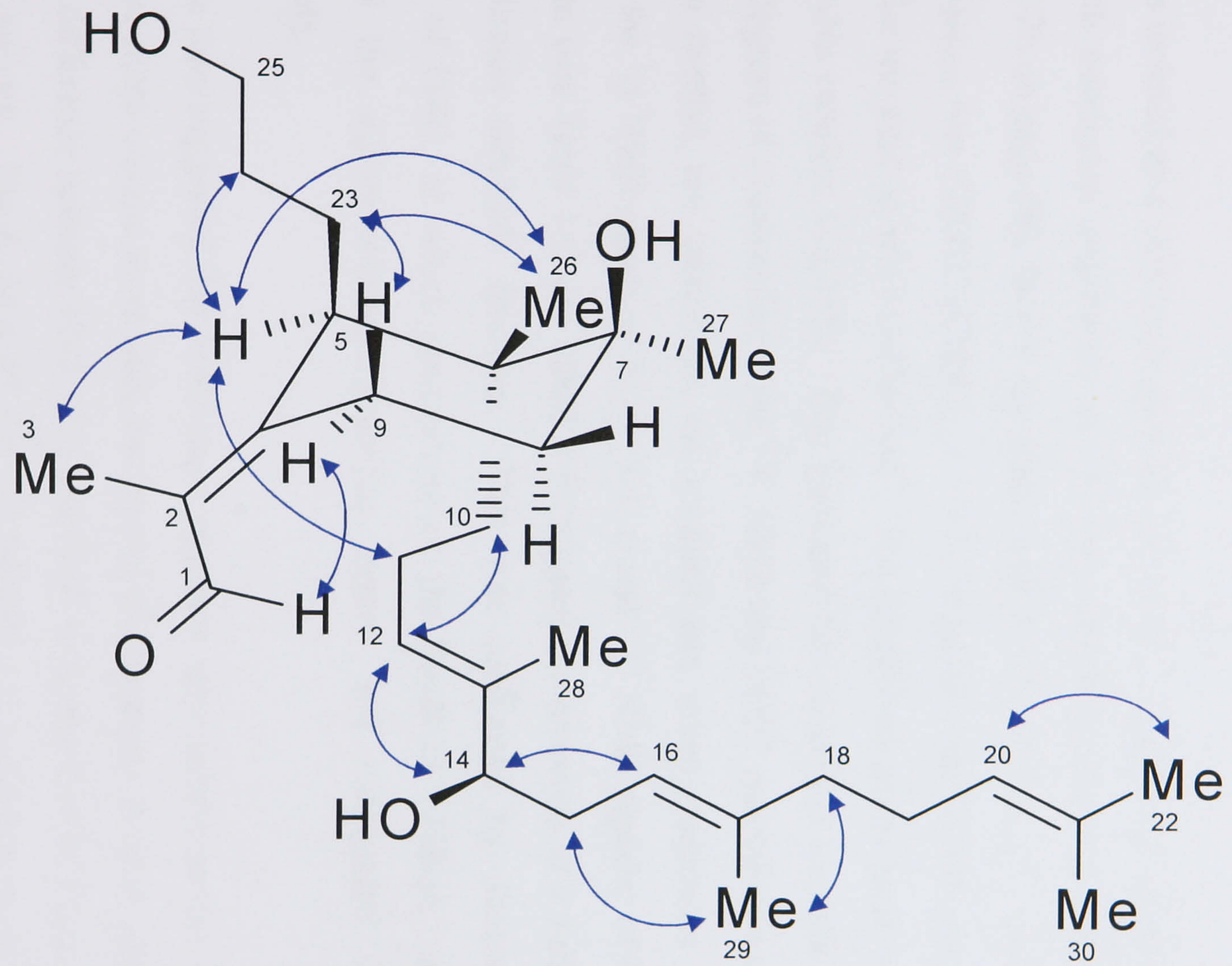

Figure 2-17: Observed NOESY ^{1}H-^{1}H correlation signals and proposed stereostructure of IT4E (**60**) (Some hydrogen atoms omitted for clarity).

2.5.2 Structural elucidation of novel triterpenes IT4C and IT4D

IT4C and IT4D were isolated as minor constituents along with IT4F (**57**) and IT4E (**60**) from 17g of the active sub-fraction IT4, which was obtained from the $CHCl_3$ extract of *Iris tectorum* by the application of vacuum liquid chromatography (VLC) as shown in Figure 2-6 on page 63. IT4C and IT4D showed peaks with retention times of 20 min and 21.3 min, respectively, on the HPLC chromatogram (see Figure 2-14 on page 69).

IT4C was isolated as a yellowish glass like solid, and exhibited a negative CD Cotton effect with maximum absorbance at 251.5nm and minimum absorbance at 338nm (Figure 2-26 on page 98). Its UV spectrum (MeCN) showed $\lambda_{max}(\varepsilon)$: 252.5nm (12.623) and its $[\alpha]_{589nm}$ was +28.02° (CH_2Cl_2, $c = 9.1\times10^{-3}$g/ml); Its ESIMS spectrum showed a molecular ion peak at *m/z* 513 $[M+Na]^+$. The HRESIMS gave a peak at *m/z* 513.359 ($C_{30}H_{50}O_5Na$ requires 513.355). This indicated the molecular formula of $C_{30}H_{50}O_5$, with six degrees of unsaturation. The ^{13}C NMR and DEPT spectra revealed that IT4C has seven methyl, ten methylene, six methine and seven quaternary carbons. In addition, the ^{1}H NMR signal at 10.15 (1H, *s*) and ^{13}C NMR signals, 189.8, 162.6 and 133.3 ppm (see Table 2-8 and Table 2-9) suggest the presence of a fully substituted α,β-unsaturated aldehyde function. This was confirmed by observation of IR spectrum of IT4C, in which absorptions of the bands at 1708cm^{-1} and 1609cm^{-1} suggested the α,β-unsaturated aldehyde stretch and conjugated C=C stretch, respectively.

The above data suggested that IT4C has a structure very similar to that of IT4F (**57**), but has one more oxygen atom than this known triterpenoid. A clear indication of the structural difference between IT4F (**57**) and IT4C was provided by examination of the ^{13}C NMR spectra. The δ_C 61.6 (C-12) and 63.5 (C-13) indicated the likely presence of an epoxide function in IT4C. This was confirmed by the absence of signals for a double bond assigned to 12, 13 in the ^{13}C NMR spectrum of **57**: δ_C 125.3 (C-12) and 137.0 (C-13) (Table 2-8). Moreover, IT4C differed from **57** by an upfield shift of the olefinic H-12 signal (δ_H 5.25) in the ^{1}H NMR spectrum of **57** to δ_H 2.75 in that of IT4C, consistent with an epoxide hydrogen. Similarly the signal for the C-13 methyl (H-28) was shifted upfield from δ_H 1.55 to δ_H 1.20. These values strongly suggested that the double bond at C-12 in IT4F (**57**) was replaced by an epoxide function in

IT4C, giving a proposed structure for the latter as **61**.

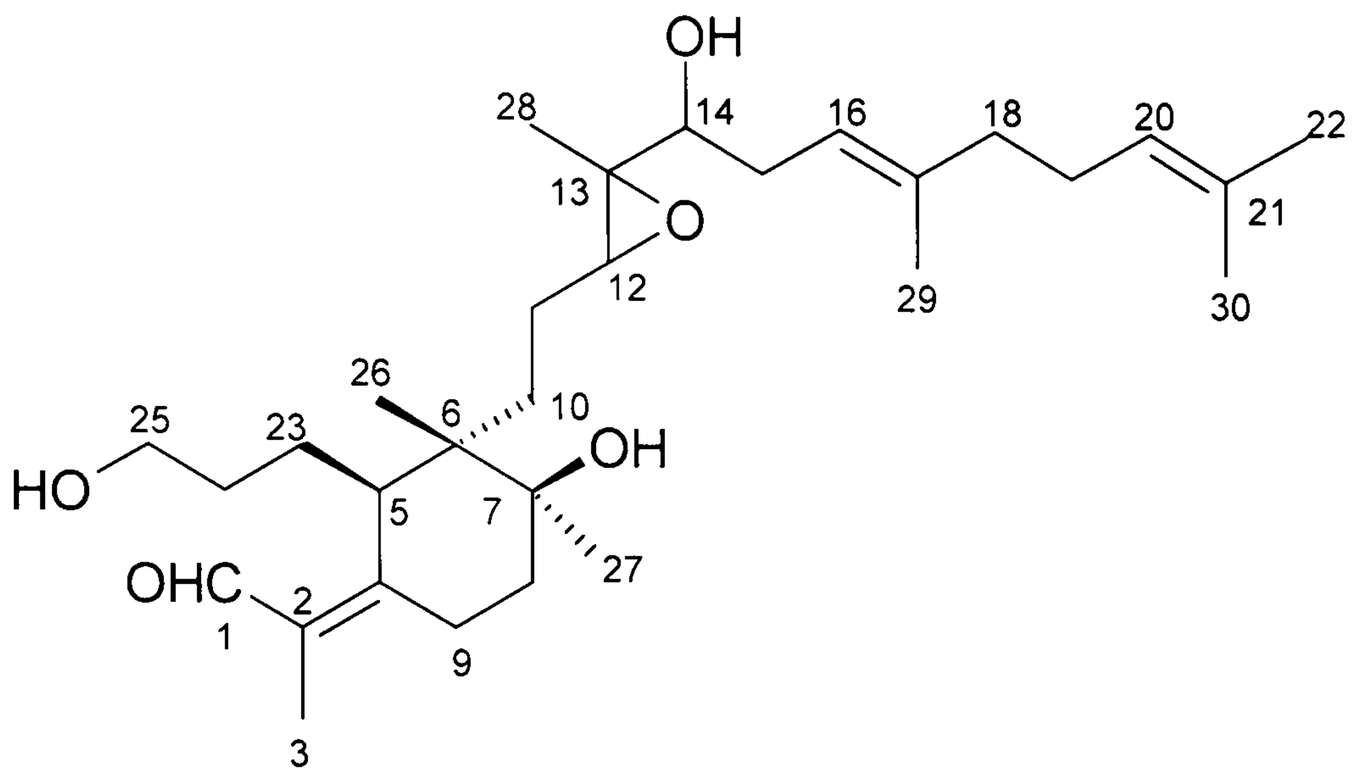

61

A range of compounds with an analogous modification between an epoxide ring and double bond in natural products have been previously reported. For example, leucanthinin (**62**) and 3α-hydroxyenhydrin (**63**) are melampolides isolated from aerial parts of *Melampodium leucanthum* (Quijano *et al.*, 1997). Their ^{1}H NMR data differ from each other by an upfield shift of the olefinic H-5 from δ_H 5.53 in the spectrum of leucanthinin (**62**) to δ_H 3.18 in that of 3α-hydroxyenhydrin (**63**). Meanwhile, the signal for the C-4 methyl (H-15) was shifted from δ_H 1.97 in **62** to1.72 in **63**. These shifts of ^{1}H NMR signals were simply due to the C-4 double bond in **62** was replaced by an epoxide function in **63** (Quijano *et al.*, 1997).

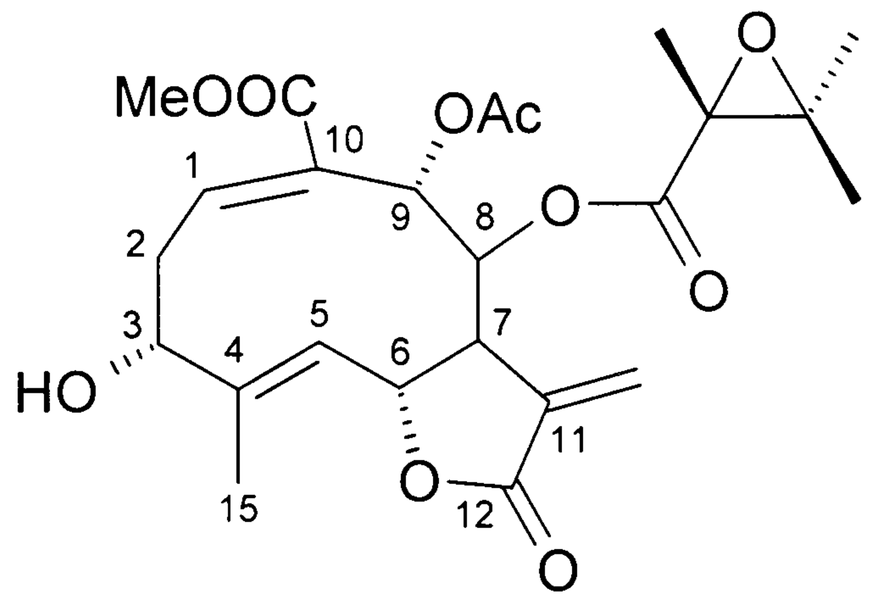

62

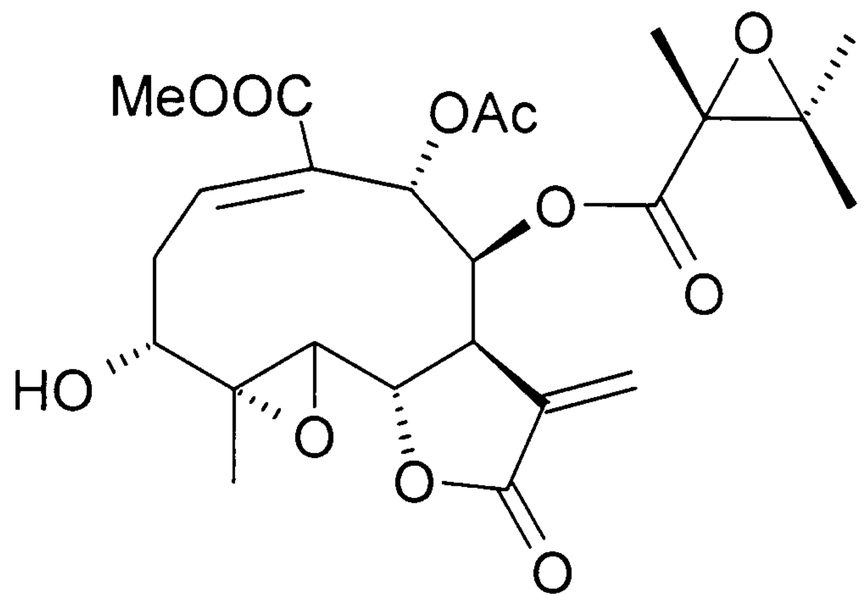

The shifts between these specific functions in the literature are very similar to those observed in the spectra of IT4F (**57**) and IT4C (**61**), and so give extra weight to the confidence in the proposed structure of IT4C (**61**). The structure elucidation of IT4C (**61**) was also supported by a review of a number of literature (Quijano *et al.*, 1997; Lenis *et al.*, 1998; Kubota *et al.*, 2003), which implied that the analogous epoxide function in different compounds exhibited similar signals in NMR spectra (summarized in Table 2-10). Except for the epoxide moiety signals, the spectral data of IT4C (**61**) closely resembled those of IT4F (**57**) (see Table 2-8). The complete structure of IT4C was drawn based on its ^{1}H-^{1}H COSY (Figure 2-20), HMBC (Figure 2-21), HMQC and NOESY measurements. Its proposed stereostructure with NOESY correlation signals is shown as Figure 2-22. IT4C therefore can be defined as (2*Z*)-2-((2*R*,3*S*,4*S*)-4-hydroxy-3-(2-(3-((3*E*)-1-hydroxy-4,8-dimethylnona-3,7-dienyl)-3-methyloxiran-2-yl)ethyl)-2-(3-hydroxypropyl)-3,4-dimethylcyclohexylidene)-propanal, **61**.

IT4D was isolated as a yellowish glasslike solid and exhibited a negative Cotton effect with a maximum absorption at 253.5nm and minimum absorption at 337.5nm in its CD spectrum (Figure 2-26 on page 98). Its UV-spectrum (MeCN) showed $\lambda_{max}(\varepsilon)$: 252.5nm (13,358) and its $[\alpha]_{589nm}$ was –31.06° (CH_2Cl_2, c = 9.4×10^{-3}g/ml). Its ESIMS spectrum showed a molecular ion peak at *m/z* 513 $[M+Na]^+$ and the EIMS gave peak at *m/z* 491 $[M+H]^+$. Its HRESIMS gave a peak of $[M+Na]^+$ at *m/z* 513.359 ($C_{30}H_{50}O_5Na$ requires 513.355), indicating the formula of $C_{30}H_{50}O_5$, with six degrees of unsaturation, identical with that of IT4C (**61**).

The ^{13}C NMR and DEPT spectra revealed that IT4D had seven methyls, ten methylenes, six methines and seven quaternary carbons. In its ^{13}C NMR spectrum,

signals at 125.8(*d*), 135.6 (*s*), 124.3(*d*) and 131.8(*s*) revealed the likely presence of two isolated trisubstituted double bonds. Moreover, the following ^{1}H and ^{13}C NMR signals: δ_H 10.16 (1H, *s*), δ_C 190.1 (*d*), 163.0 (*s*) and 133.2 (*s*) (Table 2-8 and Table 2-9) along with IR ν_{max}: 1713cm^{-1} (CHO) and 1608cm^{-1} (C=C) indicated the presence of a α,β-unsaturated aldehyde function, as that in IT4C (**61**). The relevant evidence for the structure of six-membered ring was obtained by comparison of its NMR data with those of IT4E (**60**) and IT4F (**57**). Moreover, both compounds IT4C (**61**) and IT4D exhibited NOESY correlation between the aldehyde hydrogen H-1 signal and that of H-5, also between the signals of the vinyl methyl H-3 and one H-9 in the NOESY spectrum (see Figure 2-25 on page 96). Therefore, IT4D and IT4C (**61**) have identical structure of the six-membered ring. So far they seem to be isomers.

A possible structure for IT4D as an isomer of IT4C could be the analogous 16,17-epoxide, but this is discounted because the anticipated epoxide signals (at δ_C 61.6 and 63.5 in the spectrum of IT4C) were not present in the spectrum of IT4D. There were, however, signals at δ_C 77.1 (CH from DEPT) and 84.6 (quaternary from DEPT), which are more consistent with a cyclic hydroxyether structure as in **64**. This could secondly be formed by attack by the 14-OH on a formal intermediate 16,17-epoxide, yielding **64**, as shown as Figure 2-18 on page 86.

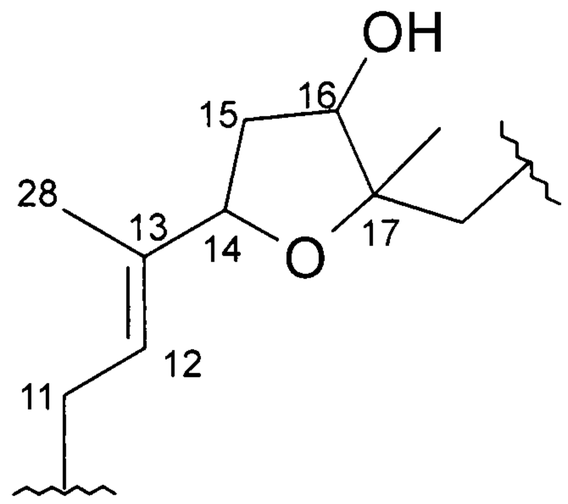

64

An estimation made by ChemDraw® Ultra 2004 (CambridgeSoft Corporation, USA) gave values for δ_C of the tetrahydrofuran moiety as 77.3 (C-14), 39.6 (C-15), 77.9 (C-16), 87.4 (C-17), similarly, ACD/i-Lab® ACD/CNMR Predictor 8.0 (Advanced Chemistry Development Inc., Canada) calculated those δ_C as 79.7 (C-14), 40.5 (C-15), 77.7 (C-16), 85.2 (C-17), which are very near to those observed values: 80.1 (C-14), 39.4 (C-15), 77.1 (C-16), 84.6 (C-17). There is literature precedent for such

rearrangement: some naturally occurring compounds with a similar type of tetrahydrofuran moiety in their structure, had fairly similar ^{13}C NMR signals for carbons 14 ~ 17: [δ_C 76.7 ~ 82.2 (C-14); δ_C 37.9 ~ 40.0 (C-15); δ_C 78.2 ~ 78.7 (C-16); δ_C 81.6 ~ 83.6 (C-17)] (Fan *et al.*, 2001; Praud *et al.*, 1995; Amico *et al.*, 1989; Kimura *et al.*, 1997). As a result, ^{13}C NMR signals of C-14, 15, 16 and 17 in IT4D (**65**) are very similar to those in the spectrum of the literature (see Table 2-11) and strongly suggested the presence of a tetrahydrofuran moiety in IT4D (**65**). Moreover, this structure is likely to be biosynthesized from IT4F (**57**), as demonstrated in Figure 2-18. The proposed structure **65** is supported by the observation of ^{1}H-^{1}H COSY and HMBC (see Figure 2-23 and Figure 2-24 on page 95). Its proposed stereostructure with observed NOESY correlation signals is shown as Figure 2-25. Thereby, the whole molecule can thus be defined as (2*Z*)-2-((2*R*,3*S*,4*S*)-4-hydroxy-3-((3*E*)-4-(4-hydroxy-5-methyl-5-(4-methylpent-3-enyl)-tetrahydrofuran-2-yl)pent-3-enyl)-2-(3-hydroxypropyl)-3,4-dimethylcyclohexylidene)-propanal, **65**.

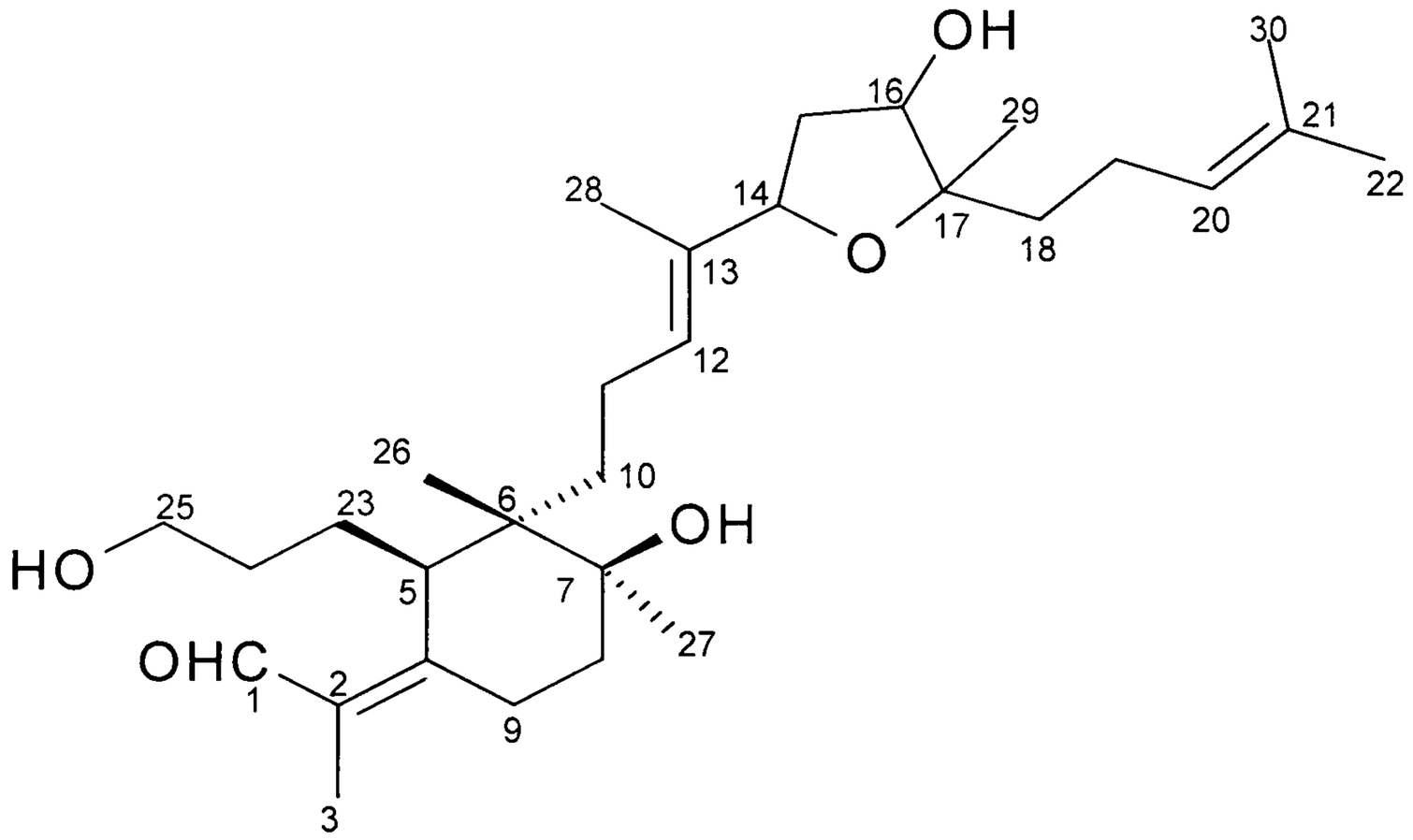

65

The ^{13}C and ^{1}H NMR data of these isolated triterpenes are summarized in Table 2-8 and Table 2-9. The IR, UV and CD spectra, and optical rotation behaviour of them showed a striking resemblance to one another (Figure 2-26 page 98 and Figure 2-27 page 100).

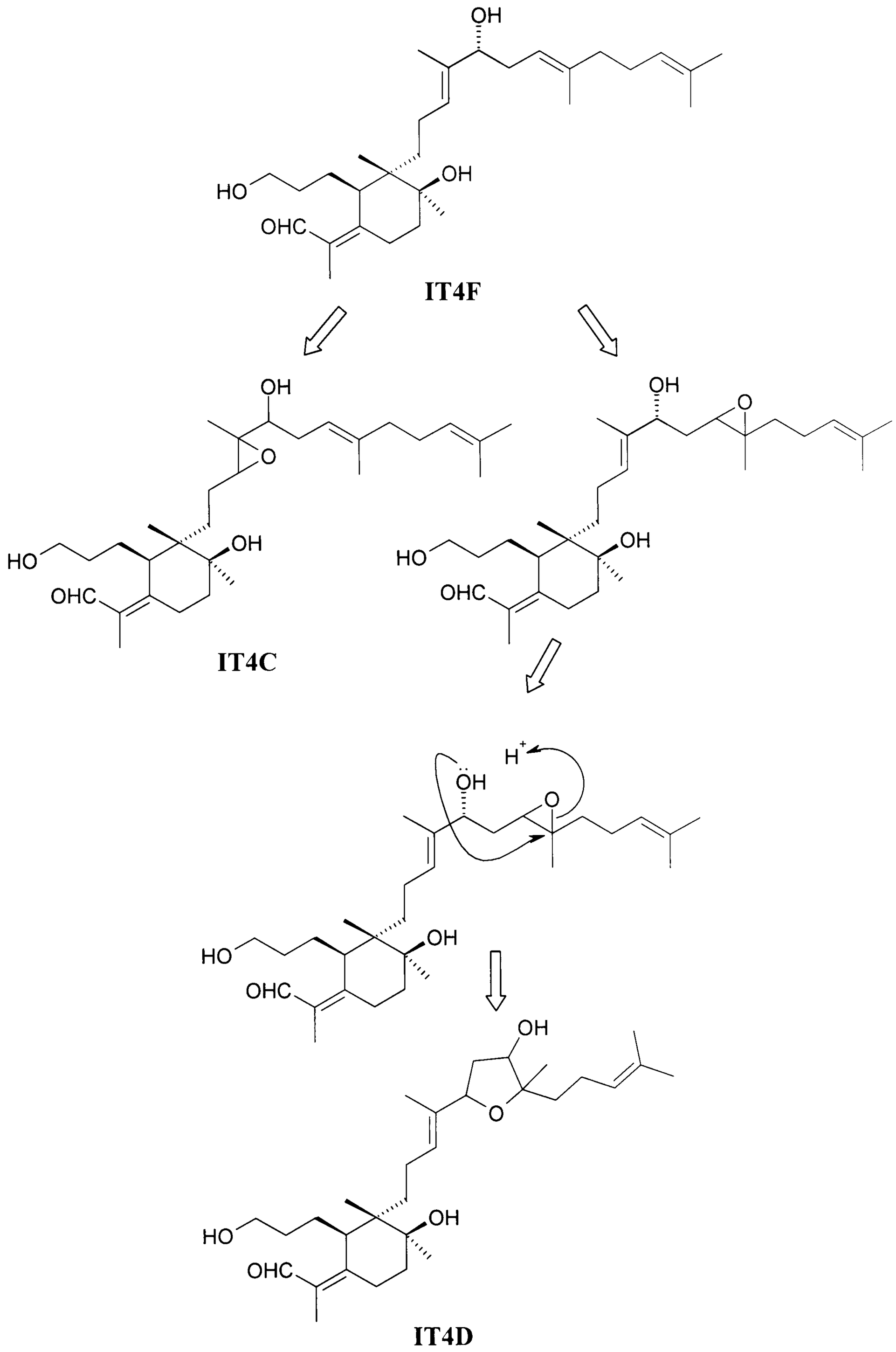

Figure 2-18: Possible subsequent biosynthetic route of IT4C (**61**) and IT4D (**65**) from IT4F (**57**)

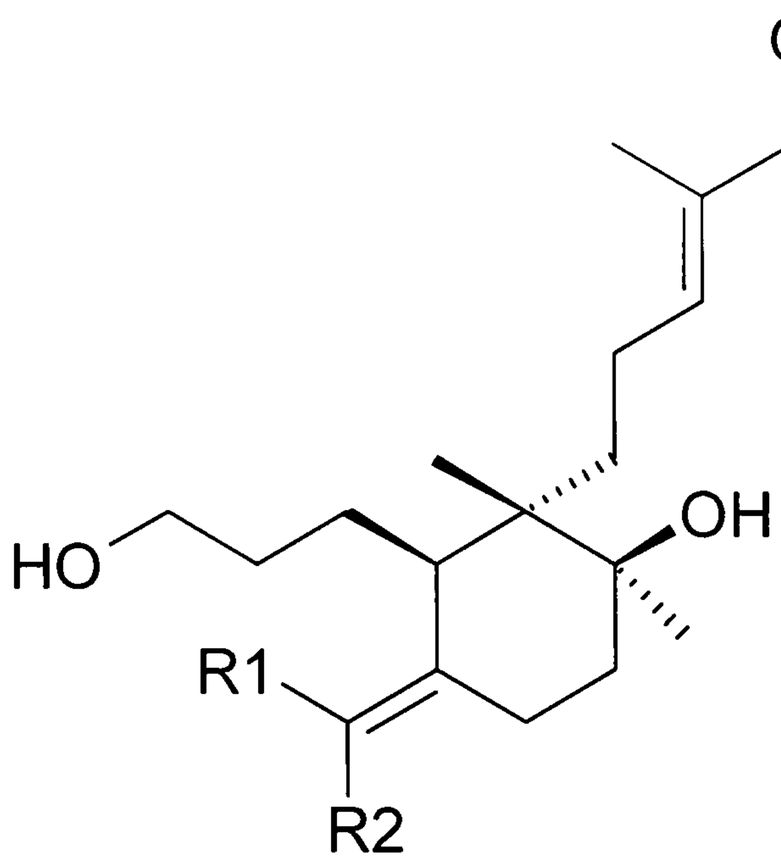

	R1	R2
57	CHO	Me
60	Me	CHO

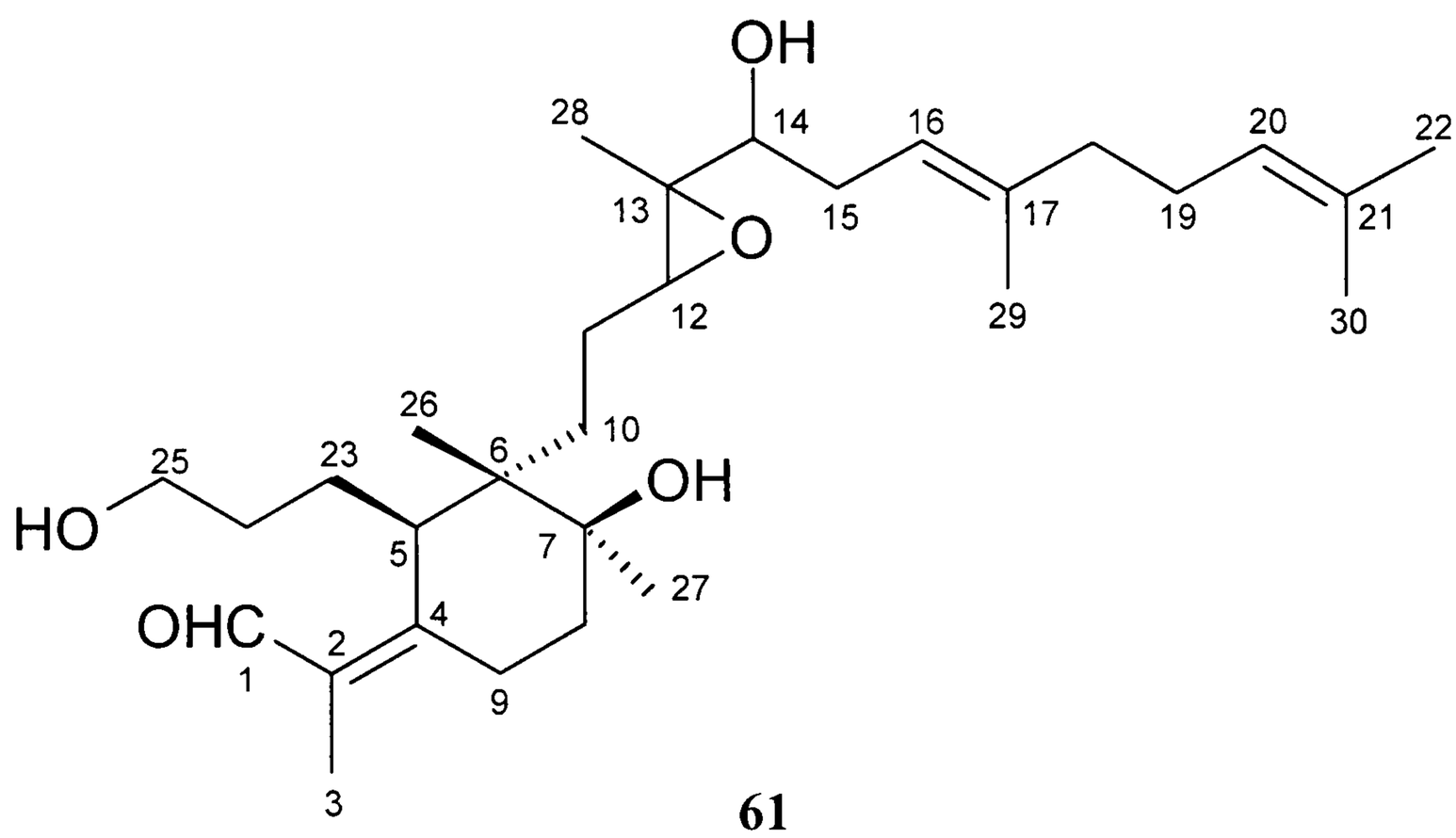

61

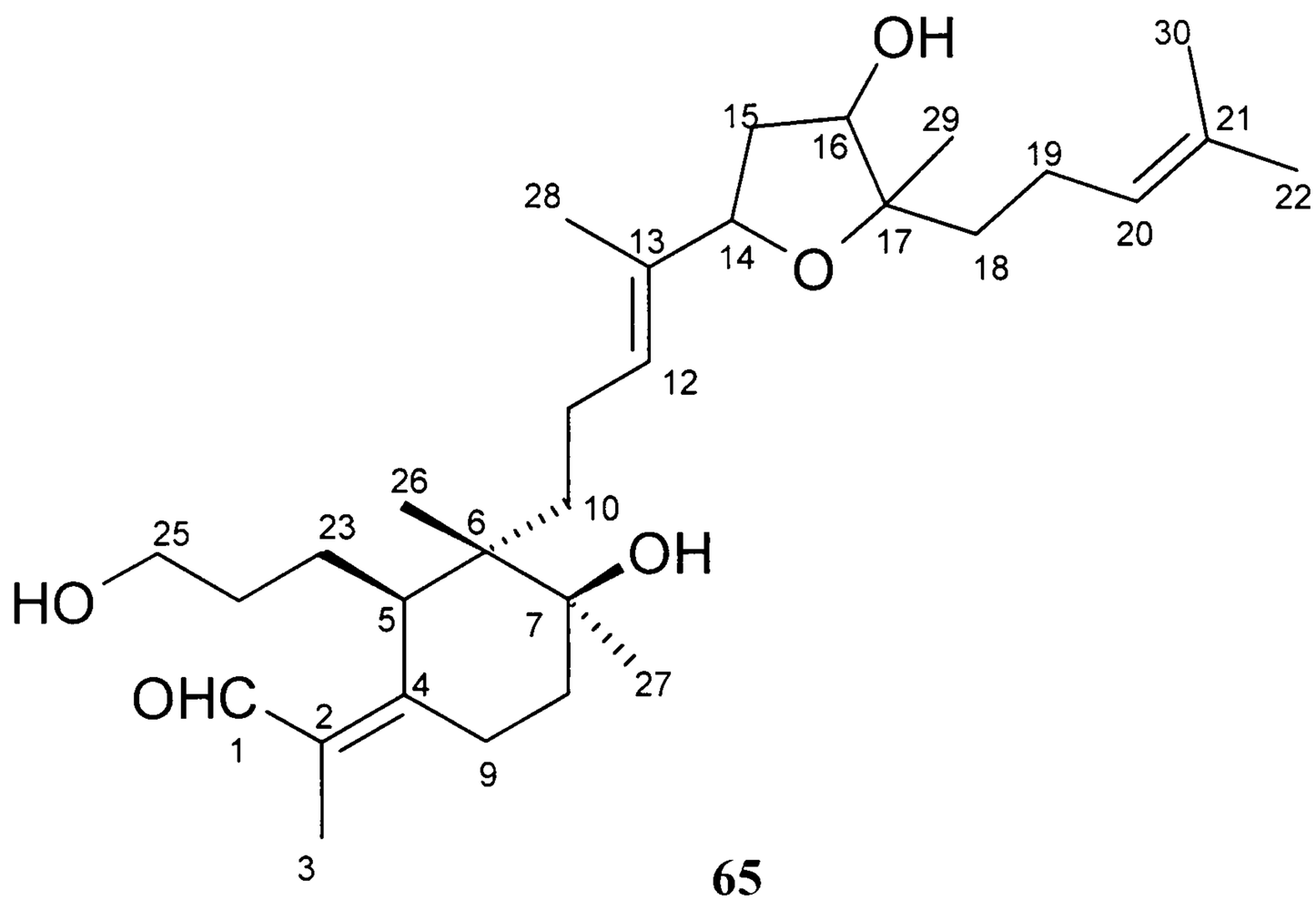

65

Figure 2-19: Summary of structures of IT4C (**61**), IT4D (**65**), IT4E (**60**) and IT4F (**57**)

Carbon No.	IT4C (61)	IT4D (65)	IT4E (60)	IT4F (57)
1	189.8	190.1	190.7	190.0
2	133.3	133.2	133.1	133.2
3	11.0	11.0	11.9	11.0
4	162.6	163.0	163.5	162.8
5	43.6	43.4	47.3	43.4
6	44.5	44.7	45.2	44.7
7	74.9	75.1	75.2	75.0
8	37.0	37.0	38.0	37.0
9	23.8	23.9	20.0	23.8
10	33.7	36.7	36.9	36.9
11	22.6	21.9	23.0	21.8
12	61.6	125.8	125.7	125.3
13	63.5	135.6	136.9	137.0
14	75.5	80.1	76.8	76.7
15	31.8	39.4	34.3	34.2
16	119.1	77.1	119.9	119.9
17	138.8	84.6	138.9	138.8
18	39.8	38.8	39.8	39.8
19	26.5	22.7	26.5	26.5
20	124.0	124.3	124.1	124.1
21	131.7	131.8	131.7	131.7
22	25.7	25.7	25.7	25.7
23	26.6	26.6	27.1	26.6
24	32.6	32.7	32.0	32.7
25	63.0	63.0	63.2	63.1
26	18.0	17.9	17.8	18.0
27	26.3	26.3	26.4	26.3
28	12.1	11.7	11.9	11.9
29	16.2	20.0	16.3	16.3
30	17.7	17.7	17.7	17.7

Table 2-8: ^{13}C NMR data of IT4C (**61**) ~ IT4F (**57**) (δ, at 125MHz, in $CDCl_3$ with TMS as internal standard). Assignments were based on DEPT, HMQC and HMBC experiments.

^{1}H	IT4C (61)	IT4D (65)	IT4E (60)	IT4F (57)
1	10.15 *s*	10.16 *s*	10.24 *s*	10.18 *s*
3	1.84 *s*	1.83 *s*	1.80 *s*	1.83 *s*
5	3.22 *br d* (*J*=10.1Hz)	3.30 *br d* (*J*=11.0Hz)	2.79 *br d* (*J*=9.9Hz)	3.31 *br d* (*J*=11.1Hz)
8	1.72 *m* 1.87 *m*	1.67 *m* 1.85 *m*	1.62-1.71 *m* 1.79-1.87 *m*	1.65 *m* 1.87 *m*
9	2.57 apparent *br t* (*J*=13.6Hz) 2.60 apparent *td* (*J*=13.6, 4.7Hz)	2.54 apparent *br t* (*J*=13.4Hz) 2.59 apparent br *td* (*J*=13.7, 4.6Hz)	3.22 apparent *br d* (*J*=13.9Hz) 2.59 apparent br *td* (*J*=13.9, 2.3Hz)	2.55 apparent *br t* (*J*=13.5Hz) 2.60 apparent *td* (*J*=14.0, 4.7Hz)
10	1.29-1.46 *m*	1.17-1.21 *m* 1.28-1.32 *m*	1.13 -1.32 *m*	1.18 *m* 1.32 *m*
11	1.33-1.49 *m*	1.82-1.68 *m* 1.93-1.98 *m*	1.90-1.96 *m* 1.99-2.10 *m*	1.86 *m* 1.96 *m*
12	2.75 *m*	5.32 *t* (*J*=6.9Hz)	5.26 *t* (*J*=6.8Hz)	5.25 *t* (*J*=7Hz)
14	3.26 *dd* (*J*=7.8, 5.7Hz)	4.19 apparent *t* (*J*=7.6Hz)	3.93 *dd* (*J*=7.5, 5.1Hz)	3.92 *dd* (*J*=7.8, 5.1Hz)
15	2.18-2.29 *m*	2.35 *ddd* (*J*=13.3, 8.0, 5.3Hz) 1.75 *m*	2.13-2.33 *m*	2.22 *m*

Continued on next page

Table 2-9: ^{1}H NMR data of IT4C (**61**) ~ IT4F (**57**) (δ, at 500MHz, in $CDCl_3$ with TMS as internal standard), assignments were based on ^{1}H-^{1}H COSY and HMQC experiments.

Continued from previous page

^{1}H	IT4C (61)	IT4D (65)	IT4E (60)	IT4F (57)
16	5.08 *m*	4.03 apparent *t* (*J*=5.8Hz)	5.07 *m*	5.07 *m*
18	2.02 *br d* (*J*=6.3Hz)	1.38-1.53 *m*	2.02 *br d* (*J*=6.5Hz)	2.02 *m*
19	2.07 *m*	2.04 *m*	2.07 *m*	2.07 *m*
20	5.06 *m*	5.10 *t* (*J*=7.0Hz)	5.06 *m*	5.06 *m*
22	1.68 *s*	1.68 *s*	1.68 *s*	1.68 *s*
23	1.79 *m* 2.03 *m*	1.78 *m* 2.05 *m*	1.80 *m* 2.10 *m*	1.79 *m* 2.03 *m*
24	1.21-1.28 *m*	1.23-1.29 *m* 1.35-1.39 *m*	1.33-1.41 *m*	1.26 *m* 1.40 *m*
25	3.61 apparent *t* (*J*=6.4Hz)	3.61 apparent *t* (*J*=6.4Hz)	3.61 apparent *td* (*J*=6.3, 2.3Hz)	3.61 apparent *t* (*J*=6.4Hz)
26	1.08 *s*	1.08 *s*	1.09 *s*	1.10 *s*
27	1.18 *s*	1.15 *s*	1.16 *s*	1.16 *s*
28	1.20 *s*	1.56 *s*	1.60 *s*	1.55 *s*
29	1.62 *s*	1.23 *s*	1.63 *s*	1.62 *s*
30	1.60 *s*	1.61 *s*	1.60 *s*	1.60 *s*

Table 2-9: ^{1}H NMR data of IT4C (**61**) ~ IT4F (**57**) (δ, at 500MHz, in $CDCl_3$ with TMS as internal standard), assignments were based on ^{1}H-^{1}H COSY and HMQC experiments.

	IT4C (61)		(6*S*,7*R*,8*R*)-6,7-Epoxy-8-hydroxydendrolasin		Piericidin C_5		3α-hydroxyenhydrin	
Solvent	$CDCl_3$ (at 125/500MHz)		$CDCl_3$ (at 125/500MHz)		$CDCl_3$		$CDCl_3$ (at 100/400MHz)	
Position	^{13}C	^{1}H	^{13}C	^{1}H	^{13}C	^{1}H	^{13}C	^{1}H
11	22.6	1.33-1.49 *m*	28.6	1.82 *m*	21.4	1.65 *d* (*J*=7.6, 6.4Hz) 1.56 *d* (*J*=7.6, 6.4Hz)	—	—
12	61.6	2.75 *m*	59.1	3.16 *t* (*J*=6.2Hz)	64.1	2.79 *t* (*J*=6.4Hz)	57.5	3.18 *d* (*J*=9.5Hz)
13	63.5	—	62.6	—	62.6	—	61.4	—
14	75.5	3.26 *dd* (*J*=7.8, 5.7Hz)	73.0	3.59 *dd* (*J*=8.0, 3.8Hz)	81.8	2.90 *d* (*J*=8.9Hz)	69.8	4.19 *br d* (*J*=6Hz)
15	31.8	2.18-2.29 *m*	31.4	2.27 *br* ? 2.13 *br* ?	—	—	29.9	3.11 *ddd* (*J*=14, 10, ~1Hz) 2.85 *ddd* (*J*=14, 8, 8Hz)
16	119.1	5.08 *m*	119.8	5.20 *t* (*J*=1.2)	—	—	147.7	7.23 *dd* (*J*=10, 7.5Hz)
17	138.8	—	134.1	—	—	—	133.1	—
28	12.1	1.20 *s*	14.3	1.26 *s*	11.0	1.30 *s*	16.0	1.72 *s*

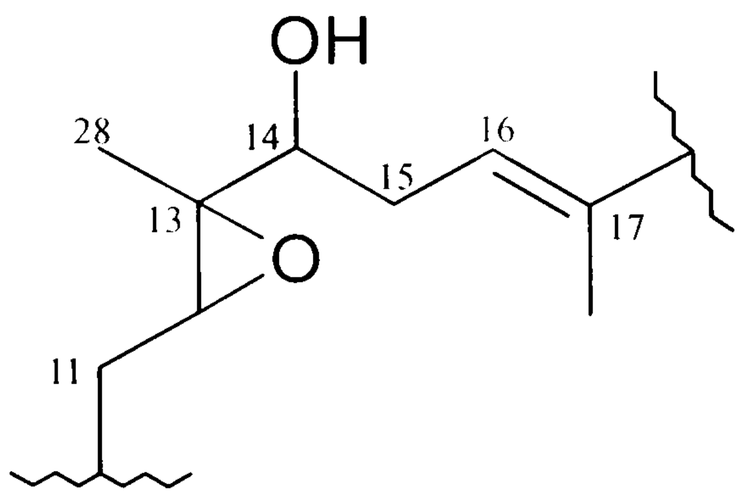

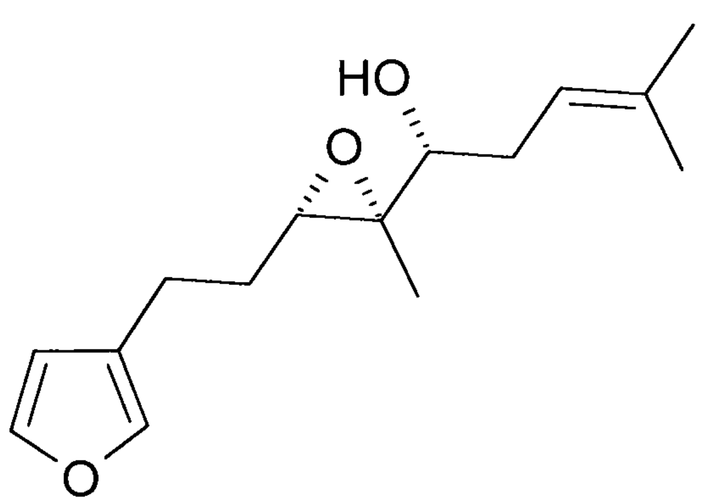

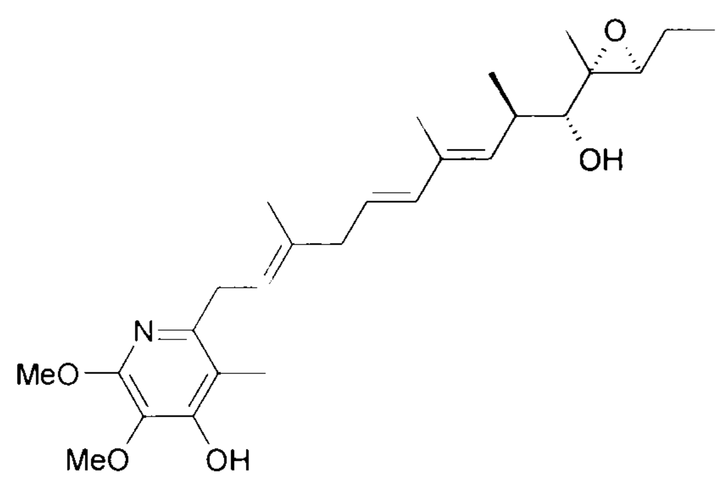

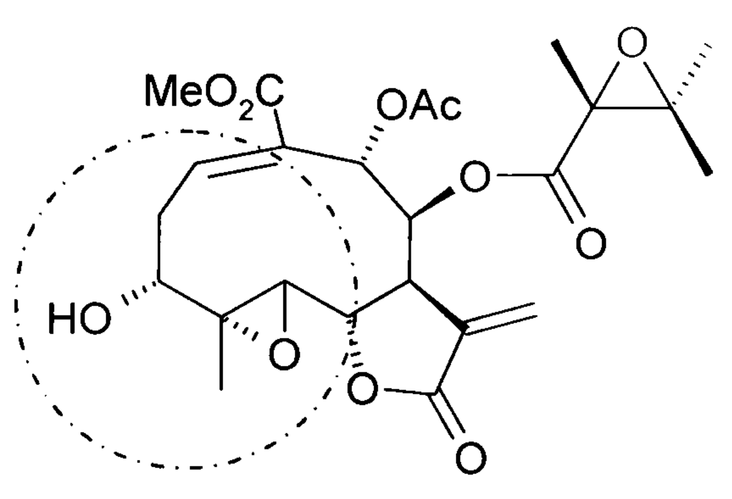

Table 2-10: Comparison of the ^{13}C and ^{1}H NMR spectral data of the epoxy moieties in IT4C (**61**), (6*S*,7*R*,8*R*)-6,7-Epoxy-8-hydroxydendrolasin, piericidin C_5 and 3α-hydroxyenhydrin (Lenis *et al.*, 1998; Kubota *et al.*, 2003; Quijano *et al.*, 1997).

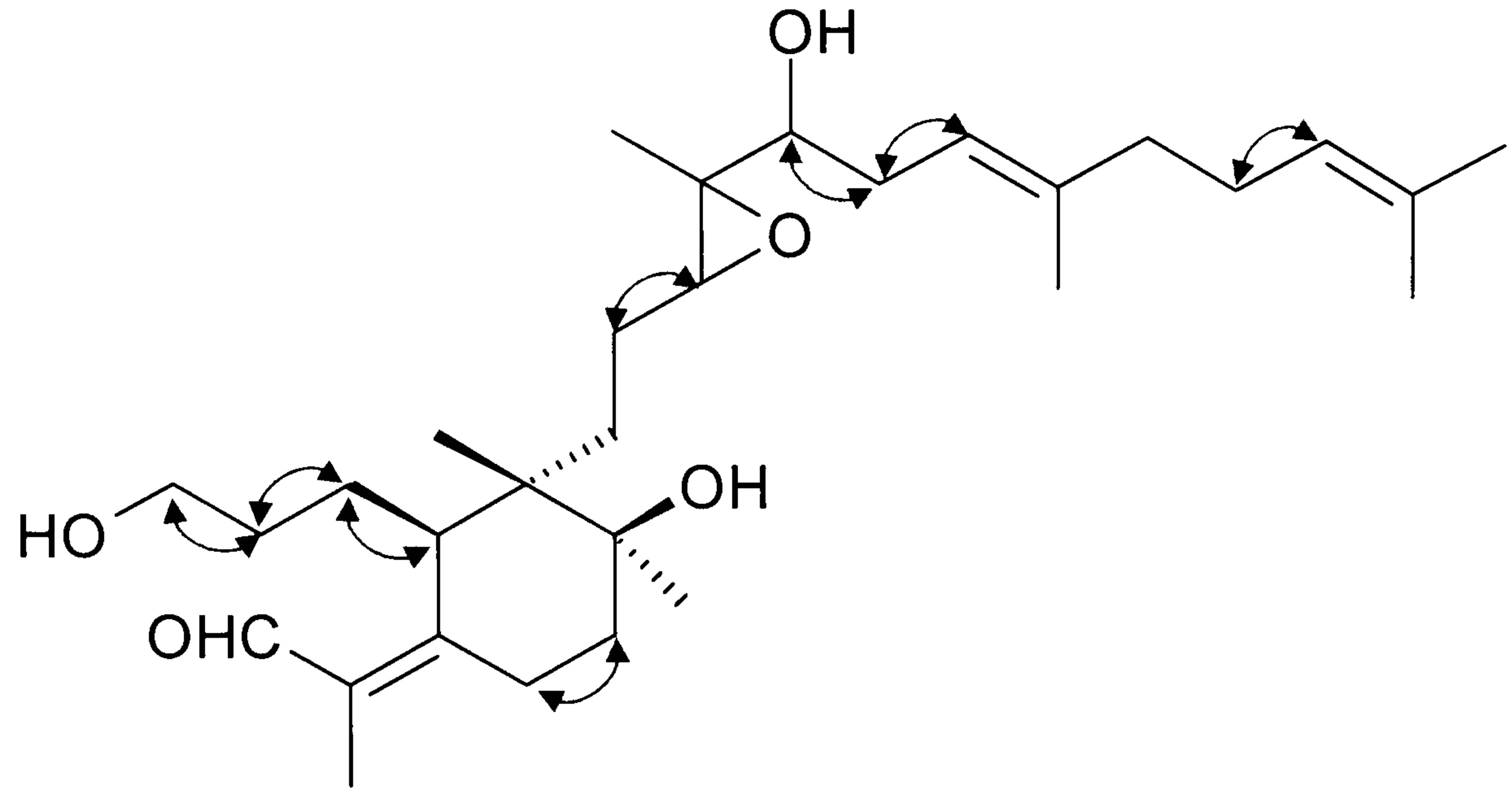

Figure 2-20: Observed correlations of the spin-spin coupled protons in ^{1}H-^{1}H COSY spectrum of IT4C (**61**)

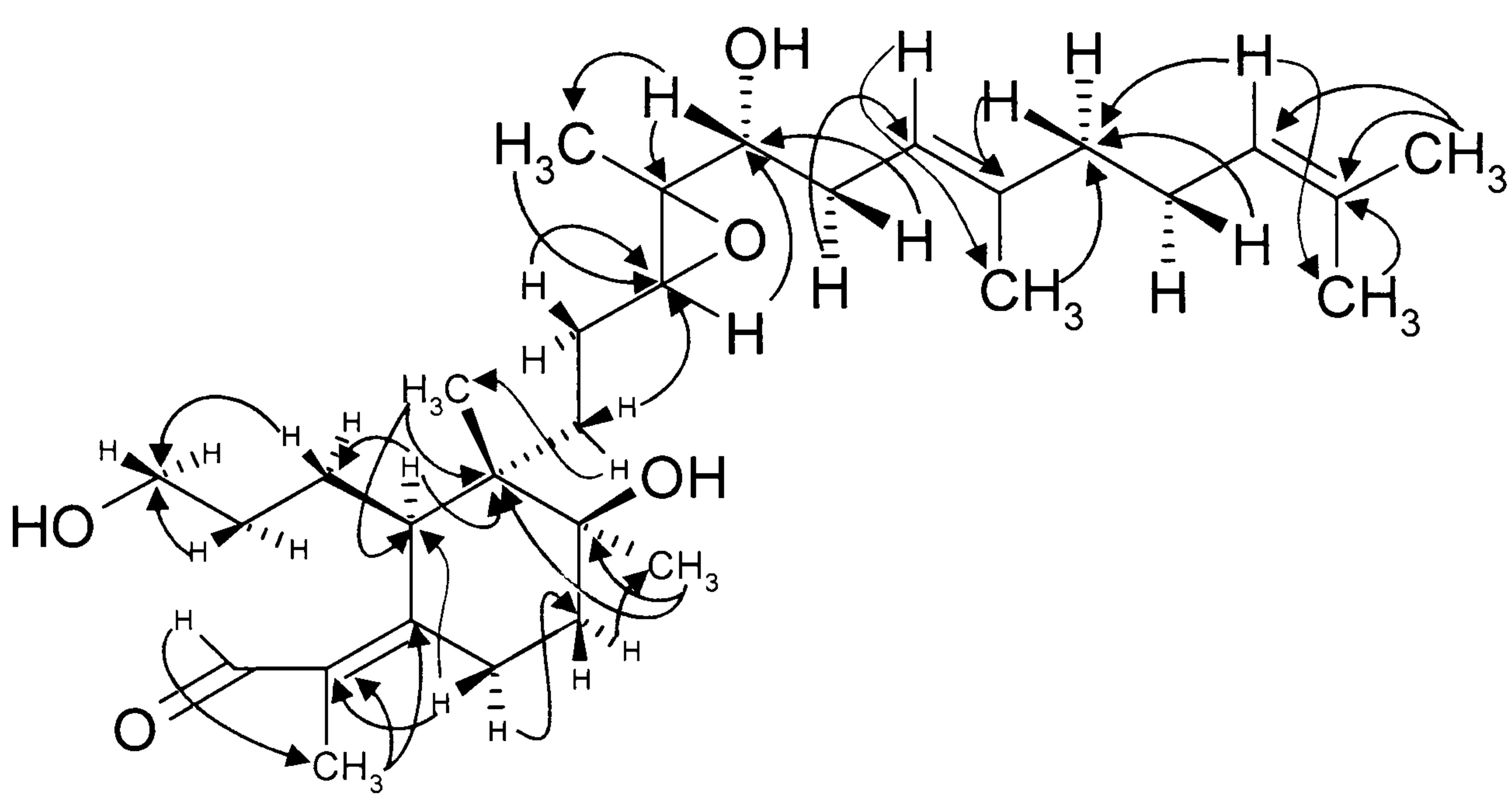

Figure 2-21: Observed HMBC (long-range ^{1}H-^{13}C COSY spectra) correlations of IT4C (**61**)

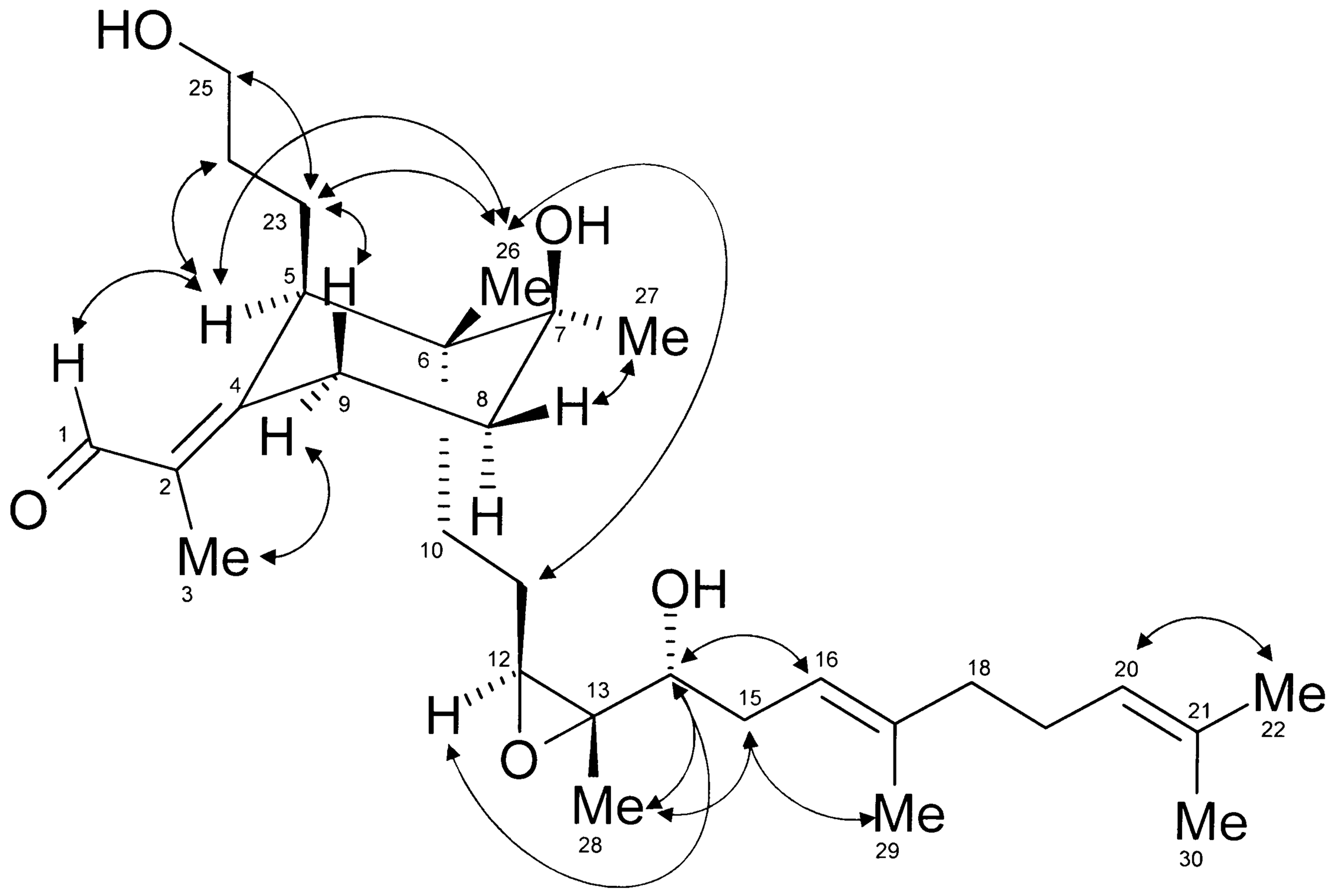

Figure 2-22: Observed NOESY ^{1}H-^{1}H correlation signals and proposed stereostructure of IT4C (**61**) (Some hydrogen atoms omitted for clarity).

	IT4D (65)		**Sachalinols B**		**Cyclokirilodiol**		**Meroditerpene-3**	
Solvent	$CDCl_3$ (at 125/500MHz)		CD_3OD (at 100/400MHz)		$CDCl_3$ (at 100/400MHz)		C_6D_6 (at 100/400MHz)	
Position	^{13}**C**	^{1}**H**	^{13}**C**	^{1}**H**	^{13}**C**	^{1}**H**	^{13}**C**	^{1}**H**
11	21.9	1.82-1.68 *m* 1.93-1.98 *m*	—	—	—	—	26.0	2.18*m*
12	125.8	5.32 *t* (*J*=6.9Hz)	125.9	5.65 *t* (*J*=6.6Hz)	—	—	124.4	5.64 *t* (*J*=7Hz)
13	135.6	—	139.0	—	—	—	135.9	—
14	80.1	4.19 apparent *t* (*J*=7.6Hz)	82.2	4.50 *t* (*J*=8.1Hz)	76.7	4.01 *ddd* (*J*=1.8, 8.1, 8.1Hz)	79.9	4.34 *br t* (*J*=7.3Hz)
15	39.4	2.35 *ddd* (*J*=13.3, 8.0, 5.3Hz) 1.75 *m*	39.8	2.06 *ddd* (*J*=12.9, 8.1, 6.1Hz) 1.99 *ddd* (*J*=12.9, 8.1, 3.9Hz)	38.7	1.67 *ddd* (*J*=4.8, 81, 13.6Hz) 2.25 *ddd* (*J*=7.0, 8.1, 13.6Hz)	40.0	2.20 *m* 1.80 *m*
16	77.1	4.03 apparent *t* (*J*=5.8Hz)	78.5	3.95 *dd* (*J*=6.1, 3.9Hz)	78.2	3.91 *dd* (*J*=4.8, 7.0Hz)	78.4	3.82 *dd* (*J*=6.2, 5.7Hz)
17	84. 6	—	84.4	—	81.7	—	82.7	—
28	11.7	1.56 *s*	12.0	1.61 *s*	—	—	12.1	1.70 *s*
	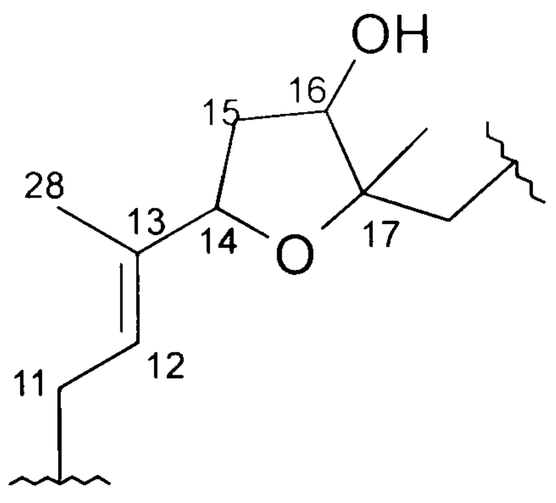		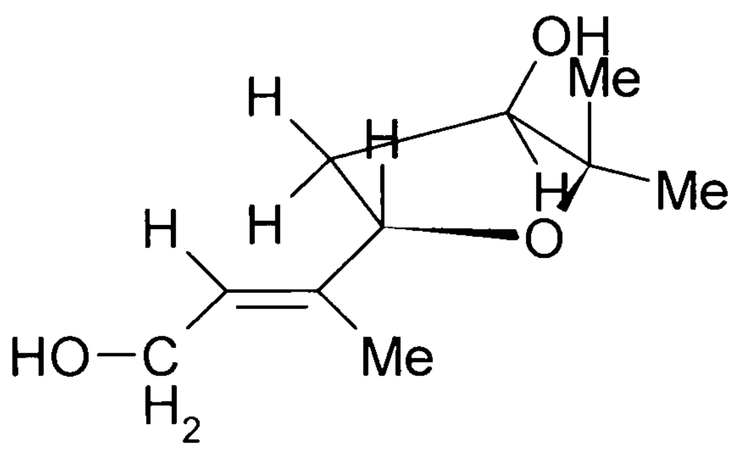		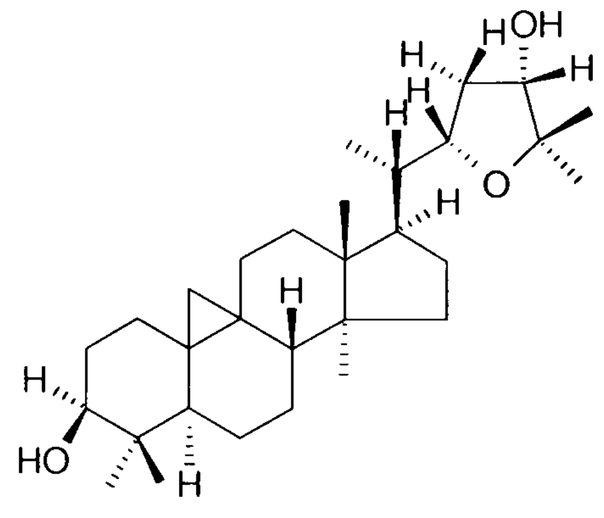		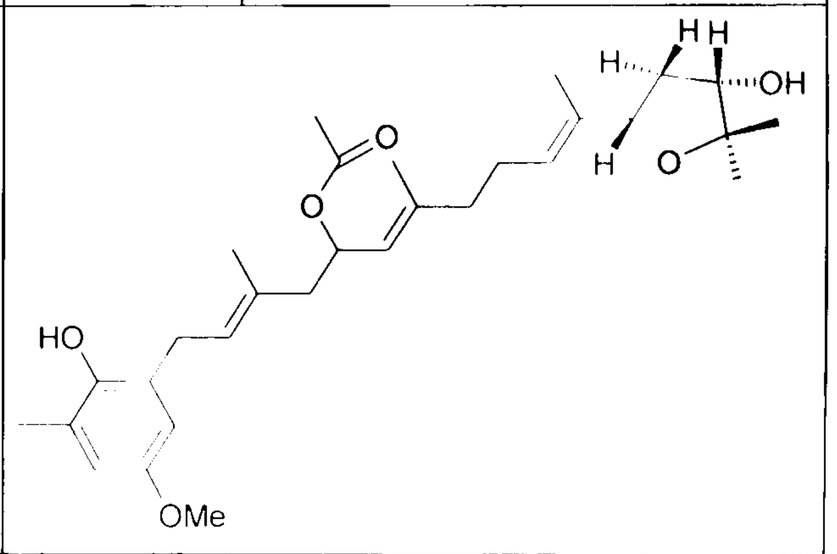	

Table 2-11: Comparison of the ^{13}C and ^{1}H NMR spectral data of the tetrahydrofuran moieties in IT4D (**65**), sachalinols B, cyclokirilodiol and meroditerpene-3 (Fan *et al.*, 2001; Praud *et al.*, 1995; Kimura *et al.*, 1997).

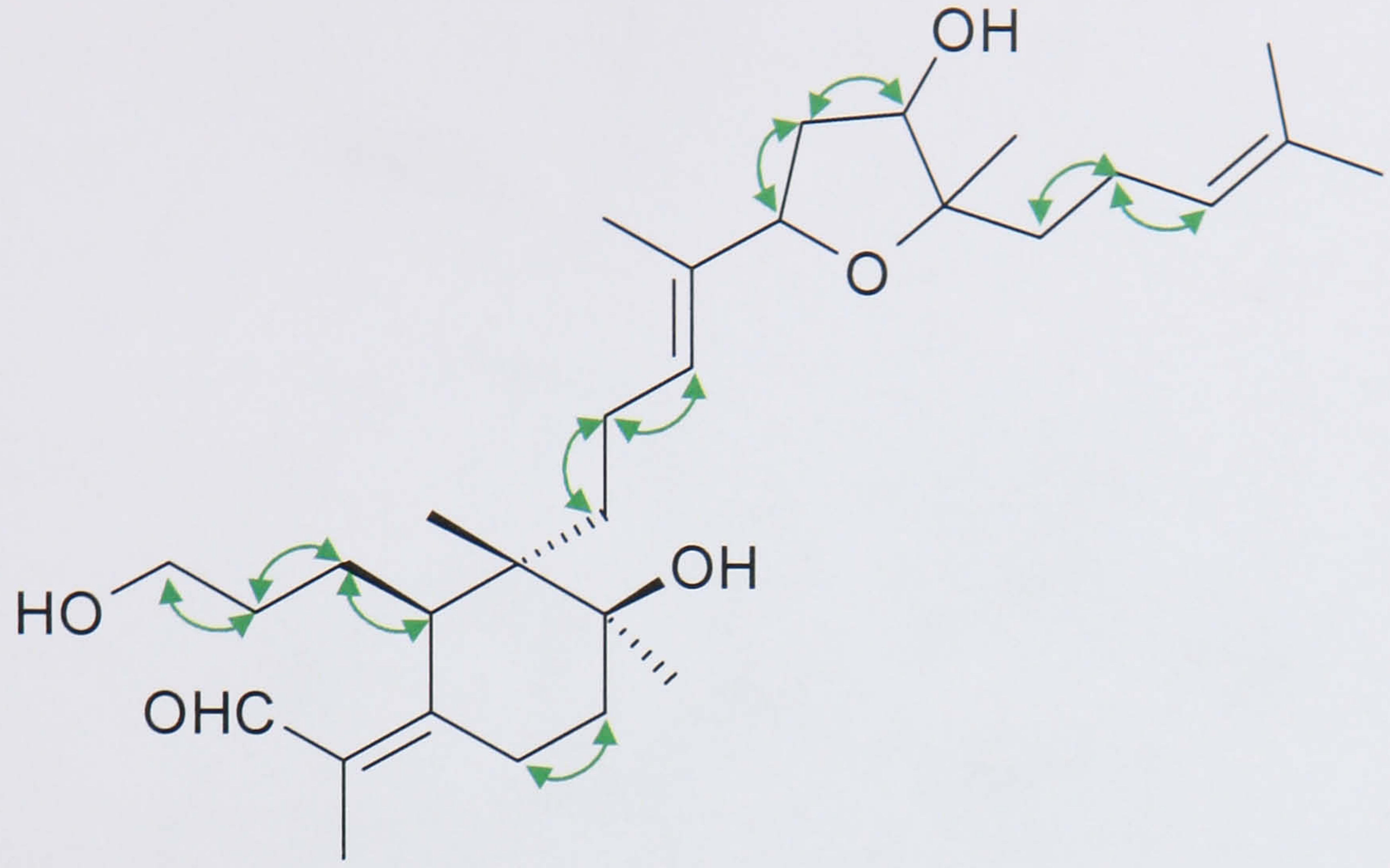

Figure 2-23: Observed correlations of the spin-spin coupled protons in ^{1}H-^{1}H COSY spectrum of IT4D (**65**)

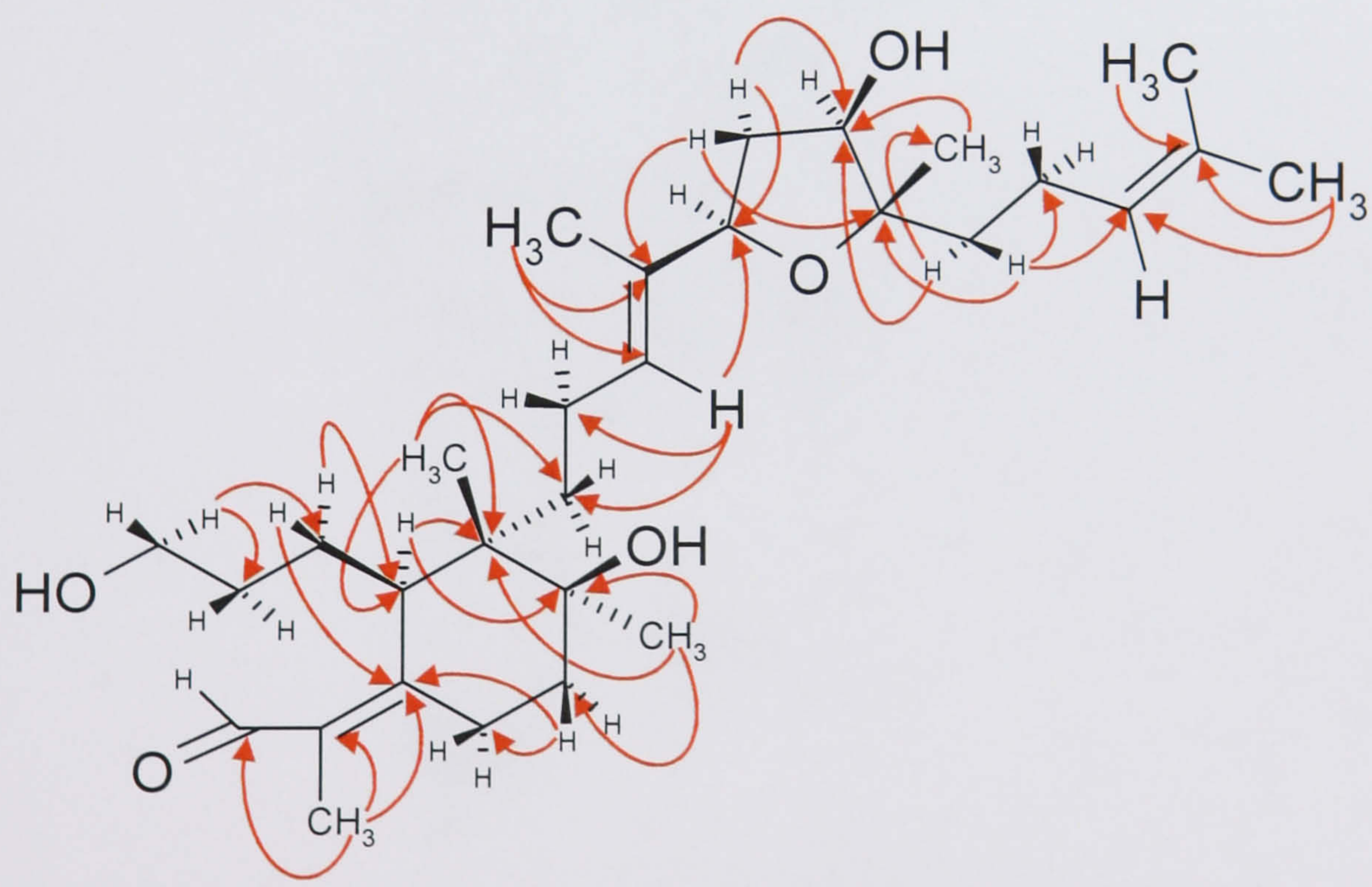

Figure 2-24: Observed HMBC (long-range ^{1}H-^{13}C COSY spectra) correlations of IT4D (**65**)

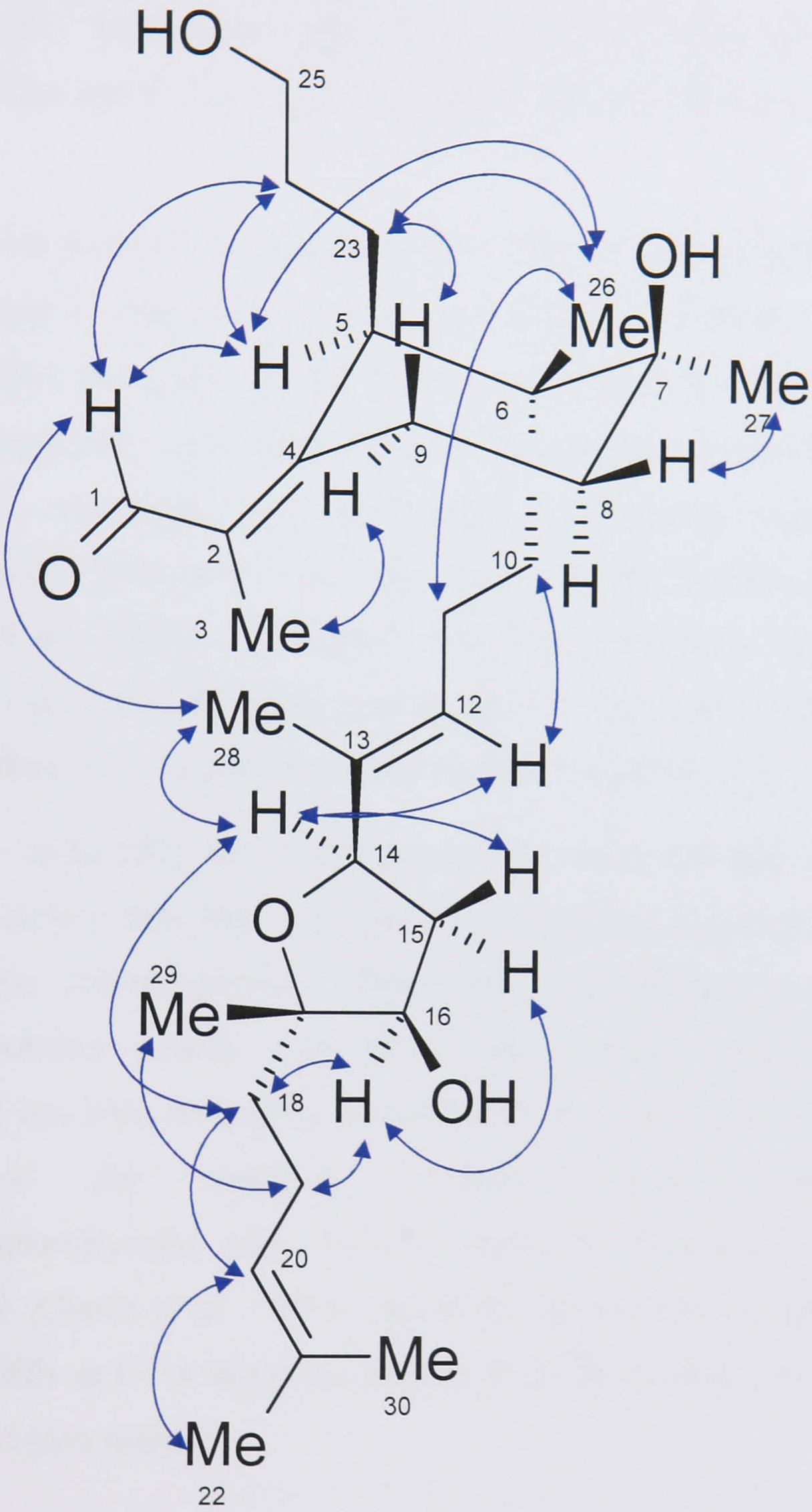

Figure 2-25: Observed NOESY ^{1}H-^{1}H correlation signals and proposed stereostructure of IT4D (**65**) (Some hydrogen atoms omitted for clarity).

Compounds IT4C (**61**), IT4D (**65**) and IT4F (**57**) were prepared in acetonitrile solution. Dilutions were then made to obtain an optimal concentration for CD determination. The spectra were acquired on a Jasco J720 spectrpolarimeter at 0.4 mg/ml. A rectangular cell with 1mm path length was employed in the region of 420–180nm wavelength. The following parameters were used: 2nm bandwidth, 4s time constant, 20nm/min speed and 0.5nm step size. All spectra were solvent baseline subtracted.

The CD spectra for iridals IT4C (**61**) and IT4D (**65**) are similar to that of IT4F (**57**). They all had negative Cotton effect with a maximum absorption around 253.5nm and minimum (multiple) absorption around 337.5nm (as shown in Table 2-12 and Figure 2-26), which are typically associated with π-π^* (conjugated carbonyl group) and n-π^* (carbonyl group) transitions in an asymmetric environment, respectively. This observation coincides with those of isoiridogermanal in the literature (Takahashi *et al.*, 2000; Miyake *et al.*, 1997). In addition, the NOE correlation signals of the six-membered ring observed in 2D NMR spectra of IT4C (**61**) and IT4D (**65**) are highly coincident with those of isoiridogermanal in the literature (Seki *et al.*, 1994b).

The monocyclic iridal (**57**) and iridals having an epoxy-function such as (**61**) or tetrahydrofuran moiety (**65**) have only an α,β–unsaturated aldehyde function as the conjugated system (chromophore). Therefore, it is difficult to determine their absolute configuration directly from those CD spectra. The configuration of isoiridogermanal has been thoroughly elucidated (Seki *et al.*, 1994b; Ito *et al.*, 1999) by means of the modified Mosher's method using methoxy-(trifluoromethyl)phenylacetic acid (MTPA) esters as described and applied in previous research (Ohtani *et al.*, 1991). However, the absolute configuration of IT4C (**61**) and IT4D (**65**) at C-14 were not examined in the present research due to the limited amount of pure sample.

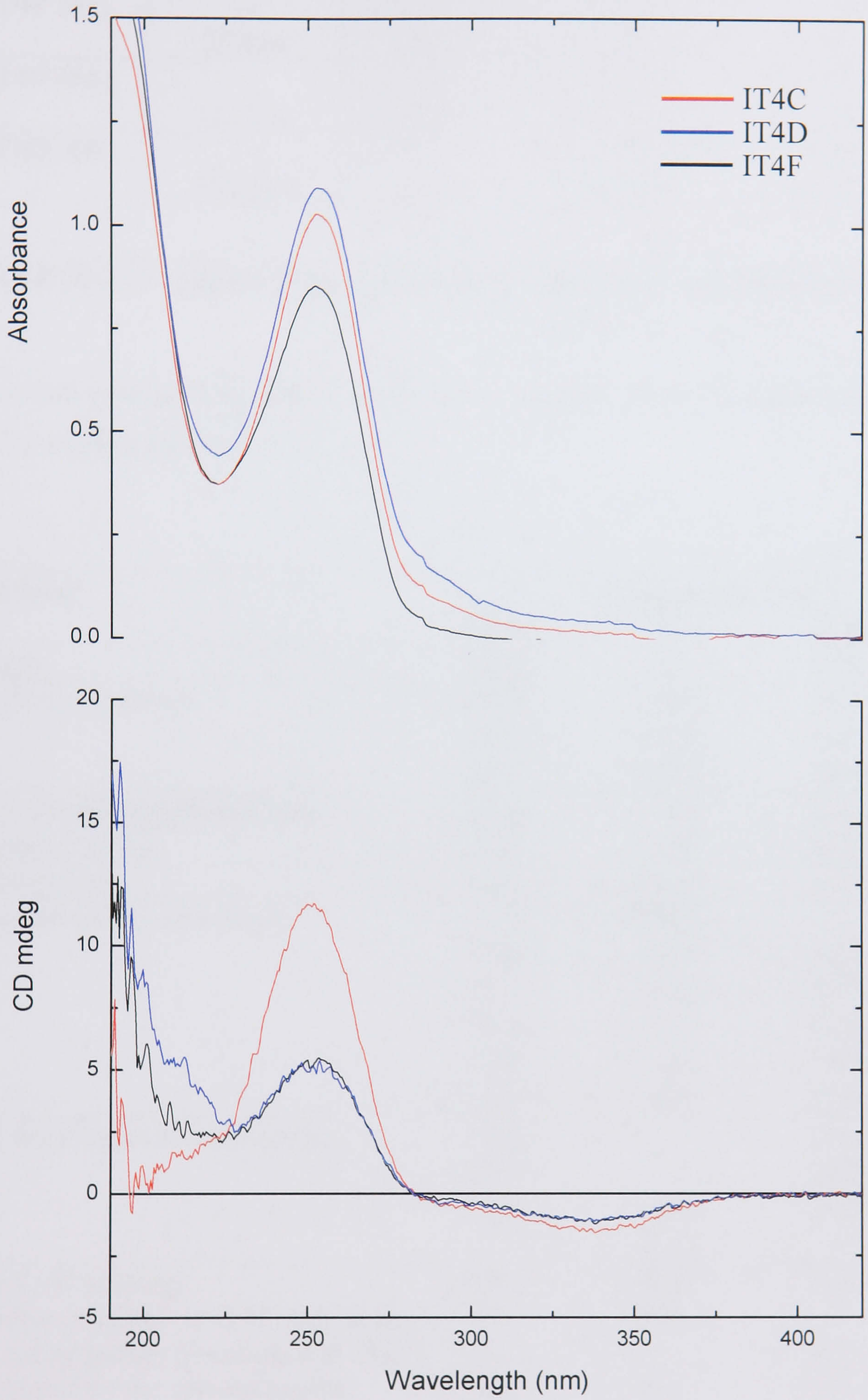

Figure 2-26: The UV/CD spectra of IT4C (**61**), IT4D (**65**) and IT4F (**57**)

Compounds	UV spectra		CD spectra	
	λ_{max}	A_{max}	λ_{max}	mdeg
IT4F (57)	—	—	335.0nm	–1.29
	252nm	0.85	253.5nm	+5.49
IT4C (61)	—	—	338.0nm	–1.60
	252.5nm	1.03	251.5nm	+11.72
IT4D (65)	—	—	337.5nm	–1.13
	252.5nm	1.09	253.5nm	+5.35

Table 2-12: The CD spectral data of compounds IT4C (**61**), IT4D (**65**) and IT4F (**57**)

The structural proposals were also supported by analysis of the IR spectra (see table Table 2-13 and Figure 2-27).

Assignment	**Wavenumber (cm^{-1})**		
	IT4C	**IT4D**	**IT4F**
Hydroxyl	3394	3402	3399
Aliphatic C–H stretch	2967	2968	2965
	2931	2928	2933
	2875	2863	2876
CHO (α,β–unsaturated aldehyde)	1708	1713	1710
C=C unconjugated	1655	1650	1651
C=C conjugated	1609	1608	1609
O–H bending of C–OH group		1515	
	1448	1449	1447
	1375	1375	1375
	1314	1313	1314
	1290	1289	1289
	1205	1203	1204
C–OH stretching of C–OH group	1182		1180
	1090		1090
	1050	1054	1050
		1016	
Alkene C–H bending	907	908	906
* Absorbance at 863 in IT4C was likely due to epoxy group; absorbance at 734 in IT4D caused by the solvent residue ($CHCl_2$).	863	879	
	812		812
	742	734	741
		701	

Table 2-13: Summary of assignments and peaks of the infrared spectra of IT4C (**61**), IT4D (**65**) and IT4F (**57**) (The assignment was based on the characteristic group frequencies on infrared spectra) (Williams and Fleming, 1995)

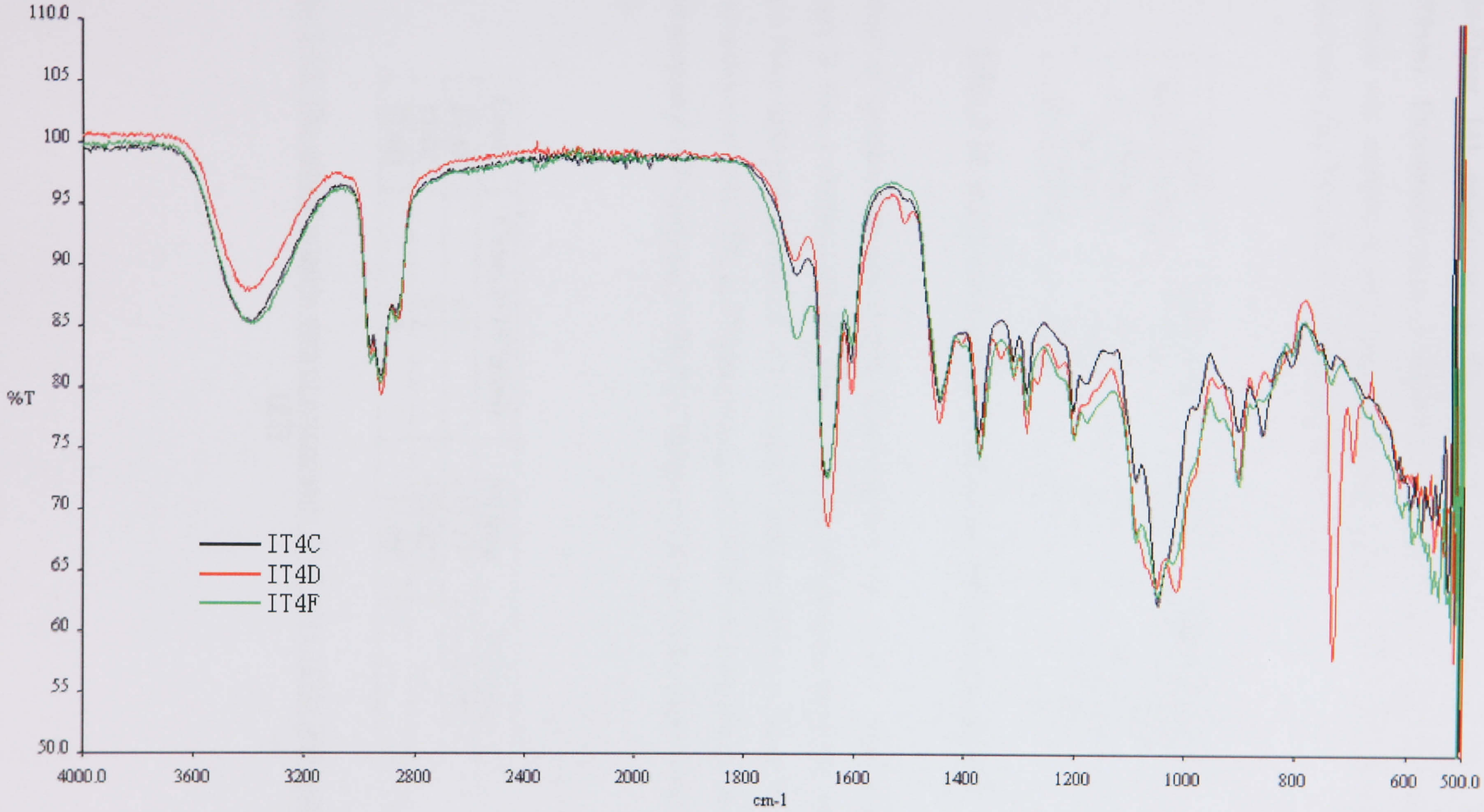

Figure 2-27: The IR spectra of IT4C (**61**), IT4D (**65**) and IT4F (**57**)

The optical rotation of IT4C (**61**), IT4D (**65**) and IT4F (**57**) were measured on a Perkin-Elmer 141 polarimeter at the sodium D line (λ=589nm) and Hg line (λ=578nm). Experiments were carried out at room temperature (23°C). Instrument calibration was completed with sucrose (obtained from BDH) at 14.59mg/ml in distilled water (see Table 2-14) as reference standard.

Laser	light path	volume	OR degree [α]
Sodium D line (λ=589nm)	10cm	6ml	+64.43°
	10cm	1ml	+65.11°
Hg line (λ=578nm)	10cm	6ml	+67.17°
	10cm	1ml	+67.58°

Table 2-14: Instrumental calibration of optical rotation using sucrose

Solutions of samples were prepared by dissolving in 1.5ml CH_2Cl_2. Optical rotation (sodium D line, λ=589nm and Hg line λ=578nm) obtained on the polarimeter by using a 10cm light path cylindrical cell (volume = 1ml) are shown in Table 2-15. The optical rotation of IT4F (**57**) at 578nm ($[\alpha]_{578nm}$ = +39.75°) is very similar to that of isoiridogermanal (**57**) ($[\alpha]_{578nm}$ = +46.7°, CH_2Cl_2, *c*=7.6) in the literature (Krick *et al.*, 1983).

Comp.	Conc. ($\times10^{-3}$g/ml)	$[\alpha]_{589nm}$	$[\alpha]_{578nm}$
IT4F	8.9	+35.27°	+39.75°
IT4C	9.1	+28.02°	—
IT4D	9.4	−31.06°	—

Table 2-15: The optical rotation data of compounds IT4C (**61**), IT4D (**65**) and IT4F (**57**)

2.5.3 Identification of 7-*O*-methyl aromadendrin

Compound IT2c and IT3Ac were isolated and crystallized from sub-fractions IT2 and IT3A respectively. They were identified as known flavonoids by comparison of their instrumental analysis data (NMR, EIMS and IR) with those in the literature.

IT2c was identified as 7-*O*-methyl aromadendrin (**66**), because the instrumental analysis data are very similar to those in the literature (Abdel-Sattar *et al.*, 2000; Balza and Towers, 1984; Hanawa *et al.*, 1991) (as shown in Table 2-16 and Table 2-17). The positive Cotton effects with a maximum absorbance at 330nm and a minimum absorbance at 292nm in the CD spectra of IT2c indicates the configuration at C-2 to be *R* in this dihydroflavonol structure (Ingham *et al.*, 1986). Since the *trans* orientation of H-2 and H-3 in IT2c was apparent from ^{1}H NMR coupling constants (both are J=11.6Hz), the *R* configuration at C-3 can be determined. These elucidations coincide with a previous report (Hanawa *et al.*, 1991).

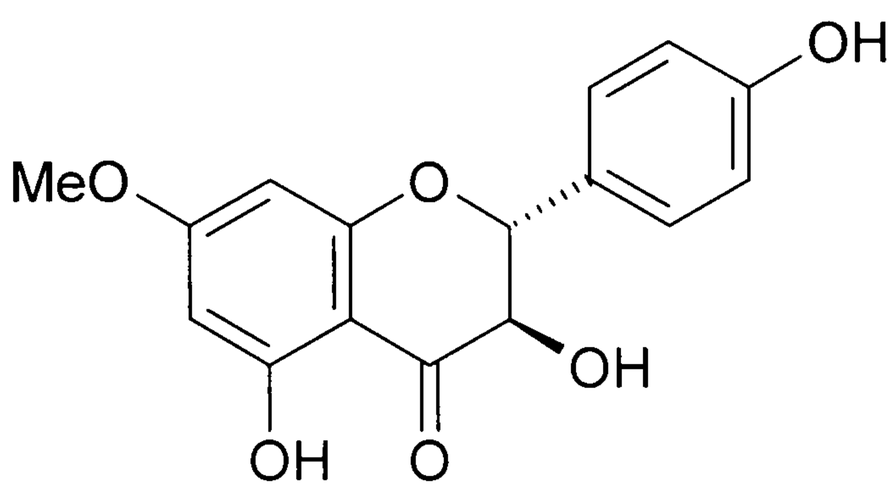

66

In a latest paper on 7-*O*-methyl aromadendrin (**66**) (Abdel-Sattar *et al.*, 2000), NMR spectra were measured in CD_3OD at 500MHz (7OMA-a), however, in an early paper (Balza and Towers, 1984), the NMR spectra were measured in $CDCl_3$ at 80MHz (7OMA-b) (shown in Table 2-16). The differences of the chemical shift values between IT2c and published data may due to the different deuterated solvents used in the NMR experiments. The assignment of the carbon signals in Table 2-16 is based on the HMBC results (shown in Figure 2-28).

It is very clear that, not only the NMR data, but also the EIMS fragments signals of IT2c matched those of 7-*O*-methyl aromadendrin (**66**) in the literature well (see Table

2-18). Moreover, the data of CD spectra of IT2c (Table 2-19 and Figure 2-29) are highly consistent with those in literature (Herz *et al.*, 1972). Thus, IT2c was identified as 7-*O*-methyl aromadendrin (**66**).

^{1}H NMR	**IT2c**	**a**	**b**
2-H	5.12 *d* (*J*=11.6Hz)	5.03 *d* (*J*=11.5Hz)	5.05 *d* (*J*=12Hz)
3-H	4.69 *dd* (*J*=11.6, 4.2Hz)	4.56 *d* (*J*=11.5Hz)	4.55 *dd* (*J*=12, 1.5Hz)
3-OH	4.79 *d* (*J*=4.2Hz)	?	3.47 *d* (*J*=1.5Hz)
5-OH	11.69 *s*	?	11.18 *s*
6-H	6.09 *d* (*J*=2.2Hz)	6.03 *d* (*J*=2.2Hz)	6.05 *d* (*J*=2.5Hz)
7-OCH_3	3.86 *s*	3.81 *s*	3.83 *s*
8-H	6.05 *d* (*J*=2.2Hz)	6.08 *d* (*J*=2.2Hz)	6.15 *d* (*J*=2.5Hz)
2'-H, 6'-H	7.43 *d* (*J*=6.8Hz)	7.37 *d* (*J*=8.8Hz)	7.45 *d* (*J*=8.5Hz)
3'-H, 5'-H	6.90 *d* (*J*=8.6Hz)	6.87 *d* (*J*=8.8Hz)	6.90 *d* (*J*=8.5Hz)
4'-OH	8.62 *s*	?	4.90 *s*

Table 2-16: Comparison of ^{1}H NMR spectral data of IT2c (δ, at 125MHz, in acetone-d_6) with those of 7-*O*-methyl aromadendrin (**66**) in the literature (**a**: Abdel-Sattar *et al.*, 2000; **b**: Balza and Towers, 1984). *Data missing from the literature are labelled with question mark.

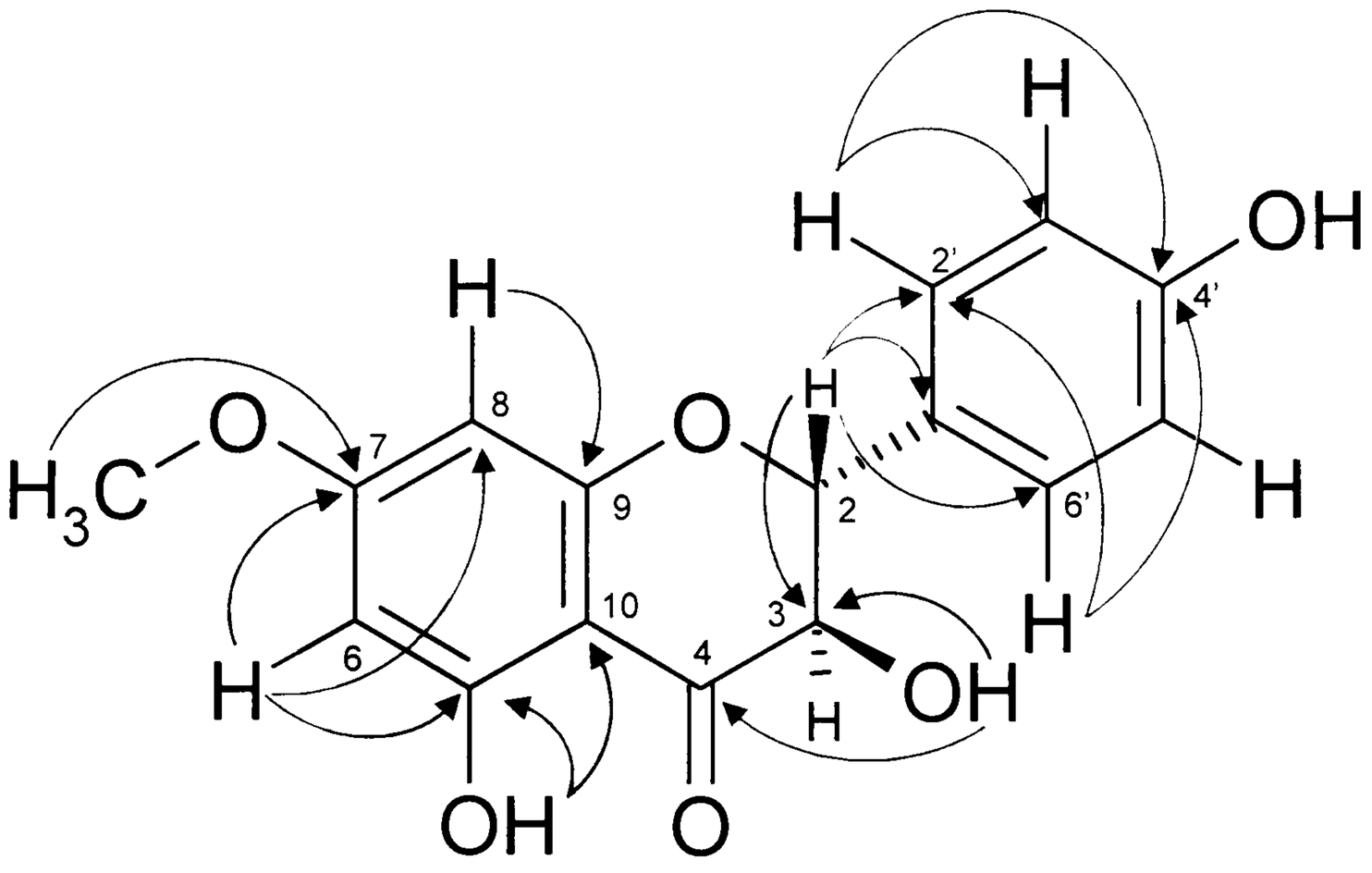

Figure 2-28: Observed HMBC correlations of IT2c

^{13}C NMR		IT2c	a
2	CH	84.5	85.1
3	CH	73.2	73.9
4	C	198.7	198.6
5	C	164.7	164.9
6	CH	95.8	96.5
7	C	169.3	169.7
7-OCH_3	CH_3	56.4	56.9
8	CH	94.7	95.5
9	C	164.0	164.2
10	C	102.1	102.8
1'	C	129.0	129.0
2', 6'	CH	130.3	130.4
3', 5'	CH	115.9	116.6
4'	C	158.9	159.1

Table 2-17: Comparison of the ^{13}C NMR spectral data (δ, at 125MHz, in acetone-d_6) of IT2c with those of 7-*O*-methyl aromadendrin (**66**) in the literature (**a**: Abdel-Sattar *et al.*, 2000)

IT2c	a	b	c
302 $[M]^+$ (50)	302 $[M]^+$ (100)	302 $[M]^+$ (30)	302 $[M]^+$ (17)
273 (58)	273 (100)	273 (50)	273 (38)
179 (17)	179 (50)	179 (35)	179 (15)
167 (100)	167 (100)	167 (100)	167 (100)
136 (19)	—	—	136 (22)
134 (36)	134 (100)	134 (70)	134 (37)
107 (20)	107 (65)	107 (75)	107 (26)

Table 2-18: Comparison of the EIMS *m/z* (rel. int.) result of IT2c with those of 7-*O*-methyl aromadendrin (**66**) in the literature (**a**: Abdel-Sattar *et al.*, 2000; **b**: Balza and Towers, 1984; **c**: Hanawa *et al.*, 1991)

UV spectra		CD spectra	
λ_{max}	A_{max}	λ_{max}	mdeg
—	—	330nm	+2.71
289.5nm	0.64	292nm	−9.83
—	—	255nm	+3.00
218nm	0.99	218nm	+17.17

Table 2-19: The CD spectra results of IT2c (**66**)

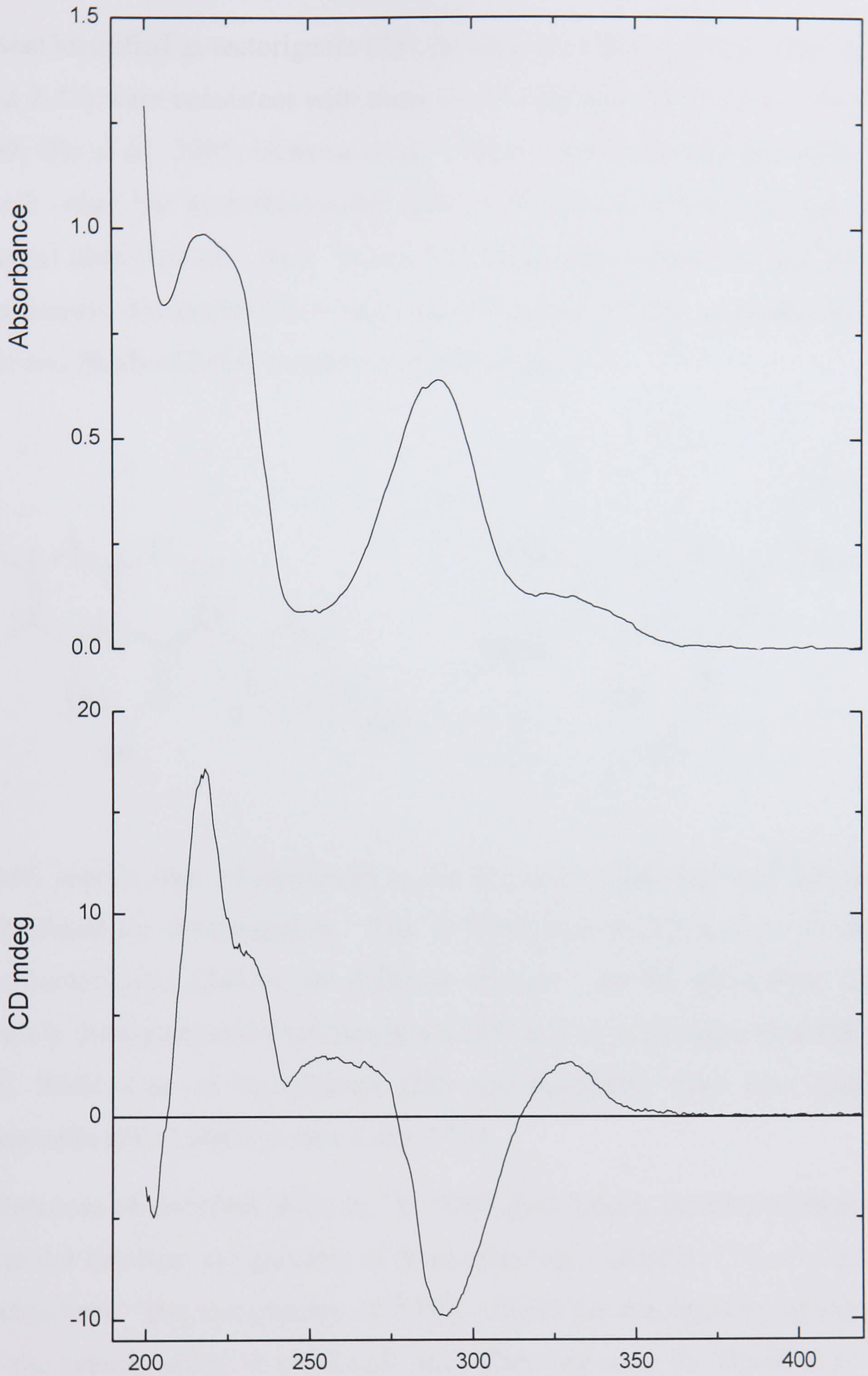

Figure 2-29: UV/CD spectra of IT2c (**66**)

2.5.4 Identification of tectorigenin

IT3Ac was identified as tectorigenin (**24**), because the spectroscopic data (Table 2-20, 2-21 and 2-22) were consistent with those in the literature (Horie *et al.*, 1998; Bae *et al.*, 1999; Qin *et al.*, 2005; Hanawa *et al.*, 1991a). The published data differ slightly from each other but nevertheless the data of IT3Ac are similar enough to allow unequivocal identification. Both ^{1}H and ^{13}C NMR data (Table 2-20 and Table 2-21) are significantly distinguishable with those of hispidulin (**67**), an isomer has similar structure and identical EIMS fragments as that of **24**.

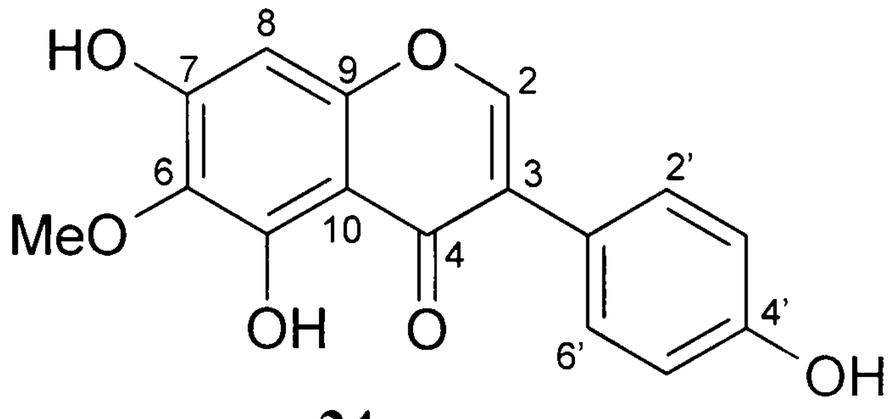

24

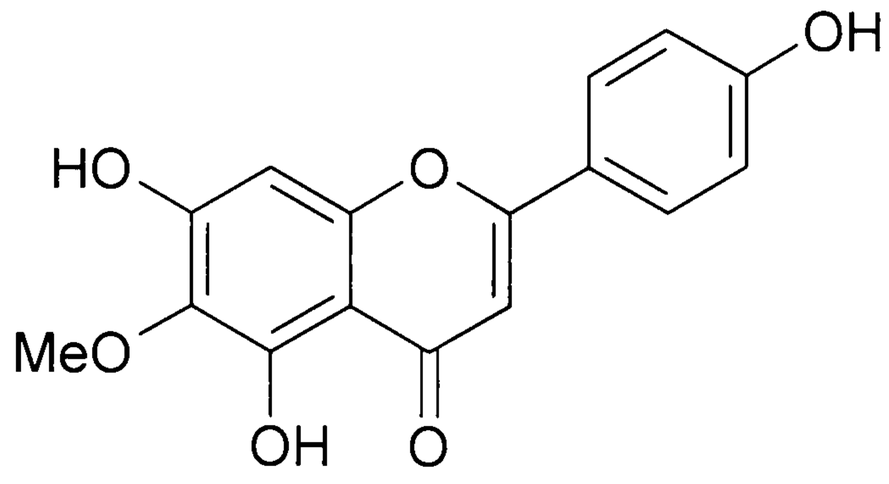

67

The NMR spectra data of hispidulin in the literature (Nakasugi and Komai, 1998) were also listed for discrimination. The ^{1}H NMR data of IT3Ac were identical with those of tectorigenin (**24**) in the different sources. At the same time they were significantly distinguishable from hispidulin (**67**) at 3-H of the latter (see Table 2-20). The ^{13}C NMR data of tectorigenin (**24**) and hispidulin were also significantly distinguishable at C-2 and C-3 (see Table 2-21).

The differences of chemical shifts in ^{13}C NMR data among the three references may be due to the incorrect assignments of three quaternary carbons: C-5, C-7 and C-9 in the publications. The assignments of NMR signals for the structure of tectorigenin (**24**) in the present study is consistent with those reported by Horie *et al.* (1998). Except for the difference in relative assignments of those three quaternary carbons, the NMR data of IT3Ac were broadly identical with those of tectorigenin (**24**) in the literature.

^{1}H NMR	IT3Ac	tectorigenin			hispidulin	
		a	b	c		
2-H	8.34 *s*	8.33 *s*	8.29 *s*	8.33 *s*	3-H	6.76 *s*
5-OH	13.06 *s*	13.07 *s*	?	13.06 *s*	5-OH	13.06 *s*
6-OCH_3	3.75 *s*	3.76 *s*	3.88 *s*	3.75 *s*	6-OCH_3	3.74 *s*
7-OH	10.78 *s*	10.78 *s*	?	10.76 *s*	7-OH	?
8-H	6.50 *s*	6.51 *s*	6.49 *s*	6.50 *s*	8-H	6.57 *s*
2'-H, 6'-H	7.38 *d* (*J*=8.6Hz)	7.38 *d*	7.38 *d* (*J*=8.3Hz)	7.37 *d* (*J*=8.1Hz)	2`-H, 6`-H	7.91 *d* (*J*=9.5Hz)
3`-H, 5`-H	6.82 *d* (*J*=8.6Hz)	6.83 *d*	6.82 *d* (*J*=8.3Hz)	6.82 *d* (*J*=8.1Hz)	3`-H, 5`-H	6.91 *d* (*J*=9.5Hz)
4'-OH	9.60 *s*	9.61 *s*	?	9.59 *s*	4`-OH	?

Table 2-20: Comparison of ^{1}H NMR spectral data (δ, at 500MHz, in DMSO-d_6) of IT3Ac (**24**) with those of tectorigenin and hispidulin (**67**) in the literature (**a**: Horie *et al.*, 1998; **b**: Bae *et al.*, 1999; **c**: Qin *et al.*, 2005; Nakasugi and Komai, 1998)

^{13}C NMR		IT3Ac	tectorigenin			hispidulin	
			a	b	c		
2	CH	154.0	154.0	153.9	153.6	C	163.7
3	C	121.7	121.7	123.8	122.1	CH	102.3
4	C	180.5	180.5	180.5	181.4	C	182.0
5	C	153.2	153.2	152.7	158.2	C	152.7
6	C	131.3	131.3	131.4	132.1	C	131.4
6-OCH_3	C	59.8	59.9	59.0	60.8	C	59.9
7	C	157.3	157.3	153.2	154.8	C	157.8
8	CH	93.8	93.8	93.8	94.7	CH	94.3
9	C	152.6	152.7	157.5	153.9	C	152.5
10	C	104.7	104.8	104.8	105.6	C	103.8
1'	C	121.1	121.1	121.0	122.6	C	121.2
2', 6'	CH	130.1	130.1	130.1	131.0	CH	128.4
3', 5'	CH	115.0	115.0	115.0	116.0	CH	115.9
4`	C	157.4	157.4	157.4	157.9	C	161.2

Table 2-21: Comparison of ^{13}C NMR data (δ, at 125MHz, in DMSO-d_6) of IT3Ac (**24**) with those of tectorigenin and hispidulin (**67**) in the literature (**a**: Horie *et al.*, 1998; **b**: Bae *et al.*, 1999; **c**: Qin *et al.*, 2005; Nakasugi and Komai, 1998)

IT3Ac	**c**	**d**
300 $[M]^+$ (100)	300 $[M]^+$ (100)	300 $[M]^+$ (100)
285 $[M\text{-}Me]^+$ (54)	285 $[M\text{-}Me]^+$ (65)	285 $[M\text{-}Me]^+$ (52)
282 $[M\text{-}H_2O]^+$ (38)	282 $[M\text{-}H_2O]^+$ (47)	282 $[M\text{-}H_2O]^+$ (38)
271 (6)	271 (8)	—
257 (49)	257	257 (65)
149 (9)	—	—
139 (8)	139 (13)	—
118 (7)	118 (22)	118 (11)

Table 2-22: Comparison of the EIMS *m/z* (rel. int.) result of IT3Ac (**24**) with those of tectorigenin in the literature (**c**: Qin *et al.*, 2005; **d**: Hanawa *et al.*, 1991a)

CHAPTER 3
ACTIVITY OF ISOLATED COMPOUNDS

3.1 Cytotoxicity

Six isolated compounds: isoiridogermanal (**57**), iridobelamal A (**60**), IT4C (**61**), IT4D (**65**), 7-*O*-methyl aromadendrin (**66**) and tectorigenin (**24**) together with two flavonoids, luteolin (**22**) and genistein (**51**) (as positive controls), were tested for cytotoxicity using the SRB assay. All of them showed dose-dependent inhibition of proliferation in the six cell lines tested for 48h. Their cytotoxicities were evaluated by calculation of the IG_{50} (the concentration that inhibits cell growth by 50%).

As shown in Figure 3-1 and Table 3-1, tectorigenin (**24**) is the least cytotoxic compound with the highest IG_{50} among the four flavonoids. Its IG_{50} values against all tested cell lines are higher than 100μM (as high as 207.2μM and 234.5μM against C32 and HBE14o-). Obviously, luteolin (**22**) is the most cytotoxic one with IG_{50} of 11μM and 9.4μM against COR-L23 and HepG2, respectively. Generally, the order of cytotoxiciy for these four flavonoids is luteolin (**22**) > 7-*O*-methyl aromadendrin (**66**) > genistein (**51**) > tectorigenin (**24**). This result also reveals that MCF-7 seems to be quite sensitive to genistein (**51**), tectorigenin (**24**) and 7-*O*-methyl aromadendrin (**66**).

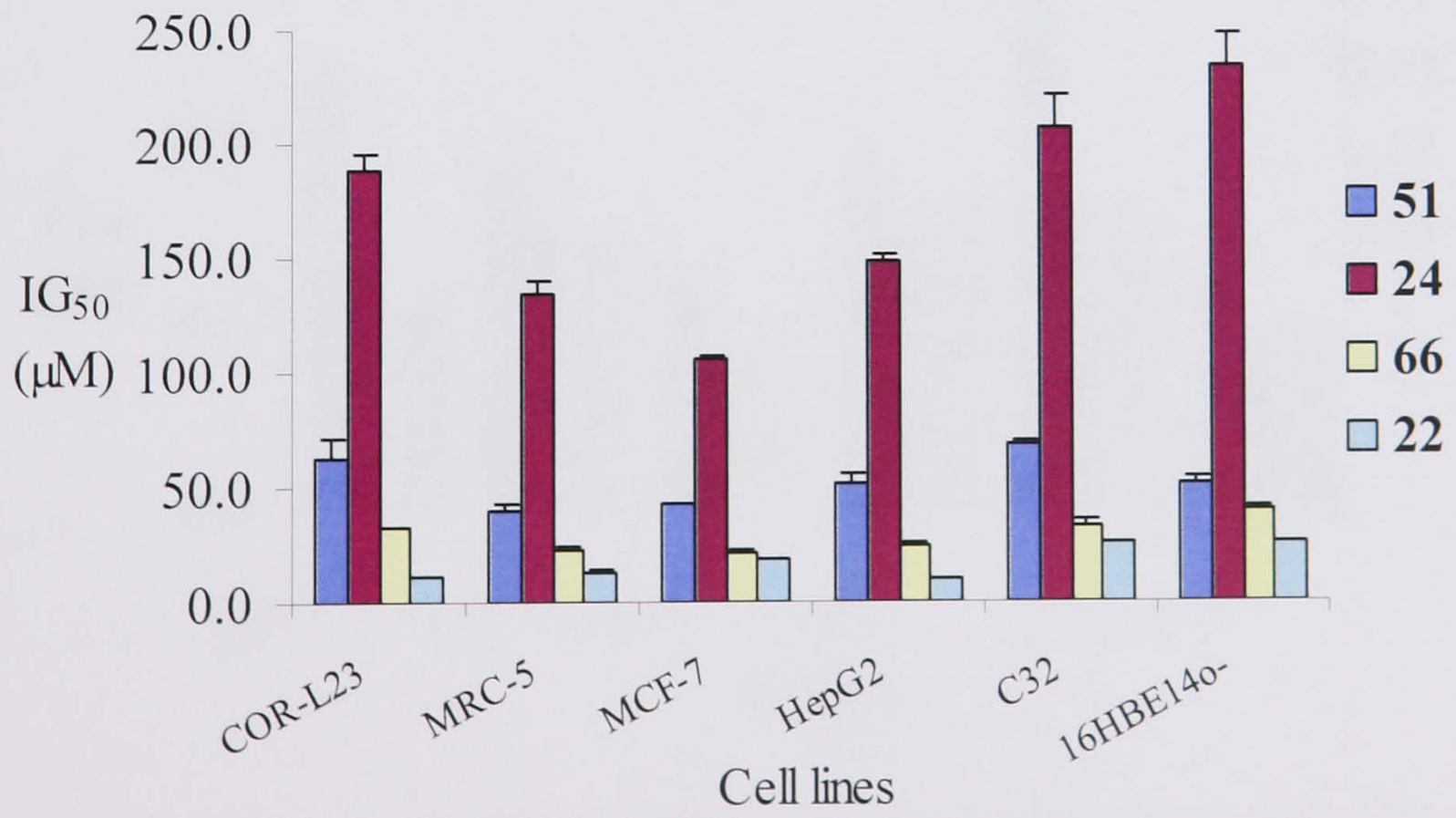

Figure 3-1: The IG_{50} values (μM) of genistein (**51**), tectorigenin (**24**), 7-*O*-methyl aromadendrin (**66**) and luteolin (**22**) against six cell lines (IG_{50}±SEM, n=3)

Cell lines	51	24	66	22
COR-L23	62.7±8.98	189.3±6.55	32.8±0.50	11.0±0.67
MRC-5	40.6±2.50	134.8±4.76	23.3±0.55	13.2±1.17
MCF-7	42.6±0.48	105.0±1.98	21.0±1.37	17.9±1.13
HepG2	51.8±4.02	148.8±2.48	24.5±1.73	9.4±1.22
C32	68.0±2.17	207.2±13.73	32.8±3.25	25.2±0.91
HEB14o-	52.0±1.91	234.5±14.14	40.4±0.74	25.9±0.24

Table 3-1: The IG_{50} values (μM) of genistein (**51**), tectorigenin (**24**), 7-*O*-methyl aromadendrin (**66**) and luteolin (**22**) against six cell lines (IG_{50}±SEM, n=3)

By comparison, the iridal-type triterpenes have the same level of cytotoxicity (shown as Figure 3-2 and Table 3-2) as those of the active flavonoids (genistein [**51**], 7-*O*-methyl aromadendrin [**66**] and luteolin [**22**]). IT4C (**61**) is the least cytotoxic compound among those four iridal-type triterpenes tested. It has IG_{50} of 34.8μM and 40.4μM against COR-L23 and C32, respectively. The other three triterpenes: IT4D (**65**), IT4E (**60**) and IT4F (**57**) showed similar cytotoxicity with IG_{50} around 11μM and 23μM against MCF-7 and C32 respectively. IT4D (**65**) and IT4F (**57**) have very similar IG_{50} against all tested cell lines. IT4E has the lowest IG_{50} of 5.7μM against HBE14o-.

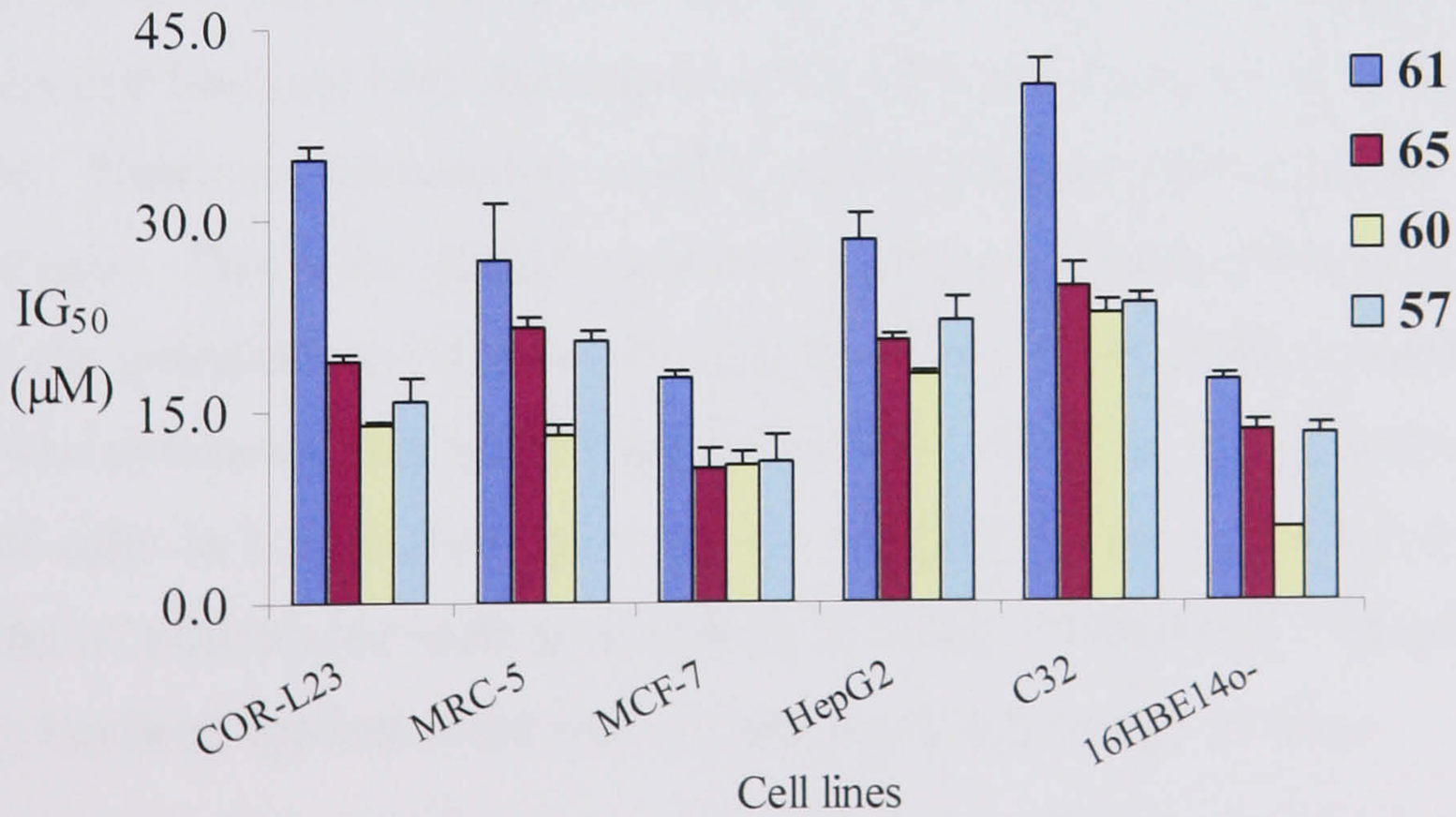

Figure 3-2: The IG_{50} values (μM) of IT4C (**61**), IT4D (**65**), IT4E (**60**) and IT4F (**57**) against six cell lines (IG_{50}±SEM, n=3)

Cell lines	61	65	60	57
COR-L23	34.8±0.86	19.0±0.44	13.9±0.27	15.7±1.84
MRC-5	26.9±4.39	21.6±0.67	13.0±0.83	20.4±0.80
MCF-7	17.6±0.51	10.6±1.42	10.7±1.22	11.0±2.11
HepG2	28.5±2.07	20.4±0.61	17.9±0.32	22.0±2.00
C32	40.4±2.29	24.6±2.02	22.6±0.97	23.5±0.80
HEB14o-	17.4±0.58	13.5±0.59	5.7±0.23	13.2±0.71

Table 3-2: The IG_{50} values (μM) of IT4C (**61**), IT4D (**65**), IT4E (**60**) and IT4F (**57**) against six cell lines (IG_{50}±SEM, n=3)

3.2 Methods used to investigate apoptotic activity

The integrity of the cytoplasmic membrane is essential to cell function. Although at least some cells can survive transient small breaches of the membrane, longer-term or larger defects may deprive the cell of materials it would normally accumulate, and may also expose it to toxins it would normally exclude. Thus, cells with a demonstrable loss of membrane integrity are dead (Shapiro, 2003). The selected methods for apoptotic investigation are dual staining systems, which are based on the changes in membrane permeability that occur during apoptosis.

3.2.1 Flow cytometry

The observation of cellular phenomena has relied primarily on microscopic analysis. The microscope has long been the symbol of the biologist for much of the last century and before. However, microscopic studies carry an inherent limitation for analyzing individual cells. That is the limited number of cells that are observable in such studies precludes the quantitative (cell-by-cell) analysis of entire populations (Ranalli *et al.*, 2003). Flow cytometry overcomes this limitation by allowing the analysis of a large number of cells in a very short time, greatly simplifying the quantitative, real-time observation of phenomena such as apoptosis in a large population. Therefore, flow cytometry has been applied to the study of apoptosis in a variety of ways.

Apoptosis was originally identified morphologically. The explosion of studies on apoptosis in recent years has clarified that it represents the mode of death that is actively driven by the cell, a complex process that is also described as programmed cell death. Conversely, necrosis represents a passive consequence of gross injury to

the cell. It is morphologically different from apoptosis, and its physiological consequences are also very different from those of apoptosis (Searle *et al.*, 1982; Buja *et al.*, 1993) (see Table 1-2 on page 24). Since apoptosis is a very common phenomenon during embryogenesis as well as adult life, and a frequent response of cells to drugs in the course of therapy, its quantitative evaluation represents an issue of considerable relevance. Flow cytometry is the technique of choice for the quantitation of apoptosis. A multitude of methods have been developed to identify apoptotic cells by flow cytometric analysis each of them differently suitable to different experimental conditions (Darzynkiewicz *et al.*, 1992).

The integrity of the plasma membrane of cells underging apoptosis is preserved and most functions of the membrane remain unchanged (Darzynkiewicz *et al.*, 1997). Apoptotic cells, thus, exclude "viability assay" dyes such as trypan blue or PI. This is in contrast to necrotic cells, where one of the earliest changes is loss of membrane function and its structural integrity; accordingly they can uptake trypan blue or PI readily. By the ability to uptake propidium iodide (PI), necrotic cells can be clearly distinguished. On the other hand, apoptotic cells can be erroneously classified by flow cytometry as viable cells (Lennon *et al.*, 1991). By using this sort of dye in combination with other markers, such as fluorescein-diacetate (FDA) or Hoechst 33258, apoptotic and healthy cells can be readily distinguished (Sasaki *et al.*, 1987; Ormerod *et al.*, 1993; Schmid *et al.*, 1994).

An unequivocal method to distinguish apoptotic from necrotic cells by flow cytometry does not exist. Rather, it is necessary to discriminate necrotic cells from apoptotic cells using different flow cytometric methodologies available to measure apoptosis. The recently developed reagents and technologies are generally based on the following distinctive features of apoptosis (Ranalli *et al.*, 2003):

- DNA fragmentation
- Plasma membrane alterations
- Mitochondrial changes
- Activation of caspases.

The plasma membrane alteration assay with annexin-V FITC and the cell viability assay with fluorescein diacetate (FDA) and propidium iodide (PI) staining have been adopted in this project for the detection of apoptosis. The cell cycle analysis assay

using PI was applied to give more detailed evidence for the features of apoptosis induced by the compounds in question. The selection was based on their features. such as high sensitivity, specificity and low cost. The physical properties of applied agents used are listed in Table 3-3.

Agent	Excitation	Emission
FITC	488nm	525nm
FDA	485nm	538nm
PI	536nm	620nm

Table 3-3: Optical properties of fluorescent probes used

3.2.2 Main features of flow cytometer

Generally, the flow cytometer is an instrument that accepts an input of liquid-suspended cells, passes them one by one through a light source, and measures a variety of light scattering and fluorescence properties for each cell. Input cells are passed through a capillary at a rate of thousands per second, and individually subjected to light, normally in the form of a focused laser beam or equivalent monochromatic light source. When the fluorescent probes are applied, fluorescence characteristics of each cell are collected by light sensors, and these data can subsequently be analysed by various software packages (Ranalli *et al.*, 2003). The instrument employed for the apoptosis assay in this project is a bench top FACScan® (BD Biosciences, San Jose, CA) flow cytometer. The histograms and dot plots presented in the results were made with Cell Quest®, which is a FCM application base on G4 Power Macintosh. Five parameters involved in cell cycle analysis and apoptosis assay are:

- Forward light scatter (FSC)
- Side light scatter (SSC)
- Fluorescence channel FL1
- Fluorescence channel FL2
- Fluorescence channel FL3.

The pulse height, area and width of each fluorescence parameter are measured at the same time as data acquisition for the tested sample. The parameter settings for the assays used are listed in Table 3-4. Forward scatter is a measure of cell size, while side scatter is a measure of cell granularity (complexity). The shrinkage and blebbing characteristic of apoptosis reduces cell size and increases cell surface complexity, resulting in a population on the dot plot with distinct light scattering properties (Ormerod *et al.*, 1995). Nevertheless, the morphological assessment of apoptosis based on a scatter plot of FSC *vs* SSC is often difficult to distinguish clearly between the apoptotic and healthy populations, as they frequently partially overlap. Furthermore, characteristic morphological changes are hidden upon detachment in some adherent cell lines. In practice, this technique is most useful for distinguishing apoptotic from healthy cells in thymocytes, freshly isolated peripheral blood cells, and some lymphoid cell lines. It is advisable to avoid this type of analysis in adherent cells lines (Mentz *et al.*, 1998). This method was therefore not employed in present project due to its poor reliability.

Emission ranges for detectors		**DNA fragmentation**	**FDA/PI staining**	**Ann/PI staining**
FL1	530±15 nm	—	FDA	FITC
FL2	585±21 nm	PI	—	—
FL3	675±25 nm	—	PI	PI

Table 3-4: Fluorescent signals (emission wavelength) detected by FCM in each assays

3.2.3 Protocols for apoptosis assay with flow cytometer

3.2.3.1 Determination of the cell cycle by DNA analysis

Propidium iodide (PI) (**68**) (Sigma-Aldrich, P4170) is the most widely-used fluorescent dye for staining DNA in whole cells (or isolated nuclei). PI (**68**) does not cross the intact plasma membrane of viable cells. However, PI (**68**) can readily enter dead cells or cells in late stages of apoptosis that have damaged plasma membranes. In cell cycle analysis assay, PI (**68**) intercalates into the DNA helix of fixed or permeabilized cells. Because PI (**68**) can stain both double-stranded RNA (dsRNA) and DNA (dsDNA), cells must be treated with RNase to ensure that PI (**68**) staining is

DNA specific (Krishan, 1975).

In a histogram of DNA analysis (as seen in Figure 3-3), cells in G_1 or G_0 will contain a single copy of the genome (see Figure 3-4), and will appear as a sharp peak, while cells in G_2 or M phase will have a double content of DNA and will appear as a second peak with approximately double intensity in the red channel. Cells in S phase will have variable DNA content and will be distributed in the area between the two peaks. The proportion of cells in each cell cycle phase can thus be determined by calculating the area of the different peaks (Wieder, 1999). Apoptotic cells will have relatively low red fluorescence intensity, due to their decreased DNA content, and will appear as a sub-G_1 peak (Darzynkiewicz *et al.*, 1992) (see Figure 3-3).

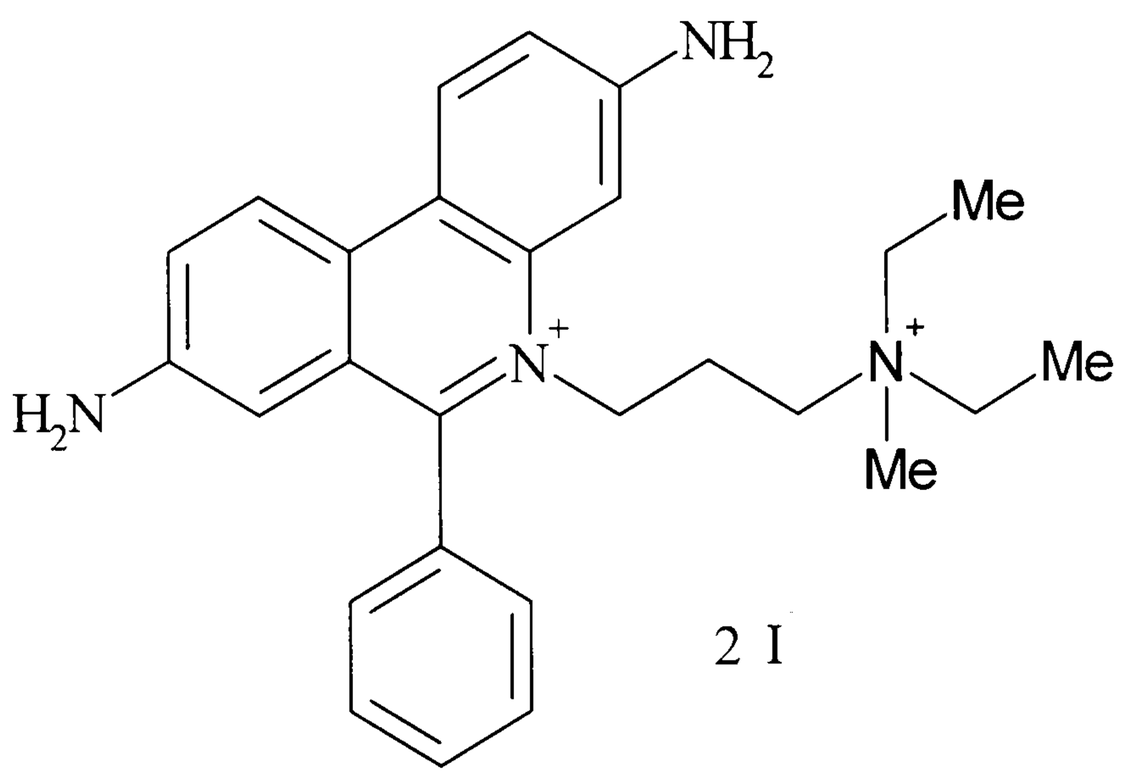

68

It has been recognized independently in several laboratories that apoptotic cells have reduced DNA stainability following staining with a variety of fluorochromes, such as PI and Hoechst dyes because of the degradation of DNA and its subsequent leakage from the cell (Ojeda *et al.*, 1990; Afanasev *et al.*, 1986). These account for the appearance of cells with low DNA stainability (lower than that of cells in G_1 phase) due to their hypodiploid DNA content. When the cultures are treated with various drugs, the sub-G_1 peak can be considered as the marker of cell death by apoptosis (Darzynkiewicz *et al.*, 1992). However, this method has been replaced by some recently developed approaches, such as annexin V staining to detect changes in membrane lipid distribution, which is capable of detecting apoptosis in an earlier stage than assays based on nuclear changes.

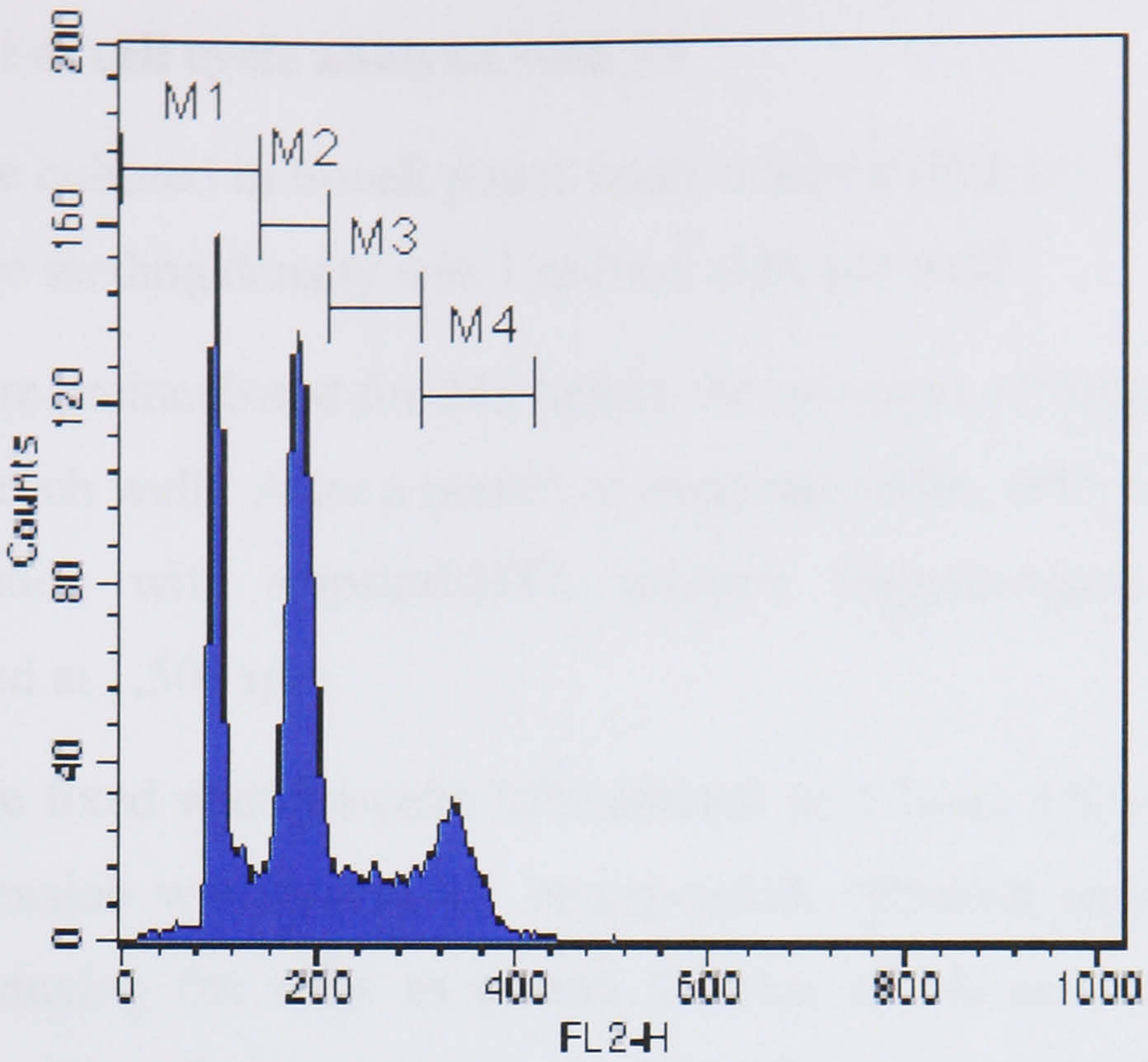

Figure 3-3: DNA content histogram of COR-L23 cells after exposure to 20µM genistein for 48h (Keys: M1= sub-G_1 peak; M2= G_0/G_1 peak; M3= S peak; M4= G_2/M peak)

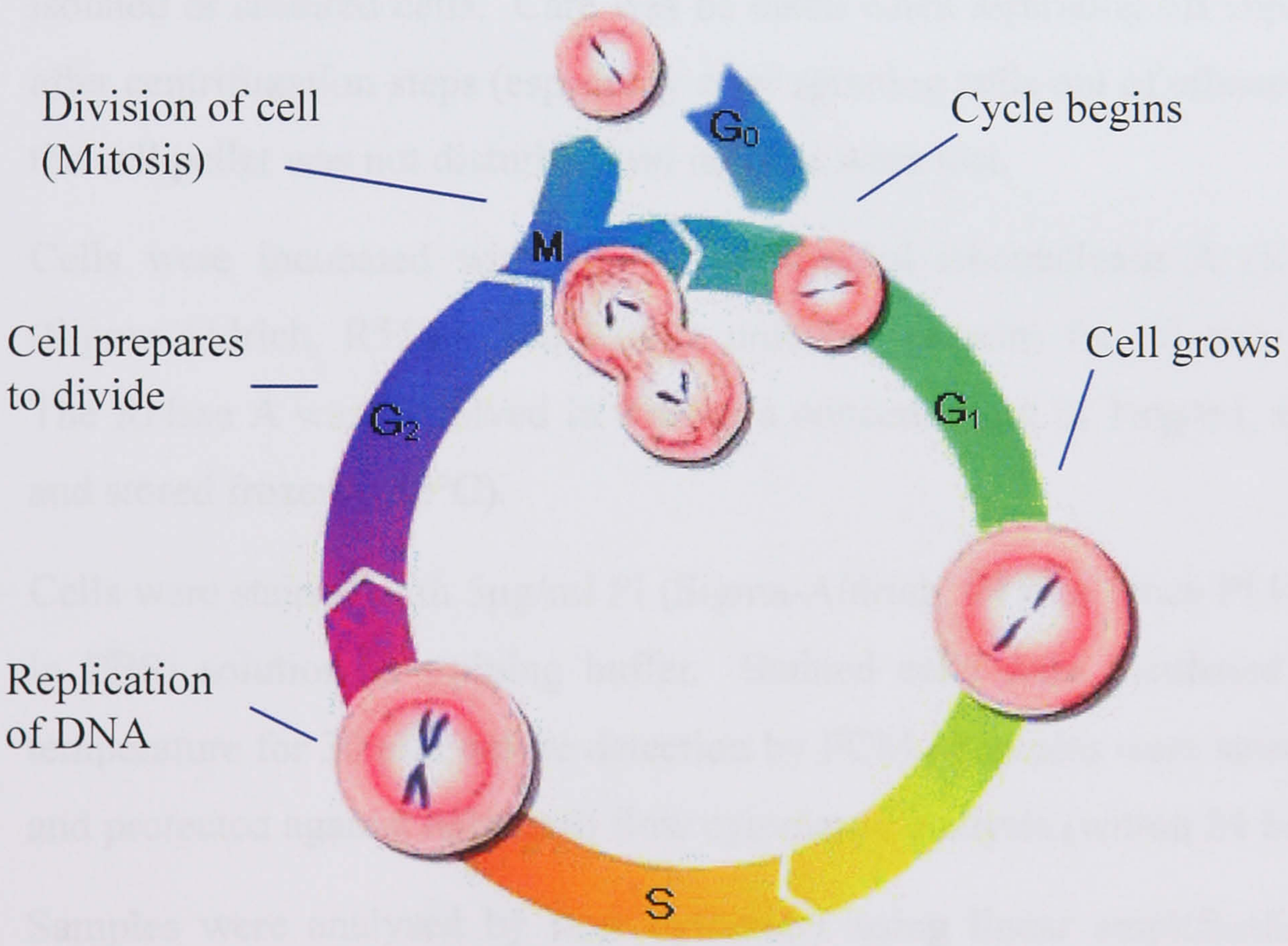

Figure 3-4: Illustration of the variation of DNA content during cell cycle (modified from http://learninglab.co.uk/headstart/images/cycle1a.jpg)

3.2.3.2 Protocol of cell cycle analysis with PI

1. Cells were cultured in 6-well plates under a humidified 5% CO_2 atmosphere at 37°C. The seeding density was 1 million cells per well.

2. Plates were preincubated for 24h before the solutions of drugs or control were added to each well. After a period of exposure (48h), cells were harvested by trypsinization with trypsin/EDTA solution (Sigma-Aldrich, T4049), and centrifuged at 1,500 rpm.

3. Cells were fixed with ice-cold 70% ethanol (≥ 1 hour, 4°C) ensuring that the cell suspension was thoroughly resuspended. Ethanol was added dropwise while vortexing the cells to ensure fixation of all cells and to minimize clumping. Once fixed, cells may be stored for months in 70% ethanol at 4°C prior to PI staining and flow cytometric analysis.

4. Cell pellets (1×10^6) were made in tubes (at 1,500rpm, 5 min) and washed once in PBS. Ethanol-fixed cells required higher centrifugal speed (2,000rpm) to be pelleted tightly since they become more buoyant upon fixation than freshly-isolated or cultured cells. Care was be taken when aspirating off supernatants after centrifugation steps (especially after spinning cells out of ethanol) so that the cell pellet was not disturbed and no cells were lost.

5. Cells were incubated with 100 µl of 1mg/ml ribonuclease A (RNase A) (Sigma-Aldrich, R5500; 100 Kunitz units/mg protein) for 30 min at 37°C. The RNase A was dissolved in PBS at a concentration of 1mg/ml, aliquoted, and stored frozen (–80°C).

6. Cells were stained with 5µg/ml PI (Sigma-Aldrich, P4170; Stock PI is 1mg/ml in PBS) solution in staining buffer. Stained cells were incubated at room temperature for 30 min before detection by FCM. Samples were stored at 4°C and protected against light until flow cytometric analysis (within 24 hours).

7. Samples were analysed by flow cytometry using linear amplification. The flow rate was maintained at less than 400 events per second. 20,000 events were acquired for each scan. A one-dimensional plot of the red channel (FL2) was engaged.

3.2.3.3 Result of positive control (vinblastine sulphate)

Vinblastine sulphate (**69**) (Sigma-Aldrich, V1377) was tested as a positive control to optimize the protocol of cell cycle analysis. As shown in Figure 3-5, cells cultured under normal conditions (control) showed the highest peak in the region of G_0/G_1 phase and a small low peak in G_2/M phase. Following vinblastine treatment, the G_2/M peak dramatically increased from 15.7% (in the control) to 71.3% after exposure to 45nM vinblastine sulphate (**69**), and the peaks of G_0/G_1 and S phases decreased from 61.3% to 5.8%, and 13.8% to 3.7%, respectively (see Figure 3-6). The significant accumulation of cells (statistical results available in Table 3-6 on page 144) clearly indicates that vinblastine sulphate (**69**) efficiently arrested the cell cycle progress in COR-L23 cells at the G_2/M phase (as shown in Figure 3-5). This result is consistent with those in the literature (Aoyama *et al.*, 1998) and testifies that the established cell cycle analysis protocol with COR-L23 cell line was working properly in the present work. Therefore, the results of the subsequent tests on the previously untested compounds may be considered reliable.

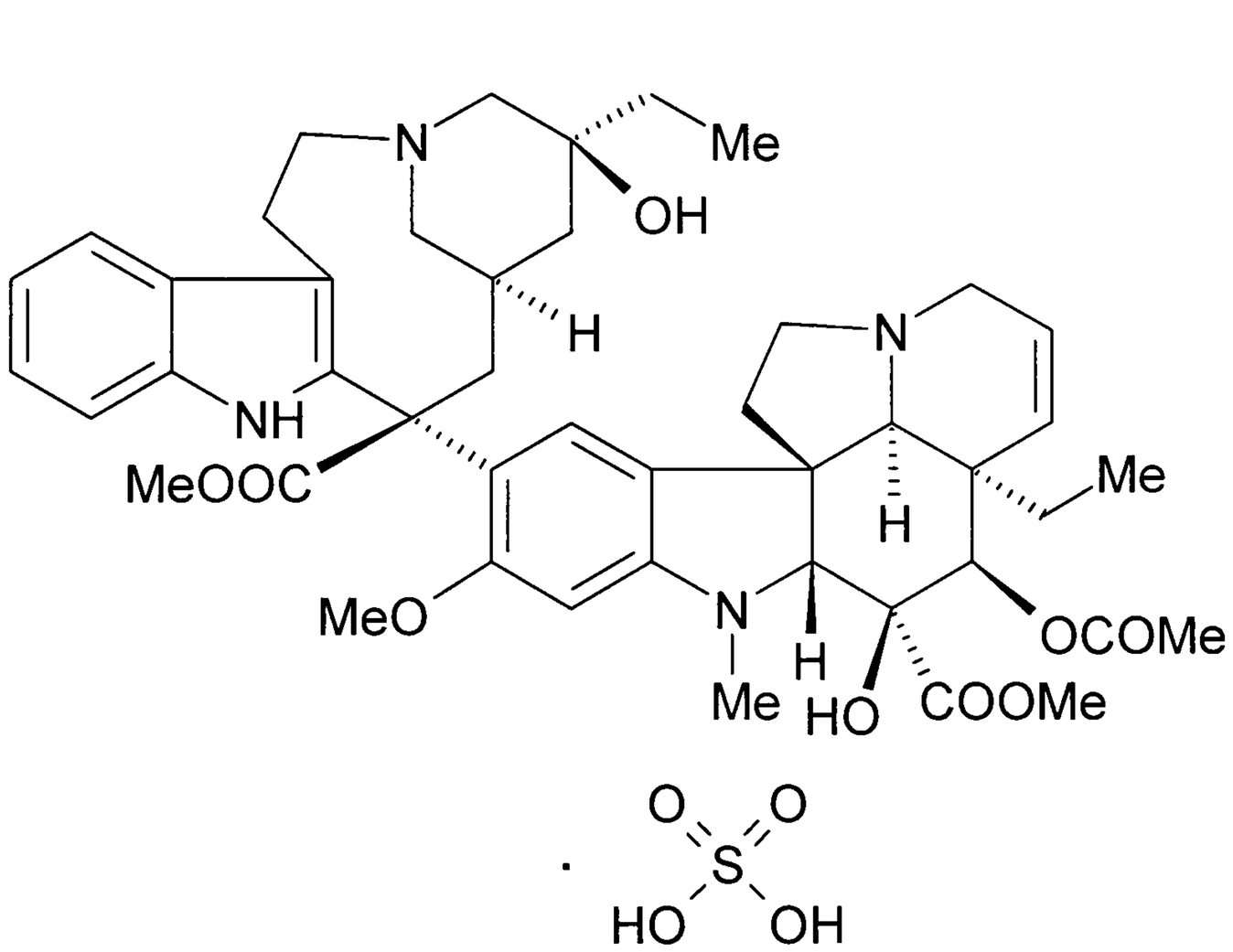

69

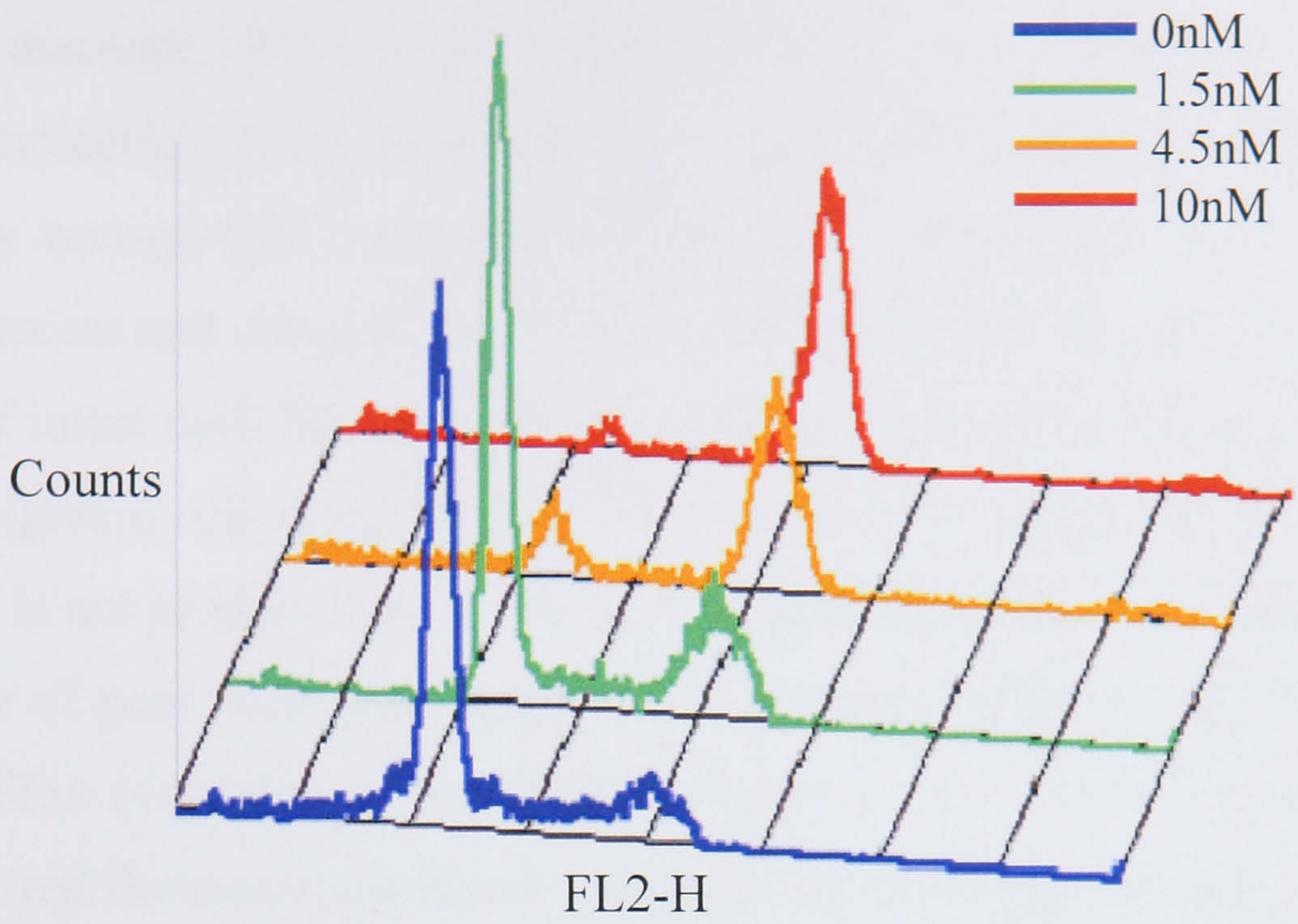

Figure 3-5: Overlay histogram of cell cycle analysis for COR-L23 treated by various concentrations of vinblastine sulphate (**69**)

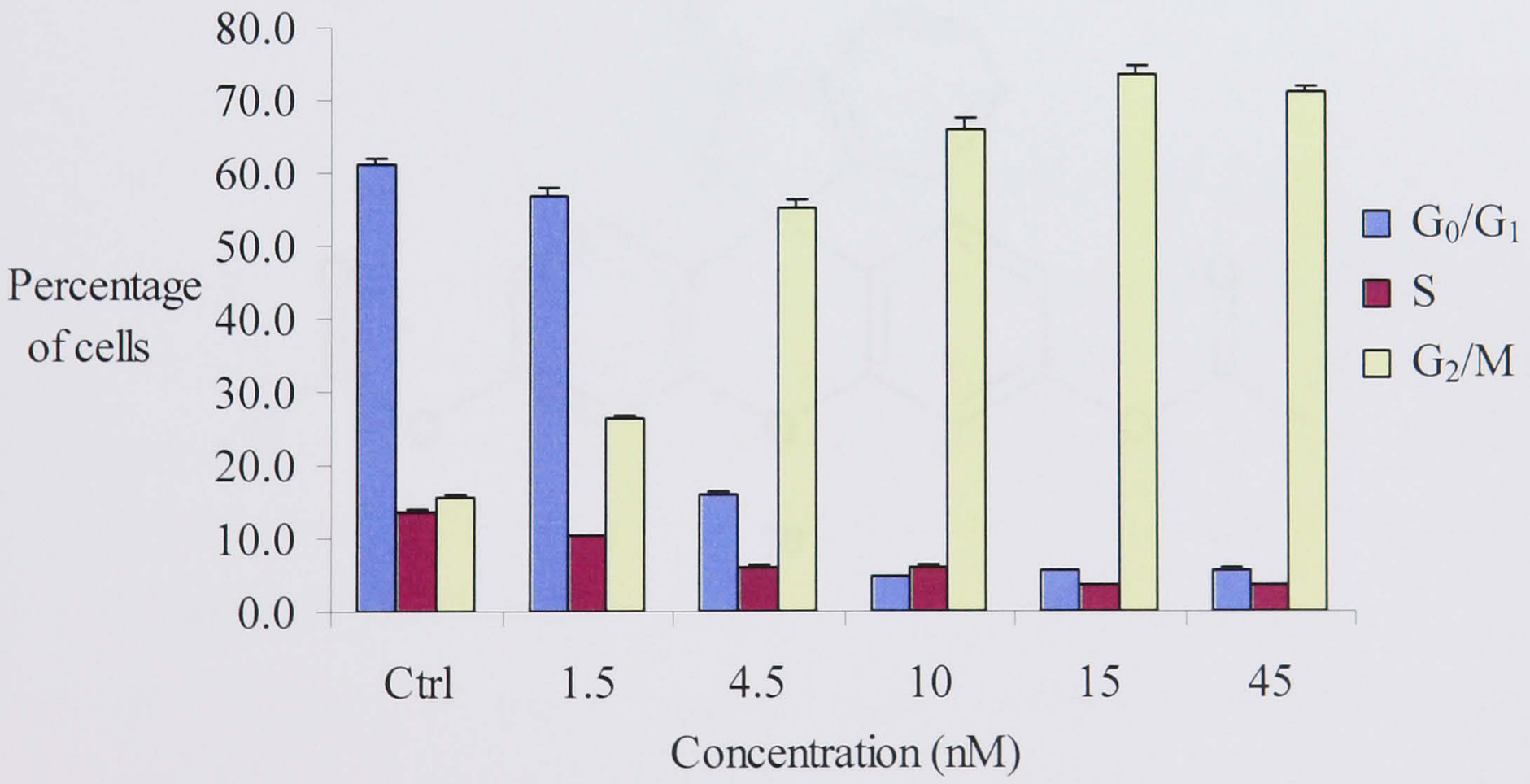

Figure 3-6: Effect of vinblastine sulphate (**69**) on cell cycle of COR-L23 cells after 48h exposure

3.2.3.4 Fluorescein diacetate (FDA)

Fluorescein diacetate (FDA) (**70**) (Fluka, 31545) is an electrically neutral, non-fluorescent molecule. It can penetrate the cell membrane and can be hydrolyzed to fluorecein by non-specific esterases in viable cells. The metabolite, fluorescein, is highly fluorescent and charged, so therefore, can accumulate in and be retained in the cytoplasm of intact cells for short periods of time, causing the living cells to become fluorescent (green) (Skehan, 1999). In the case of apoptotic and dead cells, fluorescence is not produced due to the lack of esterases or the FDA leaking out of the cells because of poor membrane integrity. In addition, an apoptotic cell is unable to metabolize FDA (Ormerod *et al.*, 1993; Tolleson *et al.*, 1996). PI, a nucleic acid binding-dye (red fluorescence), cannot penetrate the membrane of viable cells, but can enter cells readily during the cell death process due to a loss of membrane integrity. Therefore, FDA and PI co-labeling is able to distinguish viable cells (FDA positive, PI negative) (FDA^+/PI^-) and dead cells (FDA^-/PI^+) from apoptotic cells (FDA^-/PI^-) (Ranalli *et al.*, 2003).

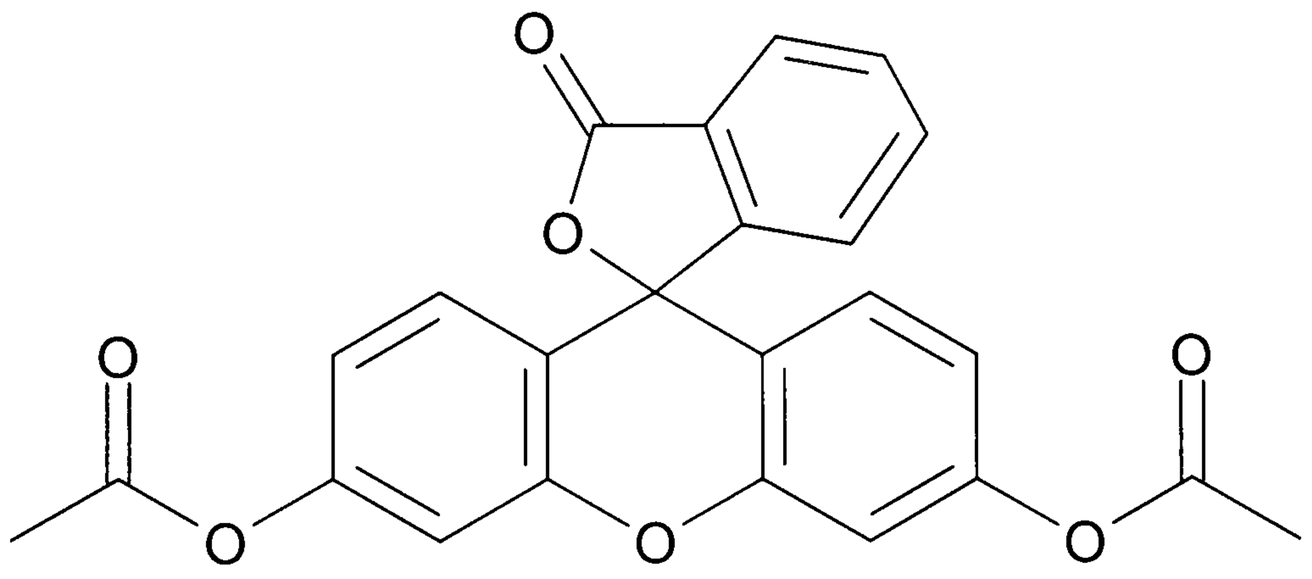

70

3.2.3.5 Protocol of FDA/PI staining

1. Cells were cultured in 6-well plates under a humidified 5% CO_2 atmosphere at 37°C. The seeding density was 1 million cells per well.
2. Plates were preincubated for 24h then the solutions of drugs or control were added to each well. After a period of treatment, cells were harvested by trypsinization with trypsin/EDTA (Sigma-Aldrich, T4049), and pelleted by centrifugation (1,500 rpm).
3. The pellet cells were resuspended in 0.98ml PBS. 10µl FDA stock solution (100µg/ml in DMSO) and 10µl PI stock solution (500µg/ml in PBS) were added and produced a 1ml cell suspension within 1µg/ml FDA and 5µg/ml PI by gentle vortex.
4. The staining samples were incubated at room temperature for 30 min in darkness.
5. The reaction was stopped by washing the samples twice with ice cold PBS.
6. Stained cells were resuspended in 800µl PBS and the samples were protected from light at 4°C until flow cytometric analysis (in 24h).
7. Samples were analysed immediately and not fixed. 10,000 events were acquired using the green channel FL1 for FDA and the red channel FL3 for PI.
8. In order to setup the quadrant analysis, four controls were required for each individual experiment. They were cells in plain buffer, cells stained with FDA only, cell stained with PI only, and cells stained with both dyes. Electronic compensation was occasionally required to remove interference form the green emission in the red channel.
9. On a FDA *vs* PI scatter plot, apoptotic cells should be double-negative, appearing in the lower left quadrant (LL). Necrotic cells or dead cells should be positive for PI only, and appear in the upper left quadrant (UL), while living cells should be positive for FDA only, appearing in the lower right quadrant (LR).

3.2.3.6 Annexin V-FITC

Changes in the plasma membrane are one of the earliest features of apoptosis. In apoptotic cells, the membrane phospholipid phosphatidylserine (PS) is translocated from the inner to the outer leaflet of the plasma membrane, thereby exposing PS to the external cellular environment. Annexin V is a 35–36 kD Ca^{2+}-dependent phospholipid-binding protein that has a high affinity for PS and binds to cells with exposed PS (Alison, 1999). Annexin V may be conjugated to fluorochromes such as FITC (fluorescein isothiocyanate) and PE (phycoerythrin). These formats retain their high affinity for PS and thus serve as sensitive probes for flow cytometry analysis of cells undergoing apoptosis (Zhang *et al.*, 1997).

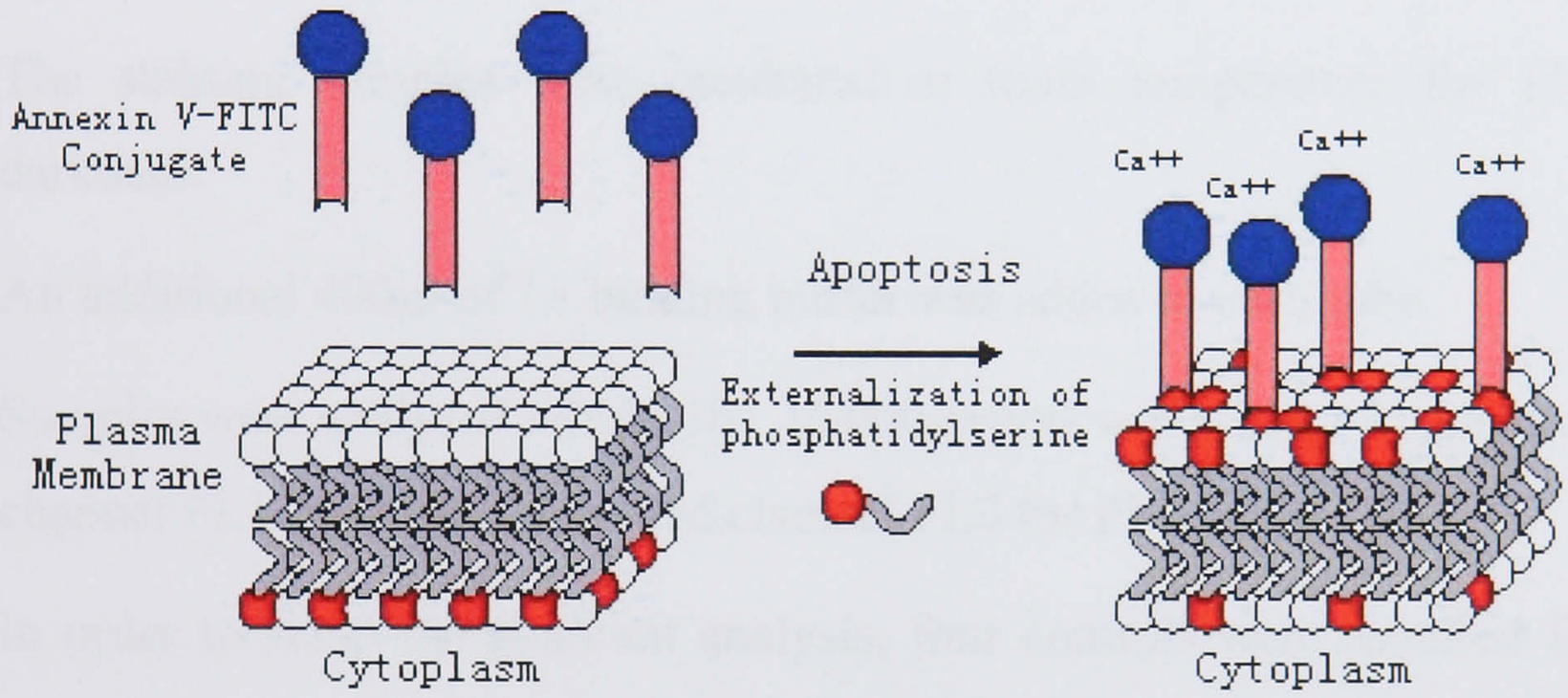

Figure 3-7: Schematic representation of the annexin V assay (from http://www.bdbiosciences.com/image_library/Annexin_Assay.jpg)

Because externalization of PS occurs at an early stage of apoptosis, staining with annexin V-FITC can identify apoptosis at an earlier stage than assays based on nuclear changes such as DNA fragmentation. Annexin V-FITC (Ann) staining precedes the loss of membrane integrity which accompanies the latest stages of cell death resulting from either apoptotic or necrotic processes. Therefore, staining with Ann in combination with propidium iodide (PI) allows the identification of early apoptotic cells (Ann^+/PI^-) from those that are in the later stages of apoptosis or already dead (Ann^+/PI^+). Nevertheless, the assay does not distinguish between cells that have undergone an apoptotic death from those that have died as a result of a necrotic pathway, because both dead cell types will stain positively with both annexin V and PI (van Engeland *et al.*, 1996).

3.2.3.7 Protocol of Ann/PI staining

1. Cell culture procedures were identical with those described in protocol of FDA/PI staining (steps 1 and 2).
2. According to the protocol in the BD Pharmingen™ techincal data sheet (supplied with the agent: annexin V-FITC, BD 556420), the cell pellet was resuspended in binding buffer (prepared from annexin V binding buffer, 10× Concentrate, BD 556454). Then, 100µl of cell suspension was transfered into a 5ml culture tube.
3. 5µl Ann and 10µl PI were added into the cell suspension, followed by gentle vortexing.
4. The staining samples were incubated at room temperature for 15min in darkness.
5. An additional 400µl of 1× binding buffer was added to each tube.
6. Samples were analysed within 1h. 10,000 events was acquired using the green channel FL1 for Ann and the red channel FL3 for PI.
7. In order to setup the quadrant analysis, four controls were required for each individual experiment. They were cells in binding buffer only, cells stained with Ann only, cells stained with PI only and cells stained with both agents. Electronic compensation was occasionally required to remove interference form the green emission in the red channel.
8. In an Ann/PI scatter plot, living cells should be double-negative (lower left quadrant), apoptotic cells should be Ann positive (lower right quadrant), and dead cells or necrotic cells should be PI positive (upper left and upper right quadrants).

3.3 Apoptosis results

In the present project a lung cancer cell line (COR-L23) was selected to test the potency of the isolated compounds in apoptosis experiments. Lung cancer is the leading cause of cancer-related death (Blair *et al.*, 1997). Its high prevalence, high death rate and ineffective current therapy have spurred the search for novel strategies in treatment of lung cancer. Two dual-colour fluorescent staining systems (Ann/PI

and FDA/PI) were applied in the present study for the detection of apoptosis. All measurements were made in triplicate and all values were represented as mean ± SEM (standard error of the mean). The results were subjected to an analysis of variance (ANOVA) using the Tukey's test to analyse the difference (p<0.05 were considered as significant).

3.3.1 Positive control for bicolour-staining apoptosis assay

An appropriate positive control for a bioassay is important. The agent must be able to induce apoptosis of certain cells and that ought to be detectable by the methods used. It is even better if the compound of positive control has a similar structure with the compounds in question. The compounds isolated from *I. tectorum* include two flavonoids: tectorigenin (**24**) and 7-*O*-methyl aromadendrin (**66**), and four iridal-type triterpenes: isoiridogermanal (**57**), iridobelamal A (**60**), IT4C (**61**) and IT4D (**65**). There is no literature about apoptosis induced by iridal-type triterpenes. However, some well known flavonoids with pharmaceutical activity, such as genistein and quercetin, have been reported to be able to induce apoptosis of human cancer cells (Vijayababu *et al.*, 2006; Lian *et al.*, 1999).

Further literature research revealed that genistein was shown to induce cell cycle progression arrest at the G_2/M phase and induce apoptosis in many different types of human cancer cell lines, including breast, stomach, prostate and squamous cell carcinoma cell lines (Alhasan *et al.*, 1999; Pagliacci *et al.*, 1994; Matsukawa *et al.*, 1993; Kyle *et al.*, 1997). Moreover, HPLC grade pure genistein is commercially available. Therefore, genistein was used as positive control for a methodological study of bicolour flow cytometry (FCM) analysis.

Since these two bicolour staining systems (FDA/PI and Ann/PI) are based on different biological mechanisms, consistent results of two testing methods will be more reliable than a single method to confirm the induction of apoptosis. Practically, FDA is much cheaper than Ann, therefore it is preferable for the primary test of potent apoptotic compounds in a large scale screening.

Firstly, the standard compound genistein (**51**) (Fluka 91955) was prepared in four concentrations from 100μM to 400μM, then incubated with COR-L23 cells for 48h before detection by FCM. The result of the present work showed that FDA/PI and Ann/PI assays gave the same trend of dose response, which indicated significant dose-

dependent apoptotic population of COR-L23 cells induced by genistein in a serial quadrant analysis.

3.3.1.1 FDA/PI assay of genistein (51)

On the scatter plot of FDA (FL1) *vs* PI (FL3) (Figure 3-8), apoptotic cells were double-negative, appeared in the lower left (LL) quadrant. Necrotic and dead cells were positive for PI only, and appeared in the upper left (UL) quadrant, while living cells were positive for FDA only, appeared in the lower right (LR) quadrant of the plot. When cells were under normal conditions, as shown on scatter plot A, most signals distributed in the LR quadrant representing 91% living cells. Signals in UL and LL quadrant indicates 2% dead cells and 7% apoptotic cells respectively.

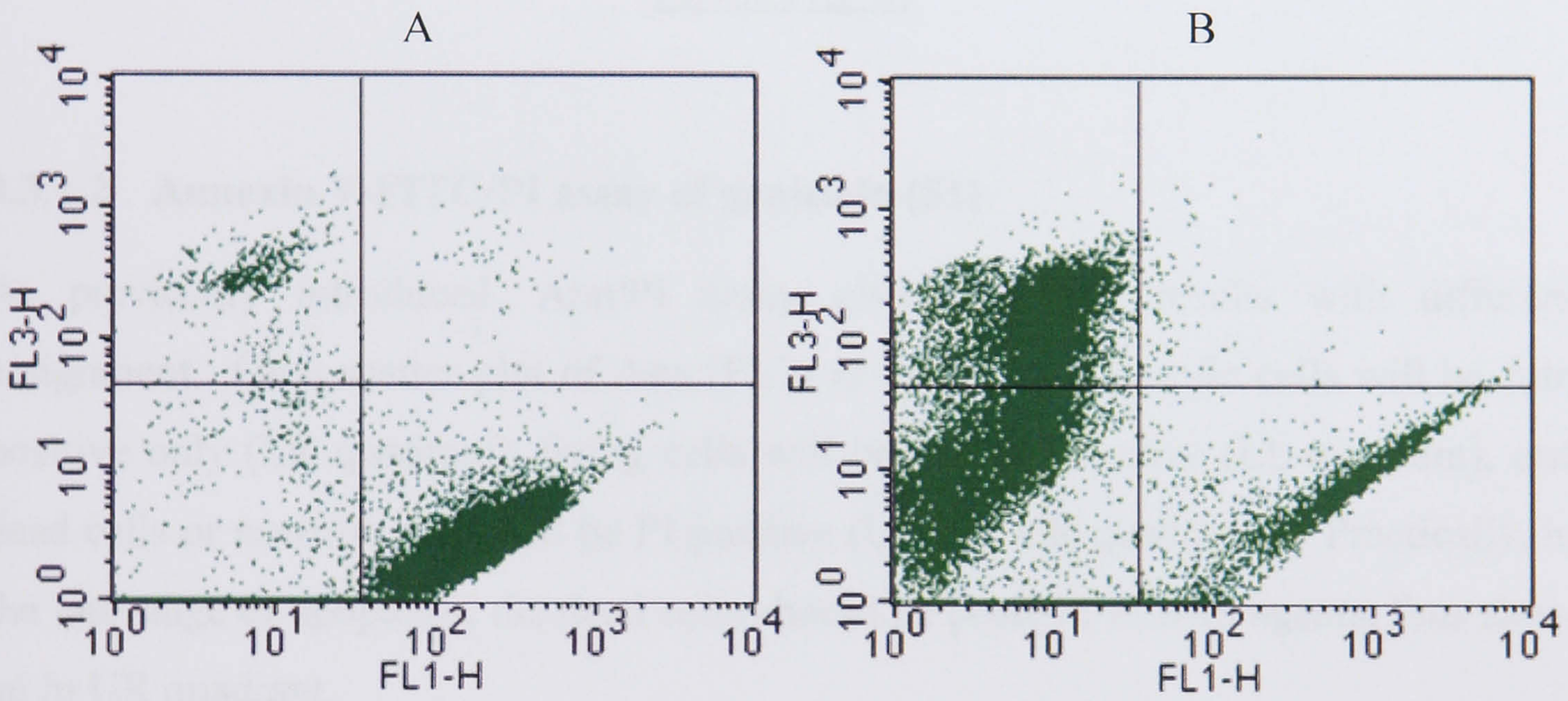

Figure 3-8: Scatter plots of FDA/PI-stained COR-L23 (lung cancer) cells under three situations in quadrant analysis, they are living cells (LR), dead cells (UL) and apoptotic cells (LL); A: control; B: exposed to 300μM genistein (**51**) for 48h

The percentage of apoptotic cells increased and that of living cells decreased, when cells were exposed to 400μM genistein (**51**) for 48hr (scatter plot B in Figure 3-8). Signals in UL and LL quadrants represent 34.2% dead cells and 51.6% apoptotic cells, respectively. Meanwhile, only 14.2% living cells were left in LR quadrant. As seen in Figure 3-9, the proportion of apoptotic and dead cells increased with the concentration of genistein (**51**). These statistic results were obtained from a series of quadrant analysis; more detailed data are available in Table 3-7 on page 145.

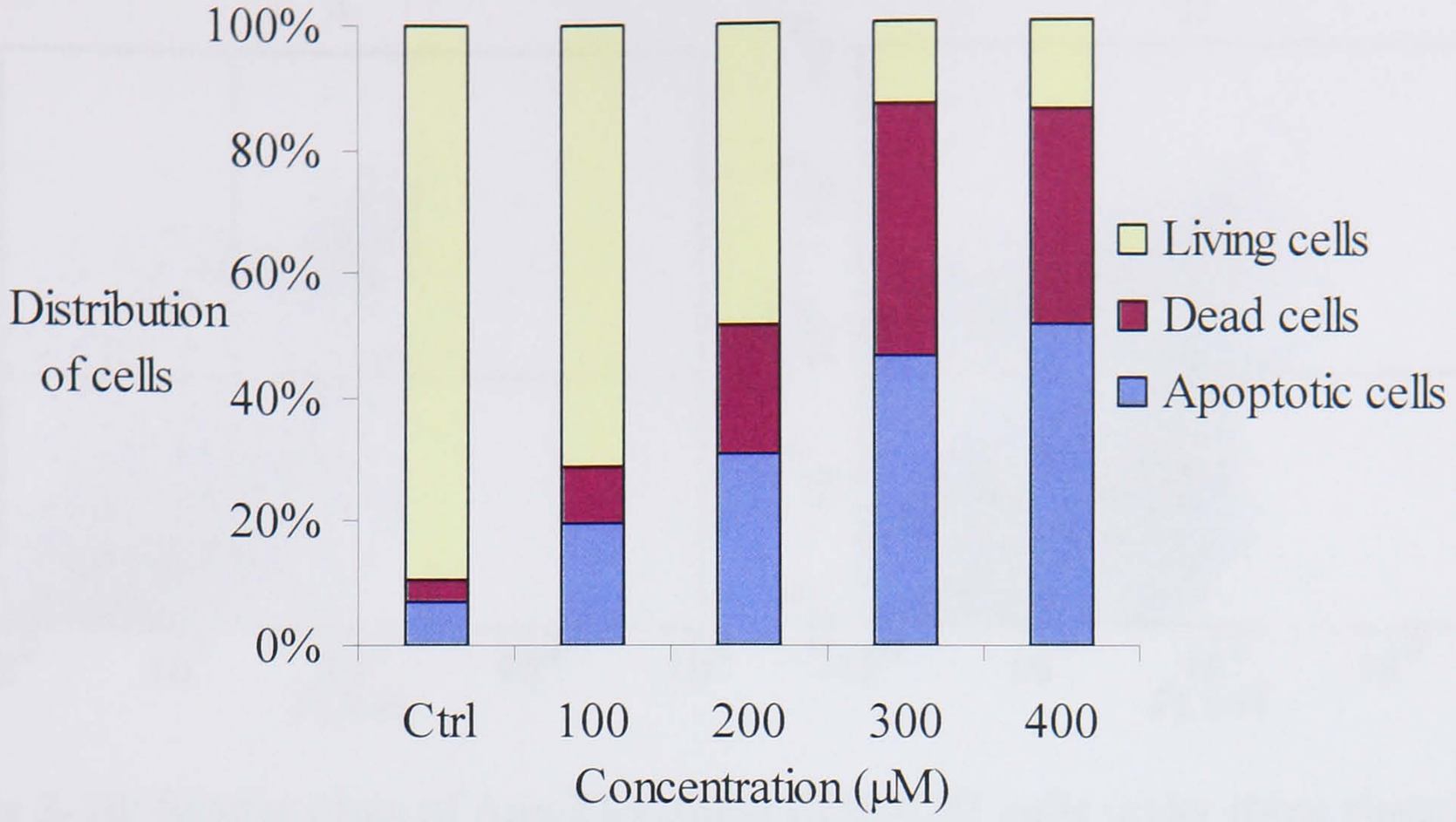

Figure 3-9: Percentage of COR-L23 cells under three different situations after exposure to various concentrations of genistein (**51**) for 48h. Specimens stained with FDA/PI (n=3)

3.3.1.2 Annexin V-FITC/PI assay of genistein (51)

As previously introduced, Ann/PI assay gives quadrant results with different assignment. On a scatter plot of Ann (FL1) *vs* PI (FL3), apoptotic cells will be Ann positive only (LR quadrant), living cells will be double negative (LL quadrant), and dead cells or necrotic cells will be PI positive (UL and UR quadrants). Practically, in the late stage of apoptosis, the dead cells should be positive to both agents, thus show up in UR quadrant.

In this assay genistein (**51**) also induced dose-dependent apoptosis with concentrations over a range of 25μM to 400μM. As seen in Figure 3-10, living cells (LL) decreased from 91.4% in control to 32.9% in 400μM, meanwhile apoptotic cells (LR) increased from 2.9% in control to 18.4% in 400μM. The total dead cells (UL and UR) are also significantly increased from 5.8% in control to 48.7% in 400μM. Practically, the percentage of dead cells, which also increased with the concentration of genistein, could be attributed to both apoptotic as well as necrotic cells because genistein can induce necrosis at high concentrations (Baxa *et al.*, 2005). Broadly, the result of the Ann/PI assay (Figure 3-11) are quite consistent with those of the FDA/PI assay.

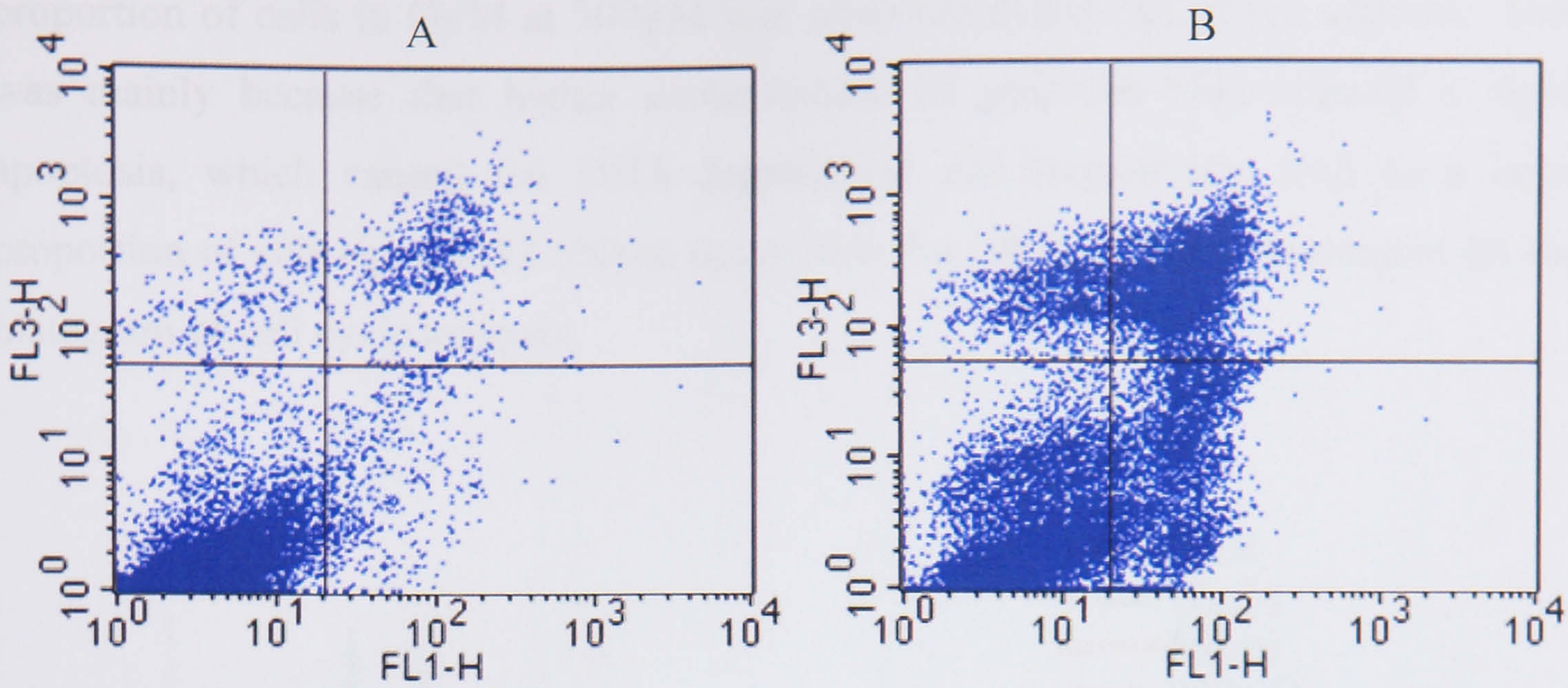

Figure 3-10: Scatter plots of Ann/PI-stained COR-L23 cells under three situations in quadrant analysis, they are living cells (LL), dead cells (UL and UR) and apoptotic cells (LR); A: control; B: exposed to 400μM genistein (**51**) for 48h

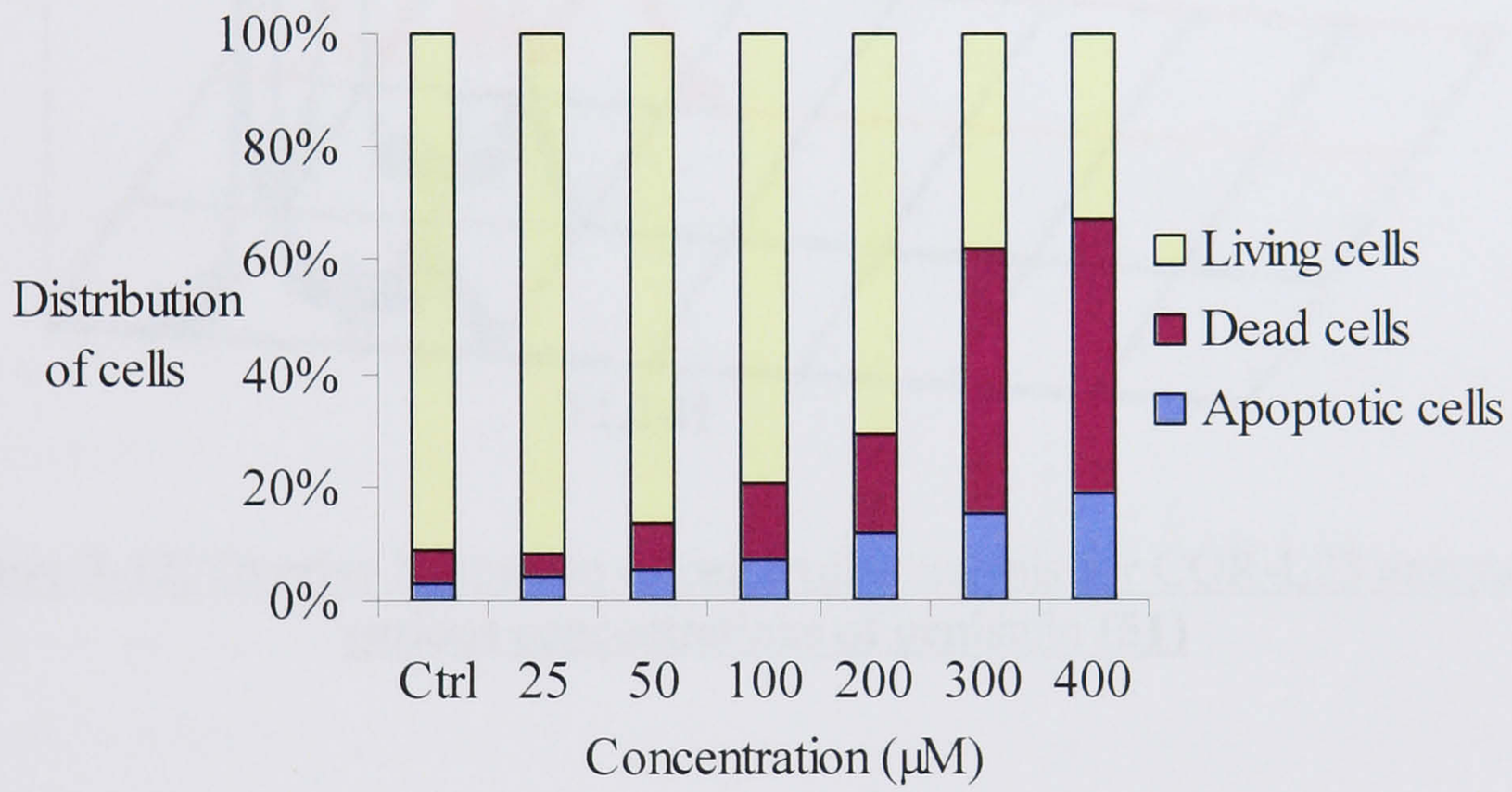

Figure 3-11: Percentage of COR-L23 cells under three different situations after exposed to various concentrations of genistein (**51**) for 48h. Specimens stained with Ann/PI (n=3)

The alteration of DNA content distribution in COR-L23 cells induced by genistein (**51**) (Figure 3-12) shows a cell cycle-specific effect similar to that of vinblastine sulphate (**69**). The proportion of COR-L23 cells in G_2/M phase gradually increased with the concentration of genistein (**51**). As shown in Figure 3-13, the cells in G_2/M phase increased from 17.2% in control to 37.5% at 200μM. On the other hand, cells in G_0/G_1 phase decreased from 62.7% to 31%. However, the proportion of cells in S phase did not significantly change over the range of tested concentrations. A drop in

proportion of cells in G_2/M at 300μM was observed at the end of the uptrend. This was mainly because that higher concentration of genistein (**51**) induced a rapid apoptosis, which caused the DNA degradation and sequentially lead to a large proportion of cell signals (33.6%) to move into the sub-G_1 DNA complement on the histogram of cell cycle analysis.

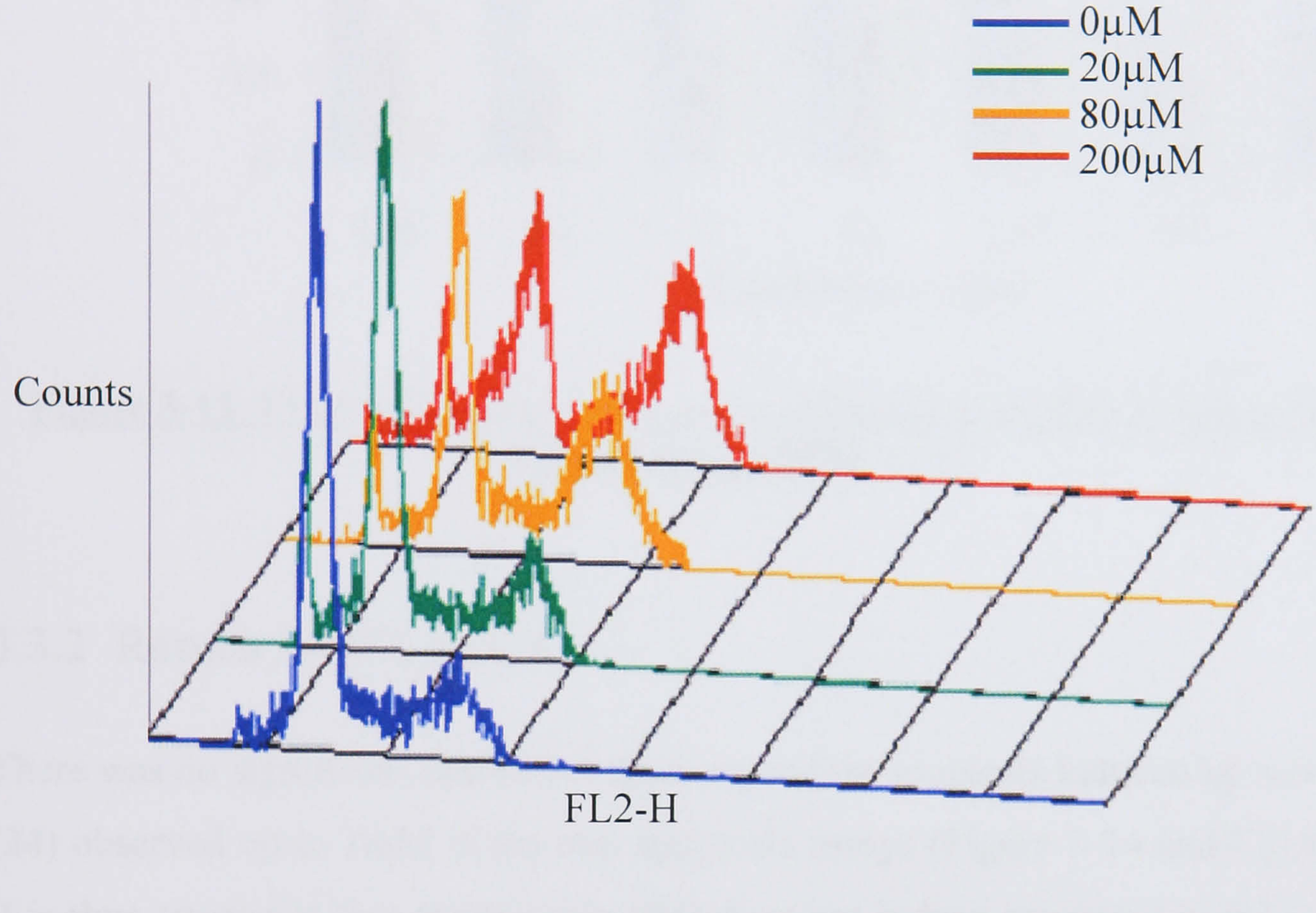

Figure 3-12: Overlay histogram of cell cycle analysis for COR-L23 exposed to various concentrations of genistein (**51**)

Apoptosis results of genistein (**51**) acquired from the two dual-colour staining assays are generally coincident to each other. The differences of the values between the counterpart treatments in two apoptosis assays are likely to be mainly due to the mechanism of the reactions, on which these bioassays are based. All the apoptotic results of genistein (**51**) were consistent with those in the literature (Matsukawa *et al.*, 1993; Salti *et al.*, 2000; Po *et al.*, 2002). This clearly indicated that the protocols of two dual-colour staining systems (FDA/PI and Ann/PI) followed in the present study were working as anticipated with the lung cancer cell line COR-L23. Thus, results of other compounds detected by identical protocols should be reliable.

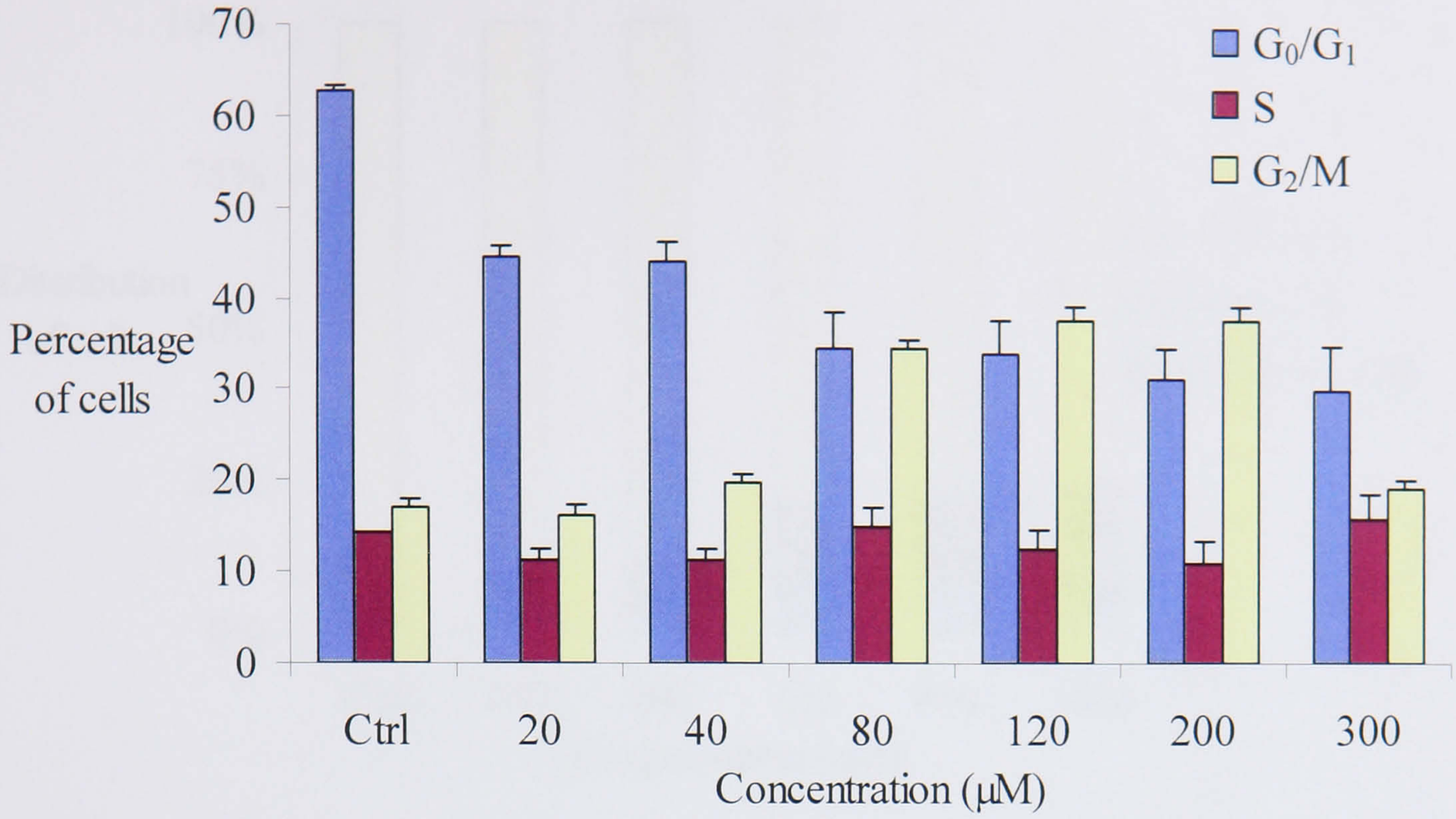

Figure 3-13: Effect of genistein (**51**) on the cell cycle of COR-L23 cells after 48h exposure (mean±SEM, n=3)

3.3.2 Results for IT3Ac (24)

There was no significant uptrend of dose-dependent apoptosis induced by tectorigenin (**24**) observed up to 1mM in the two apoptosis assays (Figure 3-14 and Figure 3-15). It is thus suggested that tectorigenin (**24**) does not induce apoptosis in the COR-L23 cell line up to the very high concentration of 1mM. This conclusion is indirectly supported by a recently published paper, in which tectorigenin (**24**) was demonstrated to protect against the cytotoxicity of HepG2 cells induced by *tert*-butyl hyperoxide (Lee *et al.*, 2005). It was also suggested that the protection may originate from inhibition of apoptosis. Moreover, these findings lead support to the traditional use of the original plant, because *Iris tectorum* has been used to treat patients with hepatic cirrhosis. This activity could be explained by the presence of tectorigenin (**24**), isolated as a principal compound from the plant (Qin *et al.*, 1996).

On the other hand, tectorigenin (**24**) arrested cell progress at S and G_2/M phases (as seen in Figure 3-16 and Figure 3-17). Furthermore, this antiproliferative effect *per se* may cause a cell cycle-mediated drug resistance if it is used in a combination with other cell cycle-specific cytotoxic agents in an inappropriate sequence (Shah and Schwartz, 2001).

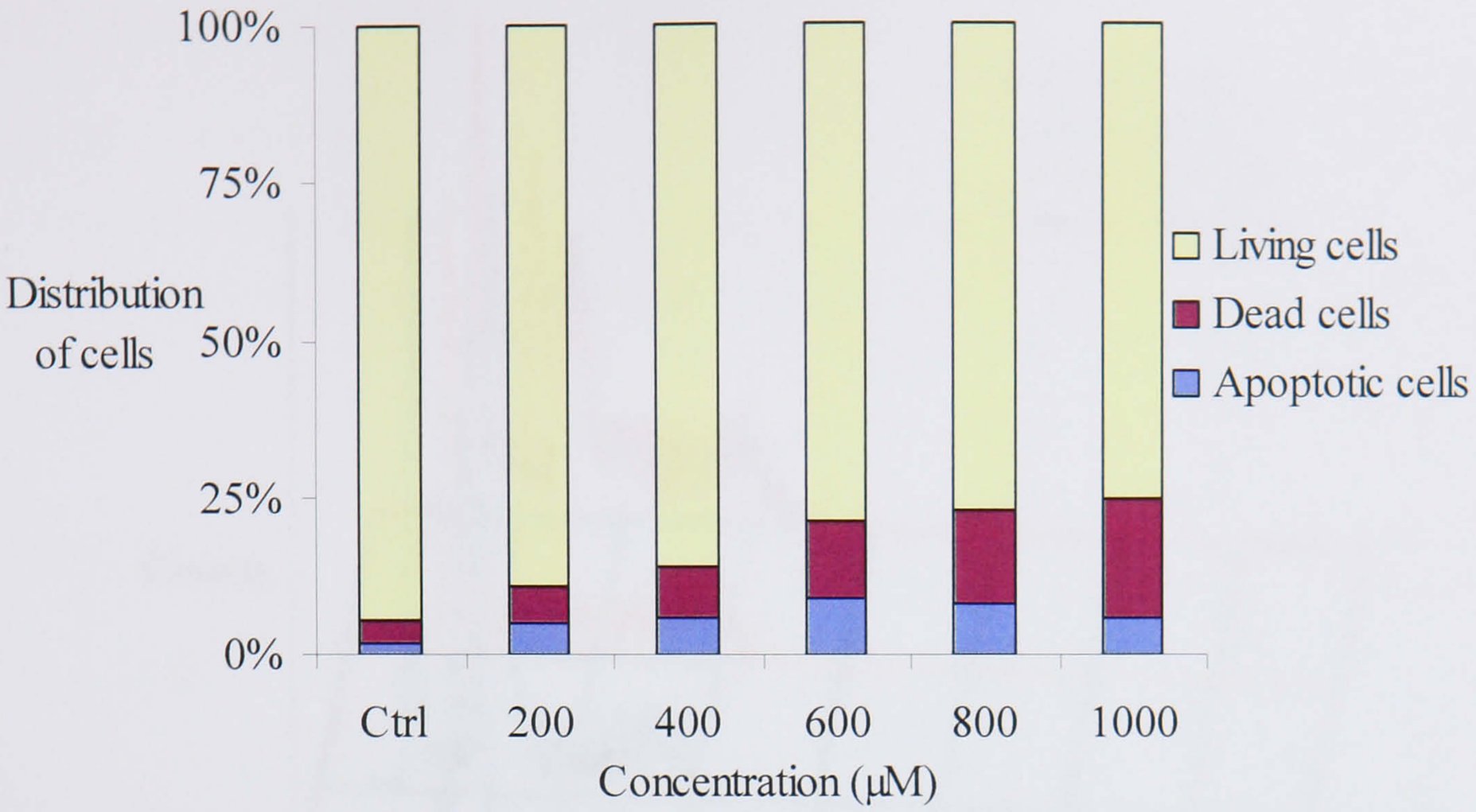

Figure 3-14: Percentage of COR-L23 cells under three different situations after exposure to various concentrations of tectorigenin (**24**) for 48h (Specimens stained with FDA/PI, n=3)

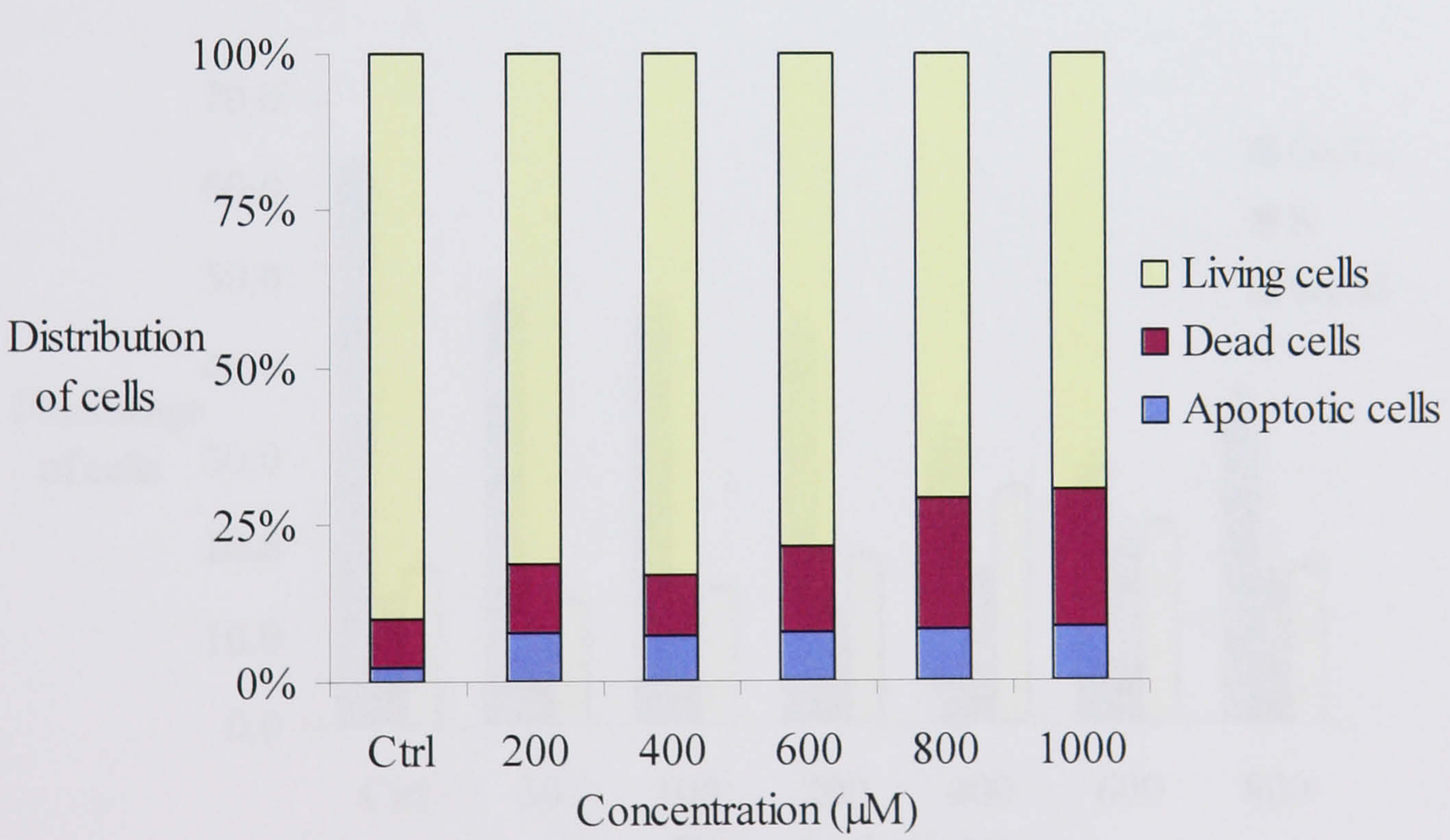

Figure 3-15: Percentage of COR-L23 cells under three different situations after exposure to various concentrations of tectorigenin (**24**) for 48h (Specimens stained with Ann/PI, n=3)

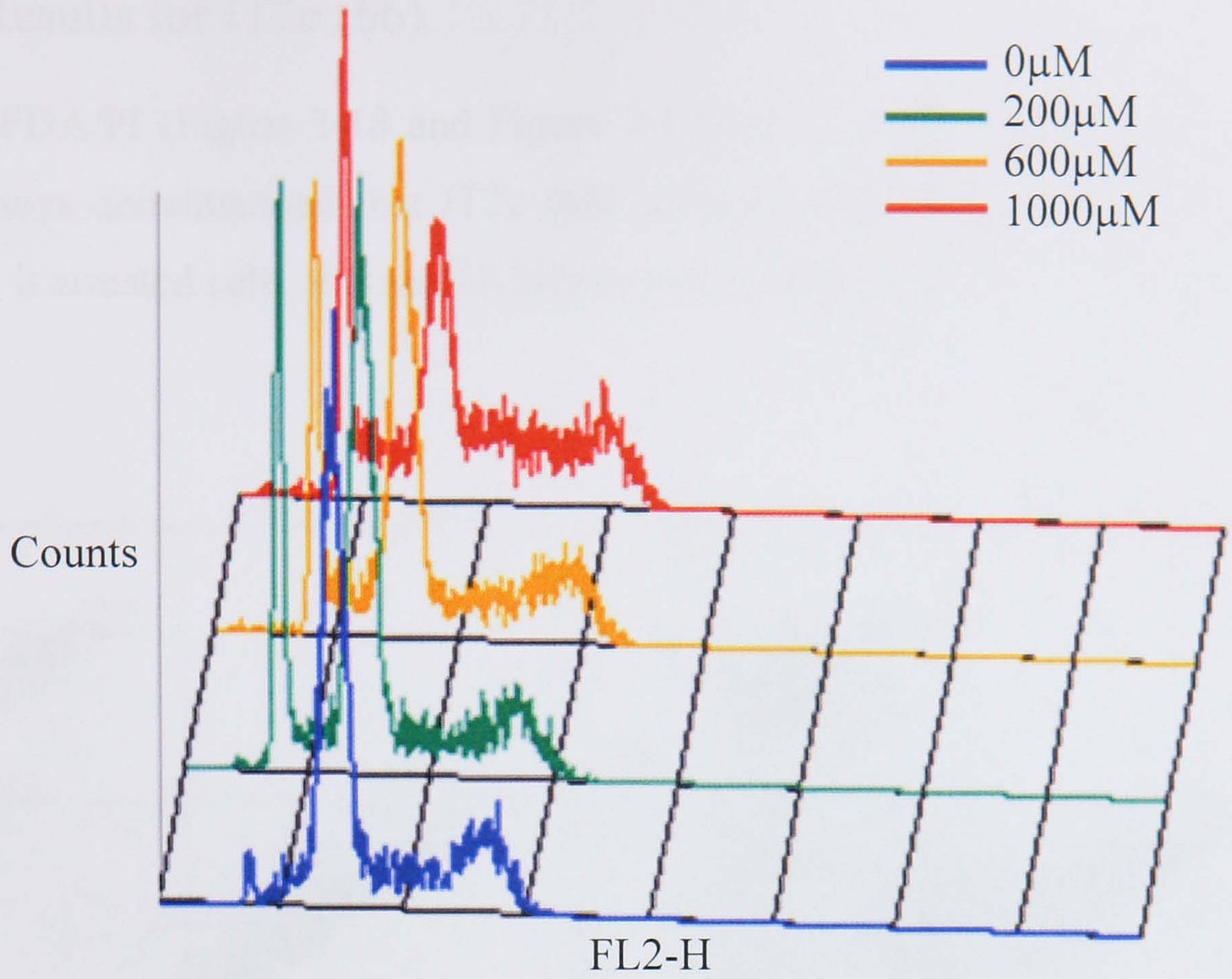

Figure 3-16: Overlay histogram of cell cycle analysis for COR-L23 exposed to various concentrations of tectorigenin (**24**)

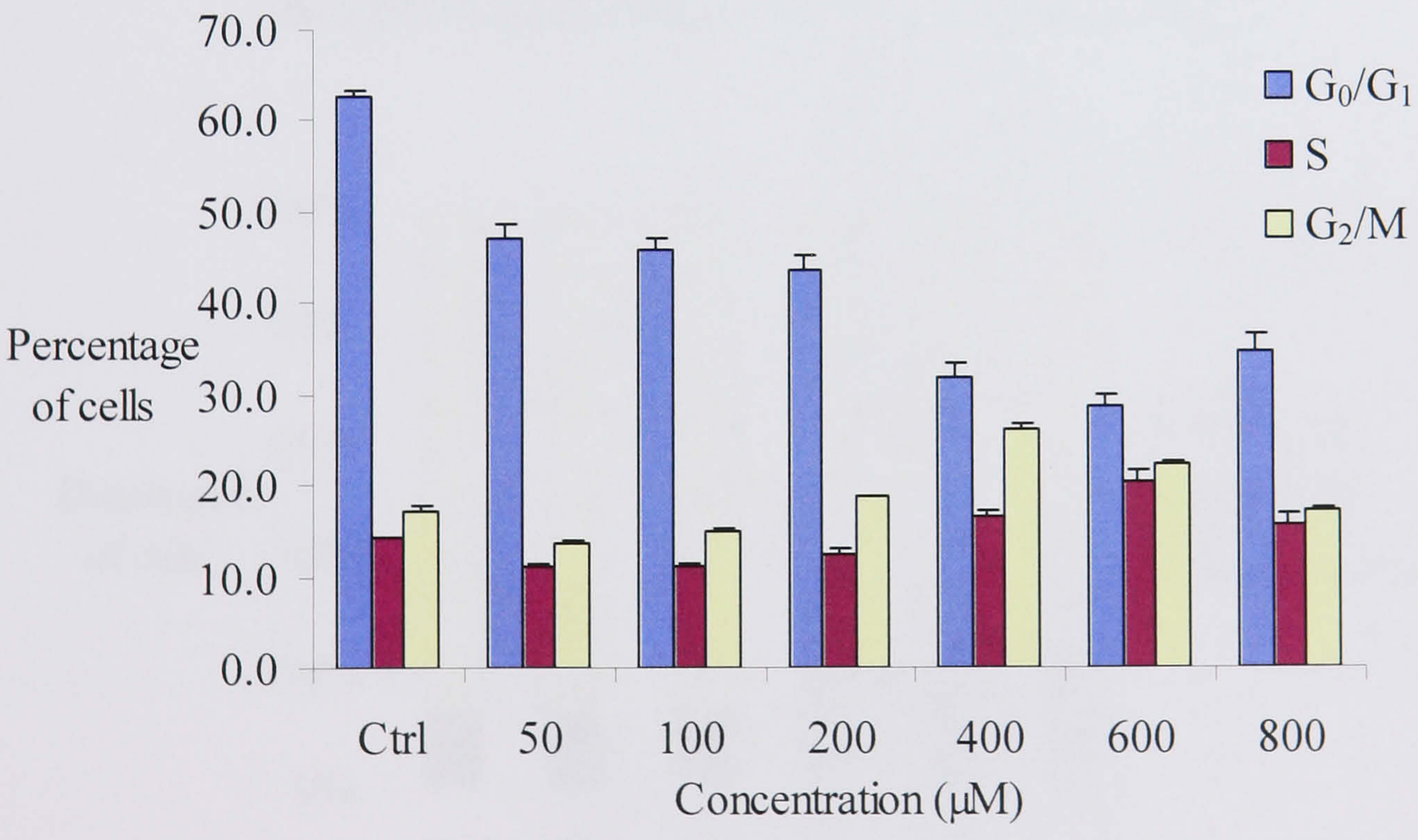

Figure 3-17: Effects of tectorigenin (**24**) on the cell cycle of COR-L23 cells after 48h exposure (mean±SEM, n=3)

3.3.3 Results for IT2c (66)

Both of FDA/PI (Figure 3-18 and Figure 3-19) and Ann/PI (Figure 3-20 and Figure 3-21) assays demonstrated that IT2c (**66**) induced apoptosis of COR-L23 cells. In addition, it arrested cells at S and G_2/M phases (see Figure 3-22).

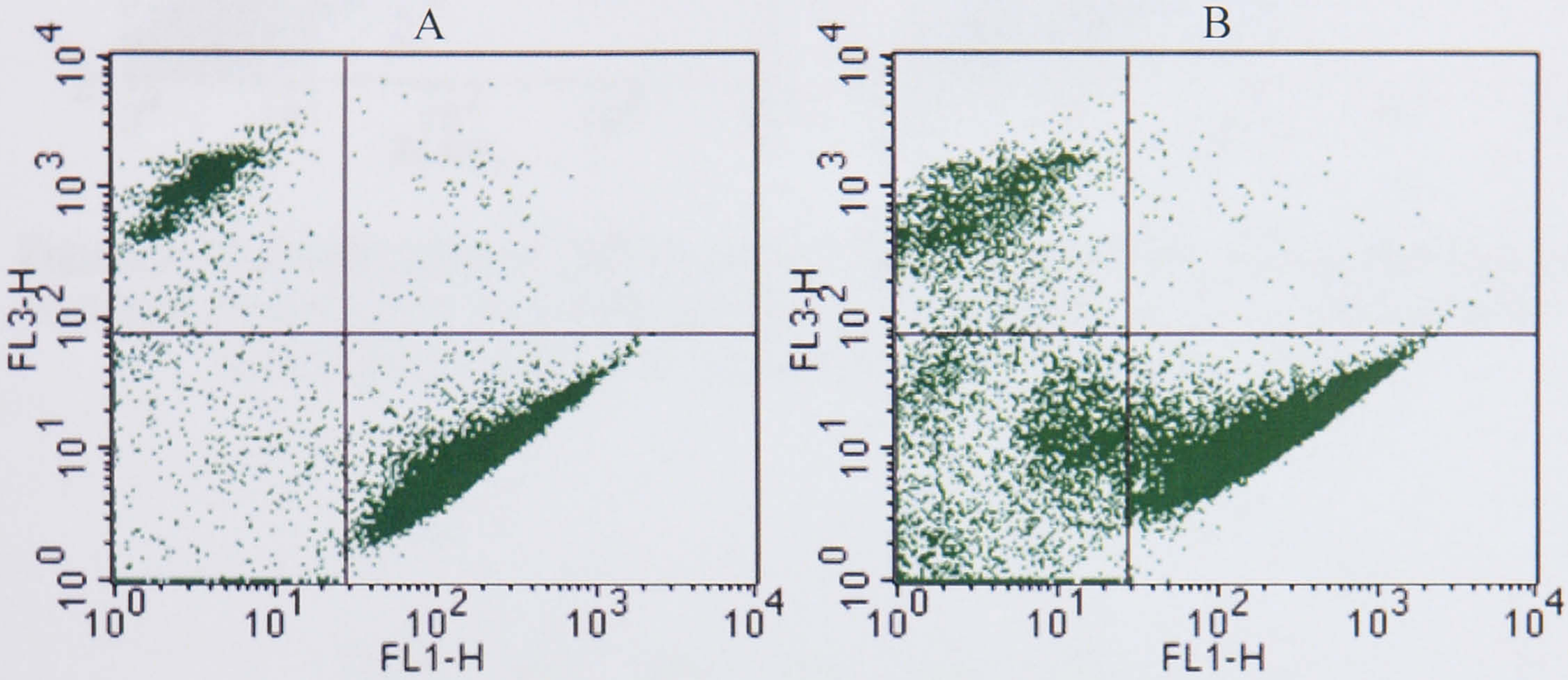

Figure 3-18: Scatter plots of FDA/PI-stained COR-L23 cells under three situations in quadrant analysis; they are living cells (LR), dead cells (UL) and apoptotic cells (LL); A: control; B: exposed to125μM IT2c (**66**) for 48h

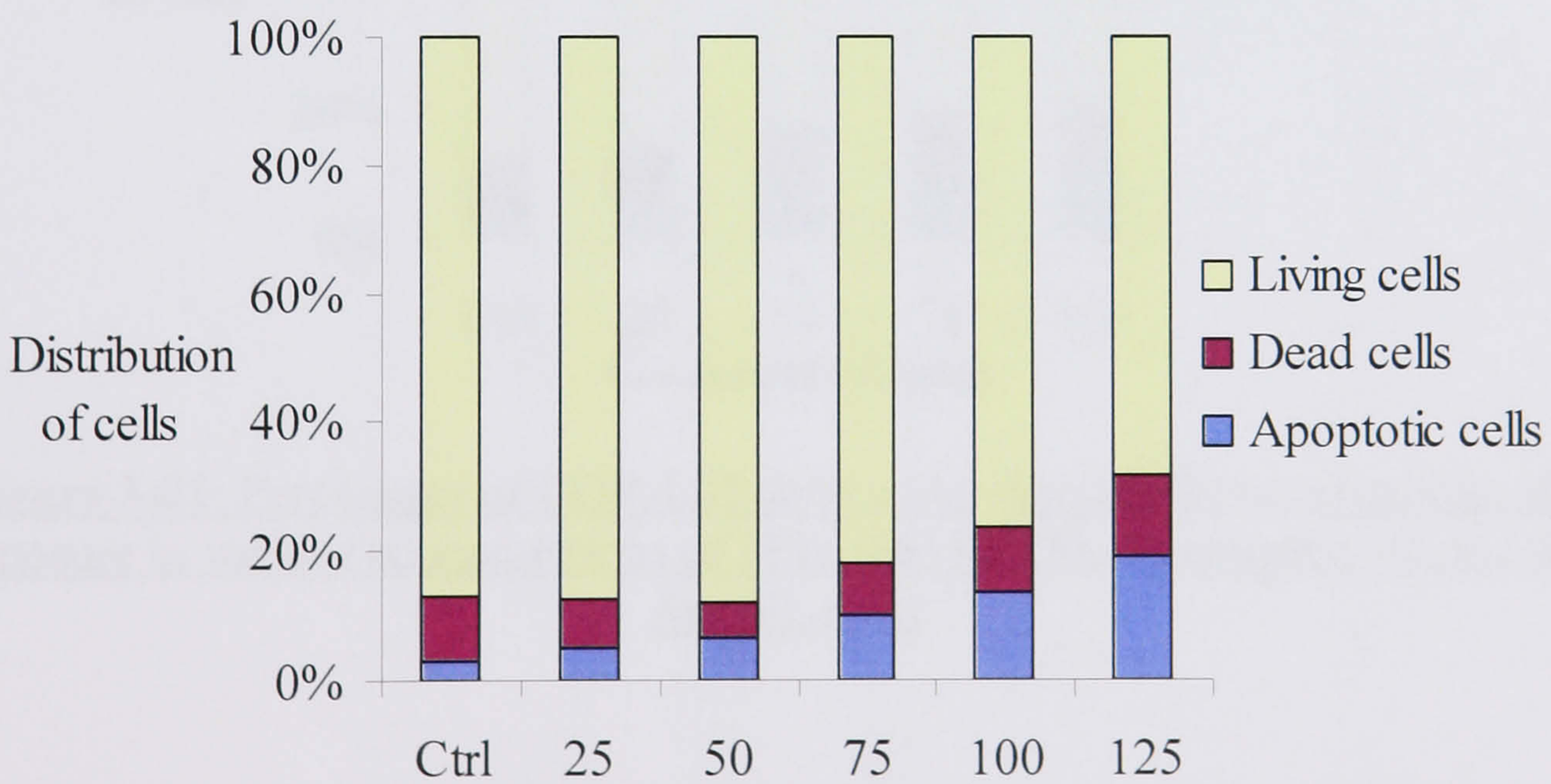

Figure 3-19: Percentage of COR-L23 cells under three different situations after exposure to various concentrations of IT2c (**66**) for 48h (Specimens stained with FDA/PI, n=3)

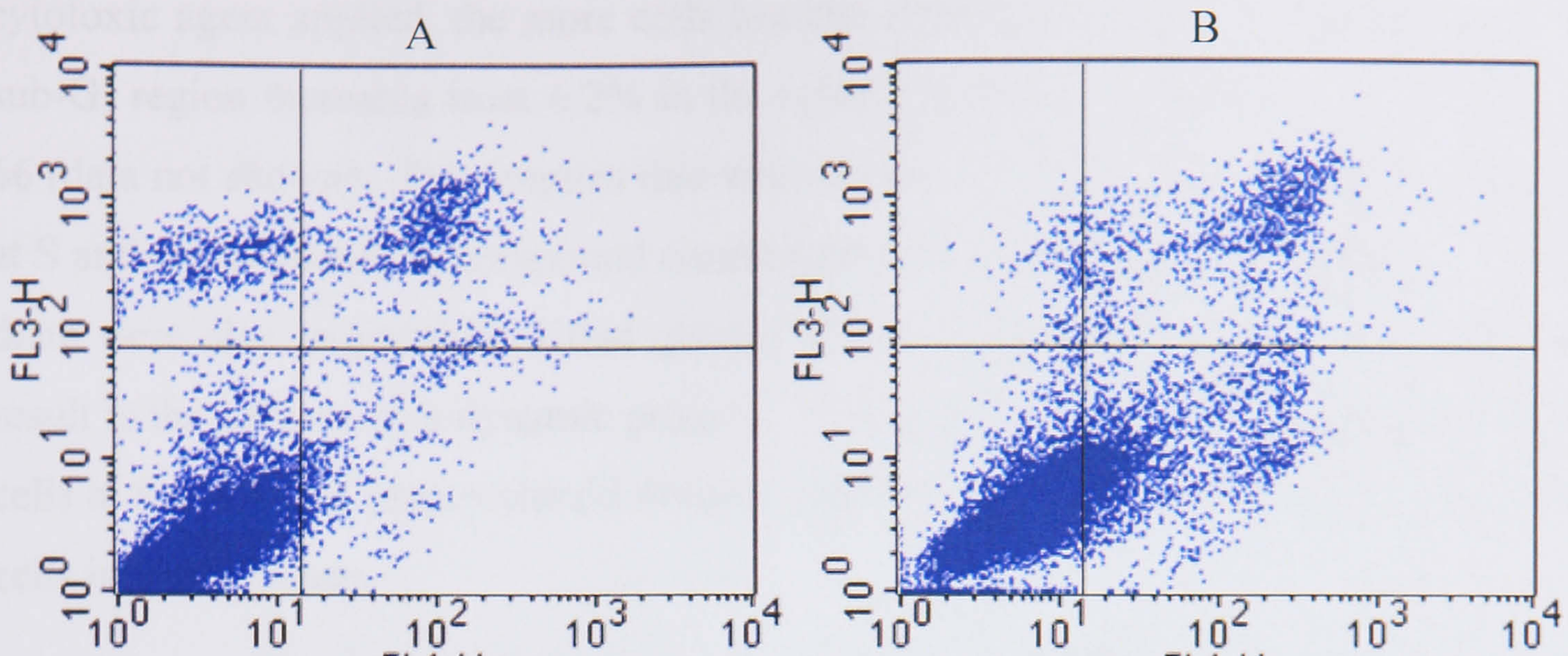

Figure 3-20: Scatter plots of Ann/PI-stained COR-L23 cells under three situations in quadrant analysis; they are living cells (LL), dead cells (UL and UR) and apoptotic cells (LR); A: control; B: exposed to 100μM IT2c (**66**) for 48h

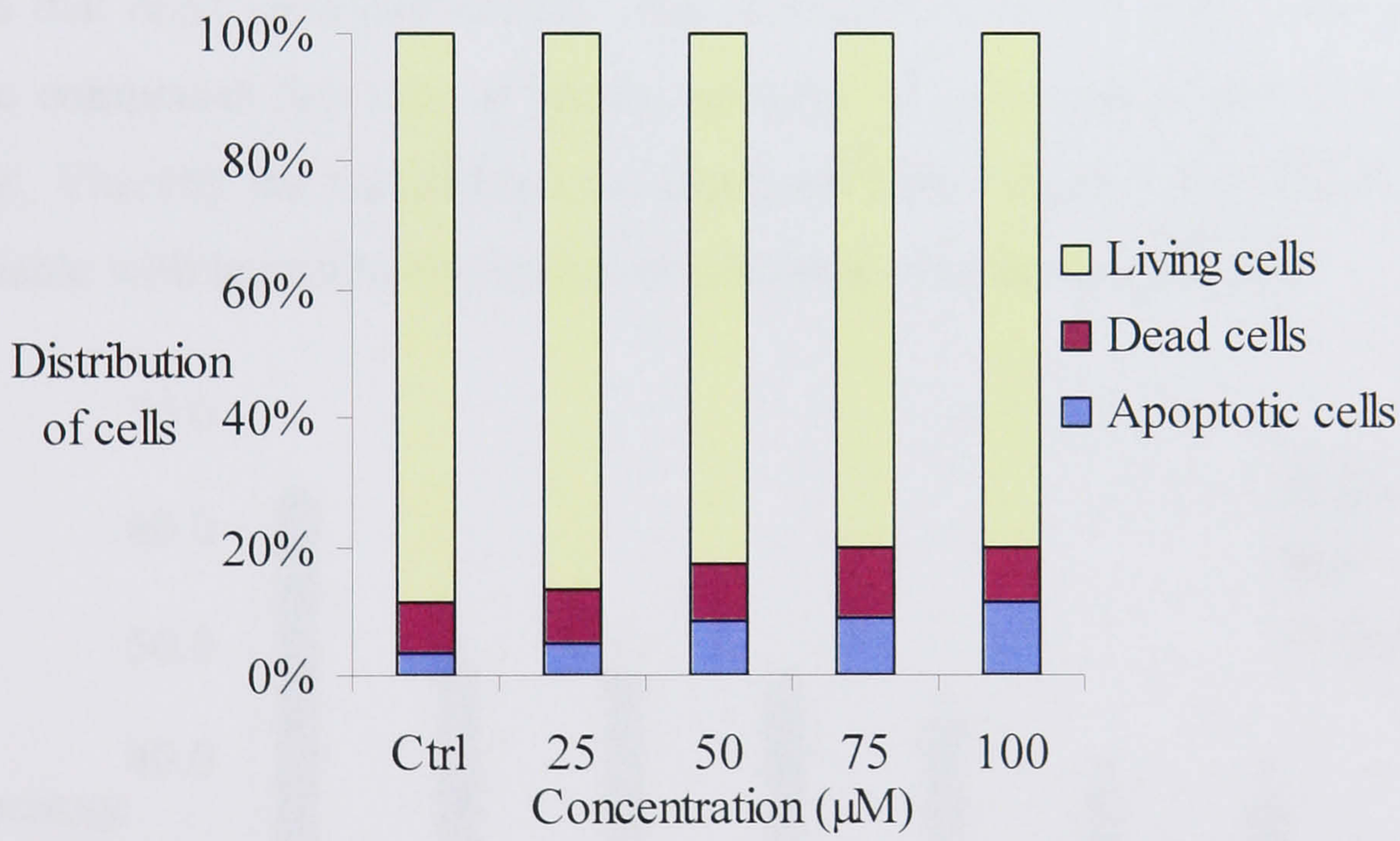

Figure 3-21: Percentage of COR-L23 cells under three different situations after exposure to various concentrations of IT2c (**66**) for 48h (Specimens stained with Ann/PI, n=3)

Comparing with the distribution of cells in the control, the proportion of cells in S and G_2/M phases did not change much when higher concentrations of IT2c (**66**) applied. However, this does not mean cells were not arrested or accumulated in certain cell cycle phase. Actually, the percentage of cells in histogram gives result of a *dynamic distribution* of cells under different conditions. The higher concentrations of

cytotoxic agent applied, the more cells became apoptotic and dead, and therefore the sub-G_1 region increases from 6.2% in the control to 29.5% on treatment with 100μM **66** (data not shown). This implies that when more and more cells were being arrested at S and G_2/M phases as compound concentration increased, at the same time some of them were also sequentially killed quickly by the compound. Thus, the quantitative result is the balance of a dynamic process. If this were not the case, the proportion of cells at S and G_2/M phases should decline, rather than only reducing the proportion of cells in G_0/G_1 phase.

A good example will be seen later in the results of IT4D (**65**) (Figure 3-28). In that case, no significant dose-dependent accumulation of cells in any cell cycle phase was observed. The proportions of cells in all phases decreased gradually when the compound concentration increased up to 60μM. Nevertheless, a drop of the proportion of cells in G_0/G_1 phase and relatively increased proportion in G_2/M phase with remarkably large error bars were observed on treatment with 100μM **65**. The reason is that most cells had already been damaged at such a high concentration of cytotoxic compound that only a limited quantity of cells was available for the cell cycle test. Thereby, the values from the treatment with 100μM IT4D (**65**) are unlikely to be reliable with regard to evaluation of cell cycle-specific cytotoxicity.

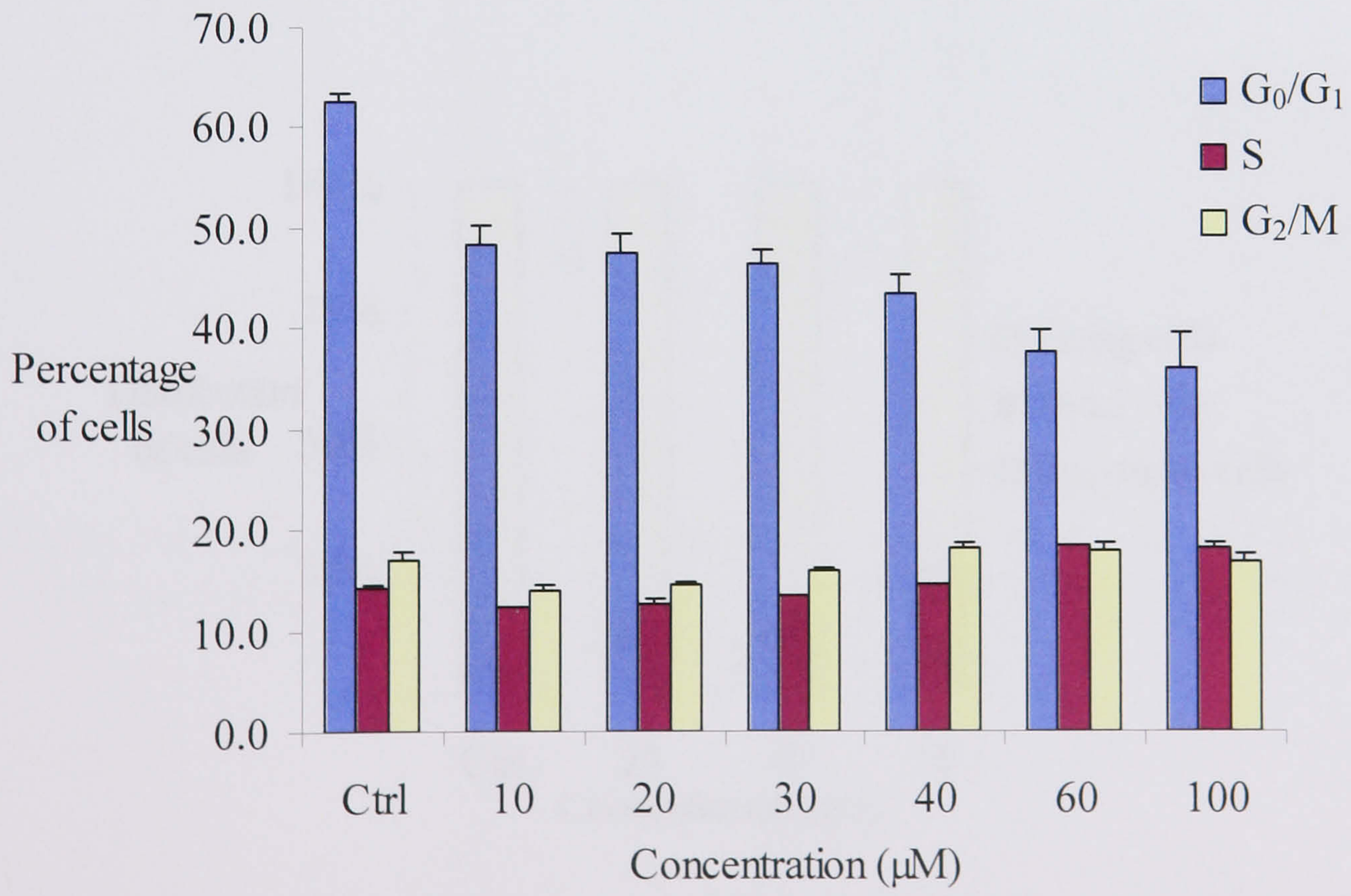

Figure 3-22: Effects of IT2c (**66**) on the cell cycle of COR-L23 cells after 48h exposure (mean±SEM, n=3)

3.3.4 Results for IT4D (65)

IT4D exhibited induction of apoptosis in both FDA/PI (Figure 3-23 and Figure 3-24) and Ann/PI (Figure 3-25 and Figure 3-26) assays. Also, it showed cell cycle non-specific cytotoxicity against COR-L23 cells (Figure 3-27 and Figure 3-28).

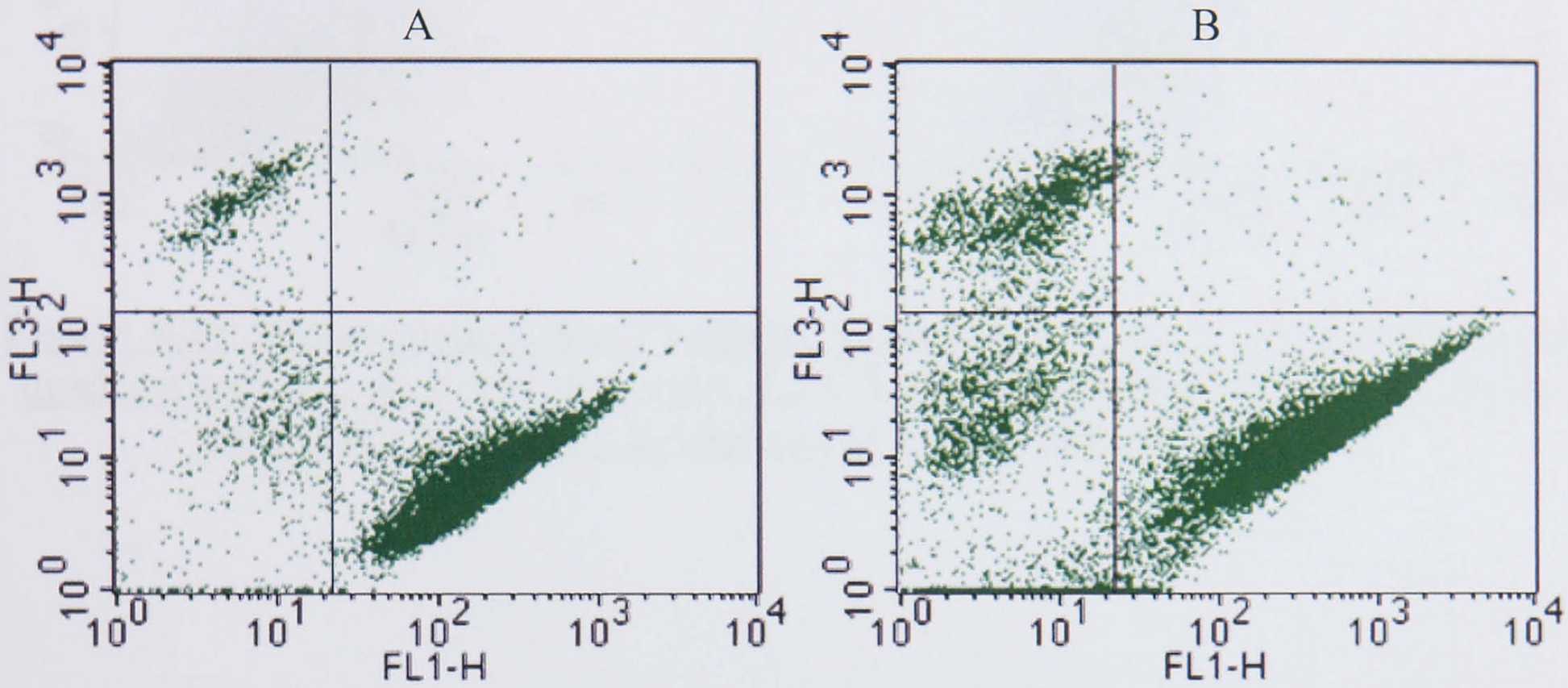

Figure 3-23: Scatter plots of FDA/PI-stained COR-L23 cells under three situations in quadrant analysis; they are living cells (LR), dead cells (UL) and apoptotic cells (LL); A: control; B: exposed to 60μM IT4D (**65**) for 48h

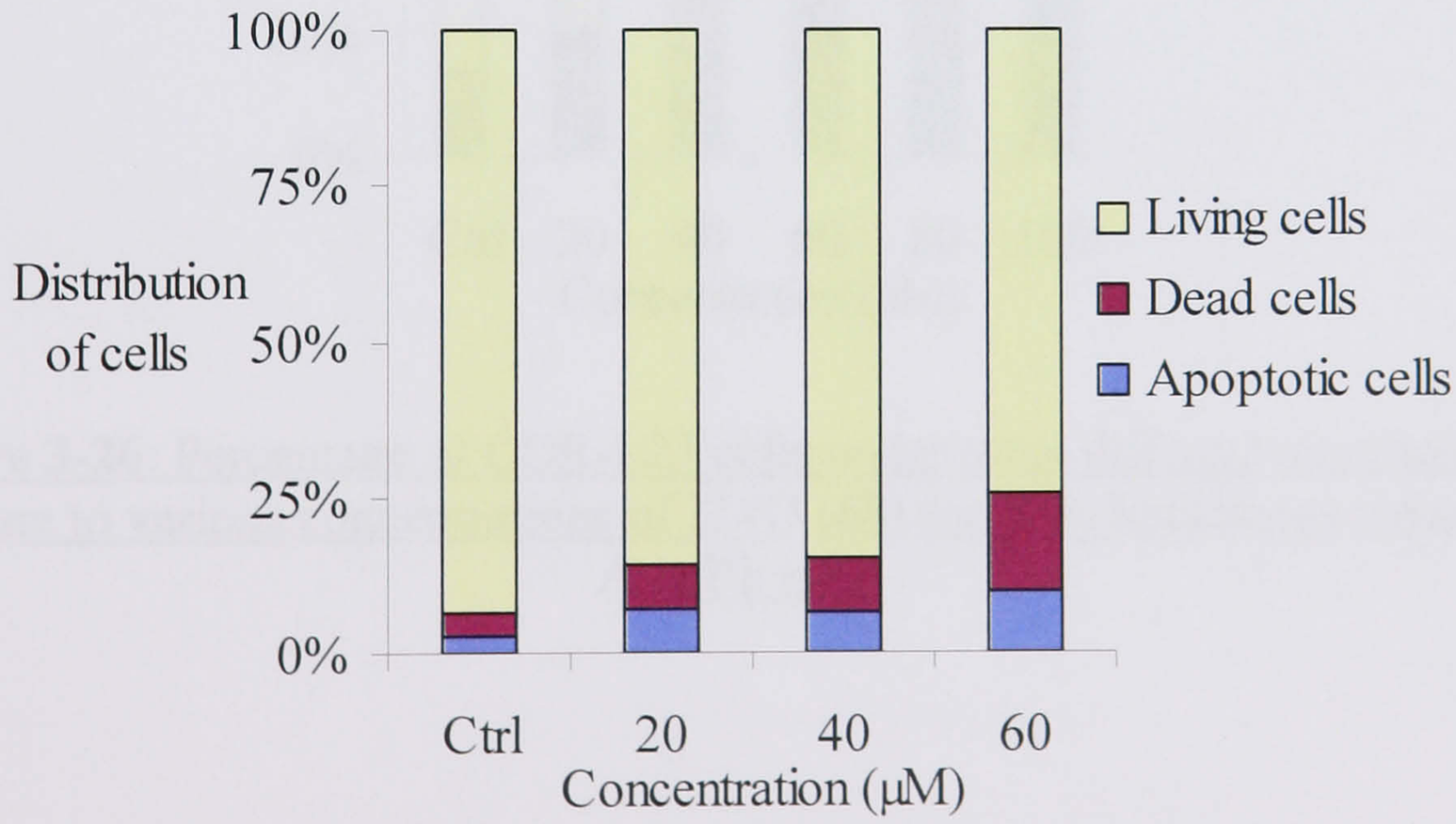

Figure 3-24: Percentage of COR-L23 cells under three different situations after exposure to various concentrations of IT4D (**65**) for 48h (Specimens stained with FDA/PI. n=3). IT4D (**65**) was tested for only three concentrations in the FDA/PI assay, due to the limited amount of material.

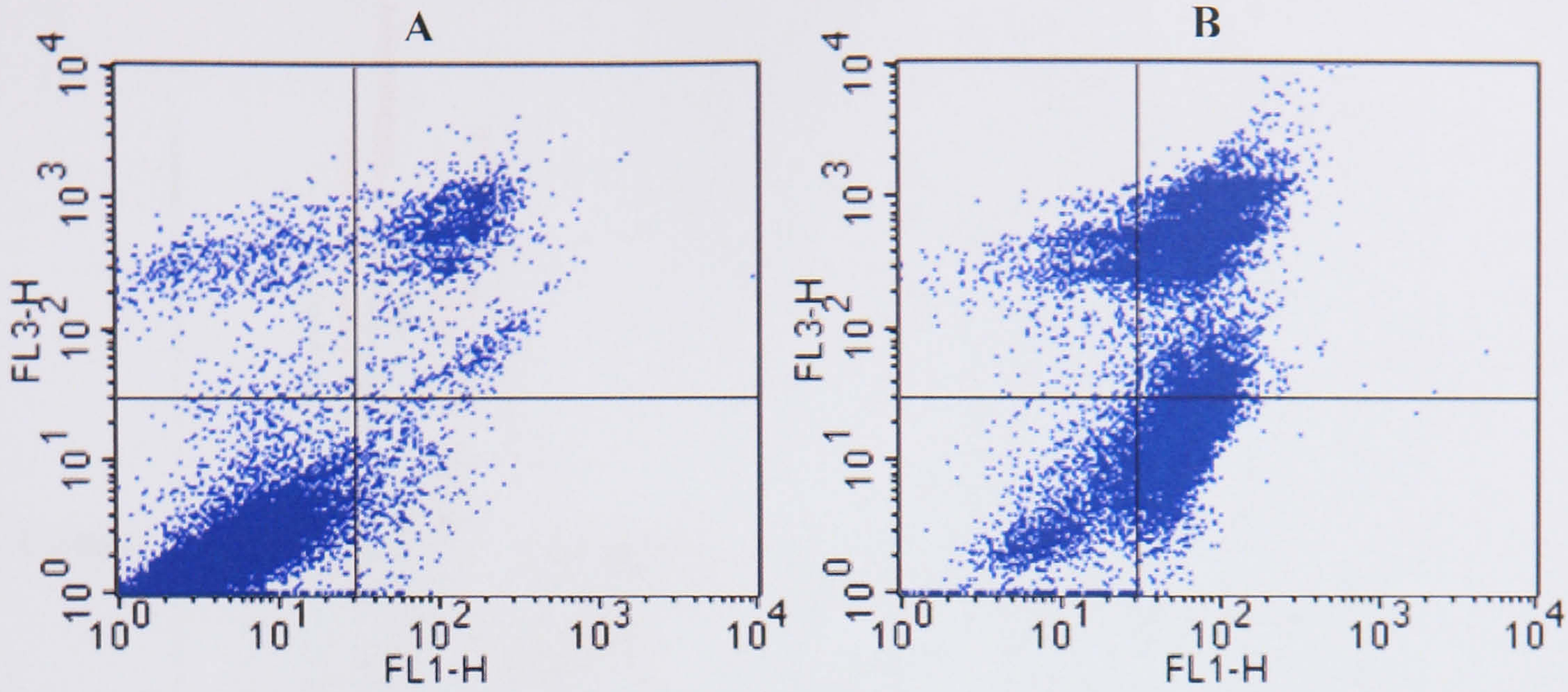

Figure 3-25: Scatter plots of Ann/PI-stained COR-L23 cells under three situations in quadrant analysis; they are living cells (LL), dead cells (UL and UR) and apoptotic cells (LR); A: control; B: exposed to 100μM IT4D (**65**) for 48h

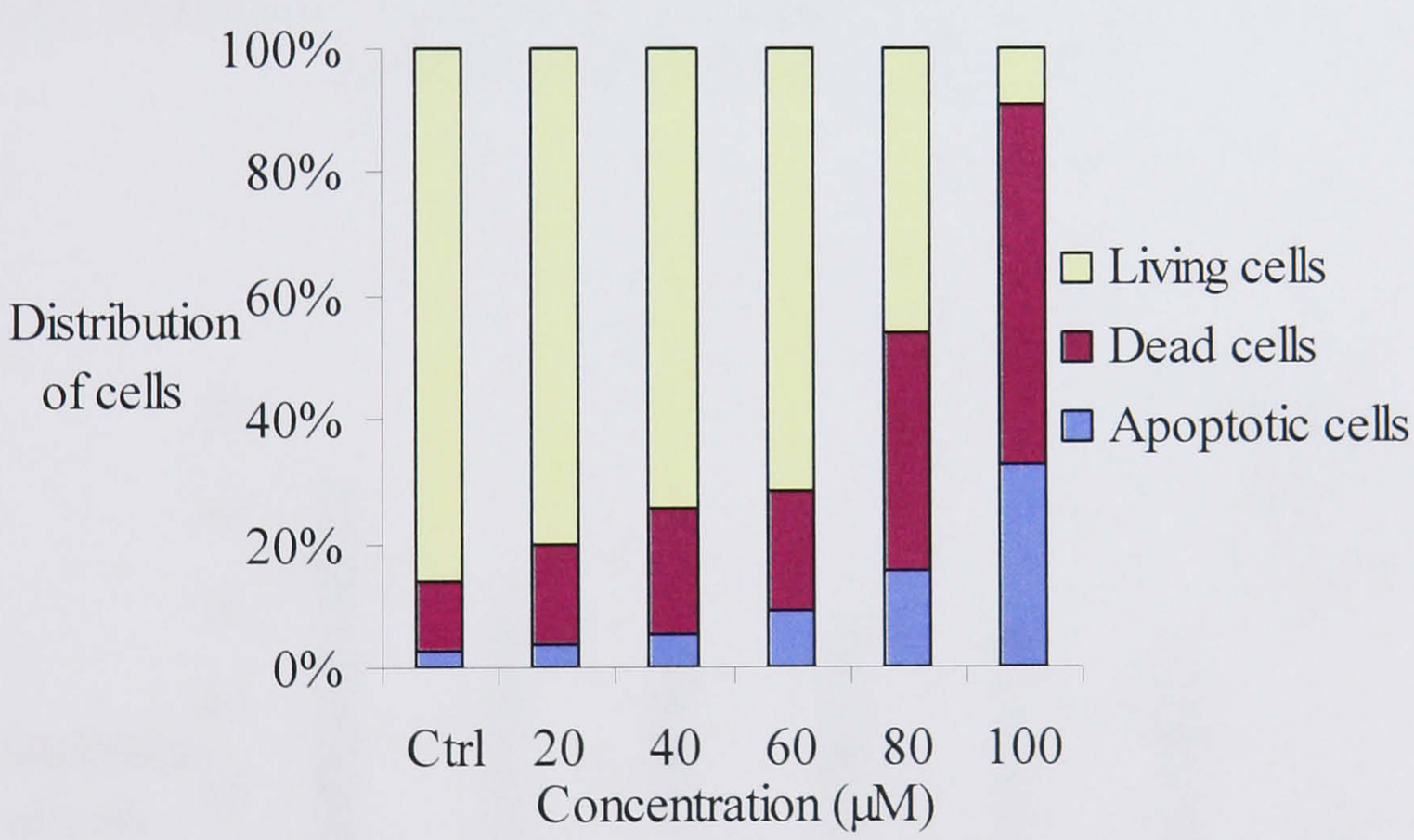

Figure 3-26: Percentage of COR-L23 cells under three different situations after exposure to various concentrations of IT4D (**65**) for 48h (Specimens stained with Ann/PI; n=3)

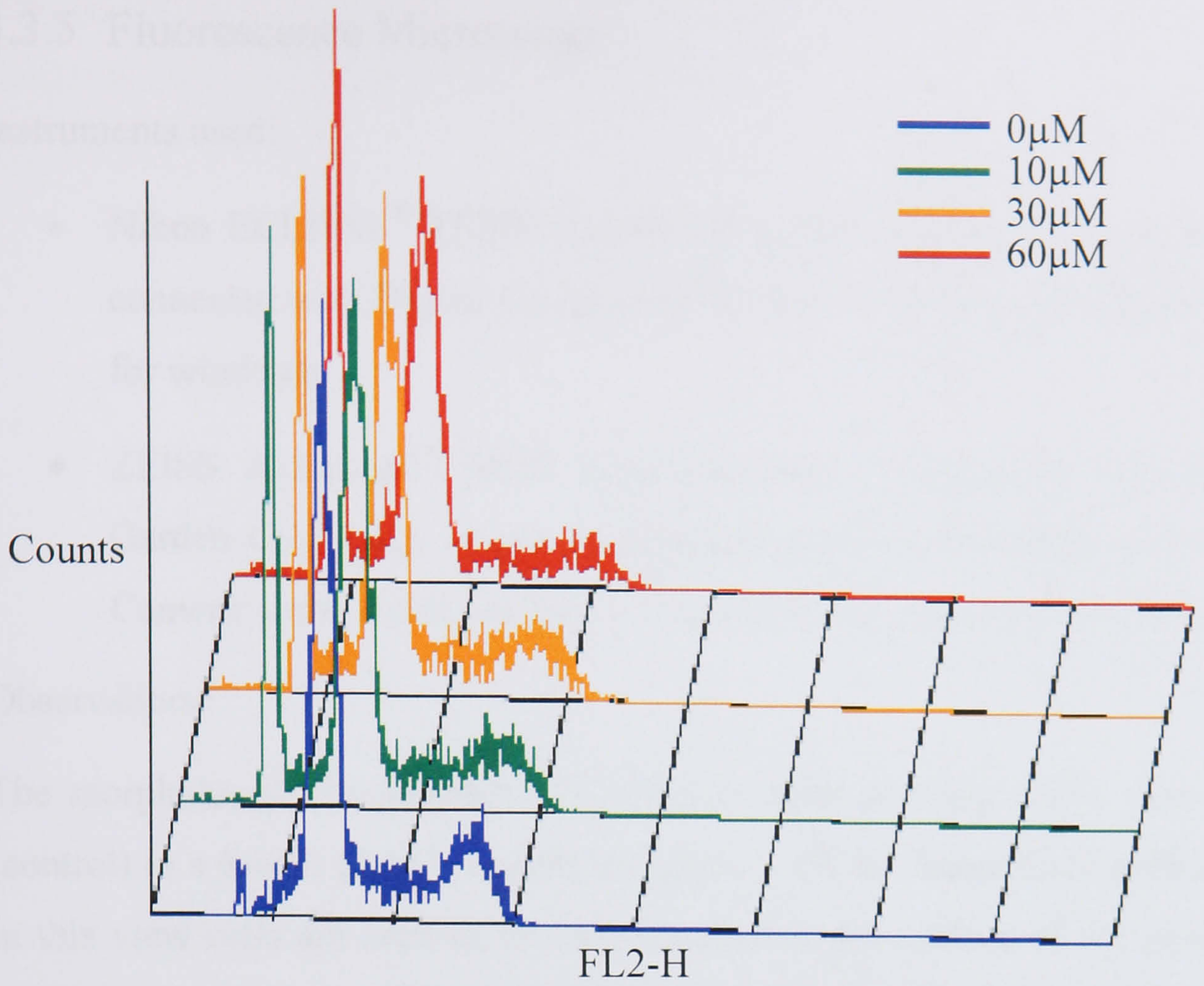

Figure 3-27: Overlay histogram of cell cycle analysis for COR-L23 cells exposed to various concentrations of IT4D (**65**)

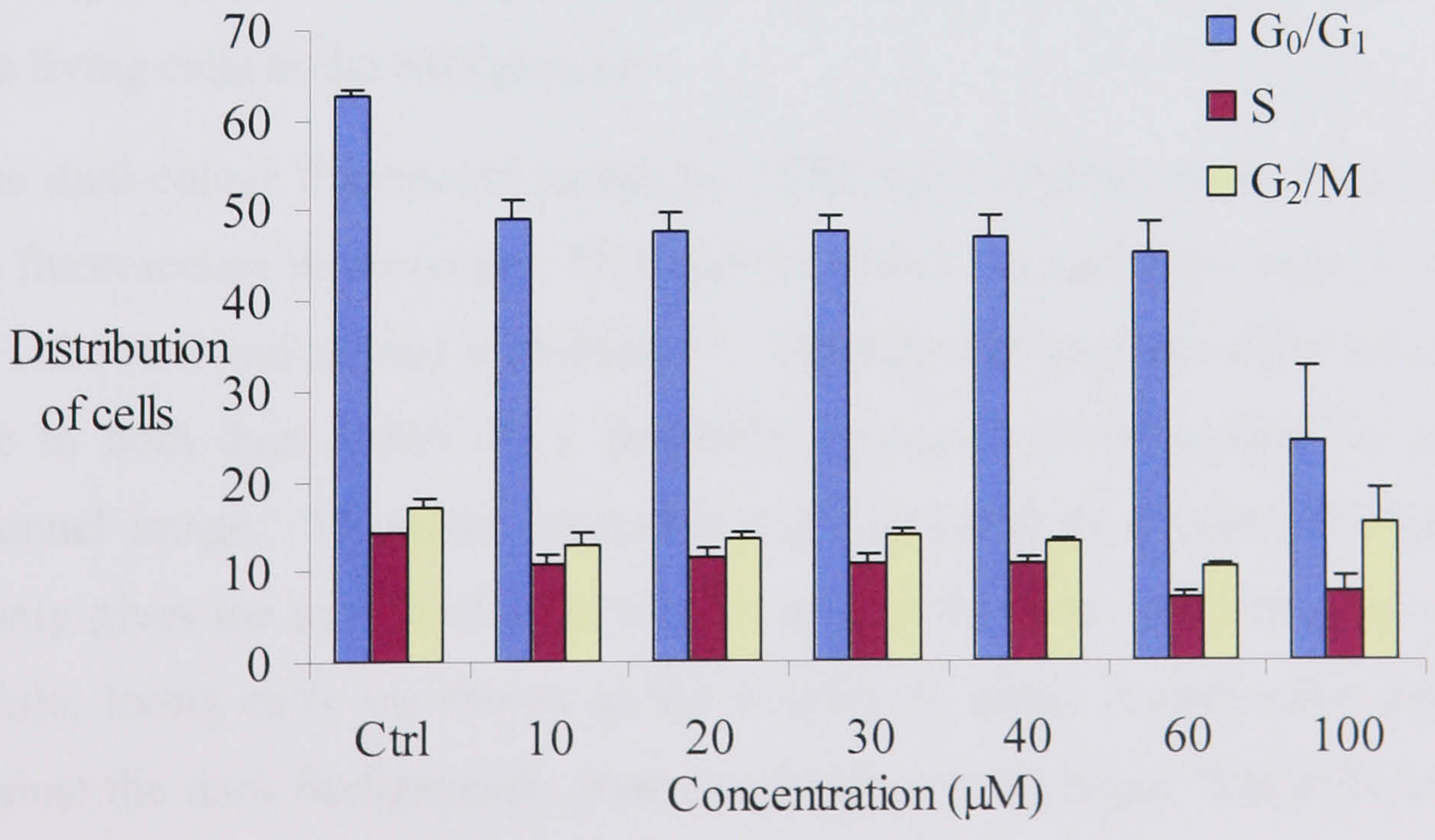

Figure 3-28: Effects of IT4D (**65**) on the cell cycle of COR-L23 cells after 48h exposure (mean±SEM, n=3)

3.3.5 Fluorescence Microscopy

Instruments used:

- Nikon ECLIPSE® TE200 microscope (Nikon Vision Co., Ltd. Tokyo, Japan) connected with Digital Camera DXM 1200. Software: LUCIA G Version 4.61 for windows.
- ZEISS Axioshop2® MOT plus microscope (Carl Zeiss Co., Ltd, Welwyn Garden City, UK); images recorded at multiple wavelengths using a Digital Camera: Zeiss AxioCam HRC. Software: Axiovision for windows.

Observations:

The morphological appearance of COR-L23 cells growing under normal condition (control) in a 6-well plate is shown as Figure 3-29, an image taken with neutral light. In this view cells are seen to be well attached to the surface of the plate, forming a confluent monolayer, and in which numerous mitotic cells can be observed. Another image (Figure 3-30) shows the morphological characteristics of apoptotic COR-L23 cells induced by 125μM IT2c (**66**). As indicated by the arrows (Figure 3-30), the presence of the formation of apoptotic bodies and cell shrinkage are highlighted by means of phase contrast-2 microscopy. When cells were observed with this function of microscope, the detached apoptotic cells stand out and can readily be distinguished from the living cells in the background.

After the dual-colour fluorescent assays by FCM, the remaining cells were observed under a fluorescence microscope. Figure 3-31 shows the apoptotic cells induced by 125μM IT2c (**66**) and stained with FDA/PI. Because the apoptotic cells were double negative to both dyes (FDA^-/PI^-), darkfield microscopy was applied to take this multichannel image. Therefore, apoptotic cells appeared as a mass of bright dots, which only gives the profile of cells without any fluorescence (indicated by arrows). Meanwhile, living cells are shown as the overlay of green fluorescence and bright dots against the dark background. Red fluorescence with bright dots indicates dead cells.

Apoptotic cells induced by 80μM IT4D (**65**) are seen as bright green in Ann/PI system as illustrated in Figure 3-32. Noticeably, the apoptotic cells in this view were undergoing mitotis and the division was not completed. The dead cells (indicated by

arrows) appear as an orange colour because of the overlay of green and red fluorescence. That might be a result of late apoptosis. Cells shown in pure red fluorescence represent dead cells.

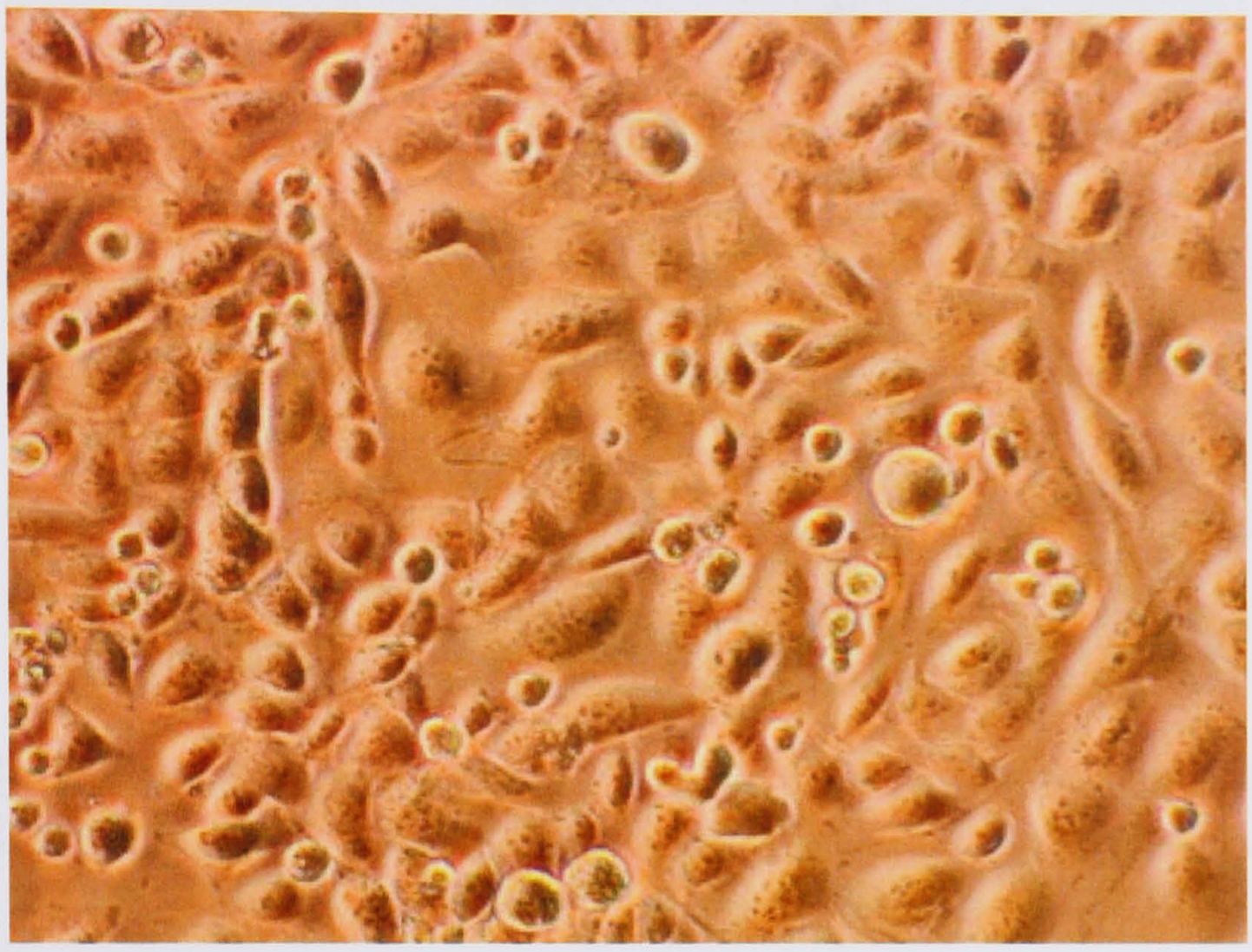

Figure 3-29: Microscopic image of COR-L23 cells after incubation in growth medium for 48h as control (taken with neutral light and phase contrast-1 at ×40 by Nikon ECLIPSE® TE200)

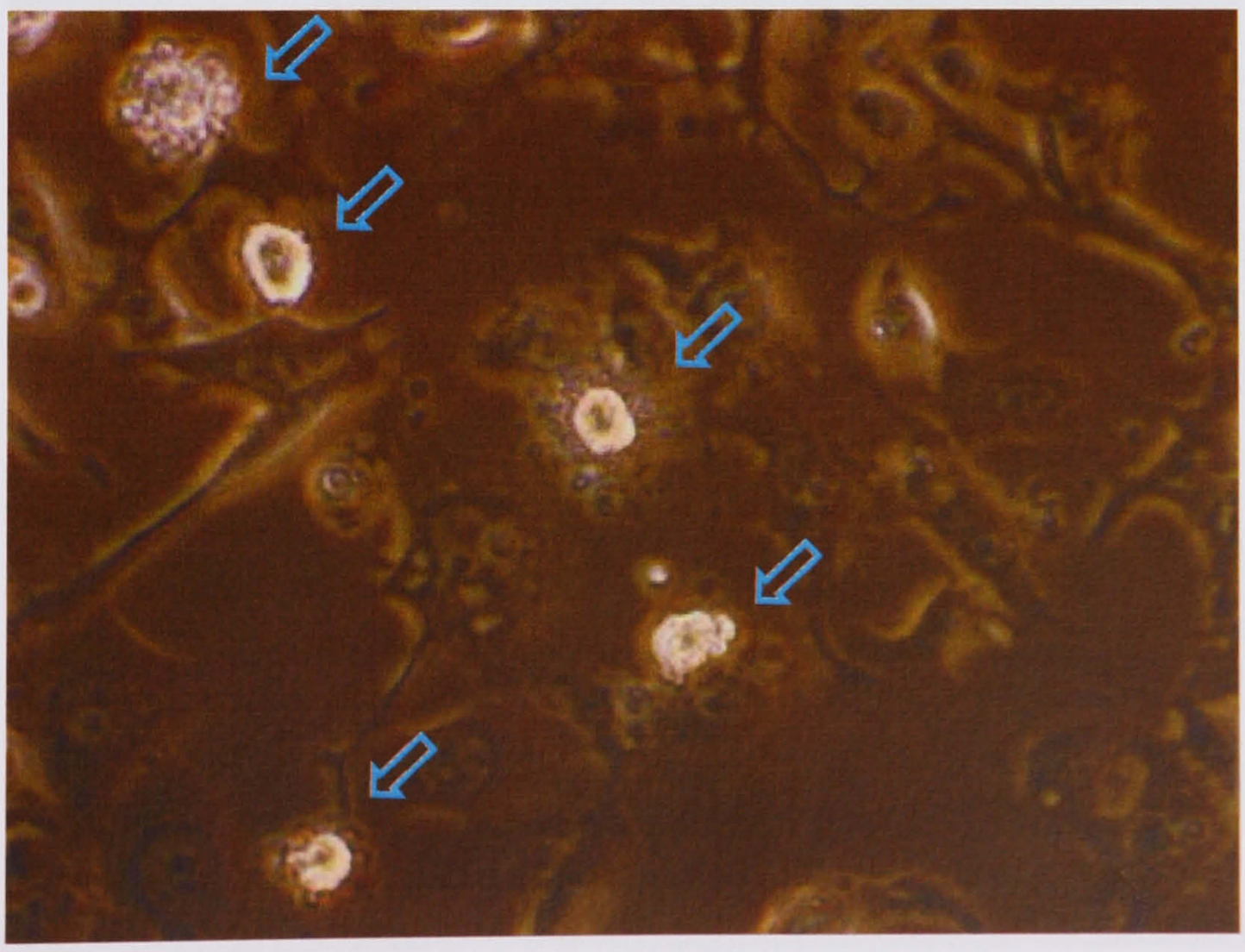

Figure 3-30: Microscopic image of COR-L23 cells after exposure to 125µM IT2c (**66**) for 48h (taken with neutral light and phase contrast-2 at ×40 by Nikon ECLIPSE® TE200)

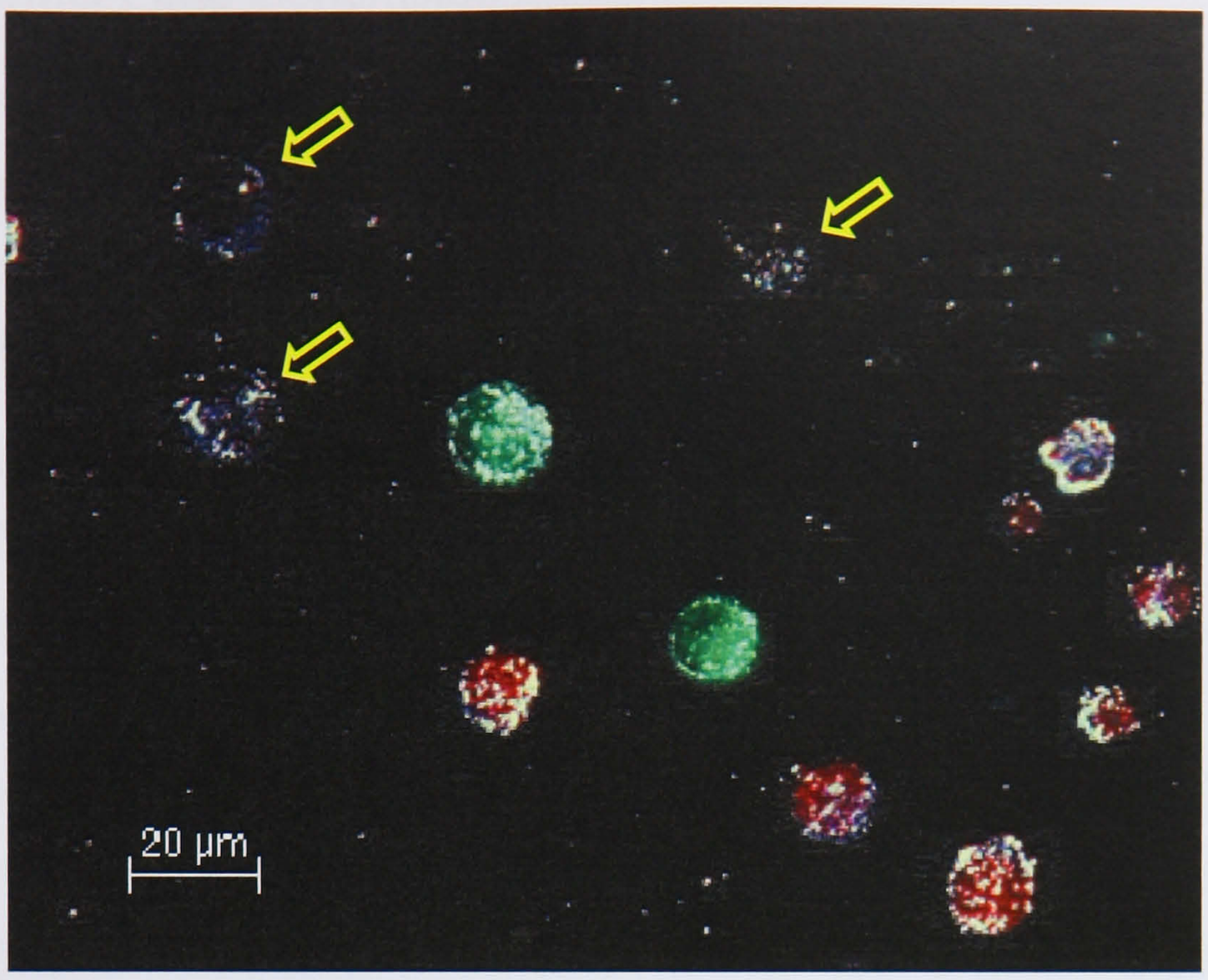

Figure 3-31: Fluorescent microscopic image of COR-L23 cells after exposure to 125µM IT2c (**66**) for 48h and stained with FDA/PI (taken as multichannel image with a view of Darkfield at ×40, by ZEISS Axioshop2® MOT plus)

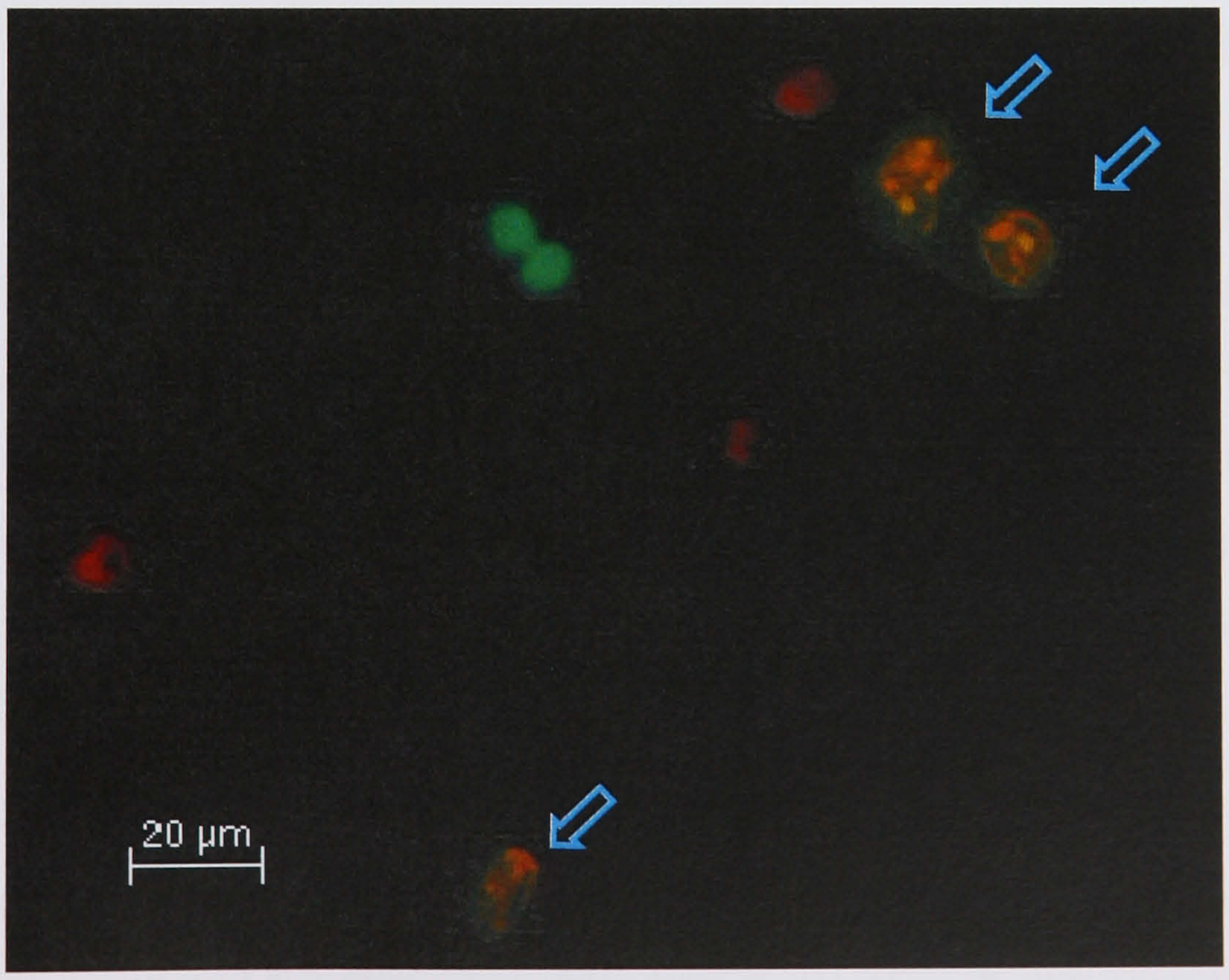

Figure 3-32: Fluorescent microscopic image of COR-L23 cells after exposure to 80µM IT4D (**65**) for 48h and stained with Ann/PI (taken as multichannel image at ×40, by ZEISS Axioshop2® MOT plus)

3.3.6 Summary and Conclusion

The measurements of cell cycle analysis were made in triplicate and all values are presented as mean ± SEM (Standard Error of the Mean). These results were subjected to an analysis of variance (ANOVA) using Dunnett's test to compare all treatments with control as seen in Table 3-6.

Statistical tests of cell cycle analysis confirmed that the positive controls, vinblastine sulphate (**69**) and genistein (**51**), as expected, significantly arrested COR-L23 cells at G_2/M phase up to 45nM and 200μM, respectively. Although it has been previously reported that genistein (**51**) induced cell cycle progression arrest at S and G_2/M phases in human head and neck squamous cell carcinoma cell line (Alhasan *et al.*, 1999), no significant increase in S phase was observed over a range of concentrations from 20μM to 300μM in the present work. After exposure to genistein (**51**) for 48h, significant cell accumulation was only shown in the G_2/M phase at concentrations of 80μM, 120μM and 200μM. There is significant accumulation of cells in S and G_2/M phases induced by tectorigenin (**24**) at 400μM and 600μM. As to IT2c (**66**), COR-L23 cells were significantly arrested in S phase at 60μM and 100μM, but no significant accumulation was observed in the G_2/M phase. Although the cell proportion did not increase significantly in G_2/M phase, the cell proportions are still keeping in relative high levels of 18.1% and 17.9% at 40μM and 60μM IT2c (**66**), if compared it with that of IT4D (**65**) (where cells proportions in all phases reduced much lower than that of control). This statistical analysis, however, can not rule out the possibility of IT2c (**66**) inducing cell cycle progress arrest in both S and G_2/M phases. The result of IT4D is rather simple - cell proportions are reduced in all cell cycle phases. The decline in G_0/G_1 and S phases are significant, whilst the percentage of cells in G_2/M phase keeps in lower level than that of the control. This means that cells were killed by IT4D at all stages of cell cycle.

The percentage of apoptotic cells calculated by quadrant analysis (either FDA^-/PI^- or Ann^+/PI^-) is summarized for each treatments as shown in Table 3-7. Moreover, these data were also compared between every two treatments of each compound detected by the same assay (shown in Table 3-8 and Table 3-9). Statistical significances of difference between every two values of apoptotic rate were subjected to One-way ANOVA with Tukey's Multiple Comparison post test, which is a built-in statistical

application of the programme GraphPad Prism version 4 for Windows (GraphPad Software, San Diego California USA). In addition, the significance is classified into four levels, which are shown as: − (p>0.05), + (p<0.05), ++ (p<0.01) and +++ (p<0.001).

According to the quadrant analysis data (Figure 3-9 on page 126) and the statistical results of genistein (**51**) (Table 3-8), the proportion of apoptotic cells significantly (p<0.001) increased with the concentration of genistein (**51**). These results indicate significant dose-dependent apoptosis in both dual-colour apoptosis assays. In addition, genistein (**51**) efficiently arrested COR-L23 at G_2/M phase of cell cycle, as did vinblastine. This conclusion is consistent with those in the literature (Baxa *et al.*, 2005; Alhasan *et al.*, 1999).

However, the trend implied by the result of tectorigenin (**24**) is not as clear as that of genistein (**51**). Although the apoptotic results of treatments significantly differ from that of control (p<0.001), there is poor significance of difference between any other treatments, especially when comparing the results of high concentration with those of low concentration, such as 200μM *vs* 1mM and 400μM *vs* 1mM (p>0.05) in the FDA/PI assay. Moreover, the statistical analysis of Ann/PI assay clearly indicates that no significant difference between any two treatments. The statistical results of both dual-colour apoptosis assays suggested that up to 1,000μM tectorigenin (**24**) did not significantly induce dose-dependent apoptosis of COR-L23 in 48h. This conclusion is contrary to a finding, in which it was claimed that tectorigenin (**24**) did induce apoptotic changes of DNA in human promyelocytic leukaemia HL-60 cells (Lee *et al.*, 2001). It also reported the IG_{50} of tectorigenin (**24**) and genistein (**51**) against HepG2 cell line were 84μM and 39.9μM, respectively. Interestingly, the results of genistein (**51**) in the present study are fairly consistent with those of the previous report; however, the observed bioactivities of tectorigenin (**24**) are different with those in literature. The main reason for the different conclusion about the apoptotic effect of tectorigenin (**24**) could be due to the difference of cell lines, experimental conditions and the assays applied. For instance, in the previous research, the cytotoxicity assay carried out by MTT assay and the induction of apoptosis in promyelocytic leukaemia HL-60 by tectorigenin (**24**) for four days (96h) was detected only by means of cell cycle analysis assay with FCM and no cell cycle specific cytotoxicity was observed. That is not a specific assay for apoptosis indeed. In present study, the cell cycle

analysis result of tectorigenin (**24**) clearly indicated that it is able to arrested COR-L23 cells at S and G_2/M phases at certain concentrations. This is the first such reported observation for tectorigenin (**24**).

As seen in Table 3-7 and Table 3-9, in the result of FDA/PI assay for IT2c (**66**), the proportion of apoptotic cells significantly (p<0.001) increased with the concentration of IT2c (**66**). This indicates significant dose-dependent apoptosis in COR-L23. However, because of the limited amount of pure compound, the Ann/PI assay of IT2c (**66**) was carried out with concentrations up to 100μM. Statistical analysis shows the apoptotic rate of 100μM significantly differs from that of control (p<0.01) and 25μM treatment (p<0.05). The overall result of IT2c (**66**) suggests that it is a medium cytotoxic flavonoid that can induce apoptsis of COR-L23 *in vitro*. Also, it might be able to arrest COR-L23 cells at S and G_2/M phases, as did tectorigenin (**24**).

Unfortunately because of lack of sample, the FDA/PI assay of IT4D (**65**) was only carried out for concentrations up to 60μM (as shown in Table 3-9). The dose-dependent apoptosis can still be observed significantly when comparing the value at 60μM with that of control and other concentrations (p<0.01). On the other hand, the Ann/PI assay (see Table 3-9 and Figure 3-26 on page 136) gave a significant increase of apoptotic rate with the concentrations of IT4D (**65**) (greater than 60μM). These observation suggest that IT4D (**65**) significantly induce apoptosis of COR-L23 cells at 60μM and higher concentrations (up to 100μM).

The activities of the compounds tested against COR-L23 cell line are summarized as Table 3-5, in which the cytoxicity and apoptosis activity of IT2c (**66**) and IT4D (**65**) are reported for the first time.

Compound	**IG_{50} against COR-L23**	**Apoptotic induction**	**Cell cycle phase specificity**
genistein (**51**)	62.7±8.98	Yes	G2/M
tectorigenin (**24**)	189.3±6.55	No	S and G2/M
IT2c (**66**)	32.8±0.50	Yes	S and G2/M
luteolin (**22**)	11.0±0.67	—	—
IT4C (**61**)	34.8±0.86	—	—
IT4D (**65**)	19.0±0.44	Yes	Non-specific
IT4E (**60**)	13.9±0.27	—	—
IT4F (**57**)	15.7±1.84	—	—

Table 3-5: Summary of results of compounds tested

Compounds	Conc.	Cell cycle distribution (%) in COR-L23 cell line		
		G0/G1	S	G2/M
vinblastine sulphate (**69**)	0nM	61.3 ±0.60	13.8 ±0.19	15.7 ±0.18
	1.5nM	56.9 ±0.96**	10.3 ±0.17**	26.5 ±0.13**
	4.5nM	16.0 ±0.49**	6.1 ±0.15**	55.2 ±1.07**
	10nM	4.6 ±0.13**	6.0 ±0.30**	66.0 ±1.68**
	15nM	5.5 ±0.10**	3.6 ±0.06**	73.7 ±1.16**
	45nM	5.8 ±0.06**	3.7 ±0.05**	71.3 ±0.81**
genistein (**51**)	0μM	62.7 ±0.68	14.3 ±0.17	17.2 ±0.79
	20μM	44.5 ±1.06**	11.2 ±1.20	16.0 ±1.32
	40μM	43.7 ±2.11**	11.2 ±1.28	19.8 ±1.02
	80μM	34.5 ±3.92**	14.8 ±2.34	34.5 ±0.90**
	120μM	33.6 ±3.88**	12.6 ±2.10	37.4 ±1.42**
	200μM	31.0 ±3.27**	11.0 ±2.31	37.5 ±1.38**
	300μM	29.9 ±4.80**	15.7 ±2.88	19.2 ±0.77
tectorigenin (**24**)	0μM	62.7 ±0.68	14.3 ±0.17	17.2 ±0.79
	50μM	46.9 ±1.69**	11.1 ±0.41*	13.6 ±0.26**
	100μM	45.9 ±1.39**	11.2 ±0.32*	15.1 ±0.07*
	200μM	43.5 ±1.88**	12.5 ±0.66	18.6 ±0.12
	400μM	31.7 ±1.60**	16.6 ±0.72	26.1 ±0.75**
	600μM	28.6 ±1.24**	20.4 ±1.16**	22.2 ±0.39**
	800μM	34.8 ±1.84**	15.6 ±1.22	17.1 ±0.49
IT2c (**66**)	0μM	62.7 ±0.68	14.3 ±0.17	17.2 ±0.79
	10μM	48.4 ±1.85**	12.3 ±0.17**	14.0 ±0.45*
	20μM	47.6 ±1.79**	12.6 ±0.52**	14.6 ±0.18*
	30μM	46.3 ±1.53**	13.3 ±0.12	15.8 ±0.45
	40μM	43.3 ±1.92**	14.5 ±0.15	18.1 ±0.63
	60μM	37.5 ±2.40**	18.3 ±0.17**	17.9 ±0.76
	100μM	35.9 ±3.75**	18.2 ±0.49**	16.8 ±0.71
IT4D (**65**)	0μM	62.7 ±0.68	14.3 ±0.17	17.2 ±0.79
	10μM	49.2 ±2.08*	10.9 ±1.02**	13.0 ±1.16
	20μM	47.7 ±1.94*	11.5 ±1.06*	13.5 ±0.80
	30μM	47.6 ±1.81*	10.9 ±1.06**	13.8 ±0.69
	40μM	46.9 ±2.48*	10.6 ±0.95**	13.3 ±0.45
	60μM	45.4 ±3.24**	6.9 ±0.70**	10.3 ±0.40
	100μM	24.2 ±8.62**	7.5 ±1.96**	15.3 ±3.79

Table 3-6: Distribution of COR-L23 cells in three cell cycle phases after exposure to various concentrations of compounds (Percentage ± SEM, n=3; comparison: values not significantly different with that of control are listed without mark, $p<0.05$ is considered as significant and marked as *, $p<0.01$ is marked as **.)

Dual-colour Assays	genistein (**51**)		tectorigenin (**24**)		IT2c (**66**)		IT4D (**65**)	
FDA/PI	Ctrl	7.1±1.05	Ctrl	1.6±0.21	Ctrl	3.1±0.29	Ctrl	2.6±0.43
	100μM	19.9±0.50	200μM	5.0±0.67	25μM	5.1±0.94	20μM	7.2±0.70
	200μM	30.9±0.58	400μM	6.1±0.68	50μM	6.7±0.83	40μM	6.5±0.52
	300μM	46.5±2.04	600μM	9.0±1.58	75μM	10.0±1.04	60μM	9.8±0.86
	400μM	51.6±2.45	800μM	8.3±1.71	100μM	13.4±1.35		
			1000μM	6.1±1.26	125μM	18.8±1.52		
Annexin V-FITC/PI	Ctrl	2.9±0.45	Ctrl	2.4±0.56	Ctrl	3.6±0.13	Ctrl	2.9±0.97
	25μM	4.0±0.52	200μM	7.5±0.54	25μM	5.2±1.68	20μM	3.9±1.57
	50μM	5.3±0.44	400μM	7.1±0.90	50μM	8.5±2.14	40μM	5.2±1.67
	100μM	6.9±1.06	600μM	7.6±0.75	75μM	8.8±2.58	60μM	8.8±2.71
	200μM	11.9±1.25	800μM	8.4±0.52	100μM	11.5±3.05	80μM	15.3±3.06
	300μM	14.9±1.63	1000μM	8.5±0.25			100μM	32.6±5.23
	400μM	18.4±1.56						

Table 3-7: Summary of the percentage of apoptotic cells in quadrant analysis (either FDA^-/PI^- or Ann^+/PI^-) corresponding to various concentrations of each compounds (Percentage ±SEM, n=3)

Apoptosis	genistein (**51**)						tectorigenin (**24**)					
FDA⁻/PI⁻ (LL)		Ctrl	100μM	200μM	300μM			Ctrl	200μM	400μM	600μM	800μM
	100μM	++					200μM	+				
	200μM	+++	++				400μM	++	−			
	300μM	+++	+++	+++			600μM	+++	++	+		
	400μM	+++	+++	+++	−		800μM	+++	+	−	−	
							1mM	++	−	−	+	−
Ann⁺/PI⁻ (LR)		Ctrl	25μM	50μM	100μM	200μM	300μM	Ctrl	200μM	400μM	600μM	800μM
	25μM	−						200μM	+++			
	50μM	−	−					400μM	+++	−		
	100μM	++	−	−				600μM	+++	−	−	
	200μM	+++	+++	+++	++			800μM	+++	−	−	−
	300μM	+++	+++	+++	+++	+		1mM	+++	−	−	−
	400μM	+++	+++	+++	+++	+++	+					

Table 3-8: Comparison of apoptotic rate induced by various concentrations of genistein (**51**) and tectorigenin (**24**), compared with that induced at a different concentration. (n=3) (− shows significance $p>0.05$; + shows significance $p<0.05$; ++ shows significance $p<0.01$; +++ shows significance $p<0.001$)

Apoptosis	7-*O*-methyl aromadendrin (**66**)					IT4D (**65**)				
FDA$^-$/PI$^-$ (LL)		Ctrl	25μM	50μM	75μM	100μM		Ctrl	20μM	40μM
	25μM	–					20μM	+++		
	50μM	++	–				40μM	+++	–	
	75μM	+++	+++	++			60μM	+++	++	++
	100μM	+++	+++	+++	++					
	125μM	+++	+++	+++	+++	+++				
Ann$^+$/PI$^-$ (LR)		Ctrl	25μM	50μM	75μM			Ctrl	20μM	40μM	60μM	80μM
	25μM	–					20μM	–				
	50μM	–	–				40μM	–	–			
	75μM	–	–	–			60μM	–	–	–		
	100μM	++	+	–	–		80μM	++	++	+	–	
							100μM	+++	+++	+++	+++	+++

Table 3-9: comparison of apoptotic rate induced by various concentrations of 7-*O*-methyl aromadendrin (**66**) and IT4D (**65**), compared with that induced at a different concentration. (n=3) (− shows significance $p>0.05$; + shows significance $p<0.05$; ++ shows significance $p<0.01$; +++ shows significance $p<0.001$)

CHAPTER 4
PRODRUG SCREENING

Generally, a prodrug is an inactive precursor of a drug, converted into its active form in the body by normal metabolic processes (Syrigos and Epenetos, 1999). The use of a prodrug strategy increases the selectivity of the drug for its intended target. This can be seen in many anticancer treatments, in which the reduction of adverse effects is always of paramount importance (Connors, 1995). For instance, irinotecan (**71**) is an anticancer prodrug that has been approved for the treatment of colon cancer. It is a member of the camptothecin class of drugs and mediated by carboxylesterases to the active metabolite SN-38 (**72**) at the tumour site and inhibits tumour cell growth by inhibiting topoisomerase I (Hyatt *et al.*, 2005). Since the prodrug has low cytotoxicity prior to this activation, there is a markedly lower chance of its "attacking" healthy, non-cancerous cells. This reduces the side-effects associated with these chemotherapeutic agents.

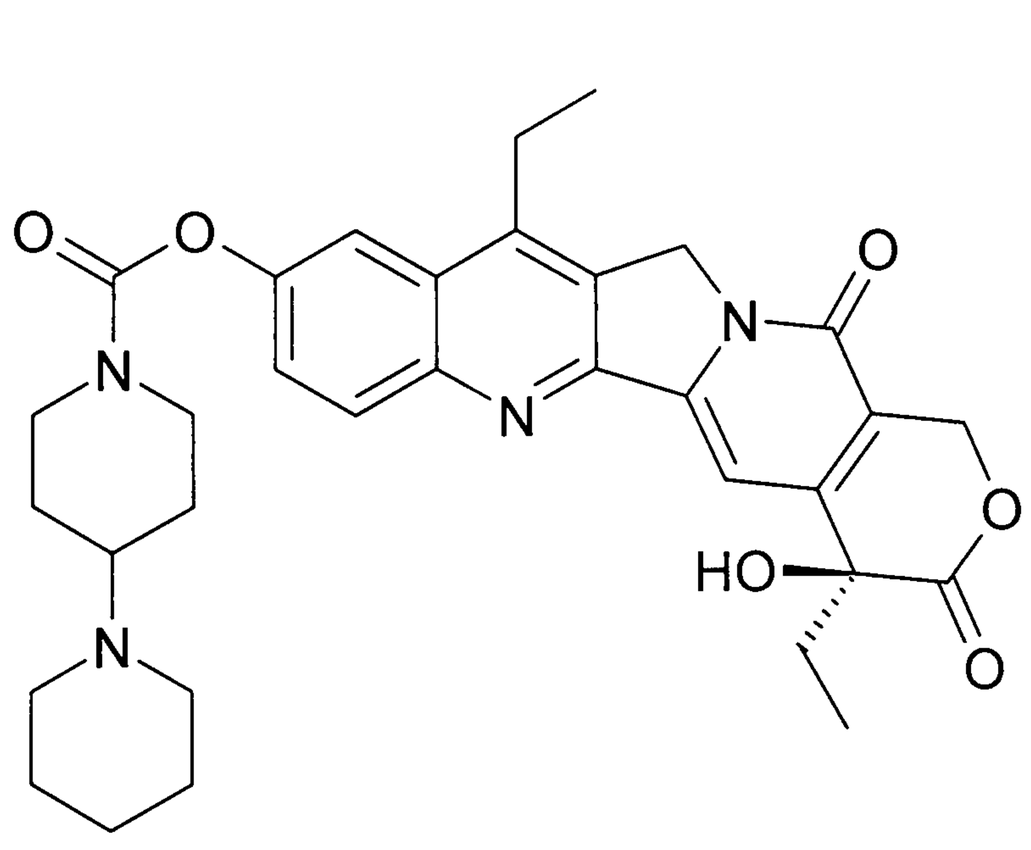

71

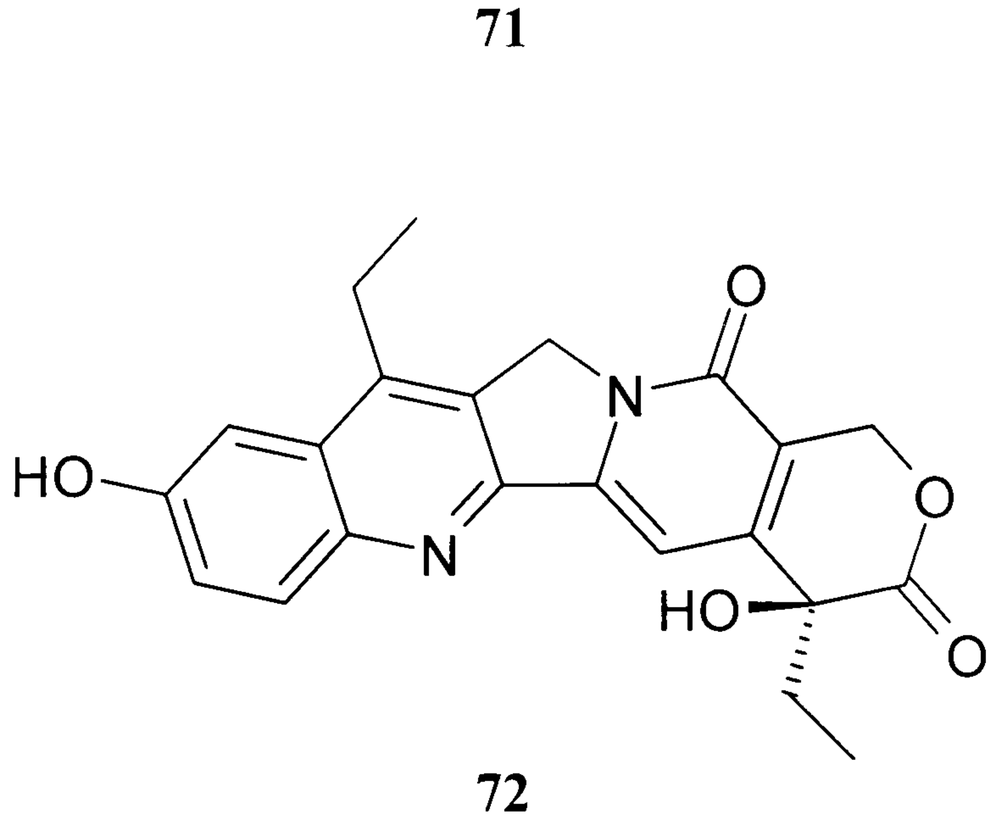

72

Besides synthetic compounds, prodrugs may also occur naturally. Sometimes the use of a prodrug is unintentional, especially in the case of serendipitous drug discoveries from natural products, and the drug is only identified as a prodrug after extensive drug metabolism studies. For example, artemisinin (**73**) is a sesquiterpene lactone isolated from a well known TCM: *Artemisia annua* L (Klayman, 1985). This natural product and its analogs are being used as antimalarials. Nevertheless it was discovered to be more toxic to cancer cells than to normal cells (Lai and Singh, 1995; Singh and Lai, 2001). Further research has shown that artemisinin induces apoptosis in cancer cells (Singh and Lai, 2004). The cytotoxic mechanism was discovered that artemisinin reacts with iron and forms intracellular free radicals, which could cause macromolecular damage and lead to cell death (Efferth *et al.*, 2004). Since cancer cells uptake relatively larger amount of iron than normal cells, they are therefore more susceptible to the toxic effect of artemisinin. This selective cytotoxicity towards cancer cells can be further enhanced by tagging artemisinin to the iron-carrying plasma glycoprotein transferrin. Because transferrin is transported into cells *via* receptor-mediated endocytosis and cancer cells express significantly more transferrin receptors on their cell surface and endocytose more transferrin than normal cells. After entry to the cell, iron is released and can readily react with artemisinin tagged to the transferrin. Thus, this tagged-compound could potentially be developed into an effective chemotherapeutic agent for cancer treatment (Lai *et al.*, 2005).

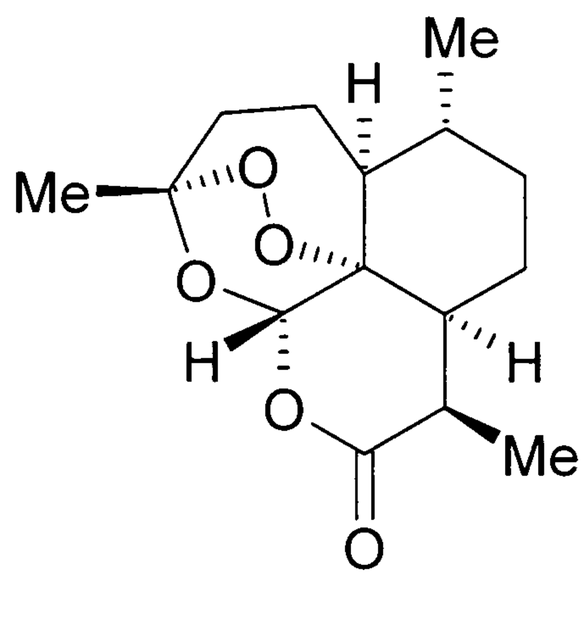

73

4.1 Possible prodrug mechanism within TCM

As most traditional medicines are administered orally, their components inevitably come into contact with intestinal microflora in the alimentary tract. Most of the components are transformed by intestinal bacteria before being absorbed from the gastrointestinal tract (Akao *et al.*, 1994; Kim *et al.*, 1998a). Practically, most TCM are traditionally used as decoctions, which is in rich of water soluble compounds, such as glycosides. Furthermore, an intensive study clearly point out that antiplatelet activity and cytotoxicity of the metabolites of flavonoid glycosides by human intestinal bacteria were more effective than those of the parental compounds. For instance, quercetin (**74**) and ponciretin (**75**) were more effective than rutin (**23**) and poncirin (**76**) on the cytotoxicity against a number of tumour cell lines, respectively (Kim *et al.*, 1998).

In previous research, tectorigenin (**24**) was isolated from *Pueraria thunbergiana* (a TCM to treat diabetes mellitus) together with structurally related compounds: tectoridin (**25**) and 6"-*O*-xylosyltectoridin (**77**) (Bae *et al.*, 1999). Further experiments revealed that the relatively hydrophilic isoflavones, tectoridin and 6"-*O*-xylosyltectoridin, can be efficiently transformed into tectorigenin (a rather hydrophobic compound) by some human intestinal bacteria, such as *Bifidobacterium breve* k-110 and *Eubacterium* A-44 (Kim *et al.*, 1998a) (see Figure 4-1). The transformed tectorigenin showed more potent hypoglycemic activity, anaphylaxis inhibitory activity and cytotoxicity against tumour cells than its glycoside (tectoridin) (Park *et al.*, 2004; Bae *et al.*, 1999).

Another experiment suggested that luteolin-7-*O*-glucoside (**50**) was absorbed after hydrolysis to luteolin (**22**) by bacteria on the surface of the intestinal mucosa (Shimoi *et al.*, 1998). This hydrolysis process was also demonstrated by using β-glucosidase *in vitro* (Gebhardt, 2002).

All the previous reports strongly suggest that some glycosides especially flavonoid glucosides should be considered as natural prodrugs in traditional medicine, and that they can be transformed into active compounds by human intestinal bacteria.

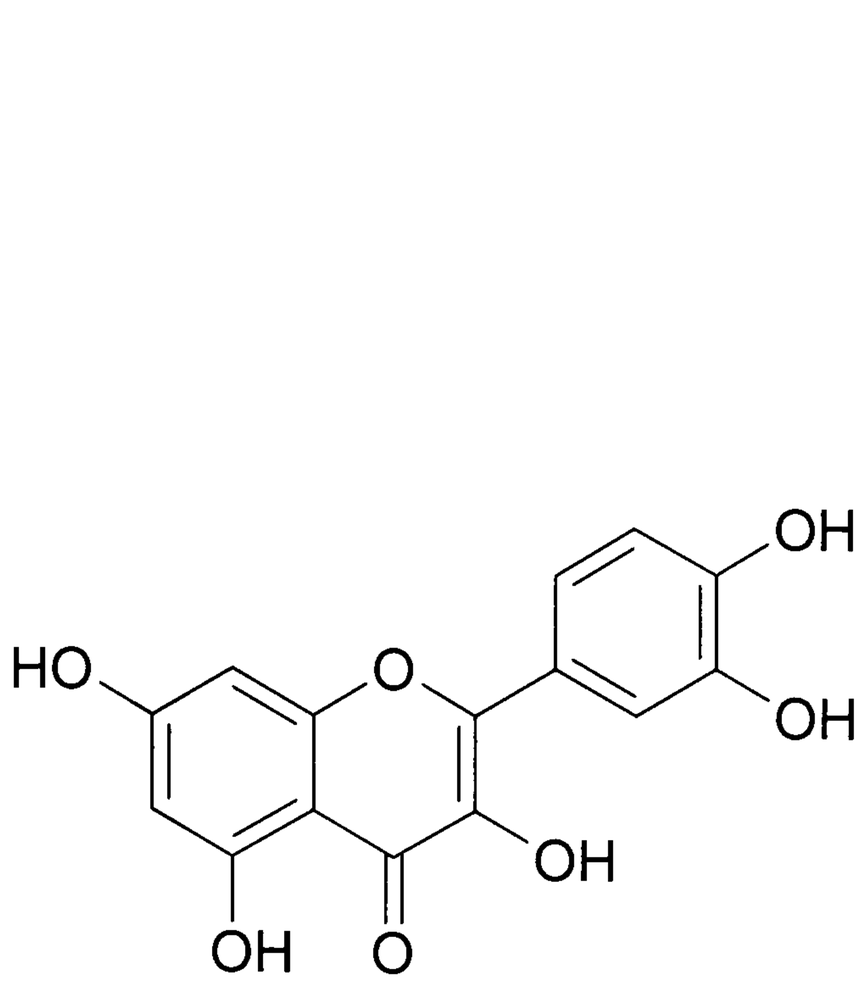

74

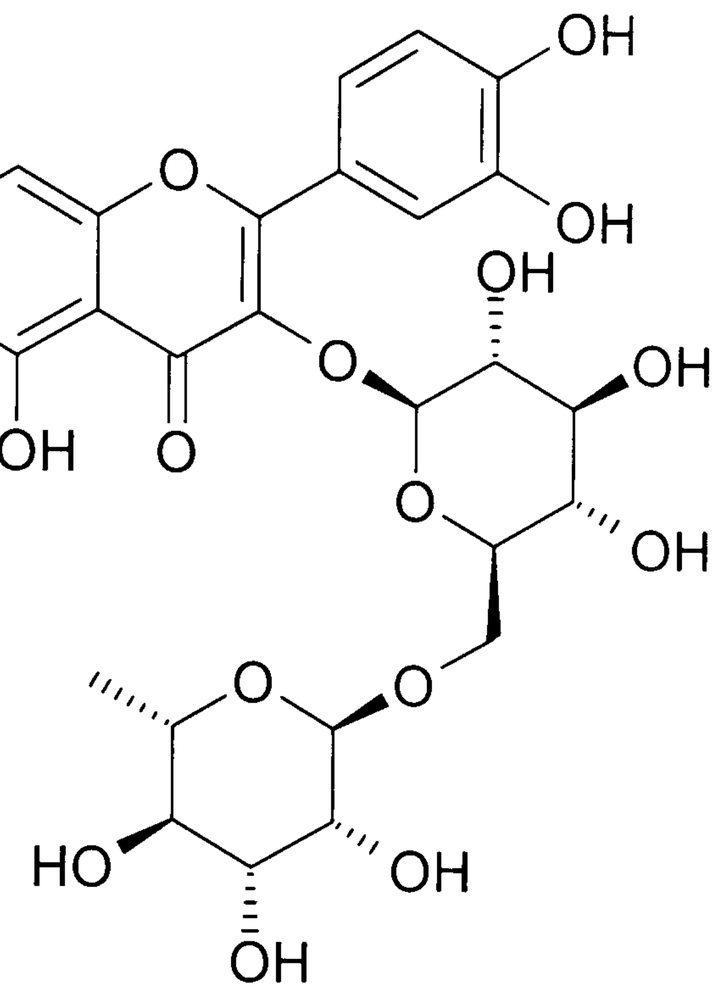

23

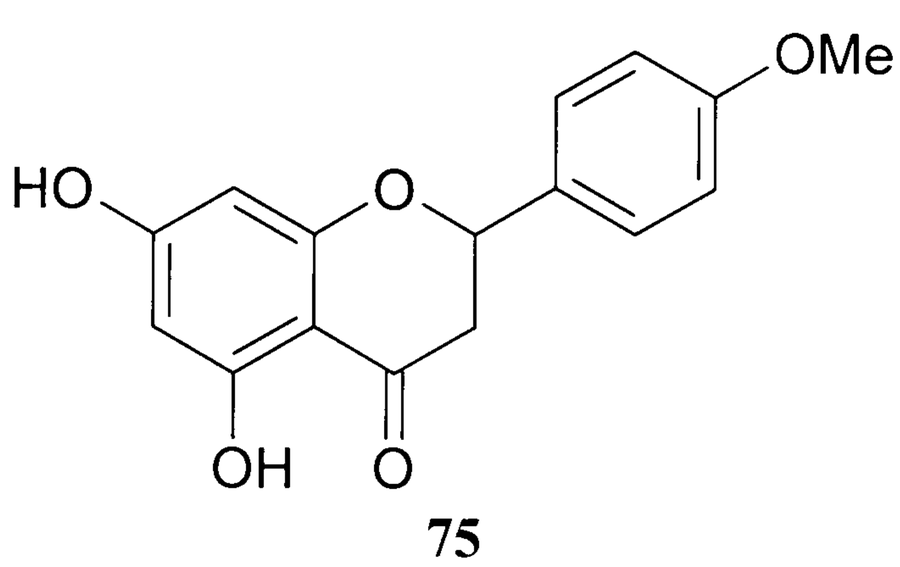

75

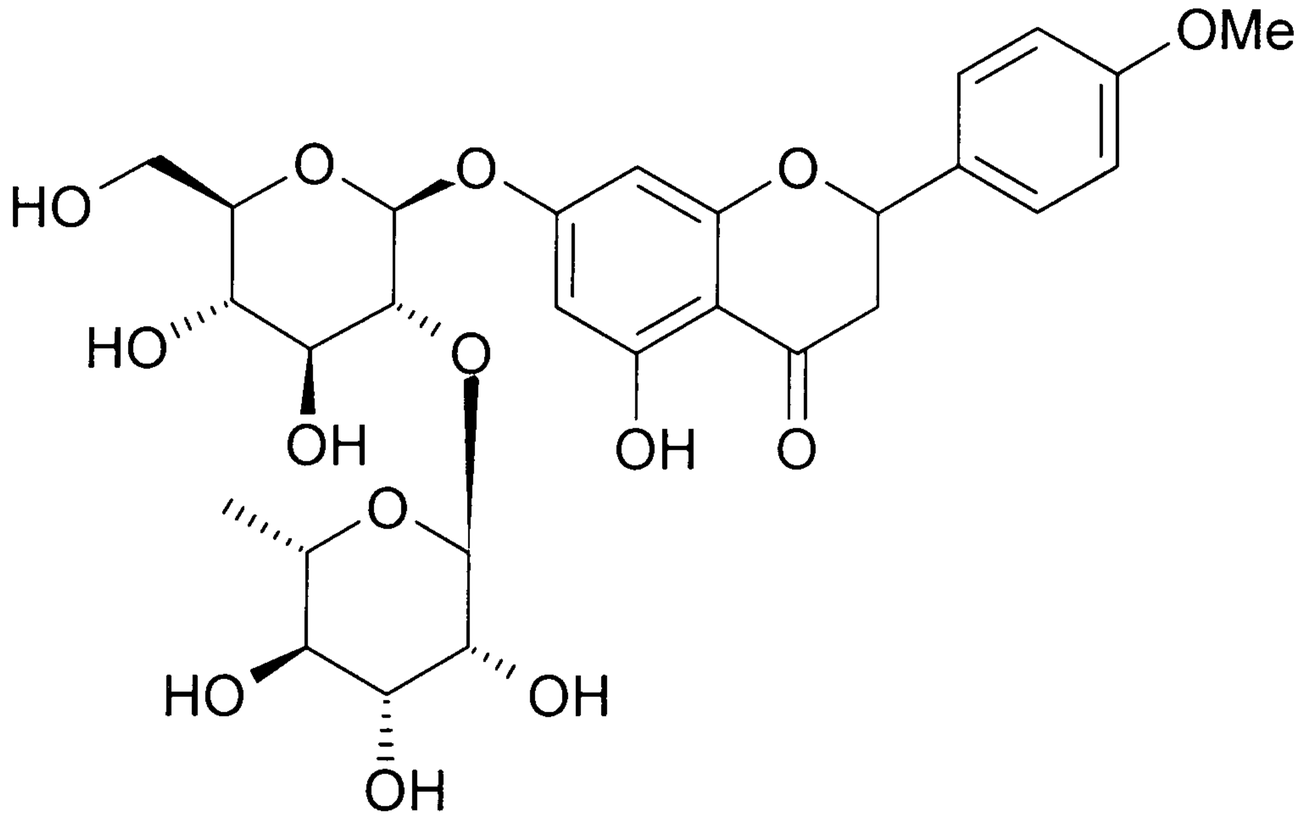

76

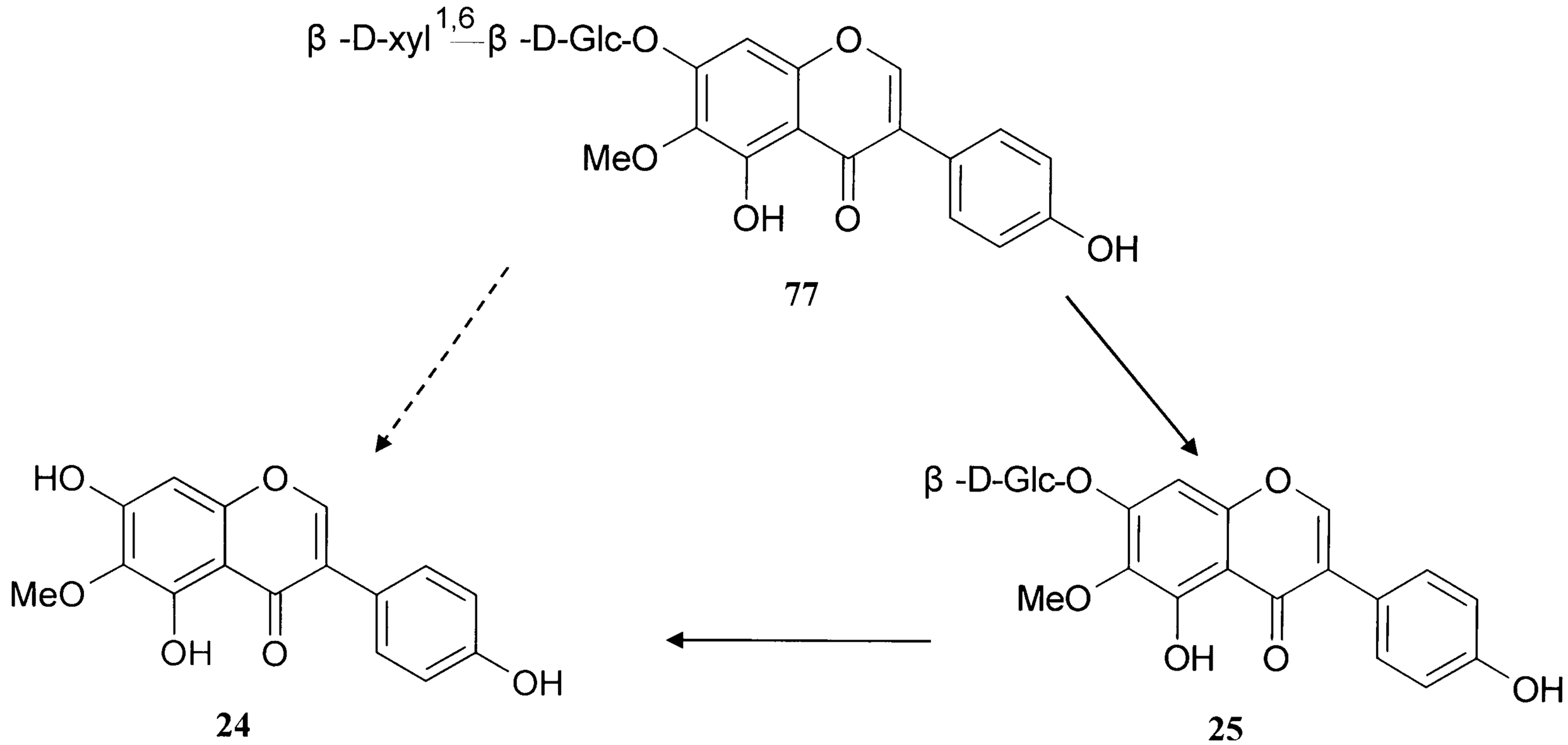

Figure 4-1: The proposed metabolic pathway of 6"-*O*-xylosyltectoridin (**77**) and tectoridin (**25**) by human intestinal bacteria (Bae *et al.*, 1999) (unbroken lines: major pathway; dashed line: minor pathway)

4.2 Enzymatic hydrolysis assay

It has been confirmed that flavonoid glucosides can be efficiently transformed into the active aglycone (the corresponding flavonoid) by some human intestinal bacteria (Park *et al.*, 2004; Bae *et al.*, 1999). However, the procedure of reaction mixture involved bacteria is difficult to combine with cell culture test as a high throughput prodrug assay, because contamination with bacteria can affect the cell growth, and metabolism requires fairly long time preincubation (12h with intestinal bacterial strains or 2 days with fresh human faeces) (Kim *et al.*, 1998).

A cytotoxicity assay with enzymatic hydrolysis procedure was established in this project to discover potential β-glucosides as prodrugs in crude extracts of TCMs. This experiment is based on the fact that the similar hydrolysis reaction of β-glucoside flavonoids would happen *in vivo*. Beside the relative enzymes produced by intestinal flora, a broad specific β-glucosidase has been found in human organs and characterized, such as the cytosol of liver (Daniels *et al.*, 1981). Moreover, the acidic environment in the digestive tract also contributes to the hydrolysis of flavonoid glycosides *in vivo*. Meanwhile, the *in-vitro* enzymatic hydrolysis assay is limited by the availability of purified enzymes.

β-Glucosidase is an enzyme which catalyzes the hydrolysis of various compounds with β-*D*-glucosidic linkages. It has been isolated from fungi, bacteria, yeast and plants (Shewale, 1982). This enzyme was employed in the present prodrug assay because about half of the naturally occurring flavonoid glycosides are β-*D*-glucosides (Mabry, 1970). The β-glucosidase from almonds was commercially acquired from Sigma-Aldrich (Fluka 49290, $\geq$6 units/mg, 1U corresponds to the amount of enzyme which liberates 1μmol glucose per minute at pH 5.0 and 35°C). The advantages of this enzyme including: high efficiency, non-toxic effect on cells and low cost.

4.2.1 Positive Control of prodrug assay

A previous publication revealed that luteolin-7-*O*-glucoside (**50**) a *β*-*D*-glucoside can be efficiently hydrolysed to luteolin (**22**) by *β*-glucosidase (Nusslein and Kreis. 2000; Gebhardt, 2002). An absorption analysis using rat everted small intestine also demonstrated that luteolin-7-*O*-glucoside (**50**) was absorbed as the aglycone after hydrolysis to luteolin in digestive tract. An HPLC analytical method in the literature (Shimoi *et al.*, 1998) allowed easy separation of luteolin-7-*O*-glucoside (**50**) (R_T 12.8min) and luteolin (**22**) (R_T 22.8min). Thus, as the precursor of luteolin (**22**), luteolin-7-*O*-glucoside (**50**) was obtained from Extrasynthese (1126S) and tested as the positive control in the prodrug assay. Luteolin (**22**) was obtained from Sigma-Aldrich (Fluka 62696).

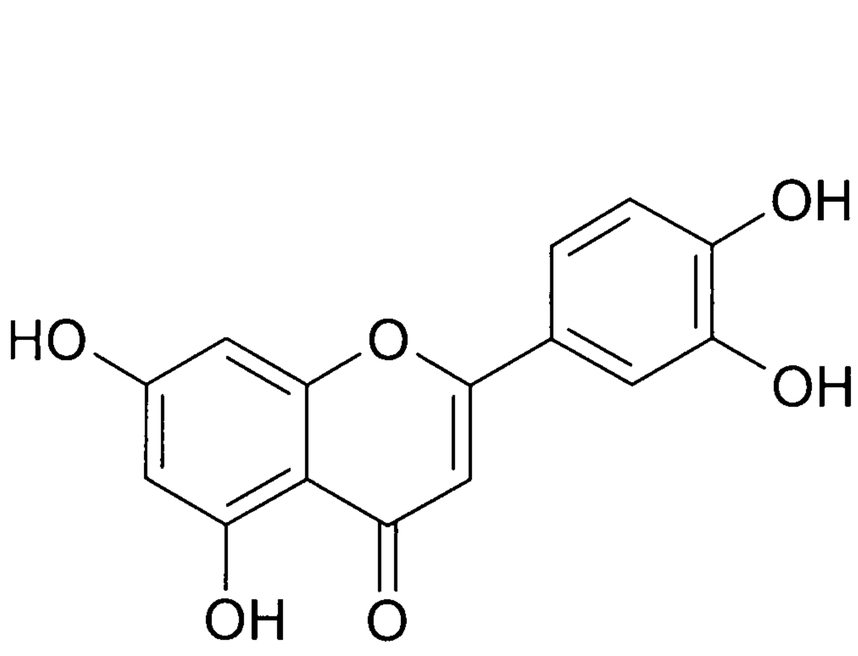

22

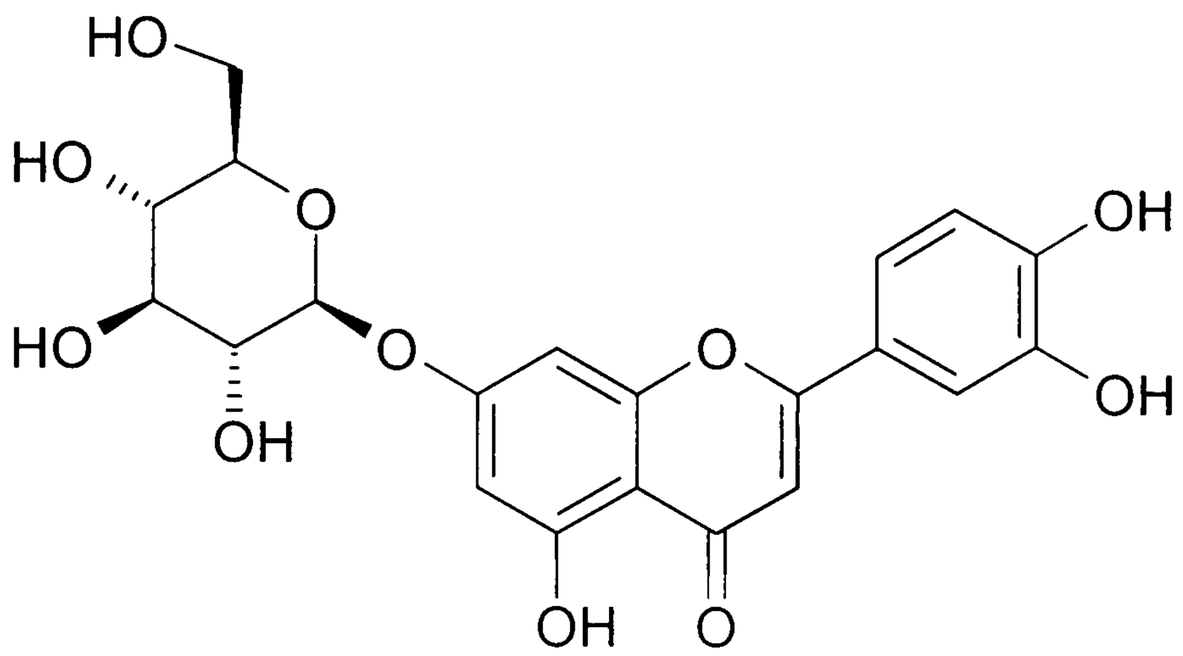

50

4.2.2 Optimization of prodrug assay

Basically, *β*-glucosidase is a non-toxic agent. With 4mg/ml of it in medium, 77% of cancer cells were still growing after 48h. When 0.5mg/ml *β*-glucosidase added into medium, the inhibition of cell proliferation caused by the enzyme was no more than 4% (see Figure 4-2). An extra experiment indicated that 0.5mg/ml was as effective as 2mg/ml *β*-glucosidase for the hydrolysis of luteolin-7-*O*-glucoside (**50**) to luteolin in this prodrug assay (data not shown). Thus, the following prodrug assay was carried out with 0.5mg/ml *β*-glucosidase.

The cytotoxic effect of the positive control against cancer cells was tested after an exposure time of 48h. Luteolin (**22**) exhibited IG_{50} of 11μM against COR-L23 cells. On the other hand, luteolin-7-*O*-glucoside (**50**) is a relatively non-toxic compound.

since there is still 77% proliferation of cells with 200μM luteolin-7-*O*-glucoside (see Figure 4-3). When incubated with *β*-glucosidase, luteolin-7-*O*-glucoside (**50**) exhibited cytotoxicity with IG_{50} of 35.7μM (see Figure 4-3). This observation is consistent with that in the literature (Gebhardt, 2002) and clearly demonstrated that luteolin-7-*O*-glucoside (**50**) was hydrolyzed to luteolin (**22**) by 0.5mg/ml *β*-glucosidase under normal cell culture conditions.

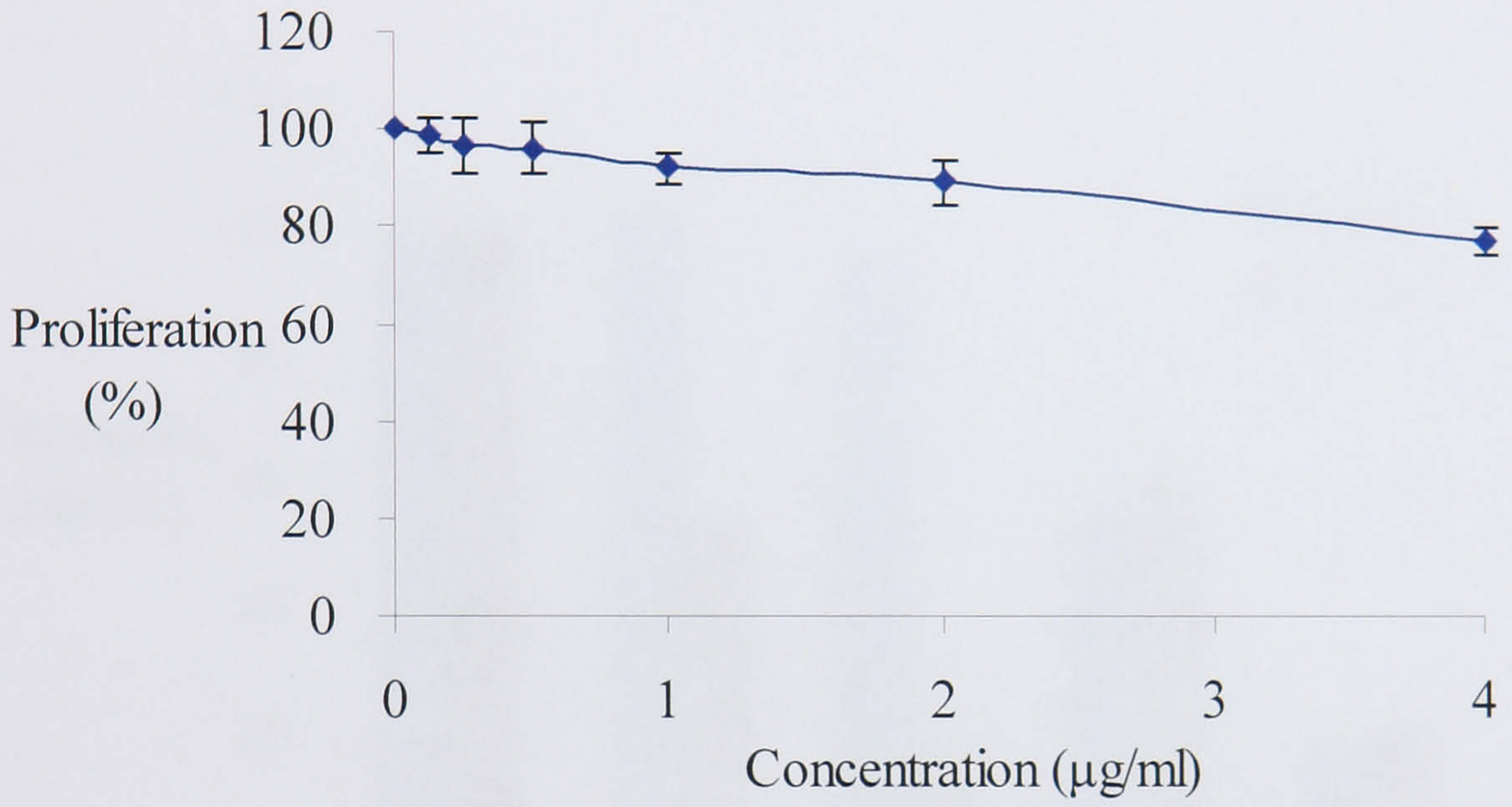

Figure 4-2: Inhibition effect of *β*-glucosidase against COR-L23 cells (mean±SEM, n=2)

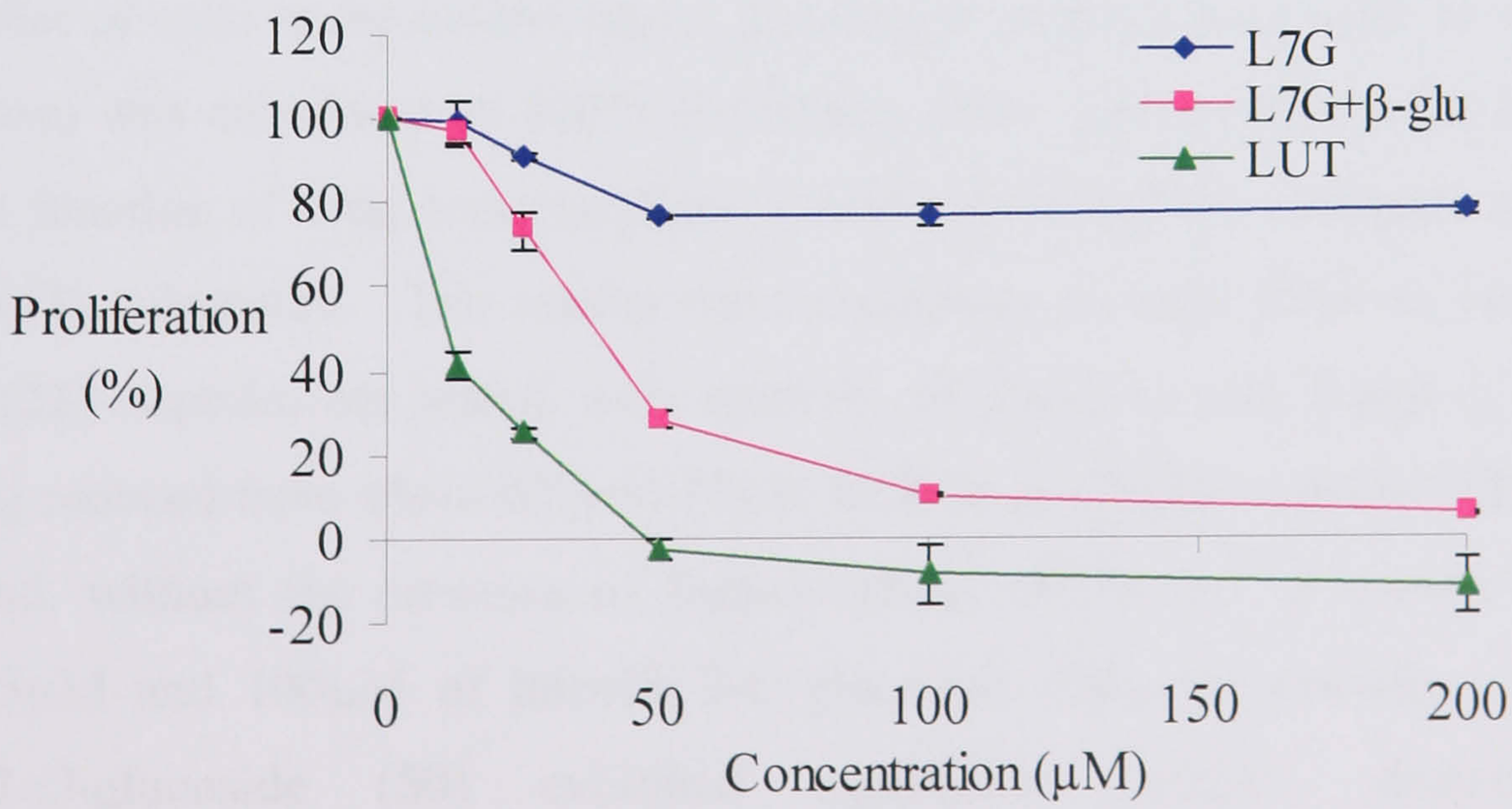

Figure 4-3: Comparison of dose-dependent cytotoxicity of luteolin (LUT) (**22**) with that of luteolin-7-*O*-glucoside (L7G) (**50**) (incubated with and without *β*-glucosidase) (mean±SEM, n=2)

As positive controls luteolin-7-*O*-glucoside (**50**) and luteolin (**22**) were tested by this prodrug assay in a pattern for all the other samples. As shown in Figure 4-4, cancer cells were treated with identical molar concentrations (15μM and 100μM) of luteolin (**22**) and luteolin-7-*O*-glucoside (**50**), respectively. Firstly, both compounds were prepared in normal medium, *β*-glu(−), and, as a counterpart experiment, they were prepared in medium with 0.5mg/ml *β*-glucosidase, *β*-glu(+). After preincubated at 37°C for 2hr, drug solutions were added into 96-well plates for 48h exposure to COR-L23 cells.

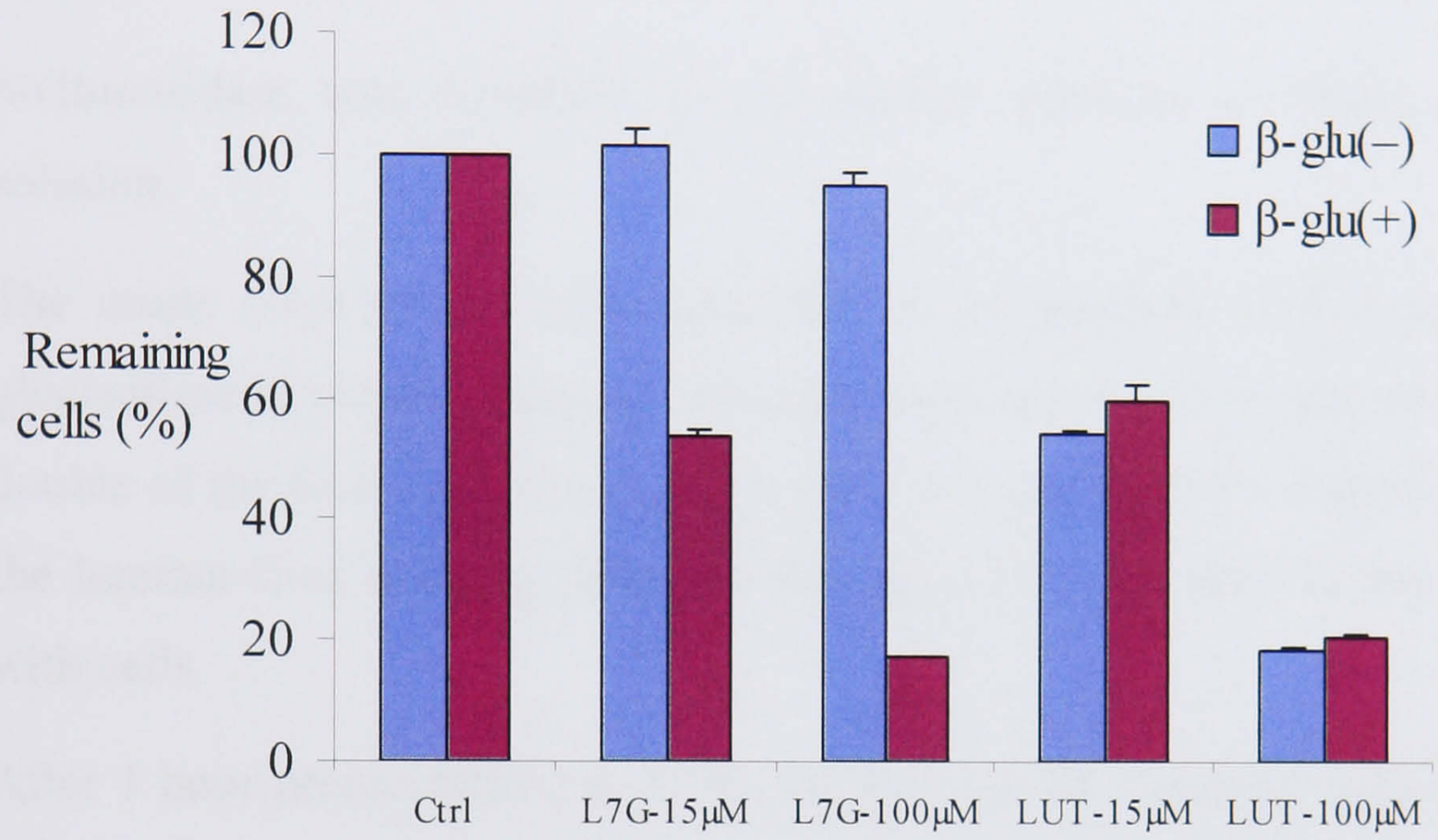

Figure 4-4: Comparison of cytotoxicity of luteolin-7-*O*-glucoside (L7G) (**50**) and luteolin (LUT) (**22**) in prodrug assay (mean±SEM, n=2)

The number of cells in the control (those growing in medium only, with or without *β*-glucosidase) was calculated as 100% remaining cells. The proportion of remaining cells as a function of drug concentrations was observed and the cytotoxic activity of luteolin (**22**) calculated. The results were consistent to each other in two sets of luteolin (**22**) experiments tested with medium of *β*-glu(+) and *β*-glu(–), the cells remaining reduced from about 60% in 15μM to 20% in 100μM luteolin (**22**). On the other hand, without the presence of *β*-glucosidase, 102% and 95% cells remained within 15μM and 100μM of luteolin-7-*O*-glucoside (**50**), respectively. However, luteolin-7-*O*-glucoside (**50**) exhibited significant ($p<0.01$) dose-dependent cytotoxicity against lung cancer cells in the *β*-glu(+) experiment. Furthermore, its inhibition potency was very similar to that of luteolin (**22**). The remaining cells declined from 54% to 17% when the concentration of luteolin-7-*O*-glucoside (**50**) was

increased from 15μM to 100μM in the *β*-glu(+) experiment. These observations suggested that luteolin-7-*O*-glucoside (**50**) was hydrolyzed to luteolin (**22**) by *β*-glucosidase in the medium, so that it showed the same cytotoxicity as luteolin against cancer cells. That means *β*-glucosidase worked as a key to activate the cytotoxicity of prodrug in this prodrug assay.

4.2.3 Protocol of enzymatic hydrolysis:

This procedure was previously established by Gebhardt, 2002 and was modified in the present work.

1. *β*-Glucosidase was dissolved in cell culture medium to obtain a 1mg/ml solution.
2. The crude plant extract was dissolved in the medium with 1mg/ml of *β*-glucosidase to obtain a range of desirable concentrations, which were made as double of the final concentrations for test. All solutions were sterilized inside the laminar-flow hood by filtration through a 0.22nM filter before incubated with cells.
3. After 1 hour preincubation at 37°C, the hydrolyzed solutions were added into 96-well plates. The final solutions were obtained by adding drug solutions into 96-well plates for 100μl per well (mixed with the original 100μl growing medium in each well).
4. The final concentrations of drug solutions thus obtained were 100μg/ml and 200μg/ml in wells (pure compounds prepared as 100μM and 200μM). Meanwhile, *β*- glucosidase became 0.5mg/ml in each well. The solutions for negative control were made with only medium and *β*- glucosidase.

4.2.4 Results of prodrug assays

All water and MeOH extracts involved in this project were tested by the enzymatic hydrolysis assay. Because the raw materials were extracted continuously by hexane, $CHCl_3$, MeOH and water, the flavonoid glucosides in question are very likely to be concentrated into MeOH and water extracts. Therefore, the prodrug assay was carried out only on all the MeOH and water extracts of TCMs. The extracts were prepared at 100μg/ml and 200μg/ml to detect possible dose-dependent cytotoxicity, which might

be noticeably changed by hydrolysis by β-glucosidase.

Comparing with the control, the water and MeOH extracts of *Gekko swinhonis* (GK), *Illicium verum* (IV) and *Dolichos lablab* (DL) did not exhibited cytotoxicity against COR-L23 cells after 48h exposure. The remaining cells were higher than 88% after exposure to those extracts. Also, no significant difference observed between the β-glu(–) and β-glu(+) experiments (see Figure 4-5).

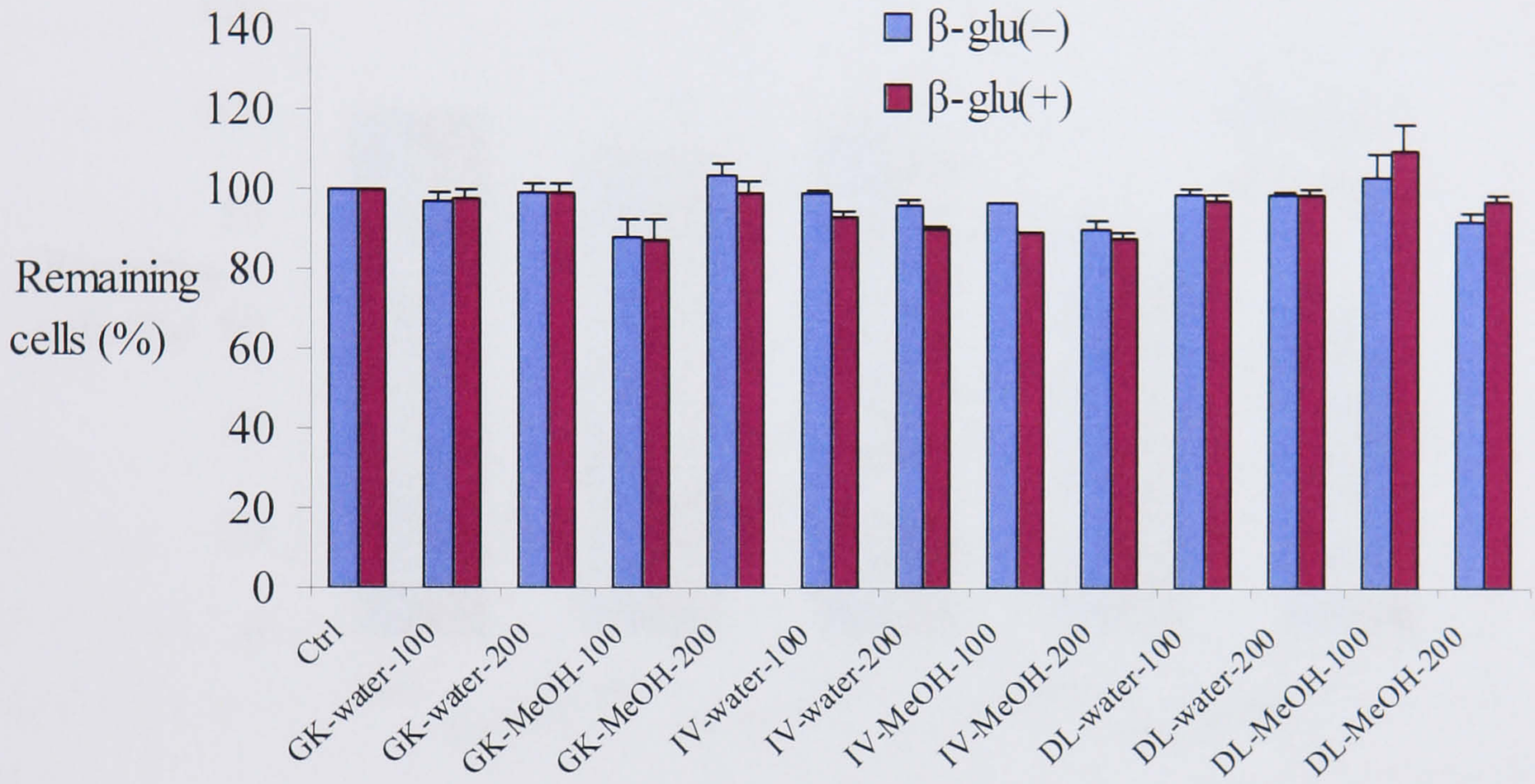

Figure 4-5: Prodrug screening for crude extracts of *Gekko swinhonis* (GK), *Illicium verum* (IV) and *Dolichos lablab* (DL) (mean±SEM, n=2; β-glu= β-glucosidase)

Although the water extracts of *Iris tectorum* (Iris-water-100 and Iris-water-200) did not show cytotoxicity, its MeOH extracts (Iris-MeOH-100 and Iris-MeOH-200) exhibited dose-dependent cytotoxicity against COR-L23 in 48h. The remaining cells decreased from 78% in 100μg/ml to 64% in 200μg/ml, for β-glu(–) experiment. Moreover, the same extracts showed slightly increased activity in an experiment with β-glucosidase in the medium. The remaining cells were 73% in 100μg/ml and 53% in 200μg/ml, respectively, for β-glu(+) experiment (see Figure 4-6). However, the difference caused by β-glucosidase was not statistically significant in this test.

The result of prodrug screening for *Lonicera japonica* showed that both water and MeOH extracts showed dose-dependent cytotoxicity. In β-glu(–) experiment, the remaining cells decreased from 79% in LJ-water-100 to 17% in LJ-water-200, and from 78% in LJ-MeOH-50 to 11% in LJ-MeOH-200. However, the extracts

demonstrated much lower cytotoxicities in β-glu(+) experiment than that of β-glu(–) experiment. Remarkably, the remaining cells in 200μg/ml LJ-MeOH significantly increased ($p<0.01$) from 11% in β-glu(–) to 54% in β-glu(+) (see Figure 4-7). This observation suggests a detoxification reaction caused by addition of β-glucosidase in the tested solution of LJ-water and LJ-MeOH extracts. This unexpected result is interesting and worth clarification in future research work.

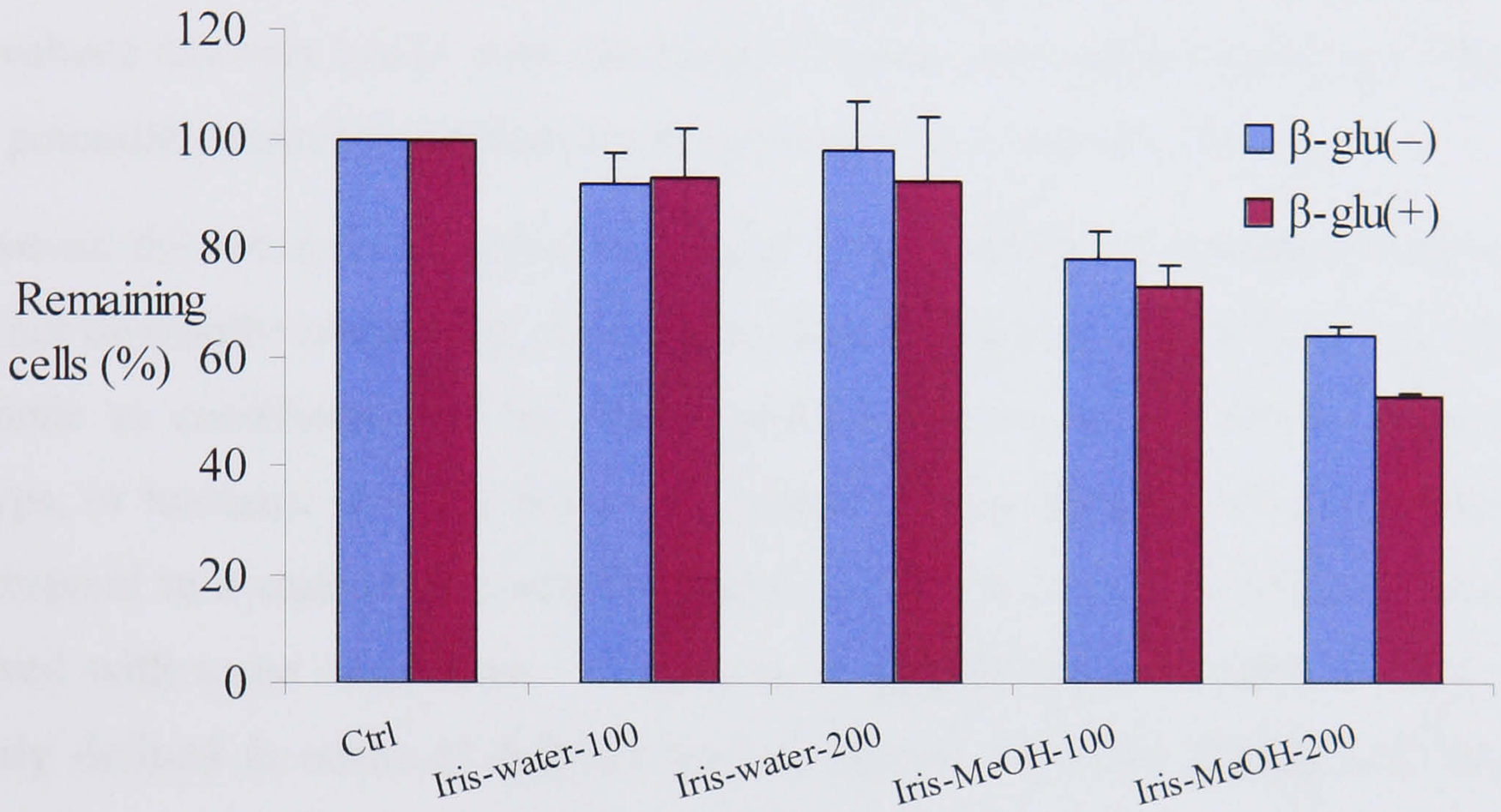

Figure 4-6: Prodrug screening for crude extracts of *Iris tectorum* (mean±SEM, n=2)

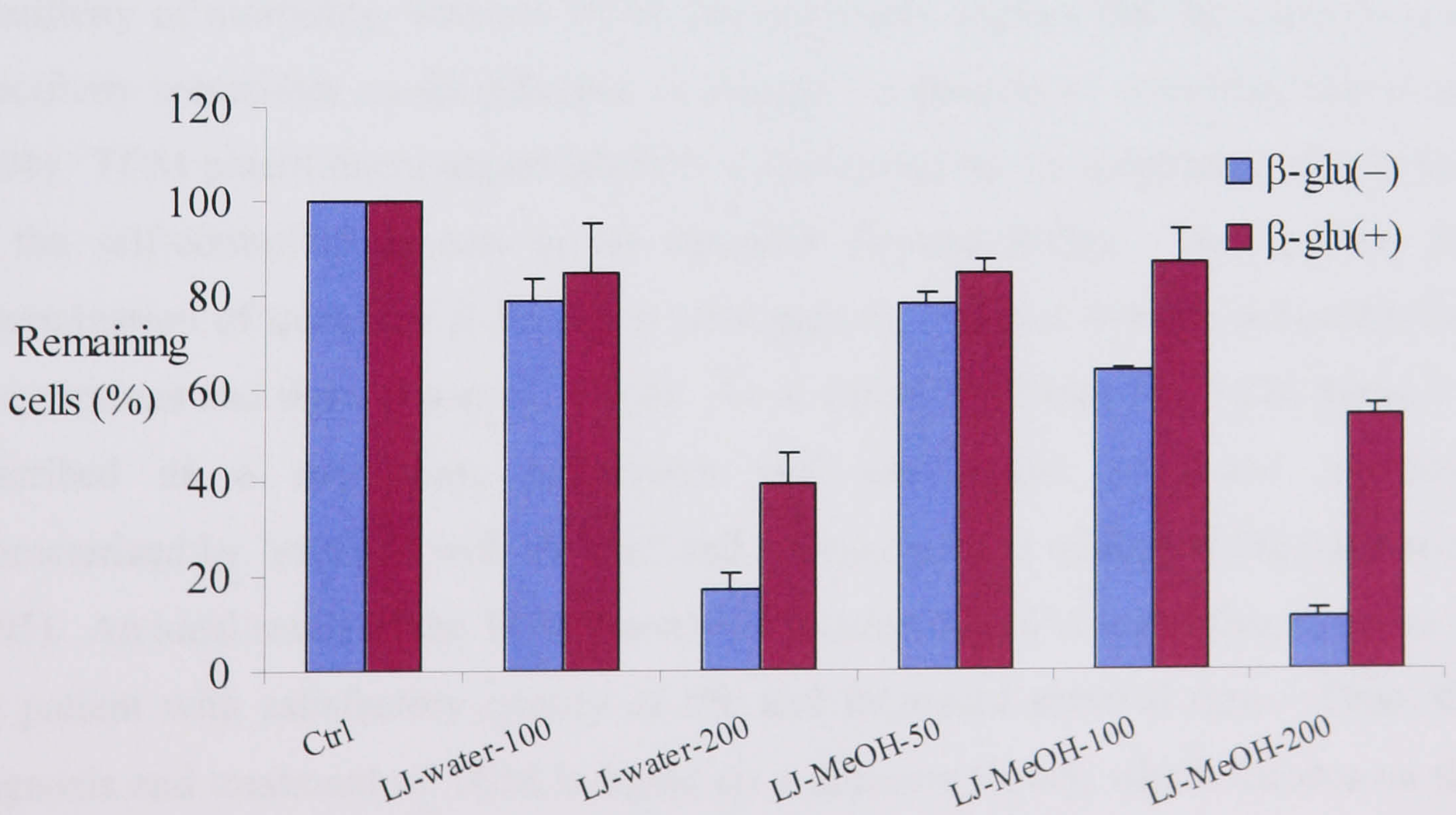

Figure 4-7: Prodrug screening for crude extracts of *Lonicera japonica* (mean±SEM, n=2)

CHAPTER 5
DISCUSSION

Plants have a long history of being used in the treatment of cancer. A survey of plants used in ethnomedicine against cancer has revealed more than 3,350 plant species (Graham *et al.*, 2000). The introduction of active compounds derived from nature into the cancer treatment has changed the natural history of many types of human cancer. Experimental agents derived from natural products offer a great opportunity to evaluate not only totally new chemical classes of anticancer agents, but also novel and potentially relevant mechanisms of action (da Rocha *et al.*, 2001).

However, the research for novel anticancer compounds from ethnobotanical sources can not be readily carried out. In many instances, "cancer" is undefined, or reference is made to conditions such as "hard swellings", abscesses, calluses, corns, warts, polyps, or tumours, to name but a few. Many of such symptoms indeed sometimes correspond to a cancerous condition, but many of the claims for efficacy should be viewed with some scepticism. Cancer, as a specific disease entity, is likely to be poorly defined in terms of folklore and traditional medicine (Cragg and Newman, 2005).

On the other hand, development of modern medicine is aimed to explore the specificity of morbidity, whereas TCM theory usually implies that the cures of non-specificity sometimes could influence or change the process of morbidity (Lu *et al.*, 2004). TCM practitioners regard disorder to be caused by the disturbance in any part of the self-controlled system in the integrity (human body). Furthermore, the determination of treatment is based on pathogenesis obtained through differentiation of symptoms and signs (Jia *et al.*, 2006). As to anticancer treatment, TCM therapy is described as a multi-way, multi-layer and multi-target integrated treatment characterized by "survival with tumour" and improvement in quality of life (Que *et al.*, 2005). An ideal result of the TCM therapy for cancer should be a positive response of the patient with satisfactory quality of life and increased survival time. Thus, the diagnosis and treatment of TCM is based on a different theory, which focuses on the result of treatment rather than a definite biomedical mechanism.

5.1 Prodrug screening

It should not be a surprise if a traditional medicine with good reputation in local culture does not exhibit any activity in screening by *in-vitro* bioassays. That means it is not guaranteed to isolate individual compounds with high bioactivity from the natural anticancer medicine. Besides the possibility of synergistic effects of the components within a TCM prescription, the metabolic process in human body after oral administration should not be ignored upon the investigation of bioactive compounds in TCM. Generally, most traditional medicines are administered orally so that the components of these medicines inevitably come into contact with microflora in the alimentary tract. Some TCM components could be transformed by intestinal bacteria before being absorbed from the intestine. It has been reported that intestinal bacteria can hydrolyze glucosides of flavonoids and produce aglycones (Hawksworth *et al.*, 1971; Kang *et al.*, 2005). Thus, a prodrug assay associated with a hydrolysis enzyme was carried out in present study.

Although no further isolation followed the prodrug assay because of lack of time, the result really provided useful information for the feasibility and necessity of using it as a routine screening assay for investigation of natural medicines. According to previous research, luteolin-7-*O*-glucoside (**50**) was hardly absorbed by itself and it was absorbed after hydrolysis to luteolin (Shimoi *et al.*, 1998). In the present prodrug assay, luteolin-7-*O*-glucoside (**50**) did not show cytotoxicity against COR-L23 cells and allowed 77% proliferation of cells at 200μM. Nevertheless, it exhibited relatively strong cytotoxicity with IG_{50} of 35.7μM after hydrolysis by *β*-glucosidase. Therefore, the activity of potent compounds like luteolin is unlikely to be detected by *in-vitro* screening when it is still in the form of the corresponding glucoside such as luteolin-7-*O*-glucoside (**50**) in TCM.

The prodrug assay for crude extracts showed that no cytotoxicity was observed in those treatments by crude extracts of *Gekko swinhonis*, *Illicium verum* and *Dolichos lablab* (see Figure 4-5). There was no significant difference of the activity observed after those extracts incubated with *β*-glucosidase either. At the same time, however, the MeOH extracts of *Iris tectorum* showed dose-dependent activity. Moreover, its water extract (at 200μg/ml) and MeOH extract (at 100μg/ml and 200μg/ml) showed increased cytotoxicity after incubation with *β*-glucosidase (see Figure 4-6). This

difference of activity is likely to be caused by the hydrolysis of glucosides components (less active) into their active aglycones in this TCM. Interestingly, the water and MeOH extracts of *Lonicera japonica* showed dose-dependent cytotoxicity. However, both extracts exhibited significant decrease of cytotoxicity in experiment with β-glucosidase in medium (see Figure 4-7). This unexpected result suggested that the integrated effect of a TCM can not readily be described thoroughly by *in-vitro* assays. As a mixture of many components the final metabolites may exhibit higher activity or lower activity *in vitro*. Before a further investigation, the mechanism behind the decreased cytotoxicity of extracts of *Lonicera japonica* caused by β-glucosidase is not clear.

5.2 Bioactivity of flavonoids from natural products

Flavonoids are one of the most widespread classes of plant secondary metabolites. They usually occur as glycosides rather than as aglycones (Zielinska *et al.*, 2003). More than 4,000 flavonoids have been isolated (Dugo *et al.*, 2005). Many flavonoids occur in the human diet, such as flavones in grains and herbs, flavonols and their glycosides in fruits and vegetables, flavanones in citrus juices, isoflavones in legumes and catechins in tea (Peterson and Dwyer, 1998).

These polyphenolic components are known as excellent antioxidants *in vitro*. They have been shown to prevent lipid peroxidation, to scavenge reactive oxygen species, to chelate iron ions (essential for the generation of hydroxyl radicals) and to inhibit NADPH-dependent oxidases and consequently superoxide anion production (Catapano, 1997; Rice Evans *et al.*, 1997; Robak and Gryglewski, 1996).

Epidemiological studies have suggested that a diet rich in isoflavonoids may play an important role in cancer prevention (Markovits *et al.*, 1989; Messina *et al.*, 1994). Further studies of the soybean phyto-oestrogens genistein (**51**) and daidzein (**78**) suggested that these flavonoids affect cancer progression as a result of their effects on apoptosis, cell cycle progression, growth and differentiation as well as their antioxidant and antiangiogenic effects (Constantinou *et al.*, 1990; Yamashita *et al.*, 1990; Okura *et al.*, 1988; Menon *et al.*, 1998). Moreover, some flavonoids such as epigallocatechin-3-gallate (EGCG) (**79**), diosmin (**80**) and hesperidin (**81**) have demonstrated a chemopreventive effect on nitrosamine-induced carcinogenesis

(Weitberg and Corvese, 1999; Yang *et al.*, 1997).

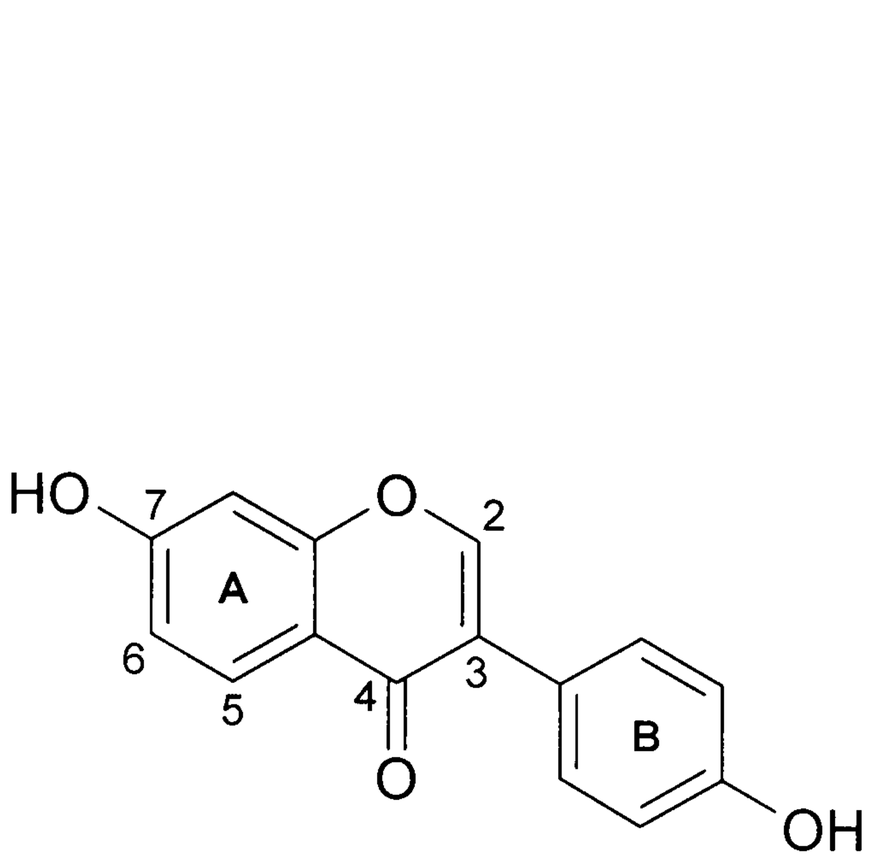

78

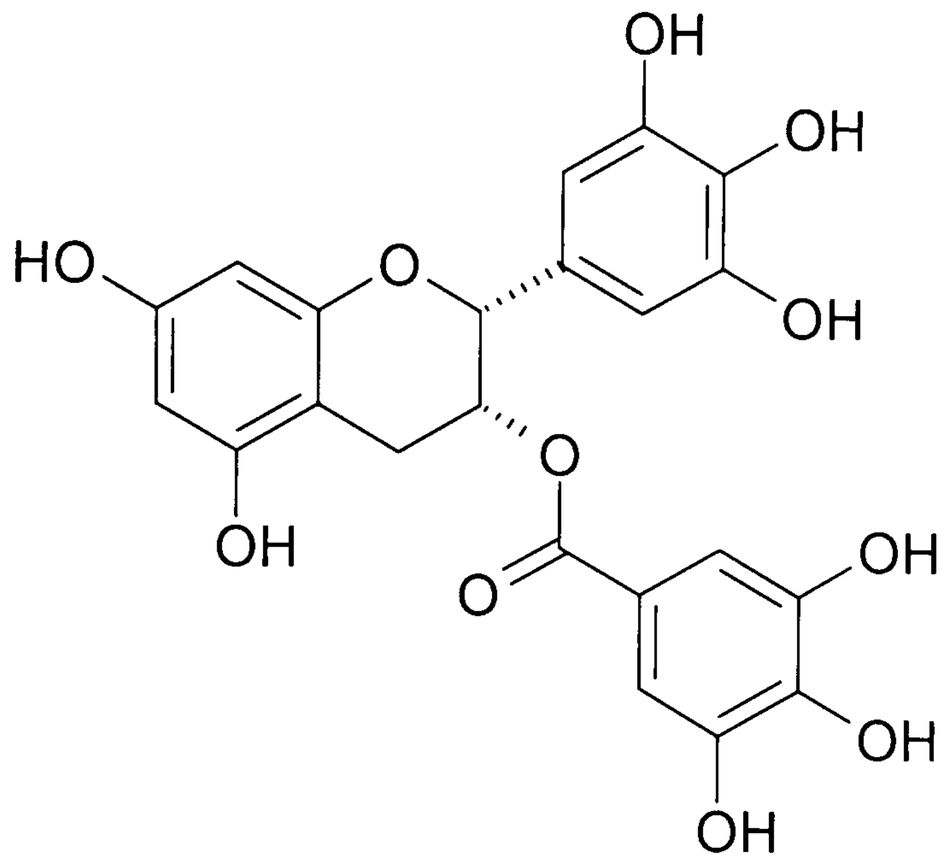

79

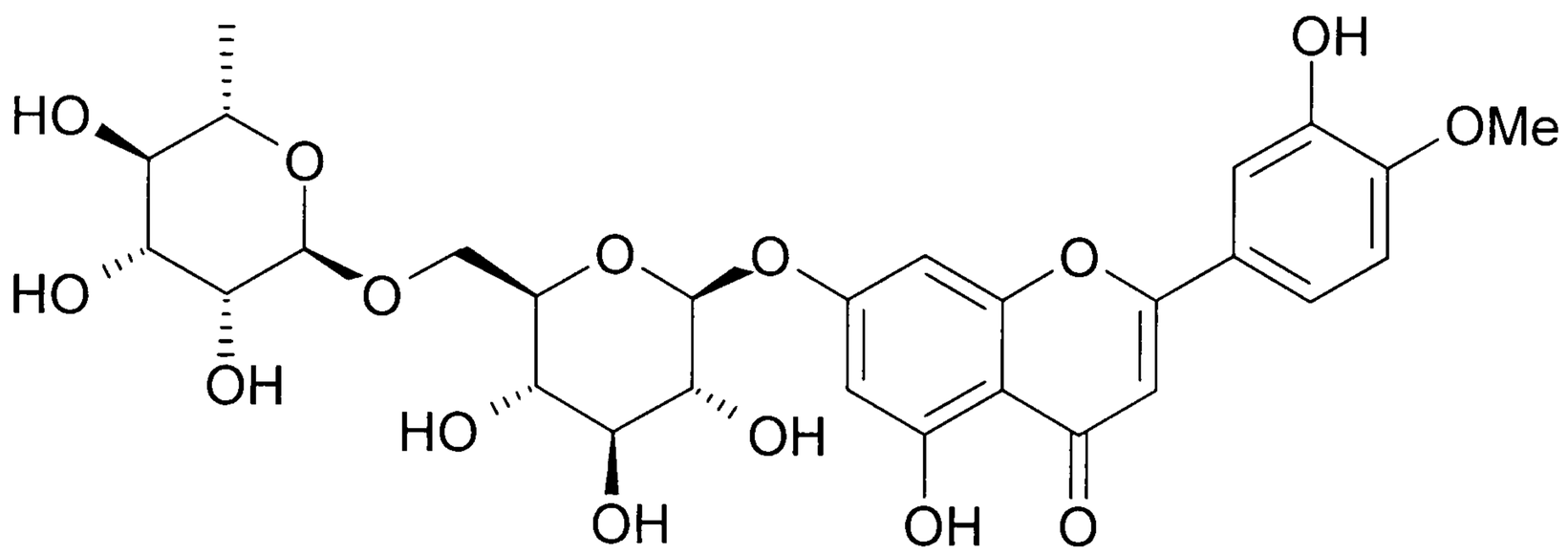

80

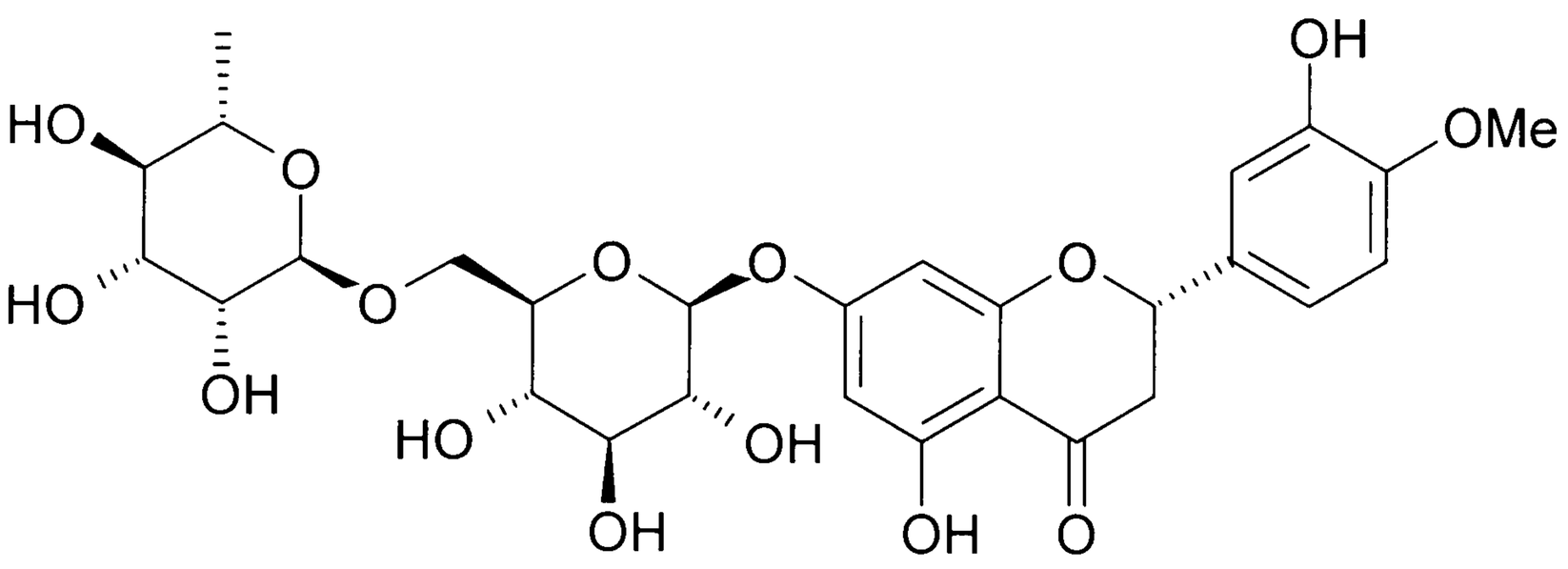

81

5.3 Structure-activity relationship of flavonoids

According to the results obtained in present study, the order of cytotoxiciy of these four flavonoids against six cell lines *in vitro* is luteolin (**22**) > 7-*O*-methyl aromadendrin (**66**) > genistein (**51**) > tectorigenin (**24**). Typically, genistein (**51**) and tectorigenin (**24**) are both natural isoflavonoids with low molecular weight (no more than 300). They differ from each other by only one methoxyl group in their structures. However, the cytotoxicity of genistein (**51**) is around 200% higher than that of tectorigenin (**24**) against various cancer cell lines in present study. Therefore, the methoxyl group at C-6 position on A-ring should be a key function to reduce the cytotoxicity of this isoflavone.

Compared with tectorigenin (**24**), 7-*O*-methyl aromadendrin (**66**) is a flavanone with similar molecular weight (MW=302). Nevertheless, it exhibited much higher cytotoxicity than genistein (**51**). The most important difference seems to be the hydroxyl function at C-3 position, which is adjacent to the oxo group at C-4. Luteolin (**22**) showed the highest cytotoxicity among those four flavonoids. Comparing with other three flavonoids, it has one more hydroxyl function on the B ring, and no methoxyl group at C-6 position on the A ring. These characteristics may contribute to its high activity.

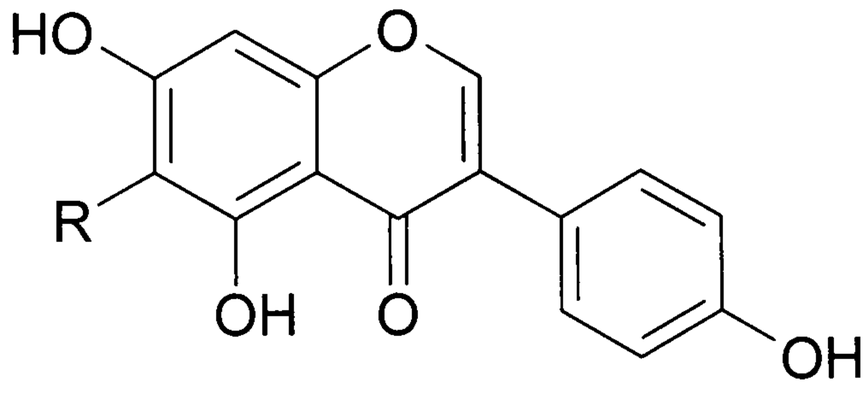

R

51: H

24: OMe

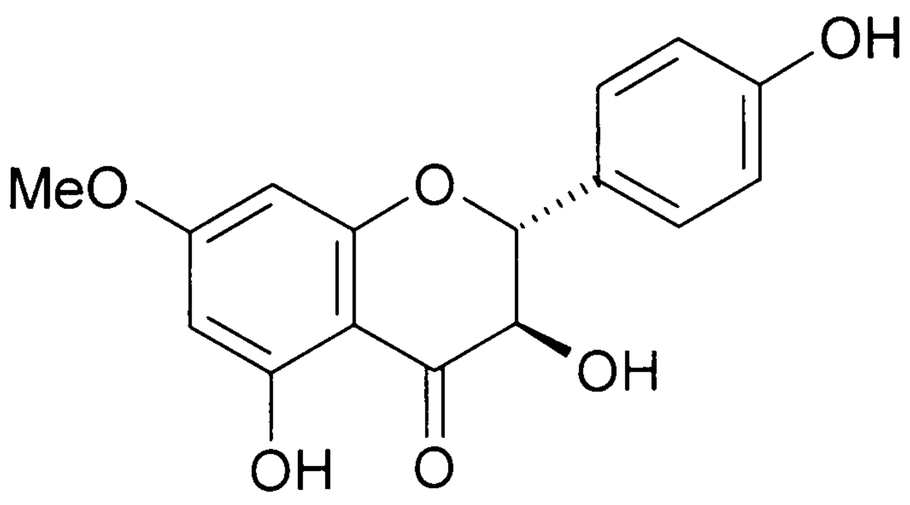

66

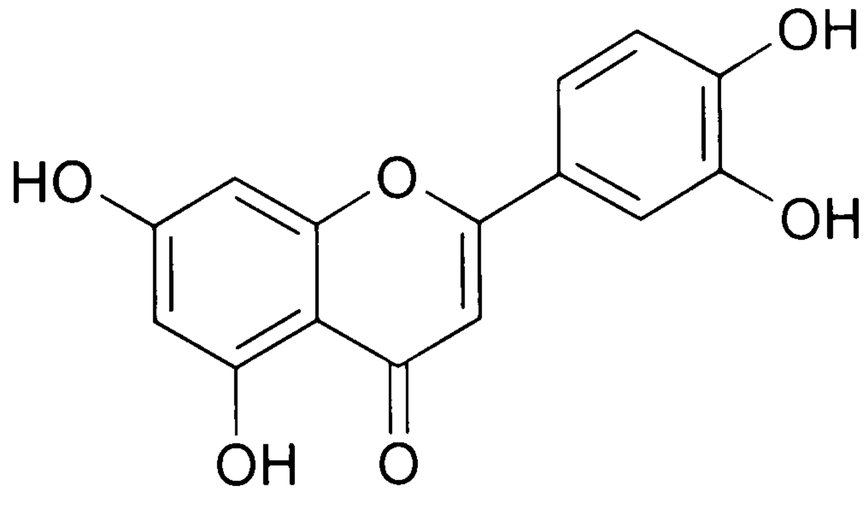

22

In order to investigate the potency of flavonoids on antagonist suppression of the transformation of cytosolic arylhydrocarbon receptor (AhR) induced by 2,3,7,8-tetrachlorodibenzo-*p*-dioxin, 34 flavonoids from natural products have been studied in previous work (Ashida, 2000). It was demonstrated that catechins and isoflavones, which have the B ring bound to the C-3 position (rather than C-2; see structure **78**), did not exhibit activity. That means an oxo group at C-4 position and a B ring bound at C-2 seems evident for the activity. Furthermore, the flavonoids glycosides showed weaker activity than their corresponding aglycones, suggesting that sugar moieties could reduce the activity.

Besides the observation in the present study (luteolin [**22**] *vs* luteolin-7-*O*-glucoside [**50**]), several studies have also reported that sugar moieties quench the bioactivities of favonoids when they were tested as glycoside *in vitro* (Park *et al.*, 2004; Bae *et al.*, 1999). Practically, those *in-vitro* bioassays used to evaluate the activites were based on cell culture experiments. Therefore the permeability of the cell membrane towards the tested compounds should be an essential factor. Obviously, flavonoids are hydrophobic compounds and can go though the cell membrane; however, the corresponding glycosides are hydrophilic and so usually do not readily enter the cells. Thus the flavonoid glycosides can hardly affect the target inside cells, and no activity could be observed *in vitro*.

5.4 Structure-activity relationship of iridal-type triterpenoids

Isoiridogermanal (**57**) isolated from petroleum ether and $CHCl_3$ extracts of the root of *Iris missouriensis* (Wong *et al.*, 1986) has been reported to demonstrate strong cytotoxicity against P-388 cells (mouse leukaemia) with ED_{50} of 0.21μM. Another study reported that iristectorene B (**36**), 16-*O*-acetylisoiridogermanal (**82**), 3-*O*-tetradecanoyl-16-*O*-acetylisoiridogermanal (**83**), 3-*O*-decanoyl-16-*O*-acetylisoirido-germanal (**84**), anhydrobelachinal (**85**), epianhydrobelachinal (**86**), belachinal (**87**) and (6*R*, 10*S*, 11*S*, 14*S*, 26*R*)-26-hydroxy-15-methylidene-spiroirid-16-enal (**88**) were isolated from *Belamcanda chinensis*, and tested for ichthyotoxic activity (Ito *et al.*, 1999). Only 16-*O*-acetyl-isoiridogermanal (**82**), belachinal (**87**) and (+)-(6*R*,10*S*,11*S*,14*S*,26*R*)-26-hydroxy-15-methylidenespiroirid-16-enal (**88**) showed potent ichthyotoxic activity against killie fish (*Oryzias latipes*) with TL_m (median tolerance limit after 24h) of 3.5μg/ml, 2.8 μg/ml and 1.6 μg/ml, respectively. All the

others showed TL_m higher than 10μg/ml (Ito *et al.*, 1999). Distinctively, the structures of **36**, **82**, **83**, **84**, **85**, **86**, **87** and **88** are numbered according to the original literature, because their names were given based on that system. However, this numbering system is not consistent with that of those triterpenes (see Figure 2-19 on page 87) isolated in present study.

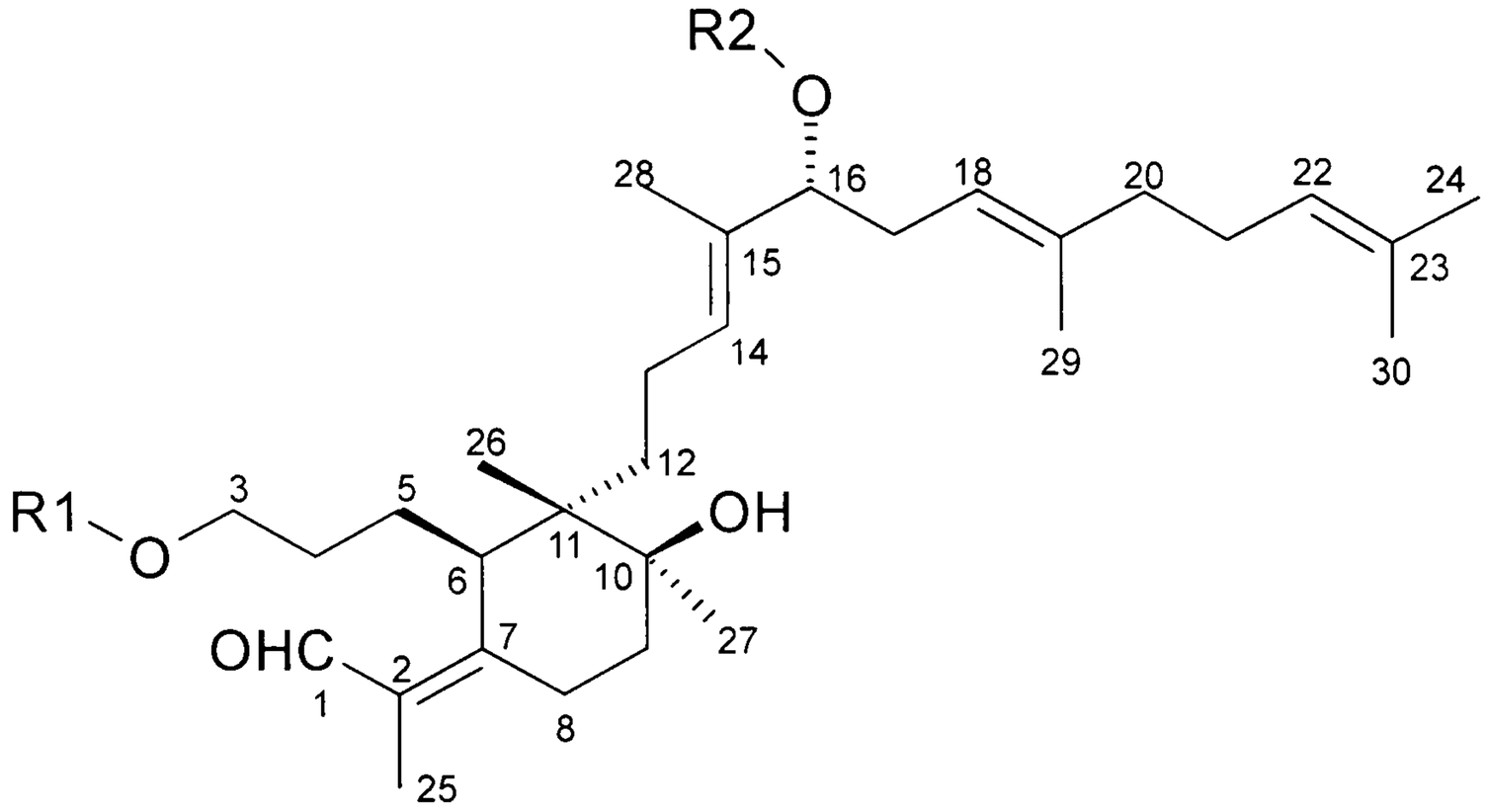

	R1	R2
36:	$CO(CH_2)_{12}Me$	H
82:	H	Ac
83:	$CO(CH_2)_{12}Me$	Ac
84:	$CO(CH_2)_8Me$	Ac

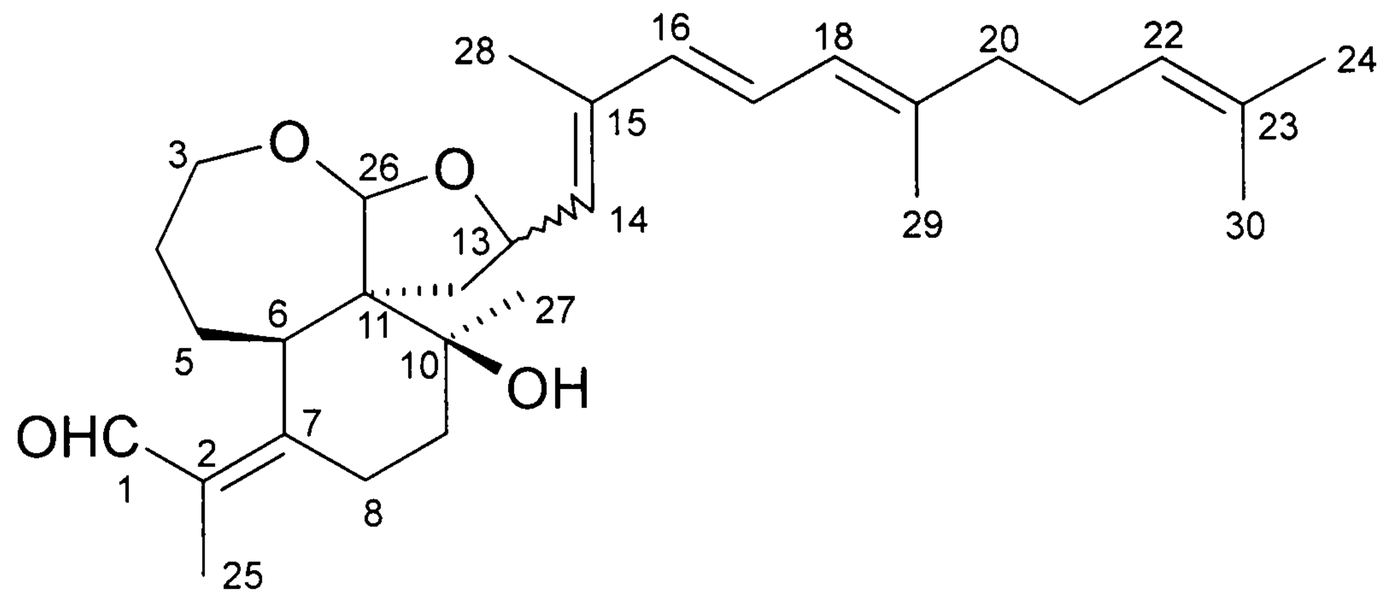

	C-13
85:	*S*
86:	*R*

By comparing the structures of those tested iridal-type triterpenes, it appears that esterification of the 3-OH of the monocyclic triterpenes (using the numbering system

shown in **79**) with a higher fatty acid, markedly lowers toxicity. Ethers such as anhydrobelachinal (**85**) and epianhydro-belachinal (**86**) were also much less toxic than those iridal-type triterpenes having the free 3-OH function. These results indicate that the free hydroxyl group at C-3 is important for toxicity. This evaluation is also supported by observations in present study, because the four iridal-type triterpenes (**57**, **60**, **61** and **65**) with the free hydroxyl group at C-25 (equivalent to C-3 in **82**, **87** and **88**) also exhibited potent cytotoxicity against various cancer cell lines (see Table 3-2 on page 111).

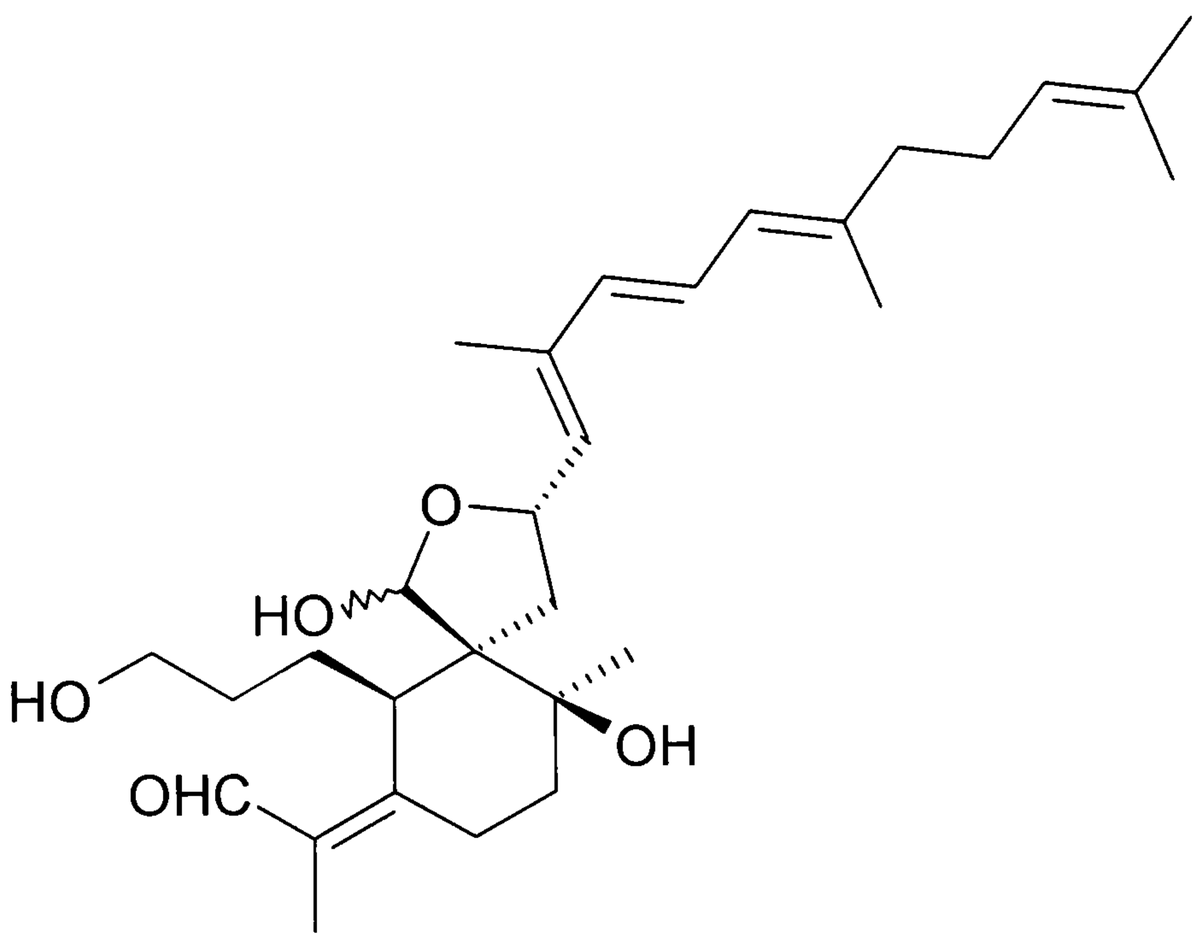

87

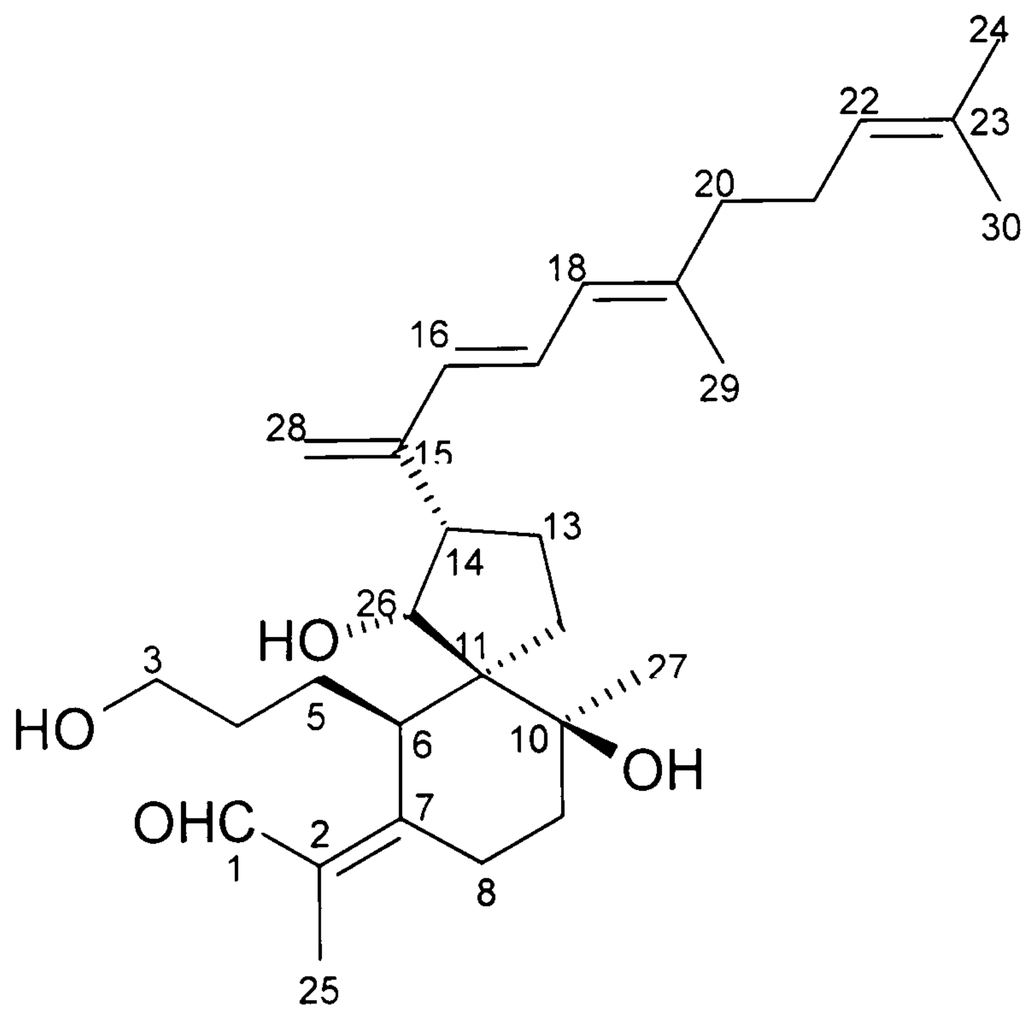

88

5.5 Possible stereostructures of IT4C (61) and IT4D (65)

The structures of IT4C (**61**) and IT4D (**65**) have been elucidated by various measurements, however, the configuration of some stereo centres in these novel compounds are still not certain. Since all isolated monocyclic iridal triterpenoids in the literature have been elucidated to have identical configurations in the six-membered ring, it is most likely for the two novel triterpenes isolated in the present work to have identical configuration of the six-membered ring. Noticeably, the results of ^{13}C NMR, ^{1}H NMR, HMQC, HMBC, ^{1}H-^{1}H COSY and NOESY experiments strongly support an identical configuration of the six-membered ring in these novel triterpenoids. Where it was possible to determine individual coupling constants, those observed (see Table 2-9) were not inconsistent with this proposed structural formulation. At the same time, IT4C (**61**) and IT4D (**65**) are suspected to be two derivatives of isoiridogermanal (**57**), thus they are likely to be biosynthesized as indicated in Figure 2-18 on page 86, and consequentially have identical absolute configuration in the six-membered ring and C-14 (*R*) as in isoiridogermanal (**57**). Therefore, the question left is the configurations of other chiral carbons on their structures.

According to the NOE correlation signals of IT4C (**61**) (see Figure 2-22 on page 93), the correlation signal between H-12 and H-14 clearly indicates that these two hydrogen atoms must be on the same side of the plane of the epoxy ring. As a result, there are only two possible configurations of the epoxy moiety in IT4C (**61**), as shown in structures **89** and **90** (the key NOESY ^{1}H-^{1}H correlation signal is indicated as blue arrow). Therefore, the absolute configuration of the whole molecule is most likely to be either of the two stereostructures shown as Figure 5-1 and Figure 5-2.

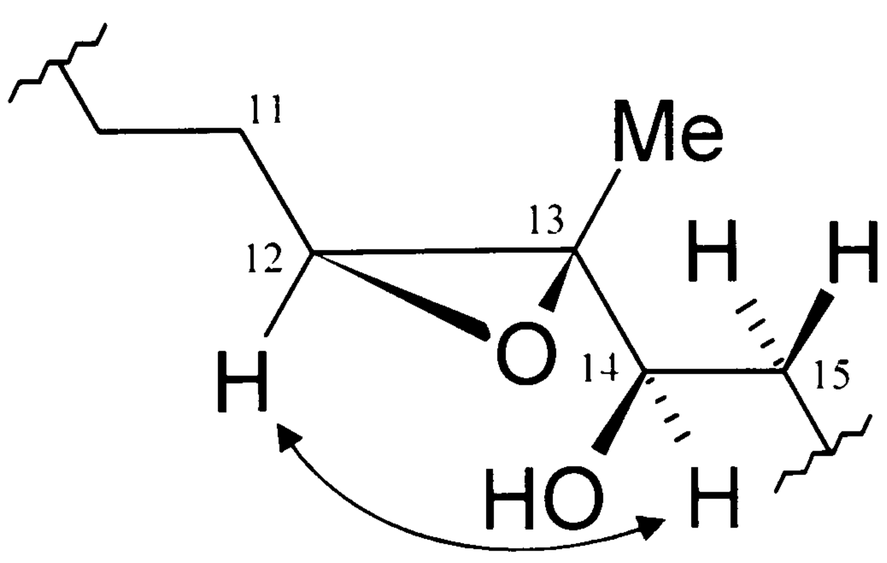

(12*S*, 13*S*) **89**

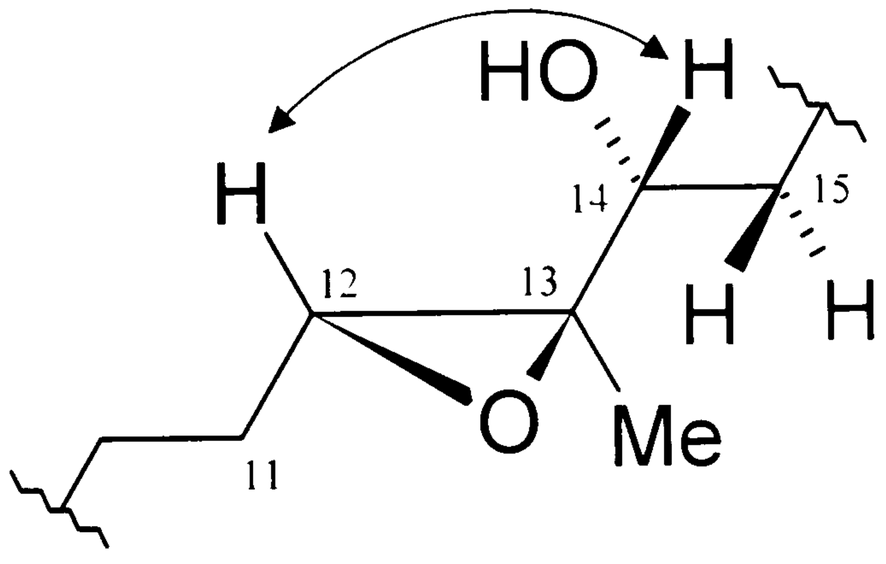

(12*R*, 13*R*) **90**

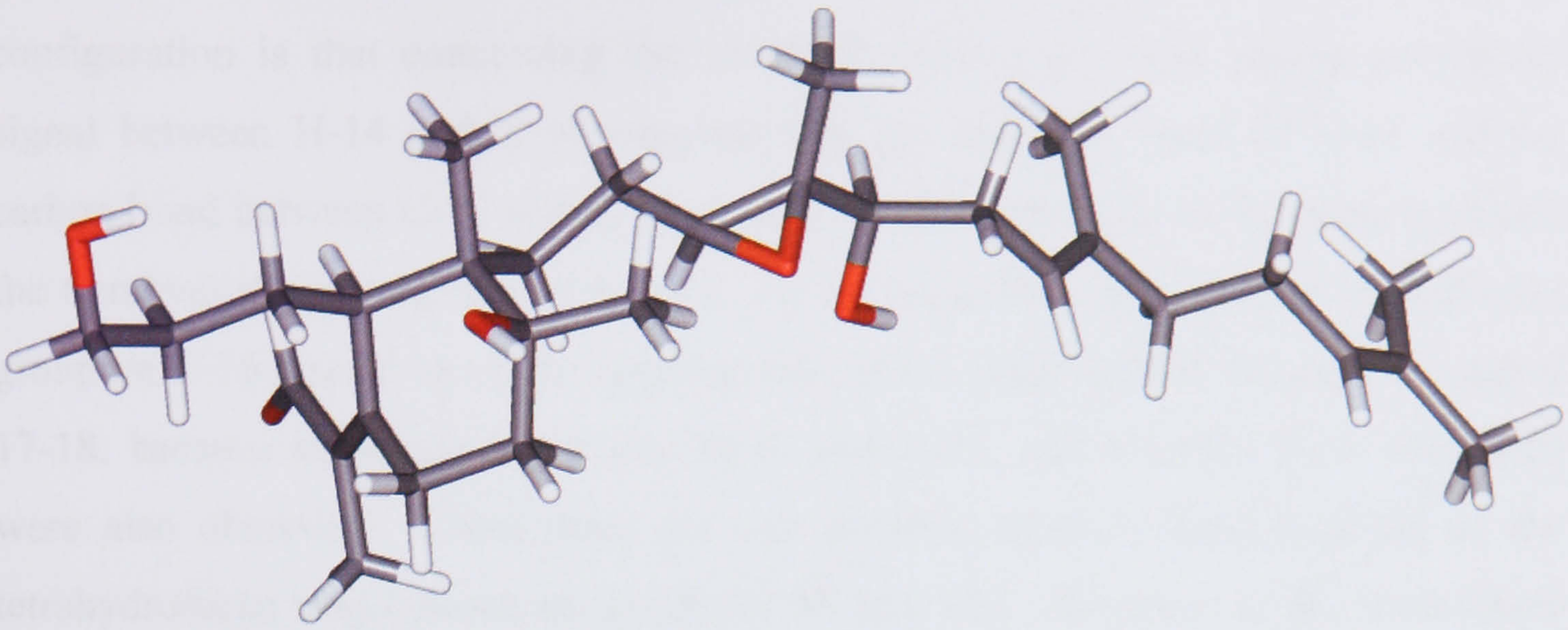

Figure 5-1: Stereostructure of IT4C (**61**) with the absolute configuration of epoxy ring as **89**

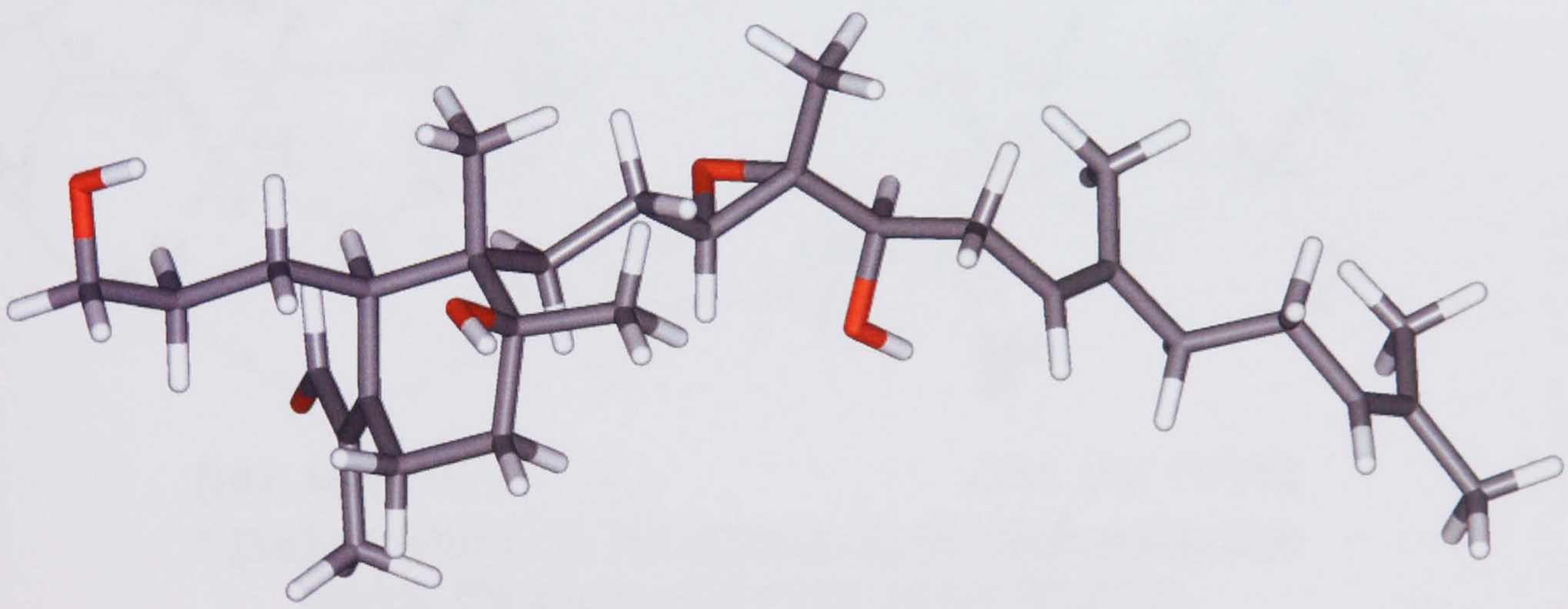

Figure 5-2: Stereostructure of IT4C (**61**) with the absolute configuration of epoxy ring as **90**

Based on the observed NOE correlation signals (see Figure 2-25 on page 96), it is likely that IT4D (**65**) has a configuration of the six-membered ring identical with those of the other three isolated iridal-type triterpenes. The only uncertain absolute configuration is that concerning the tetrahydrofuran ring. The strong correlation signal between H-14 and H-18 suggests that the hydrogen bond of H-14 and the carbon bond between C-17 and C-18 must be on the same side of the plane in which the tetrahydrofuran ring mostly resides. At the same time, the bond of the hydroxyl group on C-16 should be on the opposite side of the plane against the carbon bond of 17-18, because correlations between H-16 and H-18, and between H-16 and H-19 were also observed. Thus, there are two possible absolute configurations of the tetrahydrofuran ring (shown as structures **91** and **92**). However, if the most likely biosynthetic route of IT4D (**65**) (see Figure 2-18 on page 86) is considered, then the configuration of C-14 is most likely to be *R*, like that of C-14 in isoiridogermanal (**57**). As a result, the stereochemistry of IT4D (**65**) is most likely to be as in **91**, its 3D structure shown as Figure 5-3.

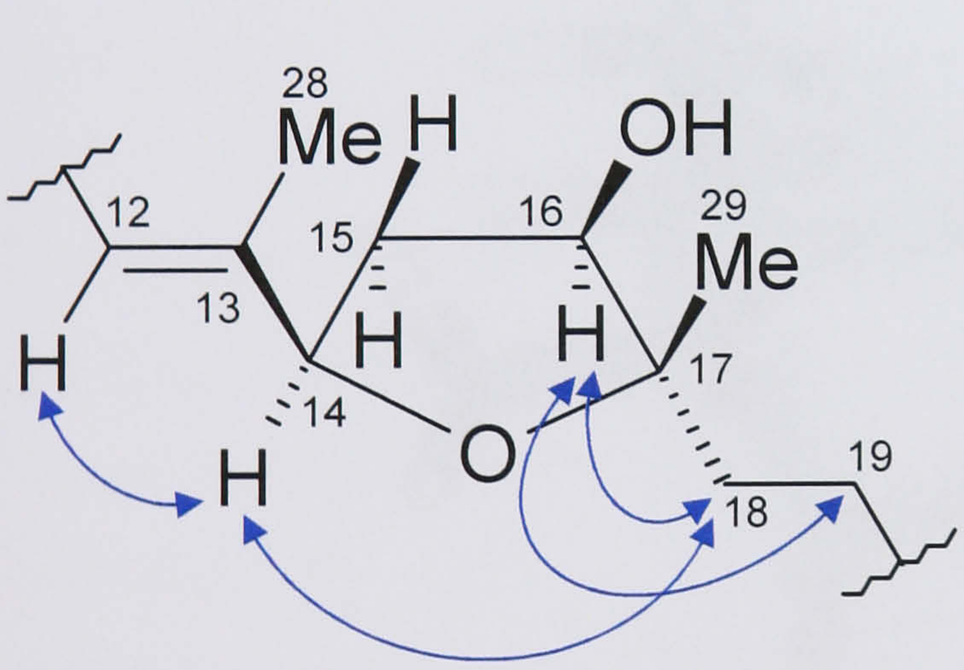

(14*R*, 16*R*, 17*S*) **91**

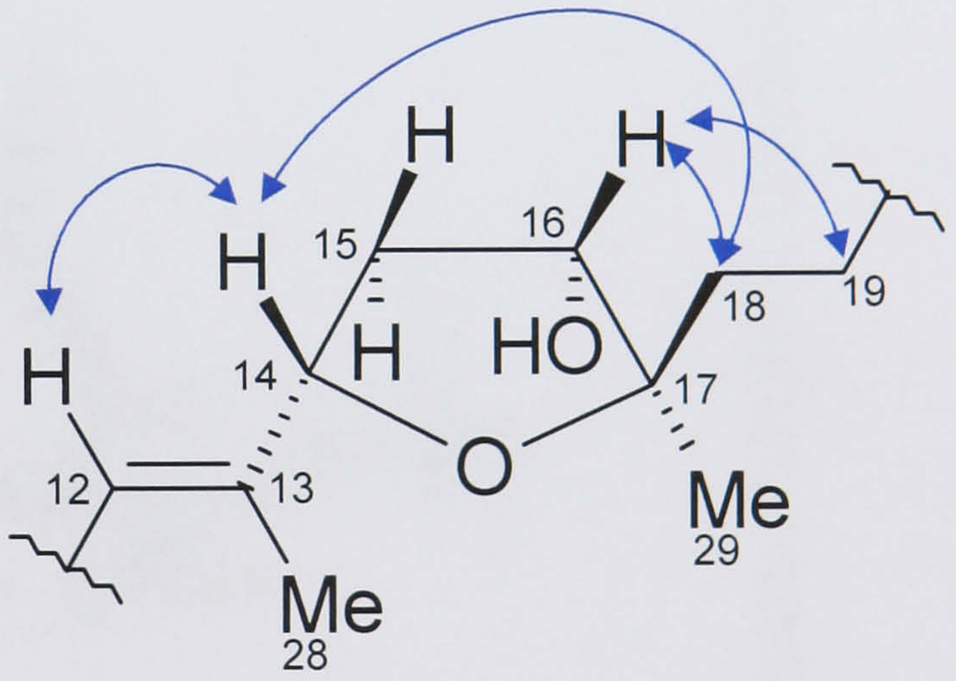

(14*S*, 16*S*, 17*R*) **92**

* The key NOESY ^{1}H-^{1}H correlation signal is indicated as blue arrows. Some hydrogens atoms omitted for clarity.

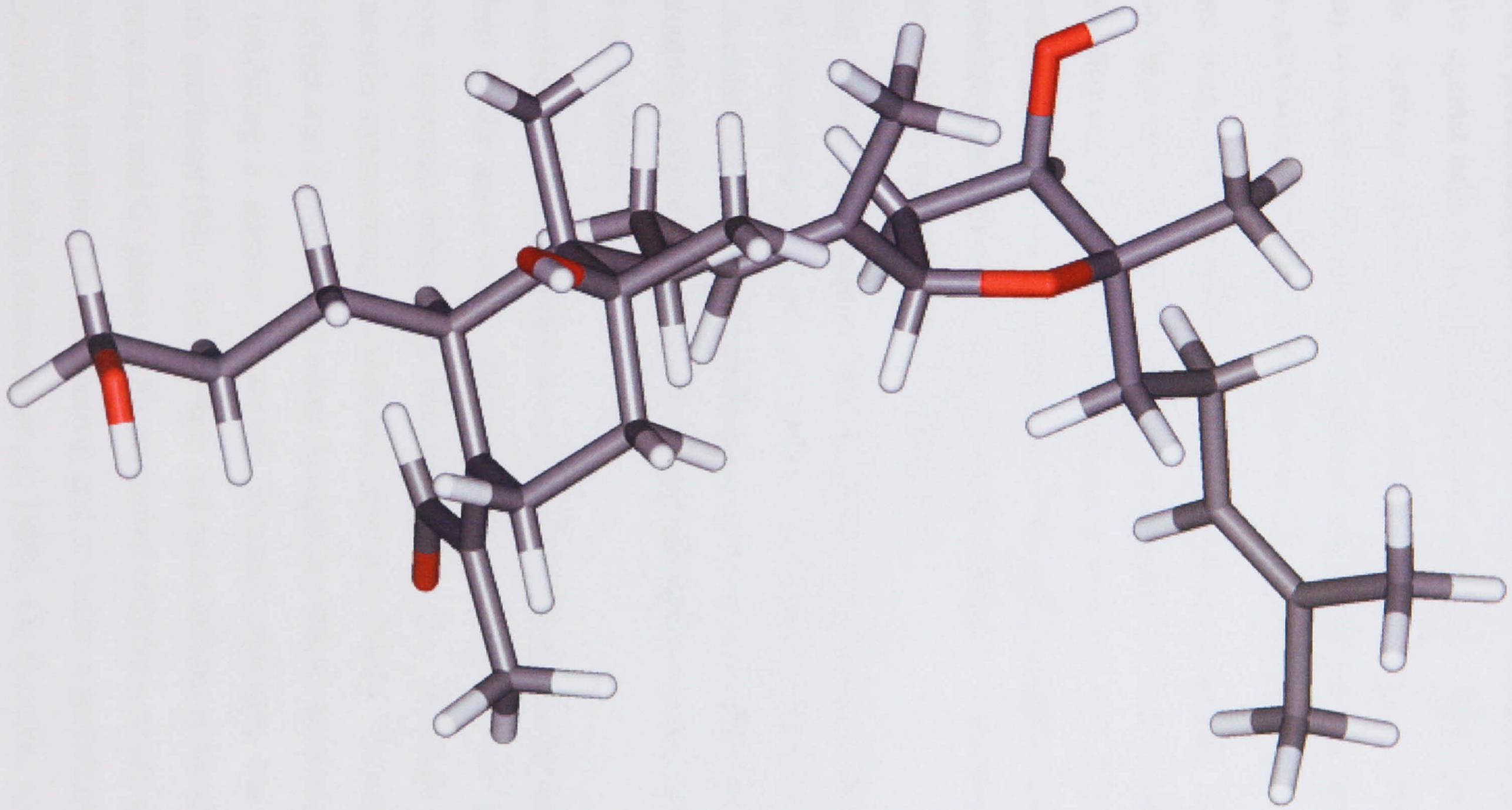

Figure 5-3: Stereostructure of IT4D (**65**) with the absolute configuration of tetrahydrofuran ring as **91**

5.6 Cell cycle specific cytotoxicity in cancer treatment

It is generally true that anticancer drugs are more effective against proliferating cells than against non-proliferating cells (Brown, 1999), because some anticancer drugs are most effective against cells in one phase of the cell cycle. Practically, they can be classified as S-phase specific (e.g., cytosine arabinoside, hydroxyurea and methotrexate), M-phase specific (e.g., vincristine and vinblastine), or cycle phase non-specific (e.g., alkylating drugs and antitumour antibiotics) (Pratt, 1994).

In the present study, the two isolated flavonoids (tectorigenin [**24**] and 7-*O*-methyl aromadendrin [**66**]) showed S and G_2/M phases specific cytotoxicity, and 7-*O*-methyl aromadendrin (**66**) was able to induce apoptosis in the COR-L23 (human non-small cell lung cancer) cell line. At the same time, IT4D (**65**) exhibited cycle phase non-specific cytotoxicity and induction of apoptosis in COR-L23. It is therefore cytotoxic for cells at any point in the cell cycle (see Table 3-5).

It is becoming increasingly apparent that apoptosis is a process intimately linked to the cell cycle (Meikrantz and Schlegel, 1995). Nevertheless, the cell cycle plays a critical role in chemosensitivity for combination chemotherapy (Mueller *et al.*, 2006). This is particularly critical for newly developed chemotherapeutic agents that have targeted cell cycle effects.

However, combination chemotherapy is not be as simple as two or more anticancer agents applied at the same time. Because cells undergo growth arrest may be protected from apoptosis induced by one agent, they may therefore be ultimately resistant to another cytotoxic agent (Shah and Schwartz, 2001). This type of adverse antagonistic effect was demonstrated when flavopiridol (**93**) (a synthetic flavone with activity of inhibiting a number of protein kinases) exposure was followed by treatment with paclitaxel (**94**). The multiple cell cycle effects of flavopiridol caused cell cycle arrest in G_1 and G_2 phases. This prevented cells from entering M-phase, the phase during which paclitaxel is most active; and so led to a significant *reduction* in paclitaxel sensitivity in culture (Motwani *et al.*, 1999). On the other hand, cell cycle-mediated drug resistance can be overcome by appropriate sequence of the drug combination. As a result, the reverse sequence of paclitaxel (**94**) followed by flavopiridol (**93**) is associated with an *increased* induction of apoptosis (Bible and

Kaufmann, 1997). Therefore, the sequence of the multi-drug chemotherapy is critical for the exploration of the synergistic effects of cell cycle-specific cytotoxic agents.

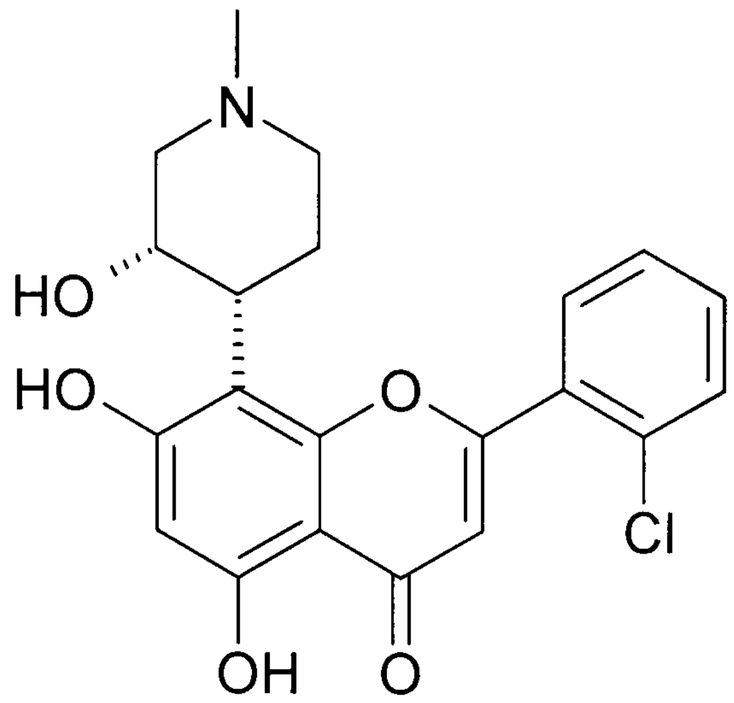

93

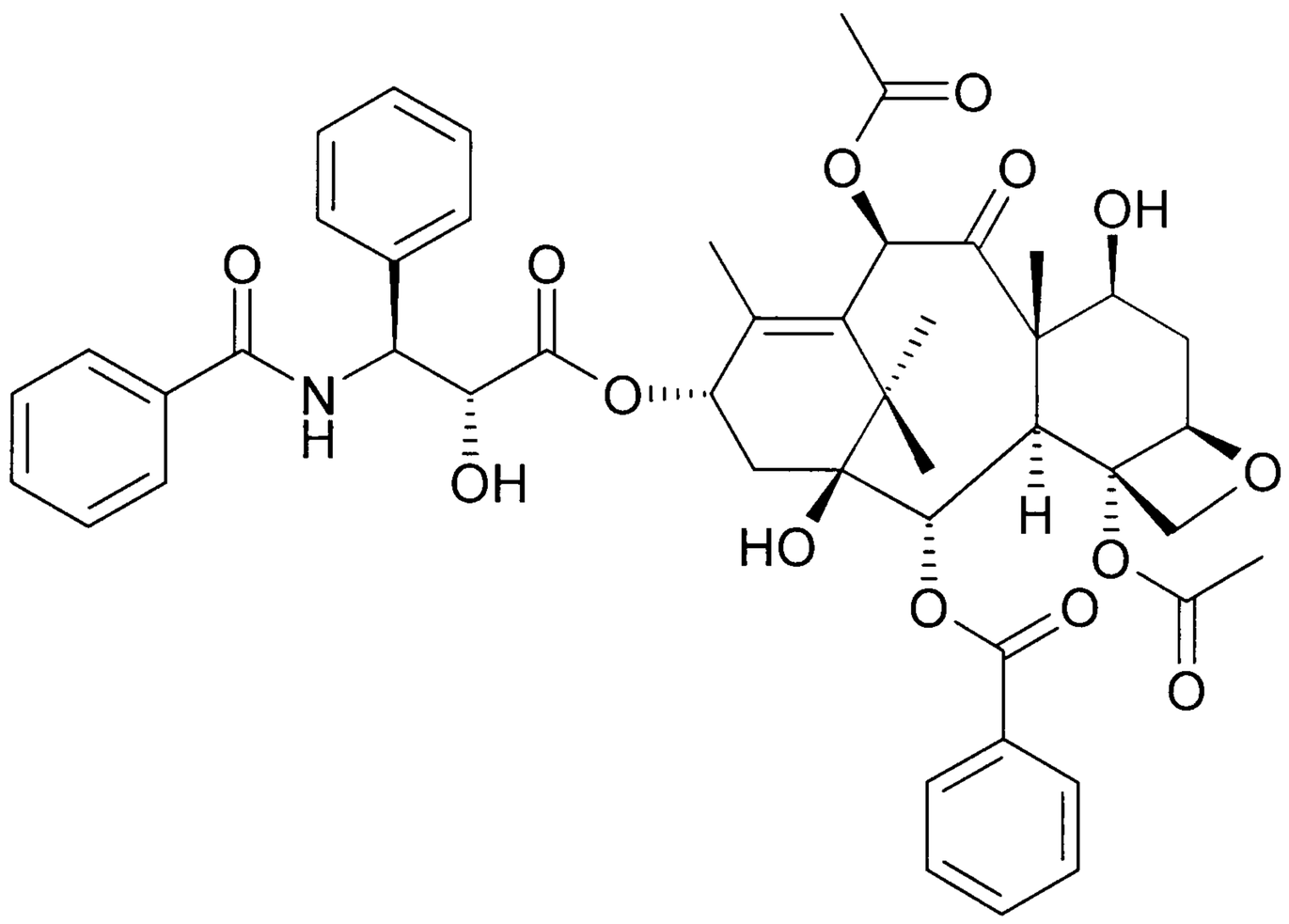

94

5.7 Possible contributions of *Iris tectorum* in anticancer treatment

Tectorigenin (**24**) should contribute to the gross activity of *Iris tectorum* when it is used as Traditional Chinese Medicine, because it is a principal compound in its rhizome. *Iris tectorum* was reported to give the highest yield rate of tectorigenin (**24**)

in an analysis of isoflavone content in rhizomatous medicinal plants belonging to Iridaceae. Those plants included *Belamcanda chinensis*, *Iris tectorum*, *I. dichotoma*, *I. japonica*, *I. germanica*, *I. confusa*, *I. blodow*, *I. lactea* var. *chinensis*, *I. ensata*, *I. sibirica*, *I. sanguinea*, *I. uniflora*, *I. leptophylla*, *I. speculatrix*, *I. versicolor* and *I. pseudocarus*. The proportion of tectorigenin (**24**) is 1.5% (w/w) in *Iris tectorum*, but no more than 0.22% in the other 15 species of Iridaceae (Qin *et al.*, 1996).

Beside its antioxidant activity (Jung *et al.*, 2004), tectorigenin (**24**) in the present study showed moderate cytotoxicity with IG_{50} of 105μM to 235μM against various cancer cell lines, and arrested cell progress at S and G_2/M phases. It has also been reported that tectorigenin (**24**) inhibited angiogenesis *in vitro* and *in vivo*. In addition, subcutaneously administered tectorigenin (**24**) at a dose of 30mg/kg for 20 days to mice implanted with murine Lewis lung carcinoma, caused a significant reduction by 30.8% of tumour volume (Jung *et al.*, 2003). At the same time, tectorigenin (**24**) exhibited a much stronger antiproliferative activity than its glycoside (tectoridin [**25**]).

As an isoflavone, tectorigenin (**24**) significantly rectified the aberrant expression of several essential gene products involved in prostate cancer (Lee *et al.*, 2001). It was reported to down-regulate prostate-derived Ets transcription factor (PDEF), prostate-specific antigen (PSA) and insulin-like growth factor-1 (IGF-1) receptor mRNA expression *in vitro* (Thelen *et al.*, 2005). It also induced differentiation and apoptosis in human promyelocytic leukaemia HL-60 cells *in vitro* (Lee *et al.*, 2001).

7-*O*-Methyl aromadendrin (**66**) has been isolated from several plants, including *Populus alba*, *Artemisia dracunculus*, *Eucalyptus maculate* and *Eupatorium* species, since 1970 (Stoessl *et al.*, 1971; Herz *et al.*, 1972; Balza and Towers, 1984; Abdel-Sattar *et al.*, 2000). However, no bioactivity has been reported. The present work is the first report of its isolation from a member of the Iridaceae and its subsequent cytotoxicity evaluation. Compared with tectorigenin (**24**), 7-*O*-methyl aromadendrin (**66**) showed much higher cytotoxicity with a range of IG_{50} from 21μM to 40μM against various cancer cell lines. In addition, it induced apoptosis in COR-L23 cell line and interrupted cell proliferation at S and G_2/M phases.

Those isolated iridal-type triterpenes exhibited high cytotoxicity against cancer cells. Since they have been isolated as major components from the cytotoxic fine fraction of *Iris tectorum*, they are supposed to be the principal cytotoxic compounds in this plant

and should contribute significantly to the cytotoxicity of this TCM. However, due to the limited amount of pure samples, only IT4D (**65**) could be tested and show the induction of apoptosis in COR-L23 cells.

In recent years, anticancer research is aimed at the development of new-targeted agents, which will likely be used in combination with established cytotoxic drugs (Broxterman and Georgopapadakou, 2005). An example of this is the application of the humanised anti-VEGF (vascular endothelial growth factor) monoclonal antibody Bevacizumab (Avastin®; Genentech, USA) used in combination with cytotoxic chemotherapy for colon cancer (Marshall, 2005).

The rationale for combination chemotherapy has focused on attacking different biochemical targets, overcoming drug resistance in heterogeneous tumours, and taking advantage of tumour growth kinetics with increasing the dose-density of combination chemotherapy. The aim is to improve clinical efficacy at the same time maintaining acceptable clinical toxicity (Shah and Schwartz, 2001).

By combination with standard chemotherapeutic drugs, novel cytotoxic compounds with a novel mechanism of action and low toxicity may give some valuable synergistic activity (Lenz, 2003). The possible synergistic effects of multi-drug chemotherapy in appropriate sequence may result in the improvement of treatment against multi-drug resistant cancer and enhancement of cytotoxicity against cancer cells with lower toxicity towards the host tissue. For instance, rapamycin (**95**) produced additive cytotoxicity with 5-fluorouracil and cyclophosphamide in a colon tumour model, and the integrated activity was such that it significantly inhibited tumour growth at any stage of development (Eng *et al.*, 1984). Further research also revealed that rapamycin (**95**) exhibited additive cytotoxicity against brain cancer cell lines when combined with cisplatin (a platinate agent) or camptothecin (**96**) (topoisomerase I inhibitor) (Geoerger *et al.*, 2001). These results indicated that the additive cytotoxicity found in combination therapy has great potential in the treatment of human cancer.

There was poor selective cytotoxicity when those isolated compounds (from the active fraction of *Iris tectorum*) were tested against both lung cancer cells (COR-L23) and lung normal cells (MRC-5). Actually most tested compounds exhibited higher cytotoxicity against lung normal cells rather than lung cancer cells (see Figure 3-1 and

Figure 3-2 on page 109). However, two most active fractions (IT3 and IT4) showed significantly higher cytotoxicity against lung cancer cells than that against normal lung cells in the earlier stage of bioassay-guided isolation (see Table 2-5 on page 67). The selective cytotoxicity against lung cancer cells is likely based on the preferable combination of some active compounds in those fractions. As to TCM used to treat cancer, the integrated activity of *Iris tectorum* ought to be attributed to those isolated and still unisolated bioactive compounds. Thus TCM is suggested to be a kind of multi-drug treatment with multi-target therapeutic activity. Even those isolated compounds in present study could be tested in a combination with standard chemotherapeutic agents for investigation of synergistic activity in future work.

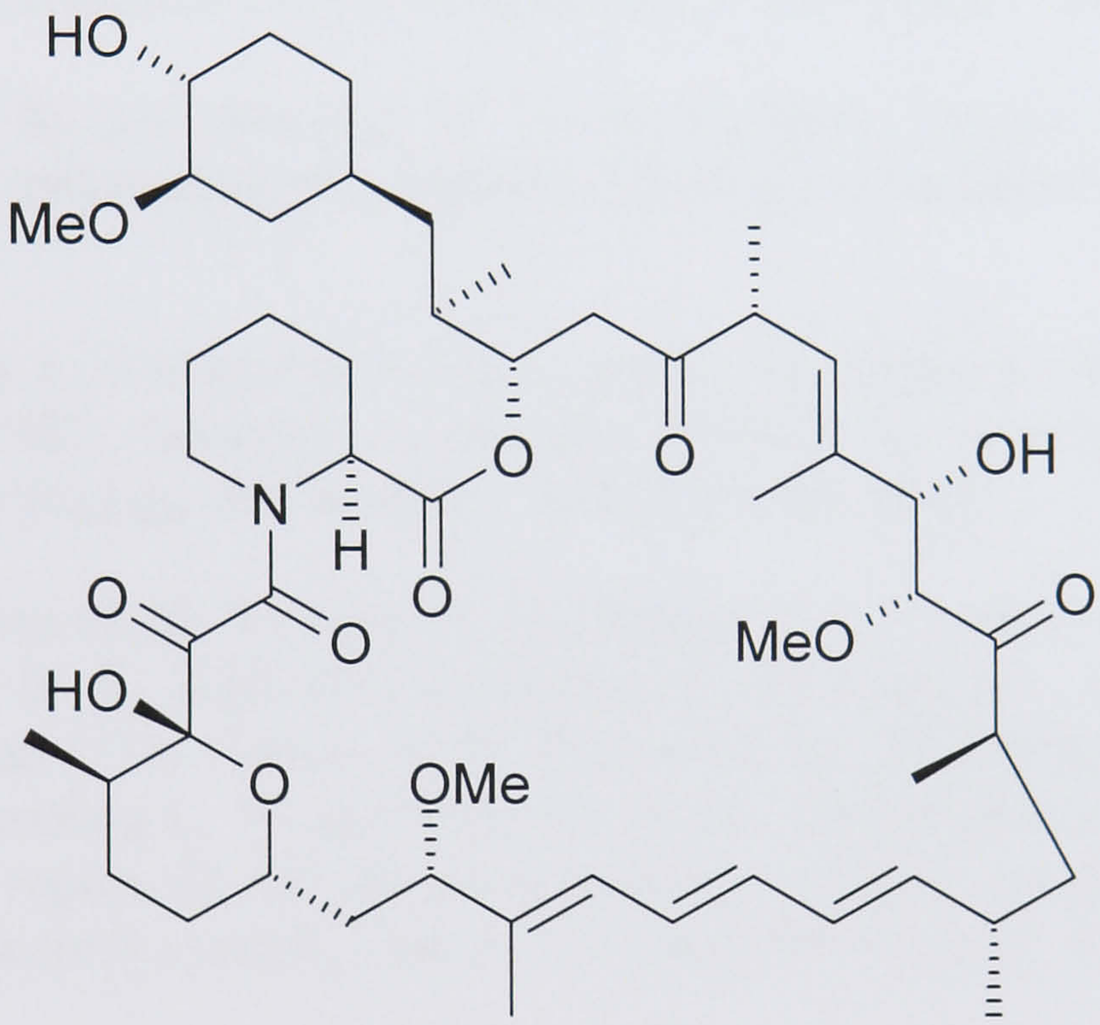

95

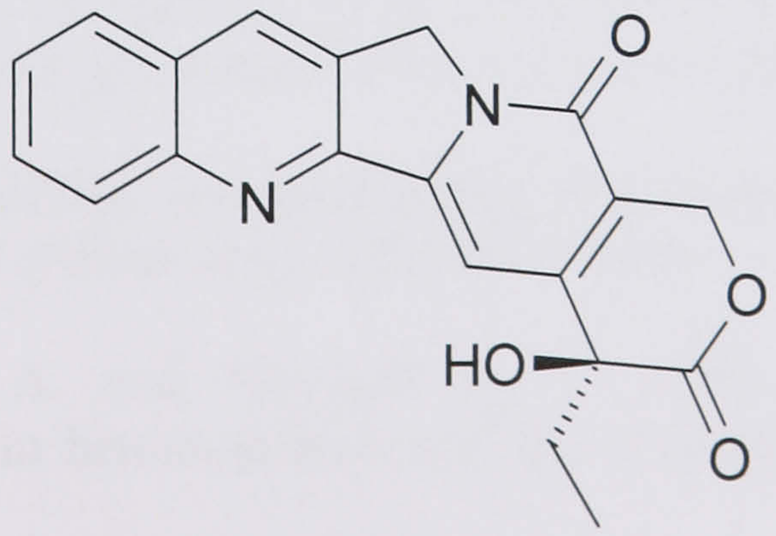

96

REFERENCES

Abdel-Sattar E., Kohiel M. A., Shihata I. A. and El-Askary H.. 2000. Phenolic compounds from *Eucalyptus maculata*, *Pharmazie*, **55**(8):623-624.

Abe F., Chen R. F. and Yamauchi T., 1991, Iridals from *Belamcanda chinensis* and *Iris japonica*, *Phytochemistry*, **30**(10):3379-3382.

Adlercreutz C. H. T., Goldin B. R., Gorbach S. L., Hockerstedt K. A. V., Watanabe S., Hamalainen E. K., Markkanen M. H., Makela T. H., Wahala K. T., Hase T. A. and Fotsis T., 1995, Soybean Phytoestrogen Intake and Cancer Risk, *The Journal of Nutrition*, **125**(3):S757-S770.

Afanasev V. N., Korol B. A., Mantsygin Y. A., Nelipovich P. A., Pechatnikov V. A. and Umansky S. R., 1986, Flow cytometry and biochemical analysis of DNA degradation characteristic of 2 types of cell death, *FEBS Letters*, **194**(2):347-350.

Akao T., Kobashi K. and Aburada M., 1994, Enzymic studies on the animal and intestinal bacterial metabolism of geniposide, *Biological and Pharmaceutical Bulletin*, **17**(12):1573-1576.

Akiyama T., Ishida J., Nakagawa S., Ogawara H., Watanabe S., Itoh N., Shibuya M. and Fukami Y., 1987, Genistein, a specific inhibitor of tyrosine-specific protein-kinases, *Journal of Biological Chemistry*, **262**(12):5592-5595.

Alberts D. S., Colvin G. M., Conney A. H., Ernster V. L., Garber J. E., Greenwald P., Gudas L. J., Hong W. K., Kelloff G. J., Kramer R. A., Lerman C. E., Mangelsdorf D. J., Matter A., Minna J. D., Nelson W. G., Pezzuto J. M., Prendergast F., Rusch V. W., Sporn M. B., Wattenberg L. W. and Weinstein I. B., 1999, Prevention of cancer in the next millennium: report of the chemoprevention working group to the American Association for Cancer Research, *Cancer Research*, **59**(19):4743-4758.

Alhasan S. A., Pietrasczkiwicz H., Alonso M. D., Ensley J. and Sarkar F. H., 1999, Genistein-induced cell cycle arrest and apoptosis in a head and neck squamous cell carcinoma cell line, *Nutrition and Cancer*, **34**(1):12-19.

Ali A. A., El-Emary N. A., El-Moghazi M. A., Darwish F. M. and Frahm A. W., 1983, Three isoflavonoids from *Iris germanica*, *Phytochemistry*, **22**(9):2061-2063.

Alison M. R., 1999, Identifying and quantifying apoptosis: a growth industry in the face of death, *The Journal of Pathology*, **188**(2):117-118.

Allen P. D., Bustin S. A. and Newland A. C., 1993, The role of apoptosis (programmed cell death) in hematopoiesis and the immune system, *Blood Reviews*, **7**(1):63-73.

Amico V., Neri P., Oriente G. and Piattelli M., 1989, Tetraprenyltoluquinol derivatives from the brown alga *Cystoseira zosteroides*, *Phytochemistry*, **28**(1):215-219.

Anonymous, 2002, WHO Traditional Medicine Strategy 2002-2005, World Health

Organization, Geneva, pp 1.

Anonymous, 2005. Pharmacopoeia of the People's Republic of China, Chemical Industry Press, Beijing, pp 28-29.

Anonymous, 2006, Cancer Facts and Figures 2006, American Cancer Society. Atlanta. pp 1-2.

Anonymous, 2006a, Incidence-UK, in: *CancerStats*, Cancer Research UK. London. pp 1-2.

Anonymous, 2006b, UK cancer mortality statistics for common cancers. Cancer Research UK, London, at http://info.cancerresearchuk.org:8000/cancerstats /mortality/ cancerdeaths/, accessed on 10/07/2006

Anonymous, 2006c, Drugs, Supplements and Herbal Information, U.S. National Library of Medicine, at http://www.nlm.nih.gov/medlineplus/druginformation.html, access on 16/02/2006

Aoyama M., MacIsaac D., Bukowski R. M. and Ganapathi M. K., 1998. Interleukin-6 differentially potentiates the antitumour effects of taxol and vinblastine in U266 human myeloma cells, *Clinical Cancer Research*, **4**(4):1039-1045.

Ashida H., 2000, Suppressive effects of flavonoids on dioxin toxicity. *Biofactors*. **12**(1-4):201-206.

Bae E. A., Han M. J., Lee K. T., Choi J. W., Park H. J. and Kim D. H., 1999. Metabolism of 6''-*O*-xylosyltectoridin and tectoridin by human intestinal bacteria and their hypoglycemic and *in-vitro* cytotoxic activities, *Biological and Pharmaceutical Bulletin*, **22**(12):1314-1318.

Bagli E., Stefaniotou M., Morbidelli L., Ziche M., Psillas K., Murphy C. and Fotsis T., 2004, Luteolin inhibits vascular endothelial growth factor-induced angiogenesis. inhibition of endothelial cell survival and proliferation by targeting phosphatidylinositol 3'-kinase activity, *Cancer Research*, **64**(21):7936-7946.

Balza F. and Towers G. H. N., 1984, Dihydroflavonols of *Artemisia dracunculus*. *Phytochemistry*, **23**(10):2333-2337.

Baxa D. M., Luo X. X. and Yoshimura F. K., 2005, Genistein induces apoptosis in T lymphoma cells *via* mitochondrial damage, *Nutrition and Cancer*. **51**(1):93-101.

Beck W. T., Mo Y. Y. and Bhat U. G., 2001, Cytotoxic signalling by inhibitors of DNA topoisomerase II, *Biochemical Society Transactions*. **29**(6):702-703.

Bible K. C. and Kaufmann S. H., 1997. Cytotoxic synergy between flavopiridol (NSC 649890, L86-8275) and various antineoplastic agents: the importance of sequence of administration. *Cancer Research*. **57**(16):3375-3380.

Birt D. F., Hendrich S. and Wang W., 2001. Dietary agents in cancer prevention: flavonoids and isoflavonoids. *Pharmacology and Therapeutics*. **90**(2-3):157-177.

Blair S. L., Heerdt P., Sachar S., Abolhoda A., Hochwald S., Cheng H. and Burt M., 1997, Glutathione metabolism in patients with non-small cell lung cancers, *Cancer Research*, **57**(1):152-155.

Bonfils J. P., Sauvaire Y., Baissac Y. and Marner F. J., 1994, Iridal levels in *Iris* rhizomes - effects of wounding and dehydration, *Phytochemistry*, **37**(3):701-705.

Bonfils J. P. and Sauvaire Y., 1996, Localization of iridals in *Iris germanica* rhizomes, *Phytochemistry*, **41**(5):1281-1285

Brown J. M., 1999, The hypoxic cell: a target for selective cancer therapy - eighteenth Bruce F. Cain Memorial Award lecture, *Cancer Research*, **59**(23):5863-5870.

Brownson D. M., Azios N. G., Fuqua B. K., Dharmawardhane S. F. and Mabry T. J., 2002, Flavonoid effects relevant to cancer, *The Journal of Nutrition*, **132**(11):3482-3489.

Broxterman H. J. and Georgopapadakou N. H., 2005, Anticancer therapeutics: "addictive" targets, multi-targeted drugs, new drug combinations, *Drug Resistance Updates*, **8**(4):183-197.

Buja L. M., Eigenbrodt M. L. and Eigenbrodt E. H., 1993, Apoptosis and necrosis: basic types and mechanisms of cell death, *Archives of Pathology and Laboratory Medicine*, **117**(12):1208-1214.

Cai Y. Z., Mei S., Jie X., Luo Q. and Corke H., 2006, Structure-radical scavenging activity relationships of phenolic compounds from traditional Chinese medicinal plants, *Life Sciences*, **78**(25):2872-2888.

Cai Y., Luo Q., Sun M. and Corke H., 2004, Antioxidant activity and phenolic compounds of 112 traditional Chinese medicinal plants associated with anticancer, *Life Sciences*, **74**(17):2157-2184.

Catapano A. L., 1997, Antioxidant effect of flavonoids, *Angiology*, **48**(1):39-44.

Chang W. C. and Hsu F. L., 1992, Inhibition of Platelet Activation and Endothelial-Cell Injury by Polyphenolic Compounds Isolated from *Lonicera japonica* Thunb., *Prostaglandins Leukotrienes and Essential Fatty Acids*, **45**(4):307-312.

Chen G. C., Yang W. M., Li Y. F., Sun J. X. and Wang H. N., 1988, Study of Yun-nan SLS-Bi Hu injection, *China Journal of Chinese Materia Medica*, **13**(1):35.

Chen M. and Huang J. H., 2001, Present status of study on Traditional Chinese Medicine Gekko, *World Science and Technology Modernization of Traditional Chinese Medicine*, **3**(4):53-56.

Chowdhury A. R., Sharma S., Mandal S., Goswami A., Mukhopadhyay S. and Majumder H. K., 2002, Luteolin, an emerging anticancer flavonoid, poisons eukaryotic DNA topoisomerase I, *The Biochemical Journal*, **366**(2):653-661.

Connors T. A., 1995, The choice of prodrugs for gene directed enzyme prodrug therapy of cancer, *Gene Therapy*, **2**(10):702-709.

Constantinou A., Kiguchi K. and Huberman E., 1990, Induction of differentiation and DNA strand breakage in human HL-60 and K-562 leukemia cells by genistein. *Cancer Research*, **50**(9):2618-2624.

Cragg G. M. and Newman D. J., 2005, Plants as a source of anticancer agents. *Journal of Ethnopharmacology*, **100**(1-2):72-79.

Curran M. P. and Plosker G. L., 2002, Vinorelbine - A review of its use in elderly patients with advanced non-small cell lung cancer, *Drugs and Aging*, **19**(9):695-721.

da Rocha A. B., Lopes R. M. and Schwartsmann G., 2001, Natural products in anticancer therapy, *Current Opinion in Pharmacology*, **1**(4):364-369.

Daniels L. B., Coyle P. J., Chiao Y. B., Glew R. H. and Labow R. S., 1981, Purification and characterization of a cytosolic broad specificity beta-glucosidase from human liver, *The Journal of Biological Chemistry*, **256**(24):3004-3013.

Darzynkiewicz Z., Bruno S., Delbino G., Gorczyca W., Hotz M. A., Lassota P. and Traganos F., 1992, Features of apoptotic cells measured by flow cytometry. *Cytometry*, **13**(8):795-808.

Darzynkiewicz Z., Robinson J. P. and Crissman H. A., 1994, Flow cytometry, in: *Methods in Cell Biology* (Wilson L. and Matsudaira P., eds.), Academic Press, San Diego, pp 16-18.

Darzynkiewicz Z., Juan G., Li X., Gorczyca W., Murakami T. and Traganos F., 1997, Cytometry in cell necrobiology: Analysis of apoptosis and accidental cell death (necrosis), *Cytometry*, **27**(1):1-20.

De M., De A. K., Sen P. and Banerjee A. B., 2002, Antimicrobial properties of star anise (*Illicium verum* Hook. *f*), *Phytotherapy Research*, **16**(1):94-95.

Denis L., Morton M. S. and Griffiths K., 1999, Diet and its preventive role in prostatic disease, *European Urology*, **35**(5-6):377-387.

DeVita V. T., Hellman S. and Rosenberg S. A., 2005, Cancer: principles and practice of oncology, Lippincott Williams and Wilkins, London, pp 267.

Ding H., Duan W., Zhu W., Ju R., Subler M., Otterson G. and Villalona-Calero M., 2001, Mechanisms of regulation of Chk2 expression after exposure to the topoisomerase II inhibitor genistein, *Clinical Cancer Research*, **7**(11):3791-3791.

Dugo P., Presti M. L., Ohman M., Fazio A., Dugo G. and Mondello L., 2005, Determination of flavonoids in citrus juices by micro-HPLC-ESI/MS, *Journal of Separation Science*, **28**(11):1149-1156.

Effers K., Scholz B., Nickel C., Hanisch B. and Marner F. J., 1999, Structure determination of tigridial, an iridopentaene from *Tigridia pavonia* (Iridaceae). *European Journal of Organic Chemistry*, (11):2793-2797.

Efferth T., Benakis A., Romero M. R., Tomicic M., Rauh R., Steinbach D., Hafer R., Stamminger T., Oesch F., Kaina B. and Marschall M., 2004, Enhancement of

cytotoxicity of artemisinins toward cancer cells by ferrous iron, *Free Radical Biology and Medicine*, **37**(7):998-1009.

Endresen P. C., Prytz P. S. and Aarbakke J., 1995, A New Flow Cytometric Method for Discrimination of Apoptotic Cells and Detection of Their Cell-Cycle Specificity through Staining of F-Actin and DNA, *Cytometry*, **20**(2):162-171.

Eng C. P., Sehgal S. N. and Vezina C., 1984, Activity of rapamycin (AY-22,989) against transplanted tumours, *The Journal of Antibiotics*, **37**(10):1231-1237.

Fan W. Z., Tezuka Y., Ni K. M. and Kadota S., 2001, Prolyl endopeptidase inhibitors from the underground part of *Rhodiola sachalinensis*, *Chemical and Pharmaceutical Bulletin*, **49**(4):396-401.

Fox B. W., 1991, Medicinal plants in tropical medicine.2. Natural products in cancer treatment from bench to the clinic, *Transactions of the Royal Society of Tropical Medicine and Hygiene*, **85**(1):22-25.

Freshney R. I., 2000, Culture of animal cells - a manual of basic techniques, John Wiley and Sons, New York, pp 332-340.

Fricker S. P., 1994, The application of sulforhodamine B as a colorimetric endpoint in a cytotoxicity assay, *Toxicology in vitro*, **8**(4):821-822.

Garrett M. D. and Workman P., 1999, Discovering novel chemotherapeutic drugs for the third millennium, *European Journal of Cancer*, **35**(14):2010-2030.

Gebhardt R., 2002, Inhibition of cholesterol biosynthesis in HepG2 cells by artichoke extracts is reinforced by glucosidase pretreatment, *Phytotherapy Research*, **16**(4):368-372.

Geoerger B., Kerr K., Tang C. B., Fung K. M., Powell B., Sutton L. N., Phillips P. C. and Janss A. J., 2001, Antitumour activity of the rapamycin analog CCI-779 in human primitive neuroectodermal tumour/medulloblastoma models as single agent and in combination chemotherapy, *Cancer Research*, **61**(4):1527-1532.

Gibbons S. and Gray A. I., 1998, Isolation by Planar Chromatography, in: *Natural products isolation* (Cannell R. J. P. ed.), Humana, Totowa, pp 222.

Goodman L. S., Wintrobe M. M., Dameshek W., Goodman M. J. and Gilman A., 1946, Nitrogen mustard therapy - use of methyl-bis(beta-chloroethyl)amine hydrochloride and tris(beta-chloroethyl)amine hydrochloride for Hodgkins disease, lymphosarcoma, leukemia and certain allied and miscellaneous disorders, *Journal of the American Medical Association*, **132**(3):126-132.

Graham J. G., Quinn M. L., Fabricant D. S. and Farnsworth N. R., 2000, Plants used against cancer - an extension of the work of Jonathan Hartwell, *Journal of Ethnopharmacology*, **73**(3):347-377.

Hanawa F., Tahara S. and Mizutani J., 1991, Flavonoids produced by *Iris pseudacorus* leaves treated with cupric chloride, *Phytochemistry*, **30**(7):2197-2198.

Hanawa F., Tahara S. and Mizutani J., 1991a, Isoflavonoids produced by *Iris pseudacorus* leaves treated with cupric chloride, *Phytochemistry*, **30**(1):157-163.

Harris G. K., Qian Y., Leonard S. S., Sbarra D. C. and Shi X., 2006. Luteolin and chrysin differentially inhibit cyclooxygenase-2 expression and scavenge reactive oxygen species but similarly inhibit prostaglandin-E_2 formation in RAW 264.7 cells. *The Journal of Nutrition*, **136**(6):1517-1521.

Hawksworth G., Drasar B. S. and Hill M. J., 1971, Intestinal bacteria and the hydrolysis of glycosidic bonds, *Journal of Medical Microbiology*, **4**(4):451-459.

Herz W., Gibaja S., Bhat S. V. and Srinivasan A., 1972, Dihydroflavonols and other flavonoids of *Eupatorium* species, *Phytochemistry*, **11**(9):2859-2863.

Holland J. F., Robert C. Bast J., Morton D. L., III E. F., Kufe D. W. and Weicheslbaum R. R., 1993, Cancer medicine, Lippincott Williams and Wilkins, Philadelphia, pp 651.

Horie T., Shibata K., Yamashita K., Fujii K., Tsukayama M. and Ohtsuru Y., 1998. Studies of the selective *O*-alkylation and dealkylation of flavonoids. XXIV. A convenient method for synthesizing 6- and 8-methoxylated 5,7-dihydroxyisoflavones. *Chemical and Pharmaceutical Bulletin*, **46**(2):222-230.

Horinaka M., Yoshida T., Shiraishi T., Nakata S., Wakada M., Nakanishi R., Nishino H., Matsui H. and Sakai T., 2005, Luteolin induces apoptosis via death receptor 5 upregulation in human malignant tumour cells, *Oncogene*, **24**(48):7180-7189.

Hotz M. A., Traganos F. and Darzynkiewicz Z., 1992, Changes in nuclear chromatin related to apoptosis or necrosis induced by the DNA topoisomerase-II inhibitor fostriecin in Molt-4 and HL-60 cells are revealed by altered DNA sensitivity to denaturation, *Experimental Cell Research*, **201**(1):184-191.

Hyatt J. L., Tsurkan L., Morton C. L., Yoon K. J. P., Harel M., Brumshtein B., Silman I., Sussman J. L., Wadkins R. M. and Potter P. M., 2005, Inhibition of acetylcholinesterase by the anticancer prodrug CPT-11, *Chemico-Biological Interactions*, **157-158**:247-252.

Ingham J. L., Tahara S. and Dziedzic S. Z., 1986, New 3-hydroxyflavanone (dihydroflavonol) phytoalexins from the Papilionate legume *Shuteria vestita*, *Journal of Natural Products*, **49**(4):631-638.

Ito H., Onoue S., Miyake Y. and Yoshida T., 1999, Iridal-type triterpenoids with ichthyotoxic activity from *Belamcanda chinensis*, *Journal of Natural Products*, **62**(1):89-93.

Ji Y. B., He, S.W., Ma, Y.L., Li, J., Yang, C. and Liu, L.L., 1999. Pharmacological action and application of anticancer traditional Chinese medicines. Heilongjiang Science and Technology Publishing House, Ha'erbin, pp 830 and 965.

Jia W., Liu P., Jiang J., Chen M. J., Zhao L. P., Zhou M. M., Yang L. P., Wang M. Q., Qiu M. F. and Zhang Y. Y., 2006. Application of metabonomics in complicated theory system research of traditional Chinese medicine. *Zhongguo Zhong Yao Za Zhi*.

31(8):621-624.

Jordan M. A., 2002, Mechanism of action of antitumor drugs that interact with microtubules and tubulin, *Current Medicinal Chemistry Anticancer Agents*, **2**(1):1-17.

Jung S. H., Lee Y. S., Lee S., Lim S. S., Kim Y. S., Ohuchi K. and Shin K. H., 2003, Antiangiogenic and antitumour activities of isoflavonoids from the rhizomes of *Belamcanda chinensis*, *Planta Medica*, **69**(7):617-622.

Jung S. H., Lee Y. S., Lim S. S., Lee S., Shin K. H. and Kim Y. S., 2004, Antioxidant activities of isoflavones from the rhizomes of *Belamcanda chinensis* on carbon tetrachloride-induced hepatic injury in rats, *Archives of Pharmacal Research*, **27**(2):184-188.

Kang K. A., Lee K. H., Chae S., Zhang R., Jung M. S., Kim S. Y., Kim H. S., Kim D. H. and Hyun J. W., 2005, Cytoprotective effect of tectorigenin, a metabolite formed by transformation of tectoridin by intestinal microflora, on oxidative stress induced by hydrogen peroxide, *European Journal of Pharmacology*, **519**(1-2):16-23.

Kaufmann S. H., 1989, Induction of endonucleolytic DNA cleavage in human acute myelogenous leukemia cells by etoposide, camptothecin, and other cytotoxic anticancer drugs: a cautionary note, *Cancer Research*, **49**(21):5870-5878.

Kavanagh K. T., Hafer L. J., Kim D. W., Mann K. K., Sherr D. H., Rogers A. E. and Sonenshein G. E., 2001, Green tea extracts decrease carcinogen-induced mammary tumour burden in rats and rate of breast cancer cell proliferation in culture, *Journal of Cellular Biochemistry*, **82**(3):387-398.

Keawpradub N., Eno-Amooquaye E., Burke P. J. and Houghton P. J., 1999, Cytotoxic activity of indole alkaloids from *Alstonia macrophylla*, *Planta Medica*, **65**(4):311-315.

Kerr J. F. R. and Harmon B.V., 1991, Definition and incidence of apoptosis: an historical perspective, in: *Apoptosis: the molecular basis of cell death* (Tomei L. D. and Cope F. O., eds.), Cold Spring Harbor Laboratory, New York, pp 5-29.

Kim D. H., Jung E. A., Sohng I. S., Han J. A., Kim T. H. and Han M. J., 1998, Intestinal bacterial metabolism of flavonoids and its relation to some biological activities, *Archives of Pharmacal Research*, **21**(1):17-23.

Kim D. H., Yu K. W., Bae E. A., Park H. J. and Choi J. W., 1998a, Metabolism of kalopanaxsaponin B and H by human intestinal bacteria and antidiabetic activity of their metabolites, *Biological and Pharmaceutical Bulletin*, **21**(4):360-365.

Kimura Y., Akihisa T., Yasukawa K., Takase S., Tamura T. and Ida Y., 1997, Cyclokirilodiol and isocyclokirilodiol: two novel cycloartanes from the seeds of *Trichosanthes kirilowii* Maxim, *Chemical and Pharmaceutical Bulletin*, **45**(2):415-417.

Kinghorn A. D., Su B. N., Jang D. S., Chang L. C., Lee D., Gu J. Q., Carcache-Blanco E. J., Pawlus A. D., Lee S. K., Park E. J., Cuendet M., Gills J. J., Bhat K., Park H. S., Mata-Greenwood E., Song L. L., Jang M. and Pezzuto J. M., 2004, Natural inhibitors of carcinogenesis, *Planta Medica*, **70**(8):691-705.

Klayman D. L., 1985, Qinghaosu (artemisinin): an antimalarial drug from China. *Science*, **228**(4703):1049-1055.

Klingaman G., 2005, Plant of the week: Japanese roof iris. Latin: *Iris tectorum*. Division of Agriculture, University of Arkansas, Little Rock, Arkansas. USA. at http://www.arhomeandgarden.org/plantoftheweek/articles/iris_japanese_roof_3-4-05.htm, accessed on 11/04/2006

Ko W. G., Kang T. H., Lee S. J., Kim Y. C. and Lee B. H., 2002, Effects of luteolin on the inhibition of proliferation and induction of apoptosis in human myeloid leukaemia cells, *Phytotherapy Research*, **16**(3):295-298.

Kong J. M., Goh N. K., Chia L. S. and Chia T. F., 2003, Recent advances in traditional plant drugs and orchids, *Acta Pharmacologica Sinica*, **24**(1):7-21.

Krick W., Marner F. J. and Jaenicke L., 1983, Isolation and structure determination of the precursors of alpha-irone and gamma-irone and homologous compounds from *Iris pallida* and *Iris florentina*, *Zeitschrift für Naturforschung C*, **38** c:179-184.

Krishan A., 1975, Rapid flow cytofluorometric analysis of mammalian cell cycle by propidium iodide staining, *The Journal of Cell Biology*, **66**(1):188-193.

Krishan A. and Frei E., 3rd, 1975, Morphological basis for the cytolytic effect of vinblastine and vincristine on cultured human leukemic lymphoblasts, *Cancer Research*, **35**(3):497-501.

Kubota N. K., Ohta E., Ohta S., Koizumi F., Suzuki M., Ichimura M. and Ikegami S., 2003, Piericidins C-5 and C-6: new 4-pyridinol compounds produced by *Streptomyces* sp. and *Nocardioides* sp., *Bioorganic and Medicinal Chemistry*, **11**(21):4569-4575.

Kumar N., Singh B., Bhandari P., Gupta A. P., Uniyal S. K. and Kaul V. K., 2005, Biflavonoids from *Lonicera japonica*, *Phytochemistry*, **66**(23):2740-2744.

Kumi-Diaka J. and Butler A., 2000, Caspase-3 protease activation during the process of genistein-induced apoptosis in TM4 testicular cells, *Biology of the Cell*, **92**(2):115-124.

Kyle E., Neckers L., Takimoto C., Curt G. and Bergan R., 1997, Genistein-induced apoptosis of prostate cancer cells is preceded by a specific decrease in focal adhesion kinase activity, *Molecular Pharmacology*, **51**(2):193-200.

Lai H., Sasaki T., Singh N. P. and Messay A., 2005, Effects of artemisinin-tagged holotransferrin on cancer cells, *Life Sciences*, **76**(11):1267-1279.

Lai H. and Singh N. P., 1995, Selective cancer cell cytotoxicity from exposure to dihydroartemisinin and holotransferrin, *Cancer Letters*, **91**(1):41-46.

Lee H. U., Bae E. A. and Kim D. H., 2005, Hepatoprotective effect of tectoridin and tectorigenin on tert-butyl hyperoxide-induced liver injury, *Journal of Pharmacological Sciences*, **97**(4):541-544.

Lee K. T., Sohn I. C., Kim Y. K., Choi J. H., Choi J. W., Park H. J., Itoh Y. and

Miyamoto K., 2001, Tectorigenin, an isoflavone of *Pueraria thunbergiana* Benth., induces differentiation and apoptosis in human promyelocytic leukemia HL-60 cells. *Biological and Pharmaceutical Bulletin*, **24**(10):1117-1121.

Lee L. T., Huang Y. T., Hwang J. J., Lee P. P. H., Ke F. C., Nair M. P., Kanadaswami C. and Lee M. T., 2002, Blockade of the epidermal growth factor receptor tyrosine kinase activity by quercetin and luteolin leads to growth inhibition and apoptosis of pancreatic tumour cells, *Anticancer Research*, **22**(3):1615-1627.

Lee S. J., Son K. H., Chang H. W., Kang S. S. and Kim H. P., 1998, Anti-inflammatory activity of *Lonicera japonica*, *Phytotherapy Research*, **12**(6):445-447.

Lee Y., Howard L. R. and Villalon B., 1995, Flavonoids and Antioxidant Activity of Fresh Pepper (*Capsicum annuum*) Cultivars, *Journal of Food Science*, **60**(3):473-476.

Lenis L. A., Ferreiro M. J., Debitus C., Jimenez C., Quinoa E. and Riguera R., 1998, The unusual presence of hydroxylated furanosesquiterpenes in the deep ocean tunicate *Ritterella rete*. Chemical interconversions and absolute stereochemistry, *Tetrahedron*, **54**(20):5385-5406.

Lennon S. V., Martin S. J. and Cotter T. G., 1991, Dose-dependent induction of apoptosis in human tumour-cell lines by widely diverging stimuli, *Cell Proliferation*, **24**(2):203-214.

Lenz H. J., 2003, Clinical update: proteasome inhibitors in solid tumours, *Cancer Treatment Reviews*, **29**(Supplement 1):41-48.

Lian F. R., Li Y. W., Bhuiyan M. and Sarkar F. H., 1999, p53-Independent apoptosis induced by genistein in lung cancer cells, *Nutrition and Cancer*, **33**(2):125-131.

Linassier C., Pierre M., Lepecq J. B. and Pierre J., 1990, Mechanisms of action in Nih-3t3 cells of genistein, an inhibitor of Egf receptor tyrosine kinase-activity, *Biochemical Pharmacology*, **39**(1):187-193.

Liu Y. B., Fiskum G. and Schubert D., 2002, Generation of reactive oxygen species by the mitochondrial electron transport chain, *Journal of Neurochemistry*, **80**(5):780-787.

Lodish H. F. and Darnell J. E., 1995, Molecular cell biology, Scientific American Books, New York, pp 141-188.

Lu A. P., Jia H. W., Xiao C. and Lu Q. P., 2004, Theory of traditional Chinese medicine and therapeutic method of diseases, *World Journal of Gastroenterology*, **10**(13):1854-1856.

Lu S. Z., 1985, Hepatoma treated by Gekko, *Zhejiang Journal of Traditional Chinese Medicine*, **20**(7):316.

Mabry T. J., 1970, The systematic identification of flavonoids, Springer, Berlin, pp 25.

Manca A., Bassani B., Russo A. and Pacchierotti F., 1990, Origin of aneuploidy in relation to disturbances of cell-cycle progression. I. Effects of vinblastine on mouse bone marrow cells, *Mutation Research*, **229**(1):29-36.

Mann J., 2002, Natural products in cancer chemotherapy: past, present and future. *Nature Reviews Cancer*, **2**(2):143-148.

Mao Y. Q., Varoglu M. and Sherman D. H., 1999, Molecular characterization and analysis of the biosynthetic gene cluster for the antitumour antibiotic mitomycin C from Streptomyces lavendulae NRRL 2564, *Chemistry and Biology*, **6**(4):251-263.

Markovits J., Linassier C., Fosse P., Couprie J., Pierre J., Jacqueminsablon A., Saucier J. M., Lepecq J. B. and Larsen A. K., 1989, Inhibitory effects of the tyrosine kinase inhibitor genistein on mammalian DNA topoisomerase-II, *Cancer Research*, **49**(18):5111-5117.

Marner F. J. and Kerp B., 1992, Composition of iridals, unusual triterpenoids from sword lilies, and the seasonal dependence of their content in various parts of different Iris species, *Zeitschrift für Naturforschung C*, **47**(1-2):21-25.

Marner F. J., Krick W., Gellrich B. and Jaenicke L., 1982, Irigermanal and Iridogermanal - 2 new triterpenoids from rhizomes of *Iris germanica* L., *Journal of Organic Chemistry*, **47**(13):2531-2536.

Marshall J., 2005, The role of bevacizumab as first-line therapy for colon cancer, *Seminars in Oncology*, **32**(6):43-47.

Martin S. J., Green D. R. and Cotter T. G., 1994, Dicing with death - dissecting the components of the apoptosis machinery, *Trends in Biochemical Sciences*, **19**(1):26-30.

Matsukawa Y., Marui N., Sakai T., Satomi Y., Yoshida M., Matsumoto K., Nishino H. and Aoike A., 1993, Genistein arrests cell-cycle progression at G_2/M, *Cancer Research*, **53**(6):1328-1331.

Mattson M. P., Estus S. and Rangnekar V. M., 2001, Programmed cell death, Elsevier, London, pp 142-144.

McCabe M. J. and Orrenius S., 1993, Genistein induces apoptosis in immature human thymocytes by inhibiting topoisomerase-II, *Biochemical and Biophysical Research Communications*, **194**(2):944-950.

Meikrantz W. and Schlegel R., 1995, Apoptosis and the Cell-Cycle, *Journal of Cellular Biochemistry*, **58**(2):160-174.

Menon L. G., Kuttan R., Nair M. G., Chang Y. C. and Kuttan G., 1998, Effect of isoflavones genistein and daidzein in the inhibition of lung metastasis in mice induced by B16F-10 melanoma cells, *Nutrition and Cancer*, **30**(1):74-77.

Mentz F., Baudet S., Blanc C., Issaly F., Binet J. L. and Merle-Beral H., 1998, Simple, fast method of detection apoptosis in lymphoid cells, *Cytometry*, **32**(2):95-101.

Messina M. J., Persky V., Setchell K. D. R. and Barnes S., 1994, Soy intake and cancer risk - a review of the *in-vitro* and *in-vivo* data, *Nutrition and Cancer*, **21**(2):113-131.

Minami H., Okubo A., Kodama M. and Fukuyama Y., 1996, Highly oxygenated

isoflavones from *Iris japonica*, *Phytochemistry*, **41**(4):1219-1221.

Mitchell J. H., Gardner P. T., McPhail D. B., Morrice P. C., Collins A. R. and Duthie G. G., 1998, Antioxidant efficacy of phytoestrogens in chemical and biological model systems, *Archives of Biochemistry and Biophysics*, **360**(1):142-148.

Miyake Y., Ito H. and Yoshida T., 1997, Identification of iridals as piscicidal components of Iridaceous plants and their conformations associated with CD spectra. *Canadian Journal of Chemistry*, **75**(6):734-741.

Monks A., Scudiero D., Skehan P., Shoemaker R., Paull K., Vistica D., Hose C., Langley J., Cronise P., Vaigro-Wolff A., Gray-Goodrich M., Campbell H., Mayo J. and Boyd M., 1991, Feasibility of a high-flux anticancer drug screen using a diverse panel of cultured human tumour cell lines, *Journal of the National Cancer Institute*, **83**(11):757-766.

Morita N., Shimokor.M, Shimizu M. and Arisawa M., 1972, Studies on medicinal resources. 33. Components of rhizome of *Iris tectorum* Maximowicz (Iridaceae) 2. *Yakugaku Zasshi*, **92**(8):1052-1054.

Motwani M., Delohery T. M. and Schwartz G. K., 1999, Sequential dependent enhancement of caspase activation and apoptosis by flavopiridol on paclitaxel-treated human gastric and breast cancer cells, *Clinical Cancer Research*, **5**(7):1876-1883.

Mueller S., Schittenhelm M., Honecker F., Malenke E., Lauber K., Wesselborg S., Hartmann J. T., Bokemeyer C. and Mayer F., 2006, Cell-cycle progression and response of germ cell tumours to cisplatin *in vitro*, *International Journal of Oncology*, **29**(2):471-479.

Murray A. and Hunt T., 1993, The cell cycle: an introduction, Oxford University Press, Oxford, pp 7-9.

Nakamura T., Okuyama E. and Yamazaki M., 1996, Neurotropic components from star anise (*Illicium verum* Hook. *fil*), *Chemical and Pharmaceutical Bulletin*, **44**(10):1908-1914.

Nakasugi T. and Komai K., 1998, Antimutagens in the Brazilian folk medicinal carqueja (*Baccharis trimera* Less.), *Journal of Agricultural and Food Chemistry*, **46**(7):2560-2564.

Nam N. H., Kim H. M., Bae K. H. and Ahn B. Z., 2003, Inhibitory effects of Vietnamese medicinal plants on tube-like formation of human umbilical venous cells, *Phytotherapy Research*, **17**(2):107-111.

Newman D. J., Cragg G. M. and Snader K. M., 2003, Natural products as sources of new drugs over the period 1981-2002, *Journal of Natural Products*, **66**(7):1022-1037.

Noble R. L., 1990, The discovery of the vinca alkaloids - chemotherapeutic agents against cancer, *Biochemistry and Cell Biology*, **68**(12):1344-1351.

Nusslein B. and Kreis W., 2000, Purification of cynaroside 7-*O*-beta-*D*-glucosidase from the herbal drug *Cynarae folium* (artichoke leaves), *Journal of Applied Botany*,

74(3-4):113-118.

Oda K., Matsuda H., Murakami T., Katayama S., Ohgitani T. and Yoshikawa M., 2000. Adjuvant and haemolytic activities of 47 saponins derived from medicinal and food plants, *Biological Chemistry*, **381**(1):67-74.

Ohtani I., Kusumi T., Kashman Y. and Kakisawa H., 1991. High-field FT NMR application of Mosher method - the absolute configurations of marine terpenoids, *Journal of The American Chemical Society*, **113**(11):4092-4096.

Ojeda F., Guarda M. I., Maldonado C. and Folch H., 1990, Protein kinase-c involvement in thymocyte apoptosis induced by hydrocortisone, *Cellular Immunology*, **125**(2):535-539.

Okura A., Arakawa H., Oka H., Yoshinari T. and Monden Y., 1988, Effect of genistein on topoisomerase activity and on the growth of [Val-12]Ha-Ras-transformed Nih-3t3 cells, *Biochemical and Biophysical Research Communications*, **157**(1):183-189.

Ormerod M. G., Paul F., Cheetham M. and Sun X. M., 1995, Discrimination of apoptotic thymocytes by forward light scatter, *Cytometry*, **21**(3):300-304.

Ormerod M. G., Sun X. M., Snowden R. T., Davies R., Fearnhead H. and Cohen G. M., 1993, Increased membrane permeability of apoptotic thymocytes: a flow cytometric study, *Cytometry*, **14**(6):595-602.

Pagliacci M. C., Smacchia M., Migliorati G., Grignani F., Riccardi C. and Nicoletti I., 1994, Growth-inhibitory effects of the natural phyto-estrogen genistein in MCF-7 human breast-cancer cells, *European Journal of Cancer*, **30A**(11):1675-1682.

Park E. K., Shin Y. W., Lee H. U., Lee C. S. and Kim D. H., 2004, Passive cutaneous anaphylaxis-inhibitory action of tectorigenin, a metabolite of tectoridin by intestinal microflora, *Biological and Pharmaceutical Bulletin*, **27**(7):1099-1102.

Park S. S., Kim Y. N., Jeon Y. K., Kim Y. A., Kim J. E., Kim H. and Kim C. W., 2005, Genistein-induced apoptosis *via* Akt signaling pathway in anaplastic large-cell lymphoma, *Cancer Chemotherapy and Pharmacology*, **56**(3):271-278.

Peterson J. and Dwyer J., 1998, Flavonoids: dietary occurrence and biochemical activity, *Nutrition Research*, **18**(12):1995-2018.

Pezzuto J. M., 1997, Plant-derived anticancer agents, *Biochemical Pharmacology*, **53**(2):121-133.

Po L. S., Wang T. T., Chen Z. Y. and Leung L. K., 2002, Genistein-induced apoptosis in MCF-7 cells involves changes in Bak and Bcl-x without evidence of anti-oestrogenic effects, *British Journal of Nutrition*, **88**(5):463-469.

Polkowski K. and Mazurek A. P., 2000, Biological properties of genistein. A review of *in-vitro* and *in-vivo* data, *Acta Poloniae Pharmaceutica*, **57**(2):135-155.

Pollard T. D. and Earnshaw W. C., 2002, Cell biology, Elsevier Science, Philadelphia, pp 690.

Ponder B. A., 2001, Cancer genetics, *Nature*, **411**(6835):336-341.

Potten C. S. and Wilson J. W., 2004, Apoptosis: the life and death of cells. Cambridge University Press, Cambridge, pp 18-24.

Potter A. J., Gollahon K. A., Palanca B. J. A., Harbert M. J., Choi Y. M., Moskovitz A. H., Potter J. D. and Rabinovitch P. S., 2002, Flow cytometric analysis of the cell cycle phase specificity of DNA damage induced by radiation, hydrogen peroxide and doxorubicin, *Carcinogenesis*, **23**(3):389-401.

Pratt W. B., 1994, The anticancer drugs, Oxford University Press, Oxford, pp 37 and 184.

Praud A., Valls R., Piovetti L., Banaigs B. and Benaim J. Y., 1995, Meroditerpenes from the brown alga *Cystoseira crinita* off the French Mediterranean coast, *Phytochemistry*, **40**(2):495-500.

Price P. and Sikora K., 2002, Treatment of cancer, Arnold, London, pp 11, 20 and 106.

Qin M. J., Wang Q., Wu H. G., Xu G. J. and Toshihiro T., 1996, Determination of isoflavones in 16 species of rhizomatous medicinal plants from Iridaceae, *Journal of Plant Resources and Environment*, **5**(4):55-56.

Qin M. J., Ji W. L., Wang Z. T. and Ye W. C., 2005, A new isoflavonoid from *Belamcanda chinensis* (L.) DC., *Journal of Integrative Plant Biology*, **47**(11):1404-1408.

Que H. F., Chen H. F., Xu J. N., Liu S., Lu D. M. and Tang H. J., 2005, Discussion of relationship between quality of life and clinical effect assessment of malignant tumour treated with traditional Chinese medicine, *Zhong Xi Yi Jie He Xue Bao*, **3**(4):253-256.

Quijano L., Nunez I. S., Fronczek F. R. and Fischer N. H., 1997, A guaianolide and four melampolides from *Melampodium leucanthum*, *Phytochemistry*, **45**(4):769-775.

Ranalli M., Oberst A., Corazzari M. and Laurenzi V. D., 2003, Flow cytometric studies of cell death, in: *Cell proliferation and apoptosis* (Hughes D. J. and Mehmet H., eds.), BIOS Scientific., Oxford, pp 330 and 334-341.

Rice Evans C. A., Miller J. and Paganga G., 1997, Antioxidant properties of phenolic compounds, *Trends in Plant Science*, **2**(4):152-159.

Robak J. and Gryglewski R. J., 1996, Bioactivity of flavonoids, *Polish Journal of Pharmacology*, **48**(6):555-564.

Roger J., Benjamin K. and Robins M., 2006, Cancer biology, Pearson Education, Harlow, pp 34.

Rubinstein L. V., Shoemaker R. H., Paull K. D., Simon R. M., Tosini S., Skehan P., Scudiero D. A., Monks A. and Boyd M. R., 1990, Comparison of *in-vitro* anticancer-drug-screening data generated with a tetrazolium assay versus a protein assay against a diverse panel of human tumour cell lines, *Journal of the National Cancer Institute*, **82**(13):1113-1118.

Salti G. I., Grewal S., Mehta R. R., Das Gupta T. K., Boddie A. W. and Constantinou A. I., 2000, Genistein induces apoptosis and topoisomerase II-mediated DNA breakage in colon cancer cells, *European Journal of Cancer*, **36**(6):796-802.

Sasaki D. T., Dumas S. E. and Engleman E. G., 1987, Discrimination of viable and nonviable cells using propidium iodide in 2 colour immunofluorescence, *Cytometry*, **8**(4):413-420.

Schmid I., Uittenbogaart C. H., Keld B. and Giorgi J. V., 1994, A Rapid Method for Measuring Apoptosis and Dual-Color Immunofluorescence by Single Laser Flow-Cytometry, *Journal of Immunological Methods*, **170**(2):145-157.

Scholey J. M., Brust-Mascher I. and Mogilner A., 2003, Cell Division, *Nature*, **422**(6933):746-752.

Schwartzman R. A. and Cidlowski J. A., 1993, Apoptosis - the biochemistry and molecular-biology of programmed cell-death, *Endocrine Reviews*, **14**(2):133-151.

Searle J., Kerr J. F. and Bishop C. J., 1982, Necrosis and apoptosis: distinct modes of cell death with fundamentally different significance, *Pathology Annual*, **17**:229-259.

Seki K., Tomihari T., Haga K. and Kaneko R., 1994, Iristectorene A and Iristectorene C~G, monocyclic triterpene esters from *Iris tectorum*, *Phytochemistry*, **36**(2):425-431.

Seki K., Tomihari T., Haga K. and Kaneko R., 1994a, Iristectorones A~H, spirotriterpene quinone adducts from *Iris tectorum*, *Phytochemistry*, **37**(3):807-815.

Seki K., Tomihari T., Haga K. and Kaneko R., 1994b, Iristectorene B, a monocyclic triterpene ester from *Iris tectorum*, *Phytochemistry*, **36**(2):433-438.

Shah M. A. and Schwartz G. K., 2000, The relevance of drug sequence in combination chemotherapy, *Drug Resistance Updates*, **3**(6):335-356.

Shah M. A. and Schwartz G. K., 2001, Cell cycle-mediated drug resistance: an emerging concept in cancer therapy, *Clinical Cancer Research*, **7**(8):2168-2181.

Shapiro H. M., 2003, Practical flow cytometry, Wiley Liss, New York, pp 46.

Shewale J. G., 1982, Beta-glucosidase - its role in cellulase synthesis and hydrolysis of cellulose, *International Journal of Biochemistry*, **14**(6):435-443.

Shi R. X., Ong C. N. and Shen H. M., 2005, Protein kinase C inhibition and X-linked inhibitor of apoptosis protein degradation contribute to the sensitization effect of luteolin on tumour necrosis factor-related apoptosis-inducing ligand-induced apoptosis in cancer cells, *Cancer Research*, **65**(17):7815-7823.

Shi Y.-B., Shi Y., Xu Y. and Scott D. W., 1997, Programmed cell death, Plenum Press, New York, pp 63-64.

Shimoi K., Okada H., Furugori M., Goda T., Takase S., Suzuki M., Hara Y., Yamamoto H. and Kinae N., 1998, Intestinal absorption of luteolin and luteolin 7-*O*-beta-glucoside in rats and humans, *FEBS Letters*, **438**(3):220-224.

Singh N. P. and Lai H., 2001, Selective toxicity of dihydroartemisinin and holotransferrin toward human breast cancer cells, *Life Sciences*. **70**(1):49-56.

Singh N. P. and Lai H. C., 2004, Artemisinin induces apoptosis in human cancer cells. *Anticancer Research*, **24**(4):2277-2280.

Skehan P., 1999, Cell growth and cytotoxicity assays, in: *Cell growth, differentiation and senescence* (Studzinski G. P., ed.), Oxford University Press. Oxford. pp 39. 40 and 52.

Skehan P., Storeng R., Scudiero D., Monks A., McMahon J., Vistica D., Warren J. T., Bokesch H., Kenney S. and Boyd M. R., 1990, New colorimetric cytotoxicity assay for anticancer-drug screening, *Journal of the National Cancer Institute*. **82**(13):1107-1112.

Song H. E., Song H. M., Dan G. Y. and Song H., 1996. Clinical report of two TCM prescripiton with Bi Hu used to treat 118 patients with hepatoma, *Jiangsu Journal of Traditional Chinese Medicine*, **17**(7):22-23.

Song L. R., Hong X., Ding X. L. and Zai Y. Z., 2001. Dictionary of Modern Chinese Medicine, People's Medical Publishing House, Beijing, pp 1254-1255.

Spinozzi F., Pagliacci M. C., Migliorati G., Moraca R., Grignani F., Riccardi C. and Nicoletti I., 1994, The natural tyrosine kinase inhibitor genistein produces cell-cycle arrest and apoptosis in Jurkat T-Leukemia cells, *Leukemia Research*, **18**(6):431-439.

Sporn M. B. and Liby K. T., 2005, Cancer chemoprevention: scientific promise, clinical uncertainty, *Nature Clinical Practice Oncology*, **2**(10):518-525.

Stein G. S. and Pardee A. B., 2004, Cell cycle and growth control: biomolecular regulation and cancer, John Wiley and Sons, Hoboken, pp 5.

Stewart B. W. and Kleihues P., 2003, World cancer report. Oxford University Press. Oxford, pp 9.

Stoessl A., Toth A., Hardegger E. and Kern H., 1971, 7-*O*-Methylaromadendrin from *Populus alba*. *Phytochemistry*, **10**(8):1972-1973.

Studzinski G. P., 1999. Apoptosis: a practical approach, Oxford University Press. Oxford. pp 6-8.

Sy L. K. and Brown G. D., 1998. Novel phenylpropanoids and lignans from *Illicium verum*. *Journal Of Natural Products*, **61**(8):987-992.

Syrigos K. N. and Epenetos A. A., 1999. Antibody directed enzyme prodrug therapy (ADEPT): a review of the experimental and clinical considerations, *Anticancer Research*. **19**(1A):605-613.

Szende B., Zalatnai A. and Schally A. V., 1989. Programmed cell death (apoptosis) in pancreatic cancers of hamsters after treatment with analogs of both luteinizing hormone-releasing hormone and somatostatin, *Proceedings of the National Academy of Sciences of the United States of America*. **86**(5):1643-1647.

Taillet L., Bonfils J. P., Marner F. J. and Sauvaire Y., 1999, Isolation and structure determination of three epoxidized iridals from *Iris cristata*. *Phytochemistry*, **52**(8):1597-1600.

Takahashi K., Hano Y., Suganuma M., Okabe S. and Nomura T., 1999. 28-deacetylbelamcandal, a tumour-promoting triterpenoid from *Iris tectorum*. *Journal of Natural Products*, **62**(2):291-293.

Takahashi K., Hoshino Y., Suzuki S., Hano Y. and Nomura T., 2000. Iridals from *Iris tectorum* and *Belamcanda chinensis*, *Phytochemistry*, **53**(8):925-929.

Thelen P., Scharf J. G., Burfeind P., Hemmerlein B., Wuttke W., Spengler B., Christoffel V., Ringert R. H. and Seidlova-Wuttke D., 2005. Tectorigenin and other phytochemicals extracted from leopard lily *Belamcanda chinensis* affect new and established targets for therapies in prostate cancer, *Carcinogenesis*, **26**(8):1360-1367.

Tolis C., Peters G. J., Ferreira C. G., Pinedo H. M. and Giaccone G., 1999. Cell cycle disturbances and apoptosis induced by topotecan and gemcitabine on human lung cancer cell lines, *European Journal of Cancer*, **35**(5):796-807.

Tolleson W. H., Melchior W. B., Jr., Morris S. M., McGarrity L. J., Domon O. E., Muskhelishvili L., James S. J. and Howard P. C., 1996, Apoptotic and anti-proliferative effects of fumonisin B1 in human keratinocytes, fibroblasts, esophageal epithelial cells and hepatoma cells, *Carcinogenesis*, **17**(2):239-249.

Toso R. J., Jordan M. A., Farrell K. W., Matsumoto B. and Wilson L., 1993, Kinetic stabilization of microtubule dynamic instability *in vitro* by vinblastine, *Biochemistry*, **32**(5):1285-1293.

Traganos F., Ardelt B., Halko N., Bruno S. and Darzynkiewicz Z., 1992, Effects of genistein on the growth and cell-cycle progression of normal human-lymphocytes and human leukemic Molt-4 and HL-60 Cells, *Cancer Research*, **52**(22):6200-6208.

van Engeland M., Ramaekers F. C., Schutte B. and Reutelingsperger C. P., 1996. A novel assay to measure loss of plasma membrane asymmetry during apoptosis of adherent cells in culture, *Cytometry*, **24**(2):131-139.

Vijayababu M. R., Kanagaraj P. P., Arunkumar A. A. and Arunakaran J. J., 2006, Effects of quercetin on insulin-like growth factors (IGFs) and their binding protein-3 (IGFBP-3) secretion and induction of apoptosis in human prostate cancer cells. *Journal of Carcinogenesis*, **5**(1):10-18.

Wakdikar S., 2004, Global health care challenge: Indian experiences and new prescriptions, *Electronic Journal of Biotechnology*, 7(3):218-223.

Wang T. H., Wang H. S. and Soong Y. K., 2000. Paclitaxel-induced cell death - Where the cell cycle and apoptosis come together, *Cancer*, **88**(11):2619-2628.

Webb M. R. and Ebeler S. E., 2003, A gel electrophoresis assay for the simultaneous determination of topoisomerase I inhibition and DNA intercalation, *Analytical Biochemistry*, **321**(1):22-30.

Weitberg A. B. and Corvese D., 1999, The effect of epigallocatechin gallate and sarcophytol A on DNA strand breakage induced by tobacco-specific nitrosamines and stimulated human phagocytes, *Journal of Experimental and Clinical Cancer Research*. **18**(3):433-437.

Wells A., 2000, The epidermal growth factor receptor (EGFR) – a new target in cancer therapy, *Signal*, **1**(1):4-11.

Wieder R., 1999, Selection of methods for measuring proliferation, in: *Cell growth, differentiation and senescence: a practical approach* (Studzinski G. P., ed.). Oxford University Press, Oxford, pp 2 and 7.

Williams D. H. and Fleming I., 1995, Spectroscopic methods in organic chemistry - fifth edition, McGraw-Hill, London, pp 40-47.

Wilson L., Creswell K. M. and Chin D., 1975, Mechanism of action of vinblastine - binding of (*acetyl*-^{3}H)vinblastine to embryonic chick brain tubulin and tubulin from sea-urchin sperm tail outer doublet microtubules, *Biochemistry*, **14**(26):5586-5592.

Wong S. M., Oshima Y., Pezzuto J. M., Fong H. H. S. and Farnsworth N. R., 1986, Plant anticancer agents. 39. Triterpenes from *Iris missouriensis* (Iridaceae), *Journal of Pharmaceutical Sciences*, **75**(3):317-320.

Wu Y. X. and Xu L. X., 1992, Analysis of isoflavones in *Belamcanda chinensis* (L.) DC. and *Iris tectorum* Maxim. by square wave voltammetry, *Yao Xue Xue Bao*, **27**(1):64-68.

Xiao P. G., Li D. P. and Yang. S. L., 2002, Modern Chinese Materia Medica, Chemical Industry Press, Beijing, pp 826.

Yamashita Y., Kawada S. Z. and Nakano H., 1990, Induction of mammalian topoisomerase II dependent DNA cleavage by nonintercalative flavonoids, genistein and orobol, *Biochemical Pharmacology*, **39**(4):737-744.

Yan J. H., Xiao X. X. and Huang K. L., 2002, Component analysis of volatile oil from *Illicium verum* Hook. *f*, *Journal of Central South University of Technology*, **9**(3):173-176.

Yang C. S., Landau J. M., Huang M. T. and Newmark H. L., 2001, Inhibition of carcinogenesis by dietary polyphenolic compounds, *Annual Review of Nutrition*, **21**:381-406.

Yang C. S., Prabhu S. and Landau J., 2001a, Prevention of carcinogenesis by tea polyphenols, *Drug Metabolism Reviews*, **33**(3-4):237-253.

Yang M. Z., Tanaka T., Hirose Y., Deguchi T., Mori H. and Kawada Y., 1997, Chemopreventive effects of diosmin and hesperidin on N-butyl-N-(4-hydroxybutyl)nitrosamine-induced urinary-bladder carcinogenesis in male icr mice, *International Journal of Cancer*, **73**(5):719-724.

Yip E. C., Chan A. S., Pang H., Tam Y. K. and Wong Y. H., 2006, Protocatechuic acid induces cell death in HepG2 hepatocellular carcinoma cells through a c-Jun N-

terminal kinase-dependent mechanism. *Cell Biology and Toxicology*. **22**(4):293-302.

Yoshikawa M., Murakami T., Komatsu H. and Matsuda H., 1998. Medicinal foodstuffs. XII. Saponin constituents with adjuvant activity from hyacinth bean, the seeds of *Dolichos lablab* L. (1): structures of lablabosides A, B and C. *Chemical and Pharmaceutical Bulletin*, **46**(5):812-816.

Yoshiki Y., Kim J. H., Okubo K., Nagoya I., Sakabe T. and Tamura N., 1995. A saponin conjugated with 2,3-dihydro-2,5-dihydroxy-6-methyl-4H-pyran-4-one from *Dolichos lablab*. *Phytochemistry*, **38**(1):229-231.

Yu Z. L., Li W. J. and Liu F. Y., 2004, Inhibition of proliferation and induction of apoptosis by genistein in colon cancer HT-29 cells. *Cancer Letters*. **215**(2):159-166.

Yun J., Zhong Q., Kwak J. Y. and Lee W. H., 2005. Hypersensitivity of Brca1-deficient MEF to the DNA interstrand crosslinking agent mitomycin C is associated with defect in homologous recombination repair and aberrant S-phase arrest. *Oncogene*, **24**(25):4009-4016.

Zhang G., Gurtu V., Kain S. R. and Yan G., 1997. Early detection of apoptosis using a fluorescent conjugate of annexin V, *Biotechniques*. **23**(3):525-531.

Zhao Y. T., Noltie H. J. and Mathew B. F., 2000, *Iris tectorum* Maximowicz. *Flora of China*. **24**:308.

Zhou X. J. and Rahmani R., 1992. Preclinical and clinical pharmacology of vinca alkaloids, *Drugs*, **44**(supplement 4):1-16.

Zhu H., Smith C., Ansah C. and Gooderham N. J., 2005, Responses of genes involved in cell cycle control to diverse DNA damaging chemicals in human lung adenocarcinoma A549 cells, *Cancer Cell International*. **5**:28.

Zielinska M., Gulden M. and Seibert H., 2003. Effects of quercetin and quercetin-3-*O*-glycosides on oxidative damage in rat C6 glioma cells. *Environmental Toxicology and Pharmacology*, **13**(1):47-53.